"A FAILURE CRITERION FOR FILLET WELDS"

by

Jonathan Drew Higgs

A thesis submitted to the

Faculty of Engineering

in fulfilment of the requirements

for the degree

Doctor of Philosophy

The University of Aston in Birmingham

January 1981

ABSTRACT

The work constitutes a study of the strength of mild steel fillet welds subject to static loading, and the behaviour of flange welded beam-column connections under combined bending and shear. Tests are conducted on short welds in the as-welded and stress relieved conditions, and also on full-size beam-column connections. It is shown that welds under compression have a lower strength than when under tension. Failure of the fillet weld is initiated at the weld root, the important factor controlling the initiation being weld ductility. The greater the residual stress, the lower the weld ductility and ultimate strength. Thermal stress relieving increases strength by as much as 30%. Weld failure plane is rarely at the throat and varies from 0° to 45° depending upon loading condition. Failure plane average stresses are related by a circular function which is expressed in terms of externally applied forces at limit state.

The tension weld of a flange-welded beam-column connection always fails before the compression weld. The shear load sharing between the welds is a complex function of elastic compression of the web, elastic/plastic deformation of the flanges, load/deformation characteristics, and the type of load application. Bearing forces between the compression flange and column face produce low level bearing stresses and frictional forces which make a negligible contribution to shear load resistance. Three modes of connection failure are possible; 'end mode', 'bending mode' and 'shear mode', with a sudden change taking place between the two latter.

Thesis submitted by Jonathan Drew Higgs for the degree of Doctor of Philosophy.

Key words: WELD STRENGTH CRITERION

BEAM-COLUMN FAILURE

CONTENTS

Page

ACKNOWLEDGEMENTS

This research was carried out at the Department of Civil Engineering of the University of Aston in Birmingham under the supervision of Dr.L.H.Martin, whom the author would like to thank for his continued help and guidance given throughout the course of the work.

The author would also like to thank M.W.Parsons of the Department of Civil Engineering for services rendered; the Staff of the Civil Engineering Structures Laboratory; the Staff of the Civil Engineering Workshop; the Staff of the Production Engineering Machine Tool Laboratory for advice given on the use of their machine tools, and the Staff of the Production Engineering Workshop for assistance given

---

FIGURES

Page

PLATES

TABLES

SYMBOLS

F	force
t	leg length of symmetrical weld, or thickness
P	externally applied load
ℓ	length of fillet weld or length in general
F_x, F_y	external forces acting normally to the legs of the fillet weld
F_z	external force acting parallel to longitudinal axis of fillet weld
K	resultant of external forces F_x and F_y
d	depth of beam section, or distance between welds
e	load eccentricity
σ	normal stress
τ	shear stress
M	applied bending moment
σ_c, σ_e	comparative stress
τ_I, τ_{II}	shear stresses acting on a critical plane
σ_I, σ_{II}	tensile or compressive stresses acting on a critical plane
N.A.	neutral axis
F_n	force normal to a failure plane
α, ϕ	angle of a critical plane to some reference plane
k	a constant
σ_p	strength of parent or base metal
σ_w	strength of weld metal
β	a constant used in the I.S.O. stress criterion
σ_t	ultimate tensile strength of weld metal based upon the weld throat section

Δ	deformation of a weld, or dial gauge reading
μ)	regression coefficients for behaviour of weld
)	
λ)	
θ	angle
Δ_{max}	ultimate deformation of weld
σ_y	yield strength of base metal
R	resistive force
Y_o	distance between N.A. and extreme compression fibre
r	radius of rotation
i.c.	instantaneous centre of rotation
A, m	slope of linear failure criteria
C_l	width factor
V	vertical shear load
M_T	torsional moment
s	distance
a)	ellipse half-axes
b)	
c	centre shift
m	slope of a strain line
R_{rh}	right-hand reaction
$R_{\ell h}$	left-hand reaction
x	distance from left-hand support
V_o	ultimate shear capacity of tension weld when $V/M = \infty$

SUFFIXES

s	shear
t	tensile
c	compressive (except for σ_c)
n	normal, or n^{th} weld element
x, y, z	reference planes
b	bending
α	critical plane
ult	ultimate
B	plate bearing
i	i^{th} weld element
f	flange
w	weld

CHAPTER 1

INTRODUCTION

The use of fillet welds in beam-column connections is relatively simple and cheap compared with the use of bolts. Fillet welds are extremely strong relative to their size especially the transverse, or end fillet. Unfortunately the geometry of the fillet weld combined with the inevitable eccentric loading produces a very unfavourable condition with respect to fatigue resistance and brittle fracture. Knowledge of the true strength of the fillet weld would enable the designer to select a more realistic size of weld. This is important for economic reasons, and because the weld size is a primary factor in determining the level of residual stress which in turn is influential to fatigue strength and brittle fracture.

Criteria related to fillet weld strength currently in use have been developed for the prediction of safe working loads and not ultimate strength capacities. These methods have been shown to give very conservative and variable safety factors[22,26,41,42]. European practice is to use the I.S.O[47] comparative stress criterion which is based upon the yield hypothesis of Huber-Hencky-von Mises. British and American practice is to use the vector addition method with a safe working shear stress parameter. Both of these methods assume the throat to be the critical plane.

Various researchers have proposed limit state criteria with which the ultimate strength of fillet welds can be predicted. The use of such criteria will allow the designer to select the necessary size of weld to correspond to a chosen safety factor.

Vreedenburgh[16] proposed an empirical limiting stress envelope based on the throat as critical section. This well known pearoid envelope has led to the common belief that the fillet weld under compression is considerably stronger than that under tension. There is evidence in dispute of this belief. There is now ample evidence to show that the throat is rarely the critical plane, the first researchers to explore this avenue were Archer et al[22], who proposed a maximum shear stress criterion based upon a theoretically variable critical plane. Butler and Kulak[30] considered that fillet weld deformation was a more accurate and a more useful limiting criterion and proposed an empirical relationship for the load-deformation characteristic. Use of this criterion involved a lengthy iterative procedure unsuitable for the design office. Crofts and Martin[45] proposed an empirical limiting stress criterion, based on the actual critical plane, which took a linear form and showed suitability for use in the design office.

The current design procedures used for beam-column connections are based on the procedures formerly used to analyze riveted joints. The welds are designed to transmit a direct shear stress and a moment-induced shear stress based on ordinary elastic beam analysis. Either the vector addition or the I.S.O. criterion is then applied. The I.I.W[47] recommended the allocation of the moment as a couple of forces to the flange welds and the shear force to the web welds. Generally, the position of the neutral axis is regarded as being at half-beam-depth although this is most unlikely as a result of the bearing which must occur between the flange/web of the beam and the column face. Obviously the beam is not free to rotate in the compression zone. This fact was appreciated by Dawe[42] who proposed a method for prediction of ultimate capacity of beam-column connections based upon the load-deformation characteristic of Butler et al[41].

In his analysis Dawe[42] assumed both an instantaneous centre of rotation and neutral axis. He acknowledged the probable presence of frictional forces in the bearing zone, but made no attempt to include them in his analysis. No study has yet been reported on the role that friction plays in the behaviour of beam-column connections.

Archer et al[22] assumed the tension flange weld would be critical and applied their maximum shear stress criterion to it in conjunction with an empirical shear load distribution function.

The distribution of load between the flange and web welds will obviously be influenced by the flexibility of both the column and the beam. Little work has been done in this area.

The presence of residual stresses in welded structures is not disputed but the possible effects upon weld strength are disputed.

Residual stress is a combination of direct welding stress caused by weld shrinkage, and reaction stress which results from the constraint offered by the structure to thermal deformation of the welded joint. It is believed that residual stress is purely elastic, and will store elastic strain energy. The direct welding stress energy is contained within a small volume and consequently the amount of stored energy is small. The reaction strain energy, however, is stored in the relatively large volume of the entire structure but may develop its effects in any part of that structure. Stress raisers such as the root of a fillet weld would be a prime target for the release of this stored energy.

It is commonly believed that residual stress is relieved as soon as the yield point is reached in the weld or adjacent base metal, but it is

only the direct welding stress that is necessarily relieved during plastic deformation or thermal stress relieving. The ultimate strength of the weld can still be influenced by the stored energy of the reaction stress. The role of reaction stress should be borne in mind when small laboratory test specimens are designed to simulate field conditions.

Experimental technique has very often left much to be desired, as large scatter in experimental results[16,20,22,30,55] bears witness to. Non-uniformity of fillet welds such as stop and start, poor penetration, irregular leg size and irregular surface are bound to result in scatter which might lead the investigator to draw wrong conclusions. There is every justification for an investigator endeavouring to produce uniform fillet welds, and such endeavours[44,45,46,55] have made possible a quantitative study of the position of the critical plane.

CHAPTER 2

HISTORICAL REVIEW

Prior to 1930 very little attention had been paid to the theoretical strength of fillet welds, and design methods were based on those used for rivets.

The first theoretical study was made by Bibber[1] in 1930 who looked at possible critical sections such as the bond between the weld and base metal, weld leg, and weld throat. He considered the end, or transverse fillet weld of a simple lap joint as shown in fig.7.

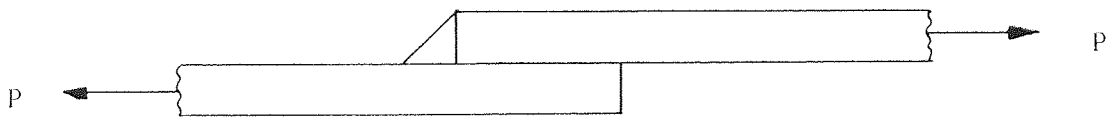

Fig.1 Transverse Lap Joint

A uniform stress distribution was assumed and the couple due to the load eccentricity was ignored. The stress at the throat section was assumed to be purely tensile and equal to

$$\text{tensile stress @ throat} = \frac{2P}{\ell t}$$

where, ℓ = length of weld, and t = leg length.

The shear and tensile stresses acting on each leg were combined using Principal Stress theory:

$$\text{combined stress} = \frac{1.618P}{\ell t}$$

Bibber concluded the throat was the critical section and would fail as a result of tension.

The analysis was extended to fillet welds of unequal leg lengths and it was shown that the critical section could change from the throat to either the parallel or transverse leg of the fillet depending upon the ratio of leg lengths. The weld profile was considered and it was concluded that a concave profile would naturally reduce the strength of the weld and ensure that the throat was generally the critical section. Convex profile increased weld strength to a point at which the leg became the critical section and further reinforcement gave no advantage to strength.

On the basis of assumed physical properties, as shown below, Bibber regarded the fillet weld under compression as having equal strength with the weld under tension.

Assumed Physical Properties

Weld Metal, *Standard Values*

Ultimate Strength in Tension	57,000 lbf/in^2
Yield Point in Tension	43,000 lbf/in^2
Modulus of Elasticity in Tension	29,000,000 lbf/in^2
Ultimate Strength in Compression	63,000 lbf/in^2
Yield Point in Compression	29,000 lbf/in^2
Ultimate Strength in Transverse Shear	41,000 lbf/in^2
Yield Point in Transverse Shear	22,500 lbf/in^2
Modulus of Elasticity in Transverse Shear	11,000,000 lbf/in^2

These properties were obtained from bare mild steel electrodes laid on mild steel plate.

For design purposes the following values of weld strength were proposed:

Ultimate Strength in Tension	36,000 lbf/in^2
Ultimate Strength in Compression	36,000 lbf/in^2
Ultimate Strength in Transverse Shear	26,000 lbf/in^2

The first reported series of tests on contemporary beam-column connections, see fig. 2, was made by Uhler and Jensen[2] in 1930.

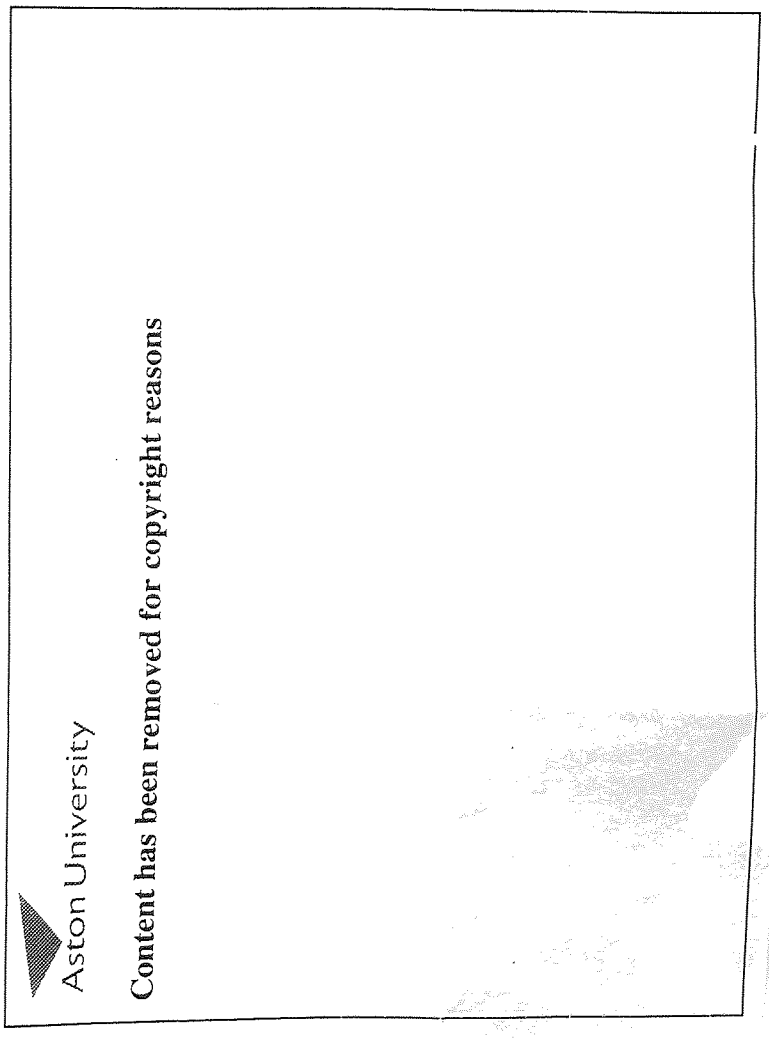

Fig.2 Contemporary Beam - Column Connections.

Their objective was to assess the stresses imposed upon the welds, and the moment resistance of the connections. Eight connections were tested to destruction, four with flange welds only, and the others with web welds only. The majority of the test specimens were made up with undefined gaps between the beam end and the column face.

Experimental technique was very poor and there is not much to be gained from the results other than from the general conclusions.

Like Bibber[1], Uhler and Jensen concluded that web welds were subjected to very high stresses at their extremities, which might lead to premature failure, for short beams however, web welds might be satisfactory. The occurrence of plate-bearing was noted and so were its effects of increased joint rigidity and reduction of maximum weld stresses.

Schuster[3] made a theoretical analysis in a similar way to Bibber[1], but pointed out the significance of the fillet weld root in terms of penetration and stress concentrations. He concluded that a study from the elastic standpoint would not serve any useful purpose, but he did not offer a method of solution. Instead, he suggested something similar to Bibber[1].

He assumed a uniform loading along a critical plane which was not necessarily at the throat. The assumed uniformity was justified with the suggestion that the stress distribution would become more or less uniform when the weld became plastic just prior to failure.

The load couple produced in the simple lap joint was neglected, and it was assumed the fillet weld to be subjected to both tensile and shear

stresses, the resultant stress being a maximum on a critical plane at an angle of 48.5° measured from the vertical leg.

$$\text{maximum stress} = \frac{1.624P}{\ell t}$$

The resultant stress at the throat was equal to $1.618P/\ell t$, the difference being so small that it was suggested to consider the throat as the critical section. No ultimate strength of weld metal was quoted, but instead, the ultimate strength of the base metal was used as the limiting strength.

Freeman[4] conducted tests in 1932 on lapped specimens in order to investigate the effect of variation in the size and length of weld, thickness, and width of plates joined. He tested longitudinal or side welds under both tensile and compressive shearing loads. There were insufficient results from which to draw any firm conclusions, but there is an indication of a fall-off in the strength per unit length with increase in weld length. Transverse welds were tested but with lack of consistency in results probably due to plate yielding

---

2.1 Important contributions, to the study of weld strength, were made by Jensen[5] in 1934:

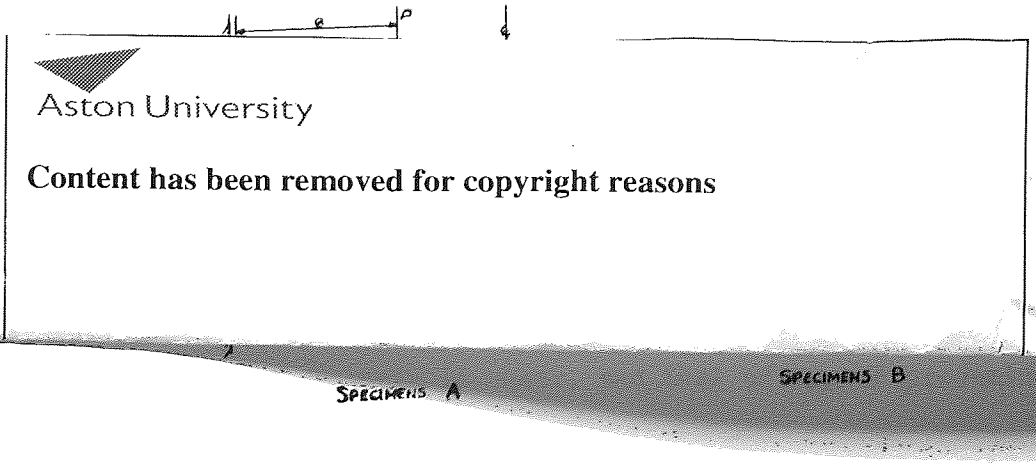

Fig.3 Jensen's Test Specimens, Styles A and B.

1. An improved experimental technique by having run-on and run-off plates for his test welds, this led to good consistency of results.
2. He developed a new style of test specimen, fig.3 in which the applied forces to the legs of the weld could be varied. Up until this time only lap joints had been studied.
3. A brief quantitative study of the possible position of the critical plane.
4. Compared contemporary theories i.e. those of Bibber[1], Schuster[3], and the one which is currently in use, the vector method, and covered in BS 449[6].

Twenty-one tests were conducted on fillet welds of 2 inch length and nominal 0.375 inch leg.

Jensen criticised what is now the current vector method,i.e.to take the resultant of the external forces acting upon the weld legs and consider it to act at the throat, because the throat is assumed to be always the critical section, and no consideration is given to the angle of the resultant load to the throat or any other section. He pointed out that simplicity was in its favour.

Jensen extended the idea of Schuster[3] that the critical plane was subjected to both tensile and shear stresses, by combining the two stresses using Principal Stress theory, but he assumed the critical plane would be at, or near the throat i.e. between 45° and 48.5° (as suggested by Schuster). The stresses used in the Principal Stress theory were in fact computed on the throat. It was suggested the weld in type A test specimen would be predominantly in shear, and that of type B predominantly in tension, see fig.4.

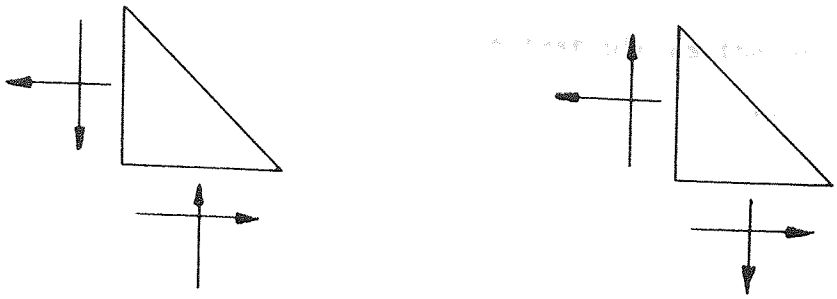

Type A Type B

Fig.4 Force Equilibrium Diagrams for Welds A and B

He assumed the couples produced by the external forces to either cancel each other in type B or, to be insignificant in type A.

Using the maximum shear stress criterion in conjunction with the value of ultimate shear strength obtained from control tests 48,100 lbf/in^2, Jensen was able to predict the ultimate strength of the welds with varying ratios of the forces applied to the weld legs. It must be noted here the maximum shear stress criterion was used for both types of welds even though Jensen himself had suggested that weld type B was predominantly in tension.

He then compared the position of actual fracture planes with the planes of maximum shear stress and maximum principal stress. This comparison was presented pictorially and actual fracture plane angles were not quoted.

For type A welds the correlation between actual and predicted weld strength was very good, and in all six tests the actual critical plane was reasonably coincident with the plane of maximum shear stress. These planes were shown to be approximately at the throat.

For type B welds the correlation between actual and predicted weld strength using the maximum shear stress criterion was not very good at low values of the ratio F_x/F_y. The plane of maximum principal stress bore

little relationship to the actual fracture plane which was generally well away from the throat. In 50% of the test-pieces the actual critical plane was reasonably close to the plane of maximum shear stress.

Jensen concluded the method proposed by Bibber[1] for lap-joints, could not be adapted to welds loaded on both legs.

Jensen found that the current method of applying the resultant force to the throat underestimated the weld strength by a maximum of approximately 37% even when using the ultimate shear strength of the weld metal instead of a safe working stress.

Jensen has clearly shown that the actual critical plane is not at the throat, but has failed to utilise his results in this respect.

He has also clearly shown that the welds of type A and B do not behave in the same way, especially with regard to ultimate strength since he has shown that weld B can be as much as 40% stronger than weld A.

His results would indicate the need for two failure criteria: a shear criterion for type A weld and a tension criterion for type B weld.

Schreiner[7] conducted tests, in 1935, on longitudinal fillet welds of lapped specimens under pure bending, and under bending and shear. These are not of direct interest to the author but four points are worth noting here:

1. Neutral axis of the weld did in fact pass through the centroid of the weld (no plate bearing).
2. At failure the stress distribution was rectangular and not triangular.

3. Yielding first occurred in the compression side of the weld near the end of the weld. This indicated a lower yield strength in compression than in tension. Schreiner suggested that this was contrary to the common belief that compression yield point was at least equal to that in tension. Bibber[1] quoted yield strengths as follows: tension yield strength 43000 lbf/in^2, compression yield strength 29000 lbf/in^2

4. Two of the specimens involved plate-bearing although they had been manufactured with gaps inbetween the web and back plates. During testing these gaps closed and bearing occurred at the compression end of the welds. This resulted in a shift of the axis of rotation from the weld centroid to the point of bearing, and great increase in the strength of the connection.

A general paper on welding design by Jennings[8] was published in 1936 and the following points of interest have been selected from it.

Jennings was the first writer to show interest in residual stresses and recommended that rigid joints should be eliminated as much as possible in order to prevent the development of excessive residual welding stresses which might cause cracked welds during fabrication or ultimate failure in service.

He highlighted the stress concentrations that occur in the fillet weld by reference tc Solakian[9], who found the stress concentration at the root to be 6 to 8 times that of the average stress intensity in the connecting plates and, at the toe, 3 to 5 times as much. Both Schuster[3] and Jensen[5], argued that such stress concentrations were relieved during yielding of the weld to give a fairly uniform stress distribution at failure.

With regard to actual fillet welds Jennings assumed the critical section to be at the throat, and for transverse welds the limiting stress was normal as opposed to shear as suggested by Jensen[5]. Jennings suggested that the bending moment which must have existed as a result of load eccentricity, see fig. 5, was significant and should be taken account of in strength prediction.

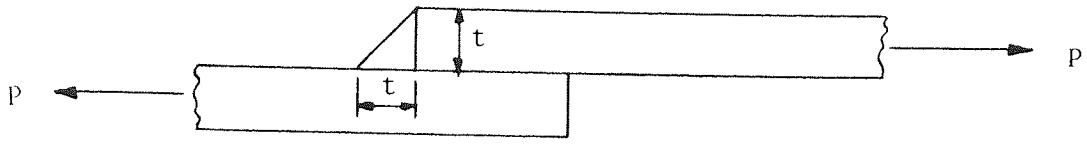

Fig. 5 Transverse Lap Joint

Jennings suggested the bending moment equalled Pt/4 and gave rise to a stress on the throat of a rectangular distribution at failure.

With regard to longitudinal welds on lapped specimens, fig. 6, Jennings suggested that the stress distribution along the weld was uniform although it had been shown, as Jennings pointed out, stress at the ends of the welds was considerably higher than the average stress but, on the other hand tests by Vogel[11] & Blackwood[10] indicated the weld strength was directly proportional to its length.

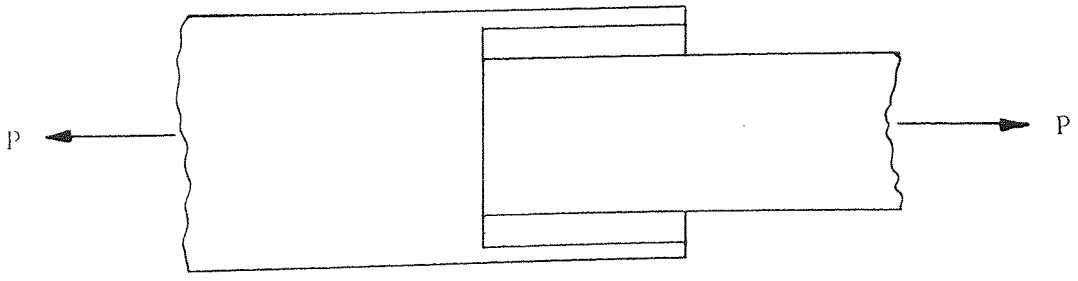

Fig.6 Longitudinal Lap Joint

Jensen and Crispen[12] 1938, looked at a simple longitudinal welded connection with plate-bearing under combined bending and shear, fig.7, in order to determine the stress distribution along the weld. Only three tests were conducted, and the stress analysis was based upon strain measurements - no stress-strain relationship was offered. One of the three test specimens had been thermally stress relieved.

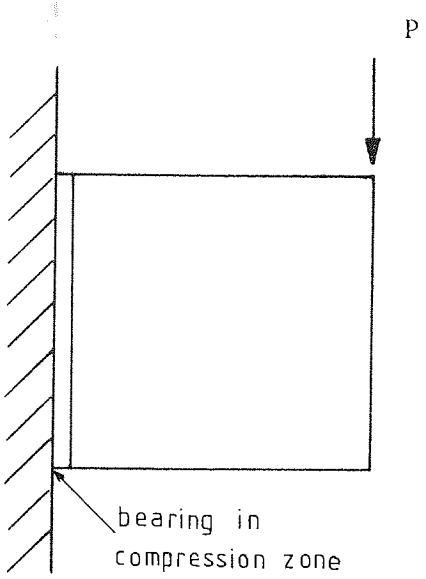

Fig.7 Connection with Plate Bearing

Jensen and Crispen, looked at contemporary theories of Shedd[13], and Schreiner[7], though these were not really applicable since the theory of Shedd[13] was concerned with repeated loads producing elastic rather than plastic strains, and Schreiner's[7] theory was applicable to connections without plate-bearing. Schreiner[7], had shown that the axis of rotation passed through the compression end of the weld when plate-bearing was present and through the weld centroid when not present.

An experimental result was presented as in fig. 8, and it was stated to be typical for all three specimens for loads above and below the yield point. It is evident from fig. 8 that the neutral axis passes through the weld centroid. It is also evident that the compression strain is much greater than the tension strain, with reference to the weld. With reference to the back-plate the strains appear to be very similar. Jensen and Crispen were apparently not aware of the effect of plate-bearing and they concluded that Shedd[13] was correct below the yield point and,

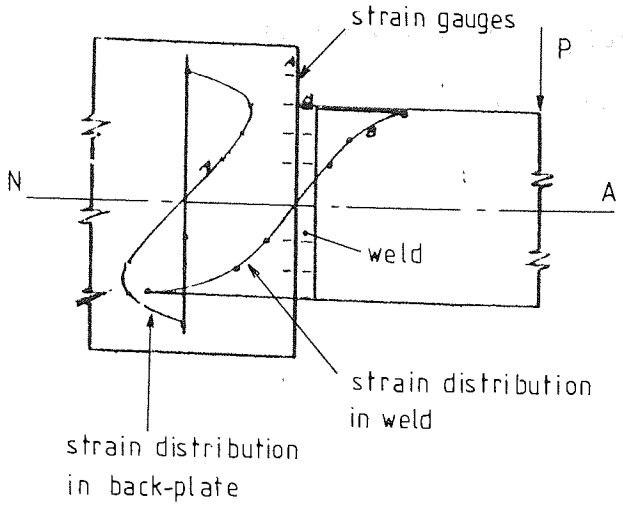

Fig. 8 Strain Distributions

Schreiner[7] was correct at limit state. These are hardly conclusions to be justified by three tests and anyway Schreiner's[7] theory is for connections without bearing, and it is difficult to see how Jensen and Crispen could verify it from their experiments.

Tests were conducted by Johnston and Deits[14], in 1942, on beam-to-column connections of established designs in order to assess moment-rotation characteristics and ability to carry vertical loads. Twenty-one specimens were tested and all were welded up with gaps inbetween the end of the beam and the column.

Only six of the twenty-one connections tested are useful with regard to obtaining the ultimate strength of the welds. Even with these six connections, yielding of the beam web around the welds took place long before fracture of the welds. Because of this, and the gaps between the beams and columns and the uncertainty of the size of the welds, the results can only be taken as a general guide to the true ultimate strength of the welds.

Johnston and Deits did notice the effect of plate-bearing which occurred during some of their tests. They noted the connections became stiffer with increased moment of resistance.

2.2 The idea of limit state design for welded connections was presented by Koenigsberger[15] in 1951, and represents a landmark in design philosophy. His method is a means of determining the working loads of welded joints by firstly evaluating the stresses in the weld in the plastic state prevailing immediately prior to failure, and then applying a load factor. Thus a known safety factor and is employed - up until this time of course analysis has been confined to the elastic state which has resulted in generally high and unknown safety factors.

Koenigsberger of course assumed that all of the weld in the joint was at a plastic state immediately prior to failure. This possibility had already been suggested by Schreiner[7].

Koenigsberger offered his analysis for brackets subjected to torsion and shear and, the detail of which is of no interest to the author. However, certain general assumptions made by Koenigsberger are of interest.

1. Fracture occurred after the weld metal had reached a plastic state throughout, with a limiting ultimate shear stress.
2. Deformations in the plastic range occurred with an approximate uniform state of stress.
3. Conditions (1) and (2) above prevailed throughout the weld throat before fracture.
4. The centre of rotation lay on an axis passing through the weld centroid.

Koenigsberger was the first investigator to treat the position of the centre of rotation as a variable.

In order to determine the ultimate strength of the weld group he considered the weld to be divided into small elements each offering a resistive force acting at right angles to a line joining the centre of the element with the centre of rotation of the complete weld group. The strength of the complete weld group was then equal to the sum of the elemental strengths.

Because of the complexity of the calculations required, he presented his solution in the form of graphs drawn for unit stress, unit weld size and unit spacing between welds.

2.3 Vreedenburgh[16] analysed all contemporary limiting stress theories, in 1954, compared them with his own test results and others, and concluded none were compatible. He suggested that some sort of empirical solution must be adopted and to this end proposed the now well known limit curve of the pearoid shape, see fig.9. The limit curve is made up of three parts joined tangentially.

(i) an ellipse with its apex at

$\sigma = +\sigma_t$; $\tau = 0$

long semi-axis = $2.39\sigma_t$

short semi-axis = $0.97\sigma_t$

Mid-point of ellipse is at

$\sigma = -1.39\sigma_t$; $\tau = 0$

(ii) an arc of a circle with mid-point at $\sigma = 0$, and radius $0.75\sigma_t$.

(iii) a tangent line to this circle passing through the point, $\sigma = -1.70\sigma_t$; $\tau = 0$. σ_t = actual breaking stress based on the throat section.

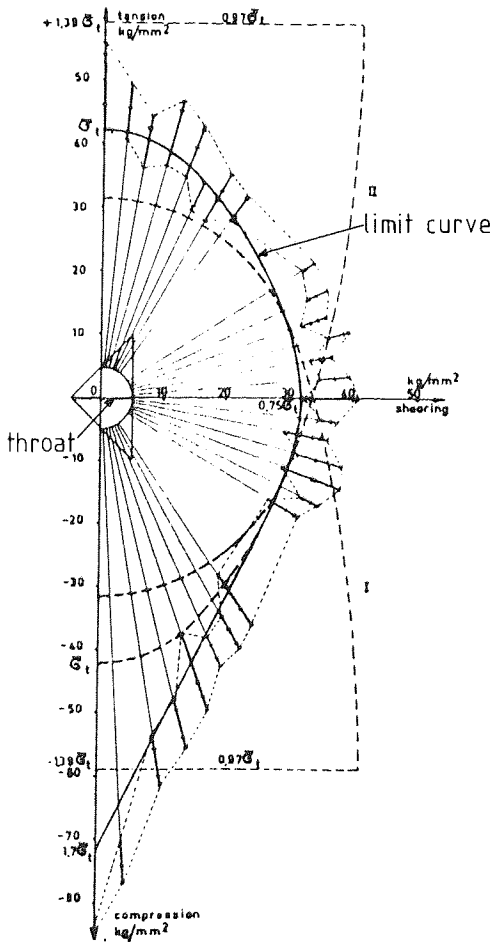

Fig. 9 Limit Curve

This limit curve is based upon tests carried out by the Netherlands Foundation for Applied Scientific Research (T.N.O) which were in fact an extension of the tests done by Jensen[5], and Kist[17].

Vreedenburgh examined the broken specimens of Kist[17], and stated that the critical plane as a rule did not coincide with the throat. In his proposed method of calculation of weld strength Kist[18], in fact assumed the throat to be the critical section. Even though Vreedenburgh had definite evidence of the position of the critical plane his limit curve is based upon the throat section. It must be concluded here that no meaningful assessment of the position of the critical plane could be made from either the Kist[17] or the T.N.O. specimens since no quantitative analysis has been presented.

Tests were conducted to establish a relationship between weld strength and weld size of transverse fillet welds. Sizes tested were 3, 6 and 9 mm throat and he concluded that there was a reduction of strength of approximately 3% per mm in excess of a 4mm throat. The maximum scatter of test results was approximately 60% of the average value and this occurred for the 3 mm welds.

Test welds for the limit curve were of 4 mm throat and maximum scatter was 20-25% of the average value of 4 specimens per test.

Vreedenburgh's limit curve can be critized on the following grounds: (i) the curve does not cover the complete range of possible load configurations, only 90° either side of the throat for the resultant force; (ii) the nearest experimental result to the normal axis to the throat in the compression region is at an angle of 87°, the point on the axis is determined by extrapolation.

(iii) the stress is based upon the throat even though there was evidence to the contrary;

(iv) the curve is based largely on the minimum values of computed stresses;

(v) the scatter is considerable;

(vi) there are large gaps in the experimental results occurringas a result of changing from test style (a) to (b), and from (b) to (c), see figs 10 and 11;

(vii) the most important criticism in the test specimen style (c), fig.11, there can be very little or no horizontal force acting on the weld and the resultant force K is in fact vertical at an angle of 135° to the throat. Such a resultant is not catered for in the limit curve and all experimental results plotted for style (c) test are probably erroneous, and as plotted must be well in excess of the true stress on a weld loaded as the limit curve suggests.

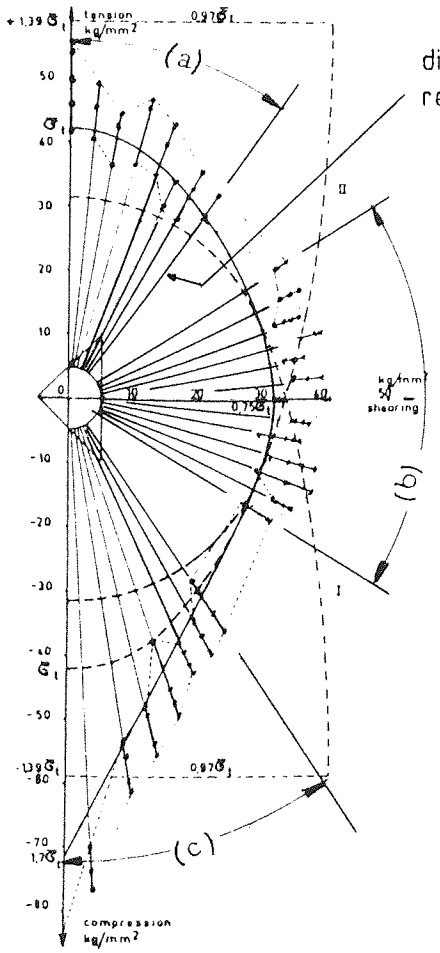

Fig.10 Vreedenburgh's Limit Curve

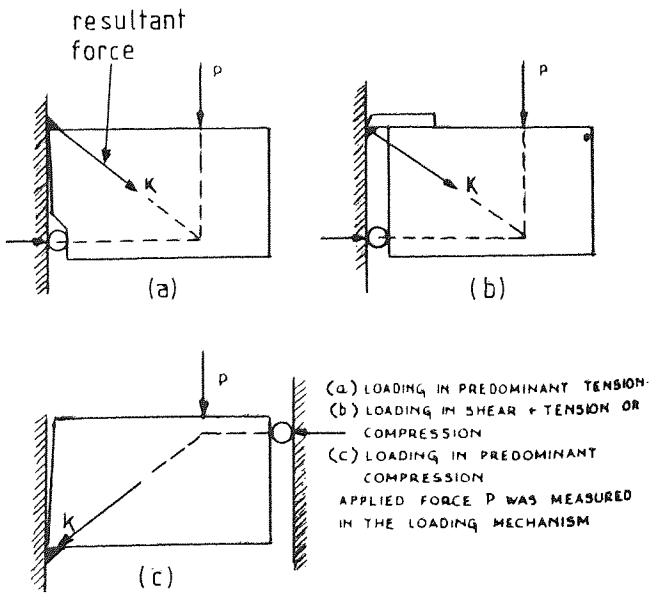

Fig.11 Styles of test specimens (a), (b) and (c).

It is possible that Vreedenburgh's limit curve has encouraged the belief that transverse welds in compression are significantly stronger than in tension. This belief is contrary to the findings of Bibber[1], and Schreiner[7].

It must be realized that Vreedenburgh used two styles of specimen for the tension/shear, and two for the compression/shear parts of the limit curve. There is no overlapping of his experimental results on the curve, in fact there are gaps as has already been mentioned. It is probably not possible to achieve overlapping, but is there any justification for assuming the three separate parts of the curve will meet with a smooth contour? The limit curve is made up of three sections, each section pertaining a different load configuration, and experimentally they do not join. The results of Vreedenburgh and Jensen[5] can be presented in another way as to give separate limit curves for each style of test specimen which will be independent of the critical plane which Vreedenburgh has chosen to be the throat knowing that it is not. This new presentation by the author is shown in fig. 12.

It is clear from both graphs that welds of specimens style (a) and (b) behave very differently with weld (a) being considerably stronger than weld (b) throughout the range of F_y/F_x plotted. Vreedenburgh's experimental results of style (c) seem to indicate a very large strength, but these results are probably erroneous as already indicated under criticisms of the limit curve. It would appear from this presentation of the results that there are different criteria for each style of test weld, and there is nothing to suggest these separate criteria will form one continuous criterion.

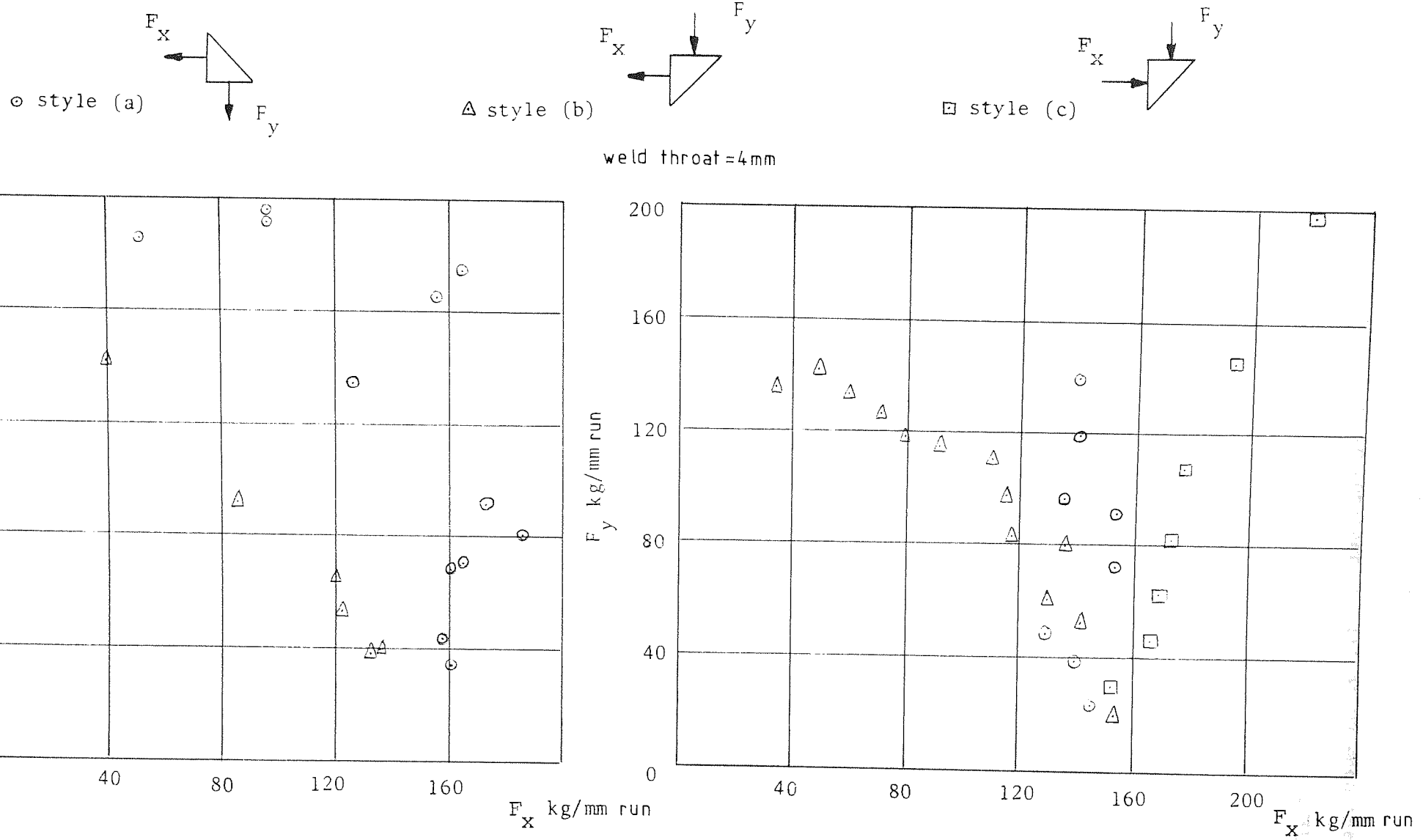

(a) Experimental results by Jensen[5].

(b) Experimental results by Vreedenburgh

Fig.12 Relationship between F_x and F_y

Vreedenburgh then goes on to consider the situation when the load is not at right-angles to the length of the weld and concludes there will be two shear stresses acting on the throat, i.e. parallel, and normal to the longitudinal axis. The resultant of these two shear stresses is to be used when considering the limit curve as a criterion.

Archer et al[19] in 1959 conducted 24 tests to destruction, of column brackets with longitudinal welds at small load eccentricities, see fig.13. They made reference to the tests of Schreiner[7], pointing out that the eccentricities involved in his tests were comparatively large and his findings were therefore not applicable to short column-brackets with small load eccentricities. Archer's test welds were of a nominal 0.21 inch leg, and varying lengths of from 3 to 4.25 inch. Load eccentricities ranged from 4.06 to 0.25 inch.

The width of the fracture plane was measured after testing, and it was noted the critical plane was always at an angle less than 45°, and further noted that the angle decreased with increase in eccentricity. However, all stress calculations have been based on the throat size.

The current vector method was considered and found to give safety factors of between 3.6 and 7.6 . Archer et al pointed to the variability of the safety factor produced and suggested a more rational method would save the unnecessary waste of weld metal and cost of fabrication.

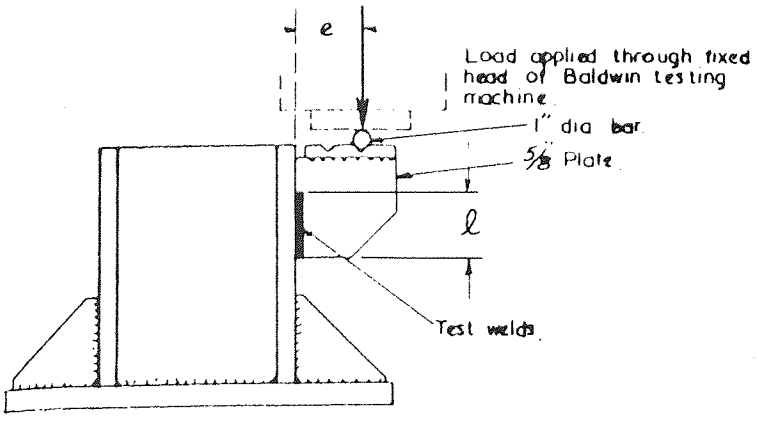

Fig.13 Column Bracket

They proposed the following empirical maximum shear stress criterion:

$$\text{maximum shear stress} = \frac{1}{2}\sqrt{0.7\sigma_b^2 + 4\tau^2}$$

where

σ_b = normal stress due to bending at extreme fibre

τ = shear stress due to vertical shear load

The empirical constant of 0.7 in the above equation is based on the belief the stress distribution caused by bending lies inbetween the triangular and rectangular blocks when the weld is in a plastic state prior to failure.

The above criterion is one of maximum shear stress and is based upon their experimental results for which the range of e/ℓ is 0 to 1.3, but they suggested the criterion was applicable to joints with any load eccentricity.

Their calculated maximum shear stress ranges from 43000 to 57000 lbf/in^2, with a quoted average value of 51000 lbf/in^2, but no comparison was made with the ultimate shear stress of 56600 lbf/in^2 which was obtained from control tests on side fillet welds.

The effect of plate-bearing was noticed since it was reported that in ten of the tests the welds did not extend to the bottom of the bracket and in three of those cases the appearance of the plate after failure indicated there had been bearing between the plate and the column below the level of the weld. It was stated this could have resulted in the weld carrying a greater moment.

2.4 The first investigative study of the ultimate strength of beam-column connections was made by Ligtenberg[20], in 1959. He reported on a series

of tests on connections in which flange and web welds were working in collaboration, see fig. 14. Uhler and Jensen[2], 1930 and Johnston and Deits[14], 1942 had reported limited tests but not of connections with both flange and web welds, and their main interest had not been in the ultimate capacity of the weld.

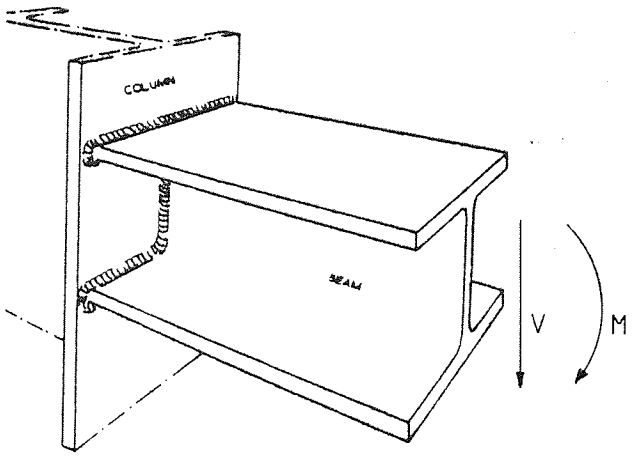

Fig.14 Beam-column Connection

Ligtenberg referred to previous studies of the strength of single fillet welds by W.J.v.d Eb who proposed the criterion

$$\sigma_c = \sqrt{\sigma_1^2 + 1.8(\tau_1^2 + \tau_{11}^2)}$$

in which σ_c was a critical stress in the order of 4000 to 5000 kg/cm^2; σ_1, τ_1 and τ_{11} were normal and shear stresses acting on the throat section, see fig. 15. This criterion was adopted by Commission XV of the I.I.W. in 1961.

Ligtenberg suggested that the important criterion for a group of welds working together was deformation since individual welds would be subjected to differing amounts of deformation. Further, welds with a predominantly tensile stress at the critical plane were brittle compared with those which were predominantly in shear on the critical plane. He pointed out that little was known with regard to these load-deformation characteristics and that such characteristics were difficult to determine accurately because of large deformations in the base material near the weld. However, he did present estimated load-deformation

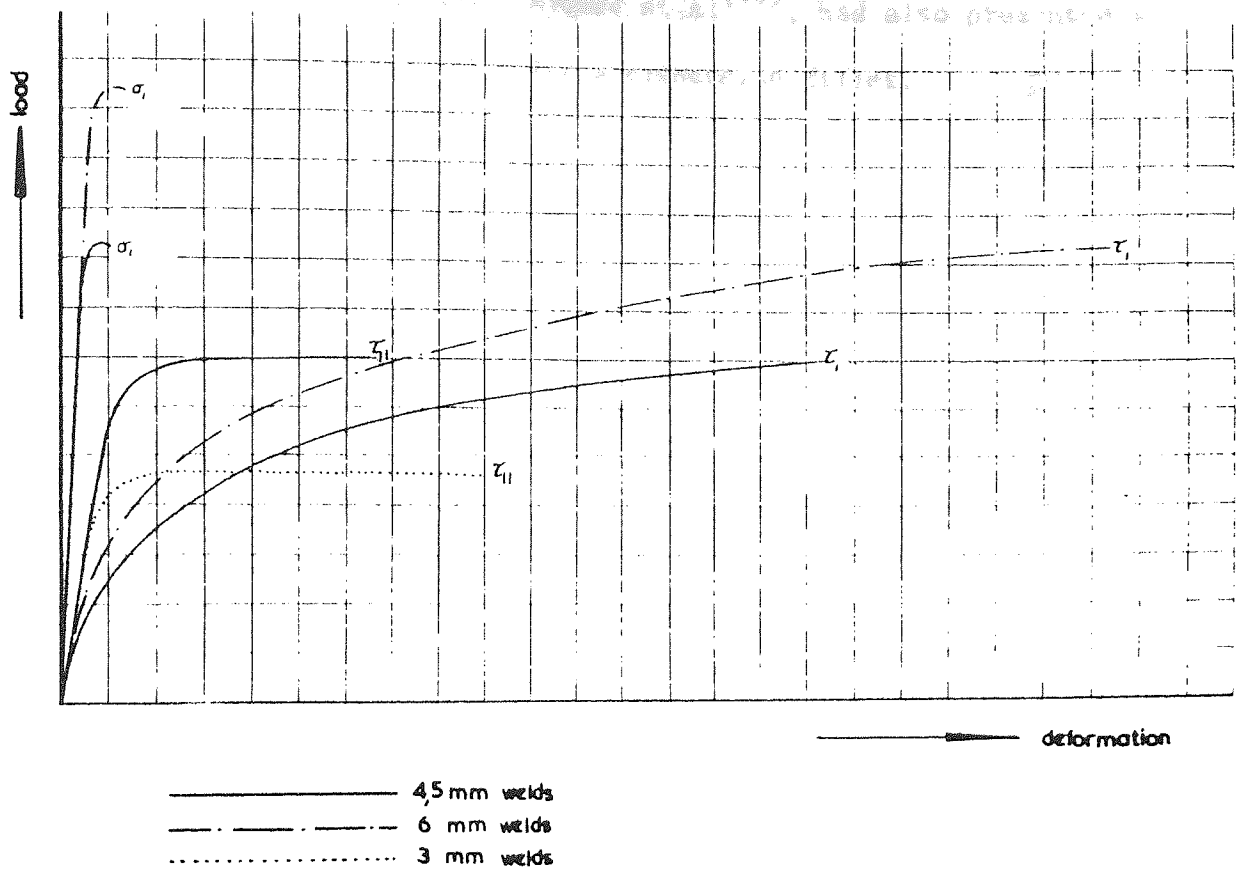

Fig.16 Estimated Deformation Characteristics

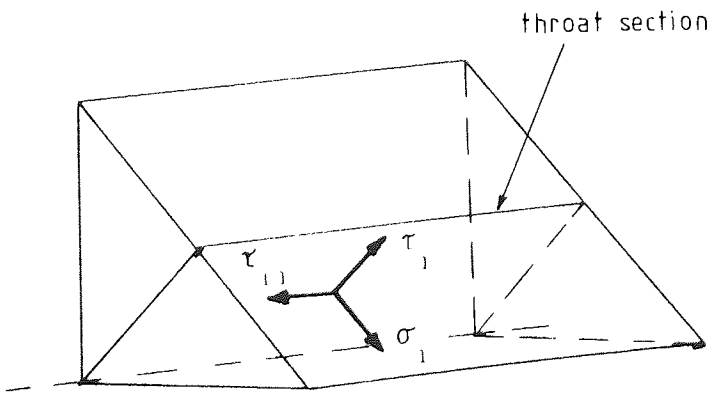

Fig. 15 Stress Notations

characteristics, see fig. 16. Archer et al[19], had also presented a load deformation characteristic for a transverse fillet.

Ligtenberg decided the most important variables with regard to stress distribution in the weld group were,

(i) the flange width - flange deformation would control the shear force distribution along the flange.

He tested two flange widths 119 mm and 200 mm.

(ii) weld size - ideally everywhere weld thickness should be compatible with profile thickness.

He tested two series (i) flange welds 6 mm, web 3 mm.

(ii) flange and web 4.5 mm.

(iii) column rigidity - this would influence the stress distribution.

He tested a "rigid" column, and a "ductile" column.

(iv) load eccentricity,

ranged from $\frac{e}{d} = \infty$ to $\frac{e}{d} = 0.54$

Using these four variables Lightenberg made 24 tests on all round welded specimens, as fig. 14, before going on to look at web and flange welds in isolation. He then proposed a theory based on the criterion of $\sigma_c = \sqrt{\sigma_1^2 + 1.8(\tau_1^2 + \tau_{11}^2)}$, but pointed out the following:

(i) there was no certainty that any of the welds would be loaded uniformly over their whole length,

(ii) forces might have been transmitted by plate-bearing,

(iii) the first weld to break would be the flange weld under tension,.

The assumption made for the theory:

(i) full plasticity at time of failure for all welds,

(ii) neutral axis at half beam-height,

(iii) uniform shear load sharing between all of the welds;
(iv) corresponding welds above and below the neutral axis had equal strengths;
(v) welds on either side of the flange had equal strengths,
(vi) critical plane was always at the throat for all welds,
(vii) rectangular bending stress distribution for the web welds,
(viii) the combined strength was equal to the summation of the strengths of the individual welds

Twelve tests were then conducted with only outside flange welds present. Four of these tests were done under pure bending from which he established a value of the critical stress σ_c at 4150 kg/cm^2. The other eight tests were done with bending and shear, and for these, it was assumed the shear load to be shared equally between the two welds.

For the 119 mm flange tests Lightenberg found the actual ultimate capacity to be well in excess of his prediction. He attributed this increased strength to the supposed greater strength of welds under compression as indicated by the limit curve of Vreedenberg[16].
Lightenberg stated that this limit curve showed that under pure compression, the weld was approximately 1.6 x the strength under pure tension.

The author has already shown the doubt concerning this limit curve.

Ligtenberg naturally assumed that his logic could be applied to the 200 mm flange specimens but found the actual strength to be only a half of the computed strength - he concluded that for wide flanges only half the flange width was effective in shear.

A further six tests were conducted with a combination of inner flange welds and web welds. He found that in pure bending, the observed strength

was greater than the computed, this he attributed to plate-bearing. The observed shear strength was again well below his expectation and he suggested that only the web welds were effective in resisting shear, whereas all the welds resisted bending.

Ligtenberg then considered the results from his main test series of twenty-four tests of all round welded specimens. He subtracted the actual strength of the flange outer welds from the total strength to give the actual strength of the weld group, the flange inner welds and the web welds. This strength bore no comparison with his theoretical predictions except for the condition of pure bending. For other conditions, actual strengths were well below predicted strengths. This led Lightenberg to suggest the connection broke down readily if the web welds carried a shear load corresponding to only $\frac{1}{2}$ to $\frac{1}{3}$ of their theoretical shear capacity.

Ligtenberg summarized his theory as follows:

Weld group (a), flange outer welds only;

(i) both welds load uniformly by bending moment

(ii) shear load was uniform for the narrow flange, i.e.119 mm

(iii) only $\frac{1}{2}$ x flange width is effective in resisting shear for the wide flange, i.e. 200 mm.

Weld group (b), flange inner welds + web welds;

(iv) all welds were fully plastic under pure bending

(v) shear forces were taken only by web welds, but only $\frac{1}{2}$ x theoretical strength if the weld thicknesses were adapted to the profile thickness, and $\frac{1}{3}$ if this was not the case.

Weld group (c), all round welded;

(vi) load proportioning was as follows

$$\frac{M_a}{P_{sa}} = \frac{M_b}{P_{sb}} = \frac{M}{P_s}$$

M_a = moment resistance of group (a) welds

M_b = " " " " (b) "

M = applied bending moment

P_{sa} = shear resistance of group (a) welds

P_{sb} = shear " " " (b) "

P_s = applied shear load.

Ligtenberg claimed his theory was a good fit with his results. It must be pointed out here that his range of results is very limited, i.e. the ratio of e/d had only three values, 0.54, 1.7 and ∞. For e/d = ∞ ultimate capacity of the connection is relatively easy to predict, which leaves only two values of e/d to verify his theory. He did not refer to the extent of his theory, but it can only be regarded as being applicable to his range of tests which are very limited. He did admit that what he had referred to as "theory" was in fact nothing more than a description of observed phenomena. He concluded that the elastic theory of beams was quite insufficient and suggested the key to the working of welds in combination lay in the weld load-deformation patterns.

2.5 Commission XV of the International Institute of Welding published a major report[21] in 1964, presenting the views and ideas of member countries regarding design methods for welded connections. The report puts forward calculation formulae for welded connections subject to static loads. All the formulae were based upon the failure criterion proposed by W.J.v.d.Eb see ref.(16).

$$\sigma_c = \sqrt{\sigma_1^2 + 1.8(\tau_1^2 + \tau_{11}^2)}$$

which was approved at the *I.S.O/T.C.44 meeting in Helsinki in 1961.

* I.S.O. International Standards Organization.

For this criterion the weld throat was assumed to be the critical plane. Uniform stress distribution was assumed, and residual stresses were ignored. For the prediction of safe working loads σ_c was related to σ_p, strength of the parent metal.

With reference to beam-column connections under combined bending and shear, for web welded connections, fig. 17, with plate bearing, it was suggested that rotation took place about the bottom end of the weld, and that stresses due to bending would be only tensile and of a triangular distribution being a maximum at the top of the weld. This is the first time that rotation is not assumed to be about a neutral axis passing through the weld centroid. The shear stress distribution was assumed to be uniform along the full length of the weld.

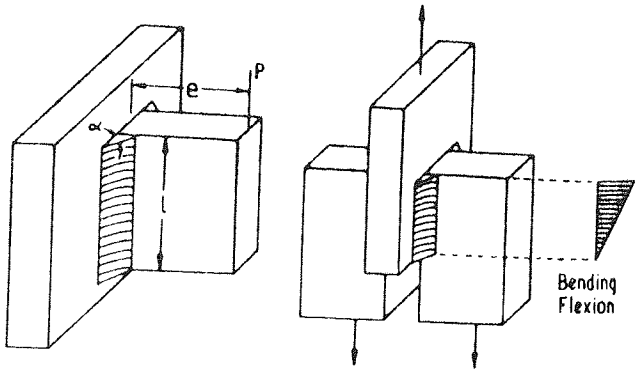

Fig.17 Web-welded Connections

For the flange welded connection, fig. 18, it was assumed rotation took place about the compression weld, i.e. only the tension weld resisted the applied bending moment.

It was recommended that this type of connection was unsuitable to withstand high shear values. Presumably this is because of the limited deformation of these transverse welds.

In the case of the combination of web and flange welds it was suggested that shear was resisted only by the web welds, whereas all welds resisted

the bending moment. This is rather an over-simplification of reality and is bound to lead to a conservative estimation of joint capacity.

The method of calculation proposed by the I.I.W. can be criticised on the following grounds:

1. the throat is assumed to be the critical plane whereas in all probability, the actual plane is variable, and by using a fixed plane of minimum area unknown safety factors will be involved.
2. bending stresses are of triangular distribution, but at failure it is probable full or partial plasticity pertains.
3. welds in compression are treated the same as those in tension - compression welds in fact may be weaker.
4. bound to be unnecessarily conservative.

2.6 An extensive study of theoretical limiting stress criteria based on Principal Stress was made in 1964 by Archer et al[22]. Their report presents a detailed analytical study of the strength of short fillet welds subjected to a single load applied perpendicularly to the longitudinal axis of the weld. They considered seven different strength theories and compared these with the experimental results produced by Jensen[5], in 1934. A failure criterion was selected and then used to estimate the ultimate capacity of flange, and web welded connections as shown in figs. 13 and 18.

Archer et al reviewed the contemporary methods of strength prediction proposed by Bibber[1], Jensen[5], Jennings[8], and the current vector addition method, BS449[6], which appears to have been in use since the inception of welding and was adopted directly from rivet design practice.

All these methods are based upon the assumption that the throat is always the critical section.
It has been reported to the contrary by Jensen[5], Vreedenberg[16], and Archer et al[19], but no theoretical corollary has been proposed until now.

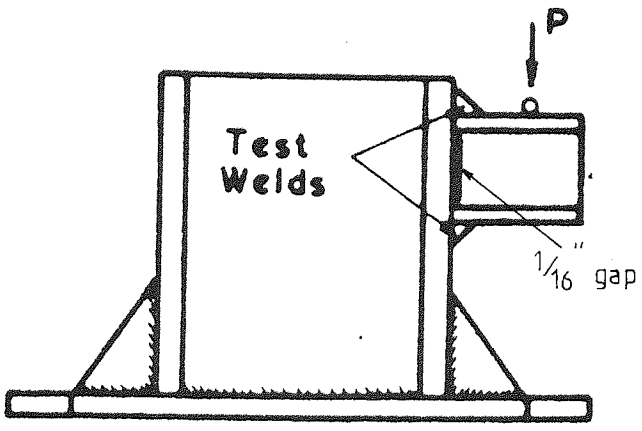

Fig.18 Flange-welded Connection

Archer et al considered the welds of the test specimens used by Jensen[5], as shown in fig.3, and for specimen B, proposed the following analysis.

Equilibrium force system, fig. 19, assuming the forces acting on the weld legs are uniformly distributed and $M = (F_x - F_y)t/4$.

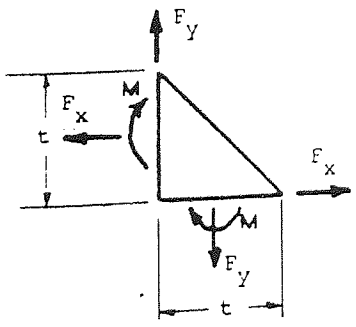

Fig.19 Equilibrium Force System.

Archer et al are the first investigators to take account of couples produced by load eccentricities.
Forces and moments are then referred to a critical plane BC as shown in the free-body diagram, fig. 20.

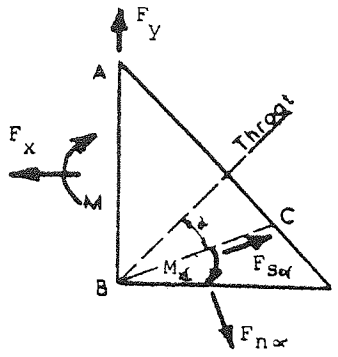

Fig.20 Free Body Diagram

For equilibrium, the tangential force on BC is,

$$F_{s\alpha} = F_x\cos(45-\alpha) - F_y \sin(45-\alpha).$$

and the normal force on BC is

$$F_{n\alpha} = F_x \sin(45-\alpha) + F_y \cos(45-\alpha)$$

and the moment on BC is,

$$M_\alpha = F_x \cdot \frac{t}{2} - F_{n\alpha} t \frac{\sqrt{2}}{4} \sec\alpha - M$$

The weld of specimen A, fig. 3, is treated in a similar manner. It is then assumed the stress distribution on the critical plane BC is uniform at the point of failure. The shear stress on the critical plane then becomes,

$$\tau_\alpha = \frac{\sqrt{2}}{t} F_{s\alpha}\cos\alpha$$

and normal stress produced by the normal force, $F_{n\alpha}$

$$\sigma_{n\alpha} = \frac{\sqrt{2}}{t} F_{n\alpha}\cos\alpha$$

and normal stress produced by the moment M_α

$$\sigma_{b\alpha} = \pm 12 M_\alpha \cos^2\alpha/t^2$$

for a triangular stress distribution, and

$$\sigma_{b\alpha} = \pm 8 M_\alpha \cos^2\alpha/t^2$$

for a rectangular stress distribution.

Then, maximum normal stress becomes

$$\sigma_\alpha = \sigma_{n\alpha} + \sigma_{b\alpha}$$

Then, using Principal Stress theory,

$$\text{maximum shear stress} = \frac{1}{2}\sqrt{\sigma_\alpha^2 + 4\tau_\alpha^2}$$

$$\text{maximum principal stress} = \frac{\sigma_\alpha}{2} \pm \frac{1}{2}\sqrt{\sigma_\alpha^2 + 4\tau_\alpha^2}$$

and, the octohedral stress is proportional to

$$\sqrt{\sigma_\alpha^2 + 3\tau_\alpha^2}$$

It is then suggested that the position of the critical plane would be determined when the above stress criteria were a maximum.

Seven limiting criteria were considered:

1. Maximum Shear Stress (M_α Neglected)
2. Principal Stress (M_α Neglected)
3. Maximum Shear Stress (triangular stress block due to M_α included)
4. Principal Stress (triangular stress block due to M_α included)
5. Maximum Shear Stress (rectangular stress block due to M_α included)
6. Principal Stress (rectangular stress block due to M_α included)
7. The Stress $\sqrt{\sigma^2 + 3\tau_\alpha^2}$ (rectangular stress block due to M_α included)

and are represented, along with the *I.S.O.[17] and *S.A.A. criteria, as limit curves for welds type A and B, see figs. 21, 22, 23 and 24.

Note: the I.S.O. criterion has been applied using Archer's theoretical angles and not the usual throat.

---

* I.S.O. International Standards Organization

* S.A.A. Standards Association of Australia.

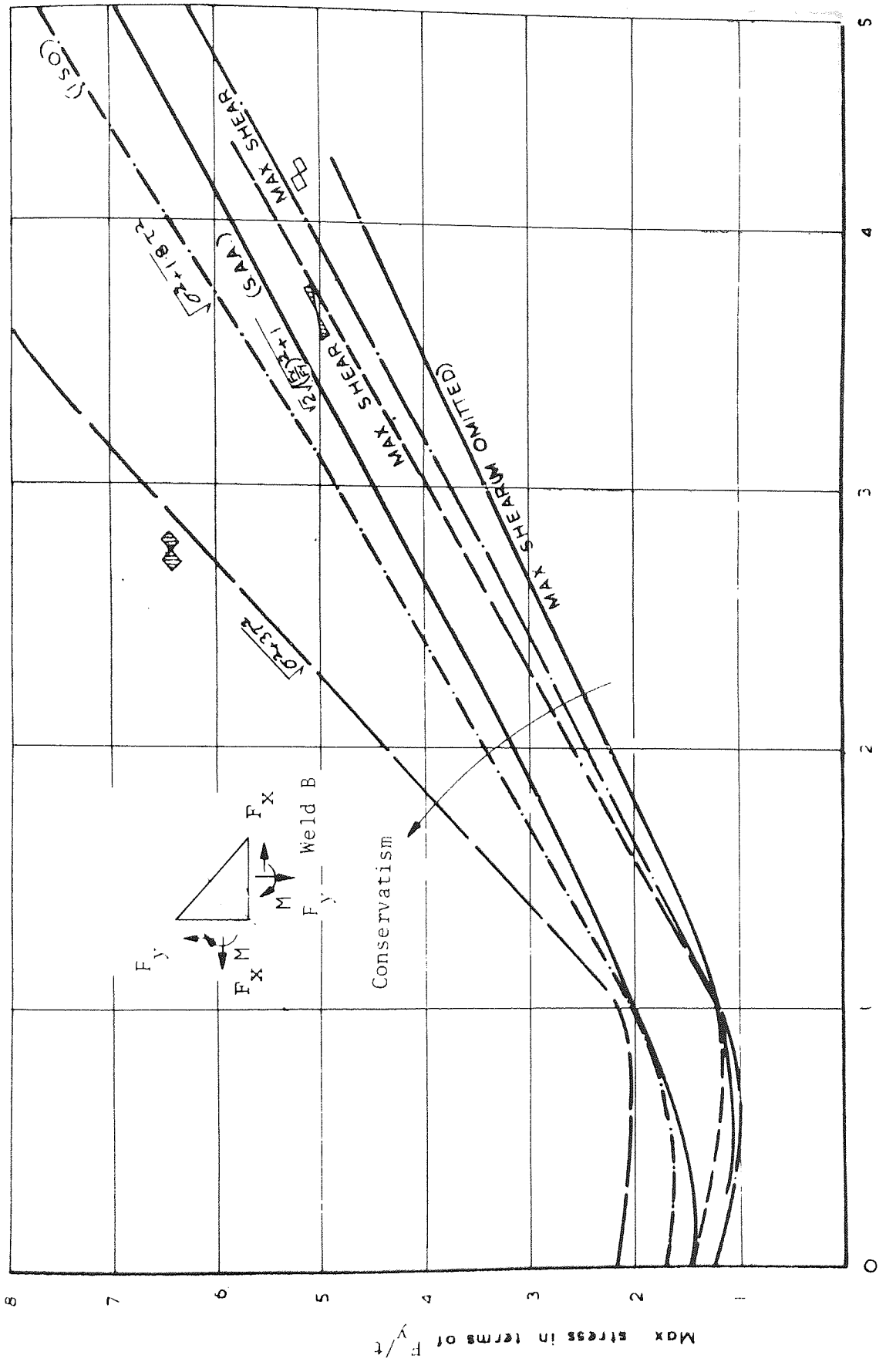

Fig.21 Relationship between (F_y/t) and (F_x/F_y)

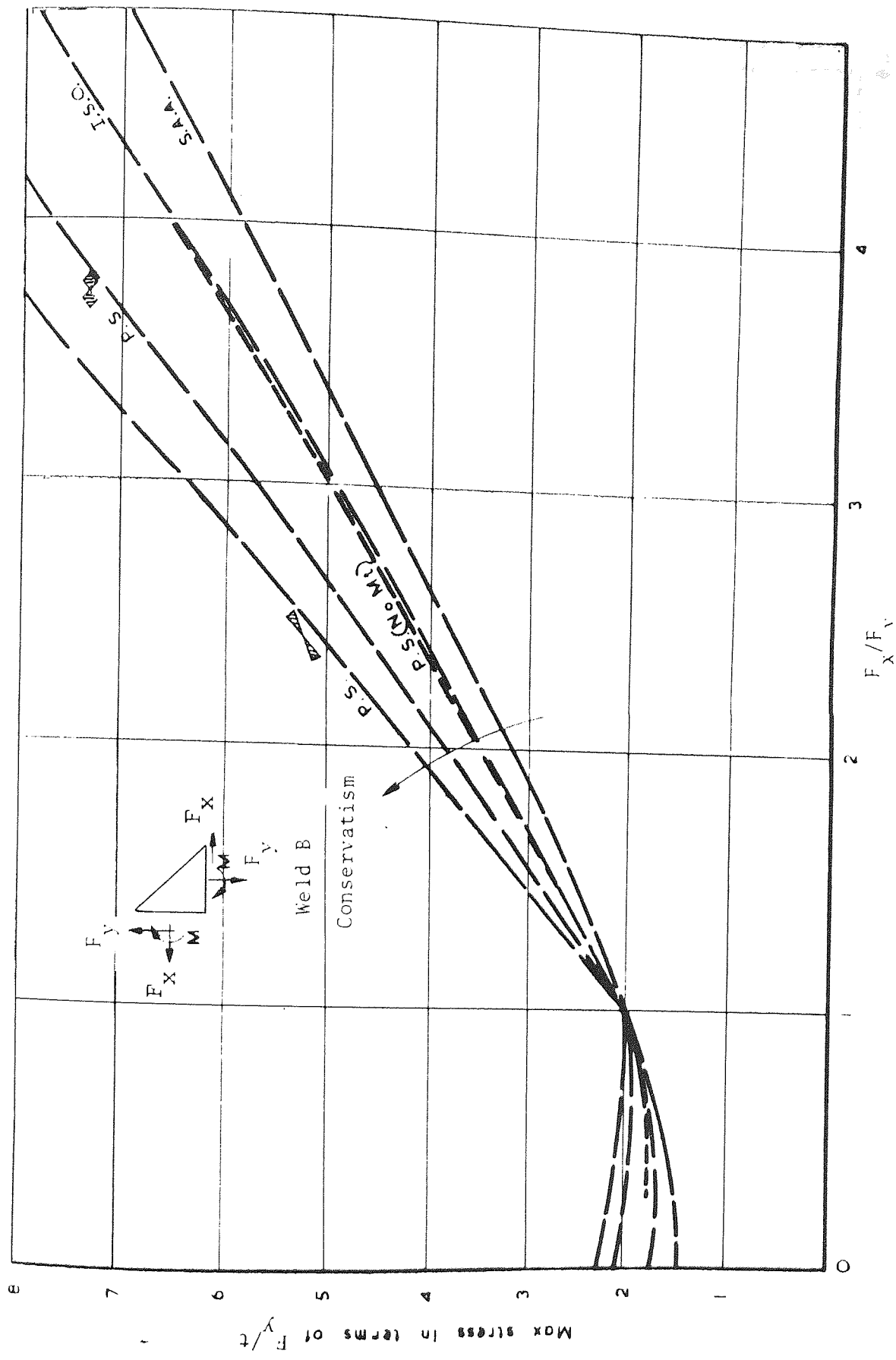

Fig.22 Relationship between (F_y/t) and (F_x/F_y)

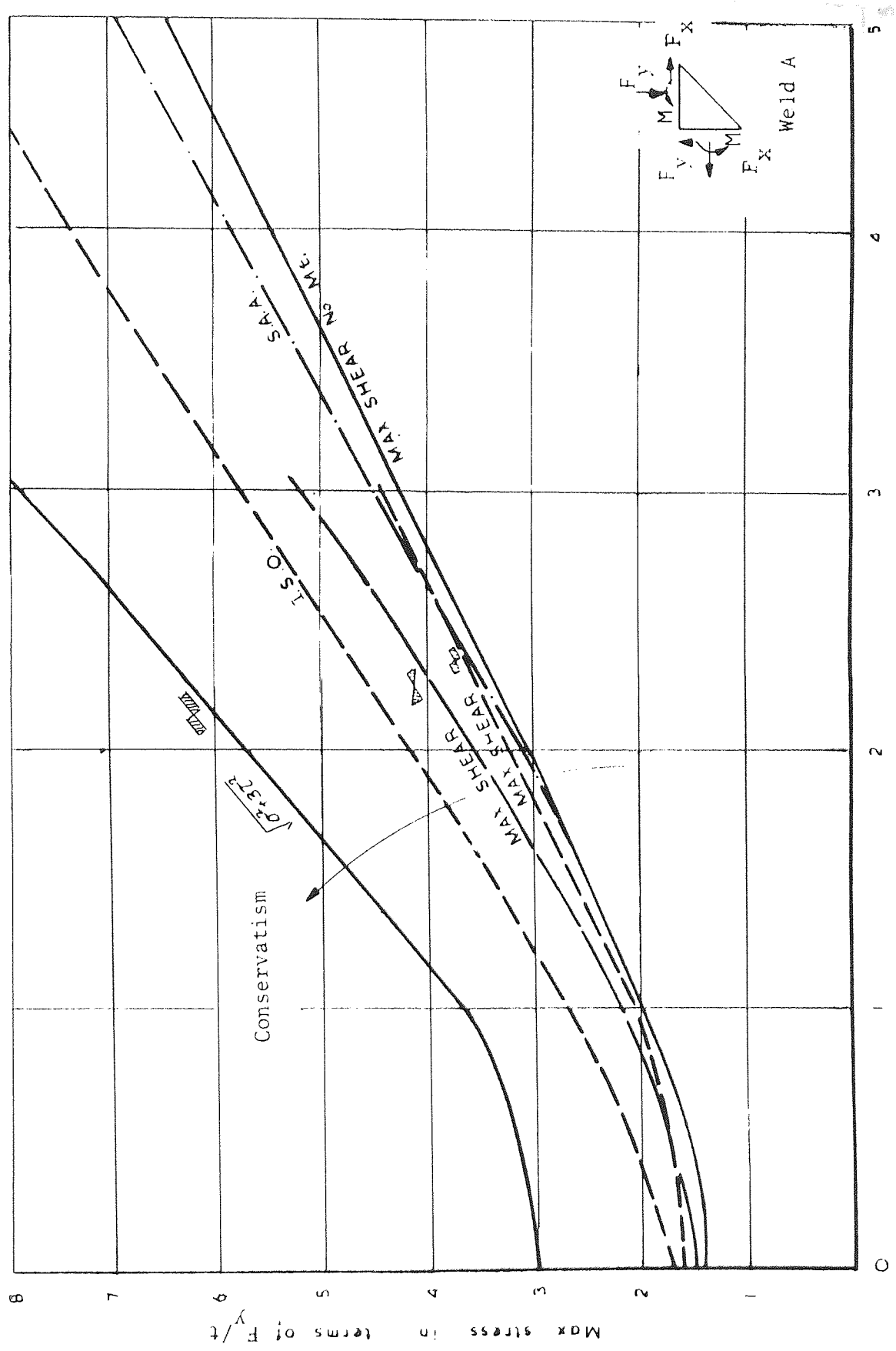

Fig.23 Relationship between (F_y/t) and (F_x/F_y)

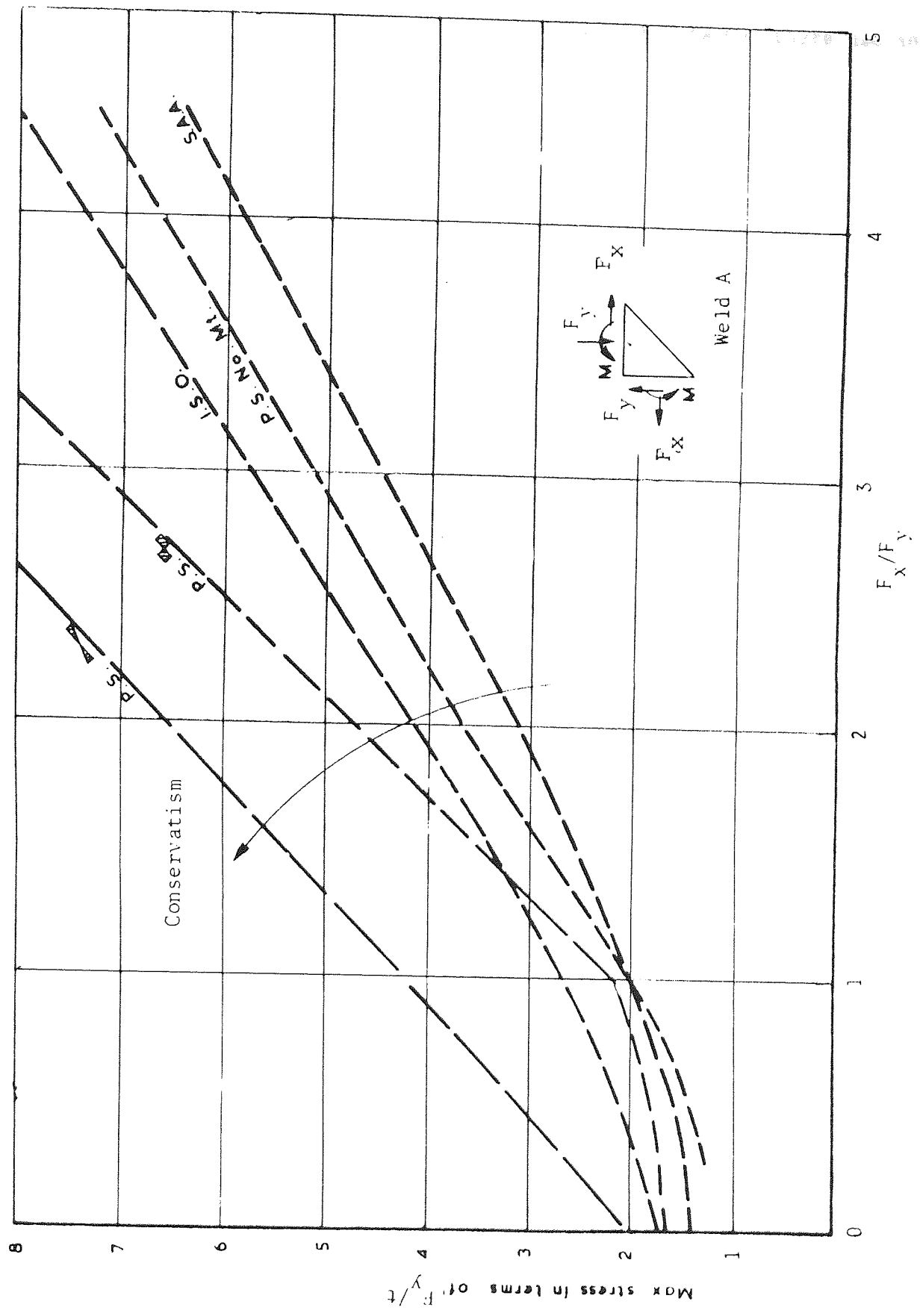

Fig.24 Relationship between (F_y/t) and (F_x/F_y)

Archer et al did not comment on these criteria but there are some points of interest:

1. for both welds the maximum shear (M omitted) criterion predicts the greatest strength,
2. the principal stress (triangular bending stress distribution) criterion predicts the lowest strength,
3. predicted strength of weld B (in tension) is much greater than that of weld A (in compression). This agrees with the results of Jensen[5] and Vreedenberg[16] as presented by the author on page 22,
4. there is very little difference in the predictions of the criteria of maximum shear (M omitted), and maximum shear (rectangular distribution). This would suggest that the unbalanced couple due to load eccentricity can be ignored.

Theoretical predictions of the seven criteria were then compared with Jensen's[5] results of 1934, and shown in figs. 25 and 26. Archer et al pointed out for the weld in tension B, the criterion of maximum shear stress with a rectangular stress block fitted the results exceptionally well, although the maximum shear (moment omitted) fitted almost as well. For the weld in compression A the maximum shear (moment omitted) fitted very well but, the maximum shear with rectangular stress block was a little conservative. Archer et al concluded that generally the maximum shear stress (moment ignored) criterion appeared to suit both types of loading situations over the full range of values of F_x/F_y.

They showed surprise that the actual weld strength was much greater than that predicted by the principal stress criteria. This is surprising since both welds A and B are predominantly in shear on the critical plane and therefore one would expect a shear criterion to be more pertinent than

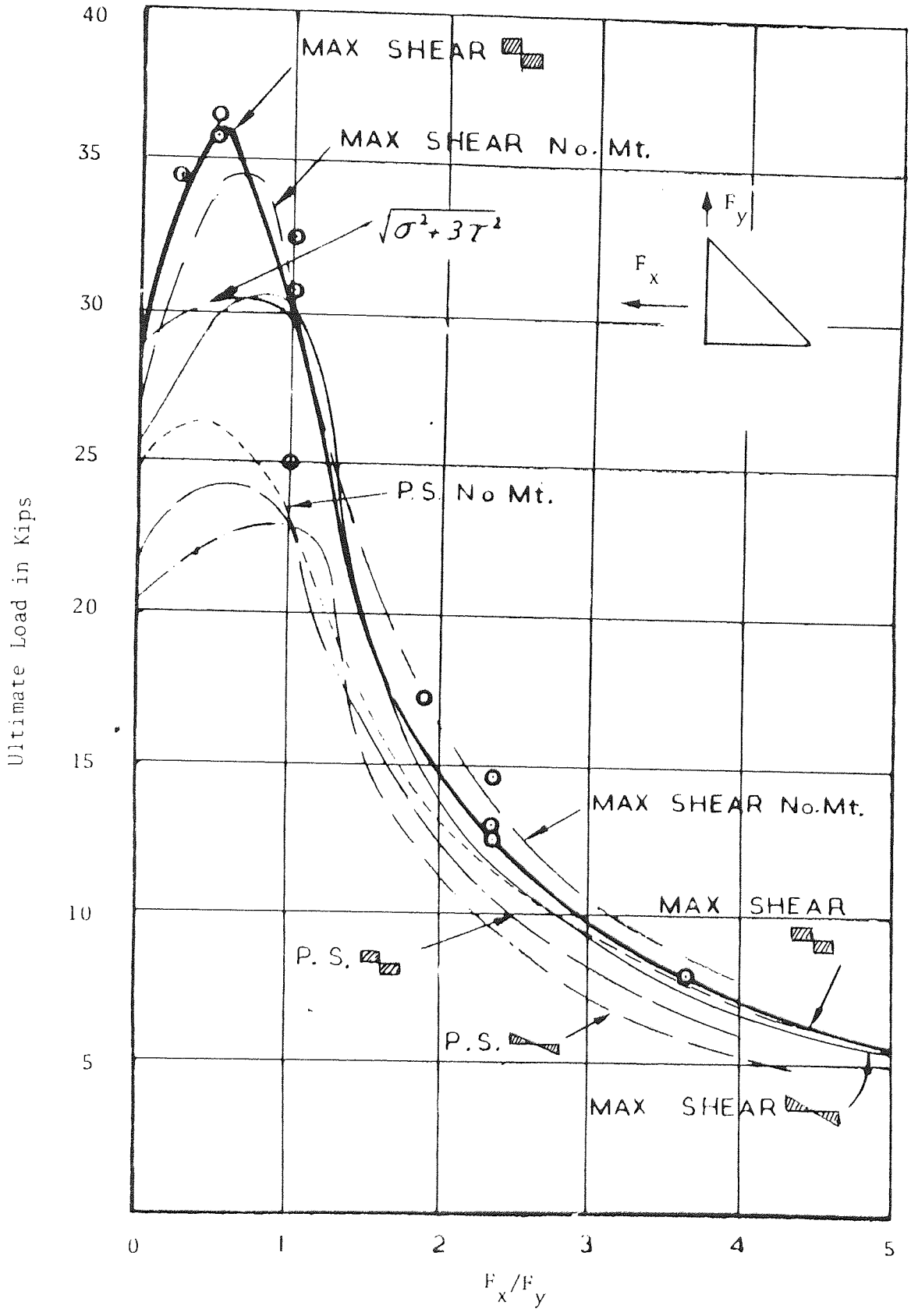

Fig.25 Relationship between Ultimate Load and (F_x/F_y)

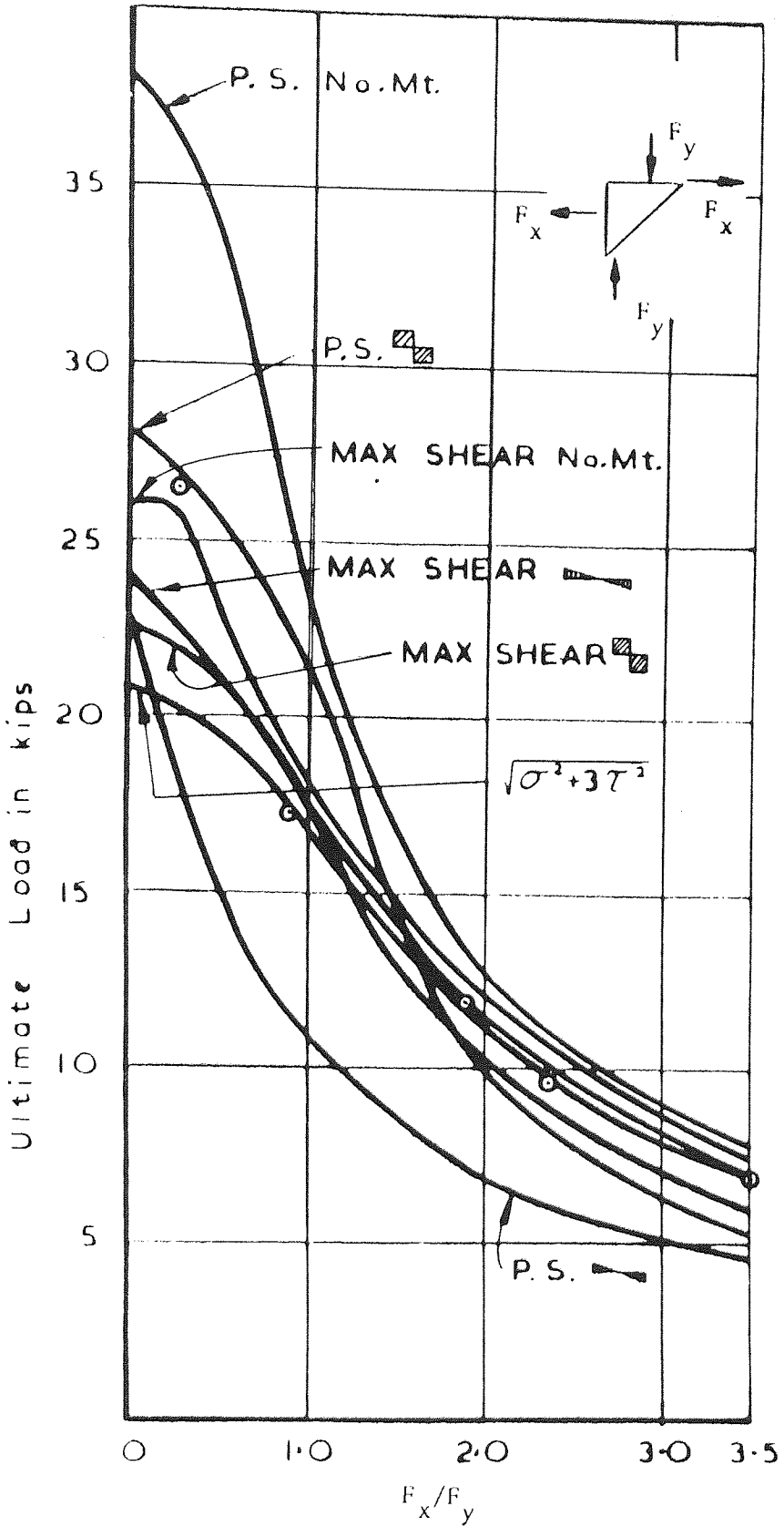

Fig.26 Relationship between Ultimate Load and (F_x/F_y)

a principal stress criterion. It must be admitted for ratios of F_x/F_y around unity, weld B would be under tension on the critical plane.

Archer et al criticised their proposed theory on the grounds that the required iterative calculations were tedious. They referred to Vreedenbergh's[16] limit curve and compared the I.S.O. criterion with it and concluded the I.S.O. criterion was well suited to design purposes on account of its simplicity, even though its predictions were rather conservative.

They then went on to study beam-to-column connections under combined bending and shear of the types shown in figs. 13 and 18. Thirty-eight tests were conducted on flange-welded (flange outer welds only) connections, the welds being 2 inch nominal length and 0.25 nominal leg length. Twenty-eight of the specimens were of depth 6 inch and the remainder were of depth 4 inch. The specimens were made up with a gap of approximately 1/16 inch between the web and column, and the ratio of e/d ranged from 0.17 to 1.5.

Some criticisms must be made here regarding the quality of the test specimens:

1. there were no run-on and run-off tags for the test welds - weld end effects of stop and start can be significant especially in short welds,
2. pairs of welds were not of equal lengths, and lengths ranged from 2.00 to 2.5 inch,
3. pairs of welds were not of equal leg length, leg lengths ranged from o.188 to 0.292 inch.

It is hardly surprising there is a great deal of scatter in the experimental results of these specimens, see fig. 27.

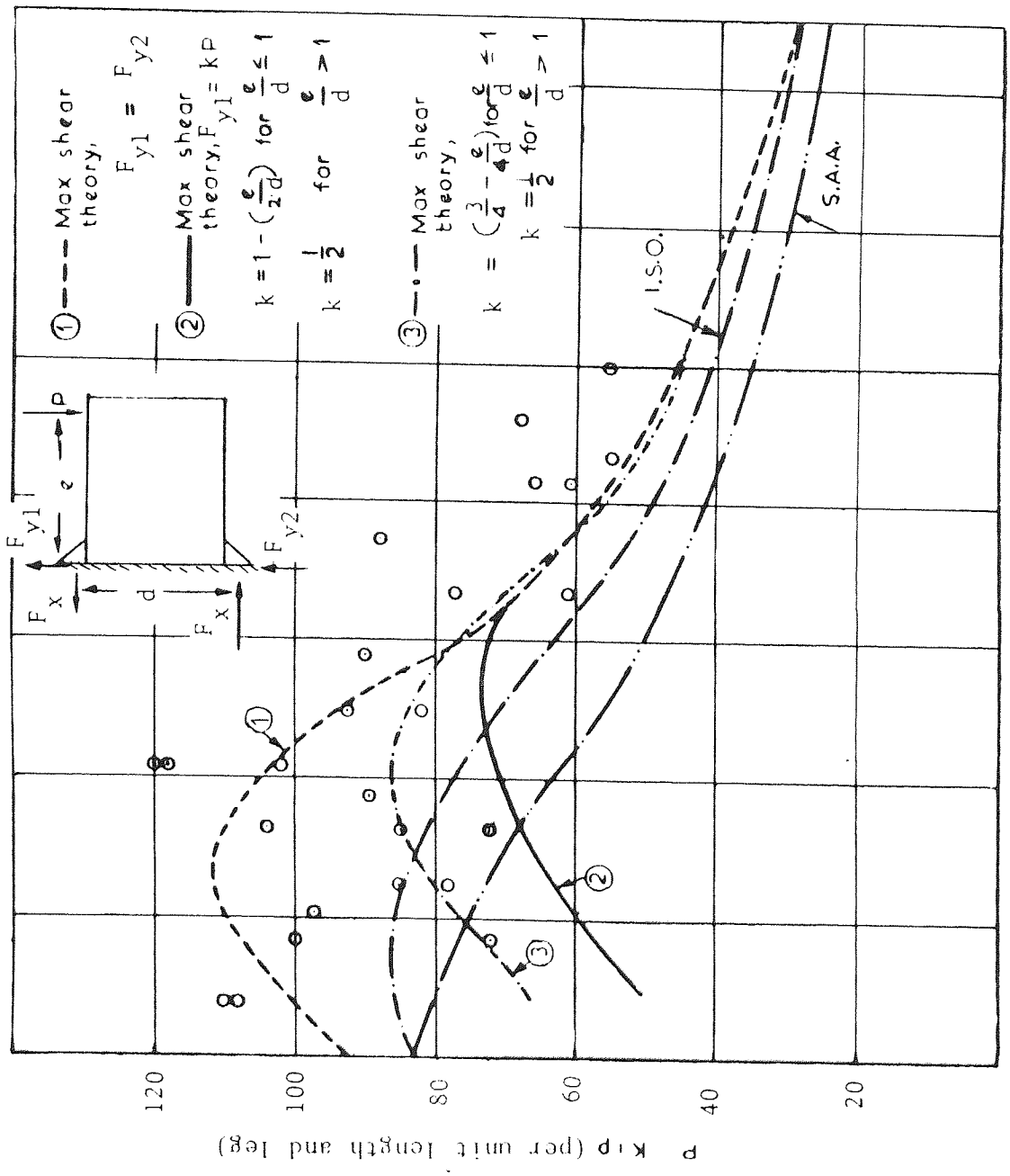

Fig.27 Relationship between Ultimate Load and (e/d)

It was stated rupture was always initiated in the tension weld, so their ultimate load calculations were done considering the tension weld only.

Archer et al used their failure criterion of maximum shear stress with rectangular stress block for weld B, and assumed rotation about an axis at mid-depth of section. The bearing between the bottom flange and the column had been ignored completely. They selected three arbitary relationships regarding the sharing of the vertical shear load between the two welds. The resulting strength predictions are shown in fig.27 in comparison with their experimental results. They did point out the distribution of the total shear force would depend upon the relative stiffness of the connection and the welds - the greater the flexibility the greater the proportion of the shear load would be carried by the top weld, i.e. the weld under tension.

It is difficult to draw any meaningful conclusions from fig.27, and in fact Archer et al erred on the safe side by suggesting theory (3) could be employed to produce an interaction diagram to be used as a design graph, see fig. 28. From this graph the ultimate load may be read for any value of e/d, the working load then obtained by dividing by a suitable load factor.

This design graph deserves merit for two important reasons:

1. it is a limit state parameter and hence a known safety factor can be employed, and

2. it is based upon the actual failure plane (a theoretical actual) and not the arbitarily chosen throat.

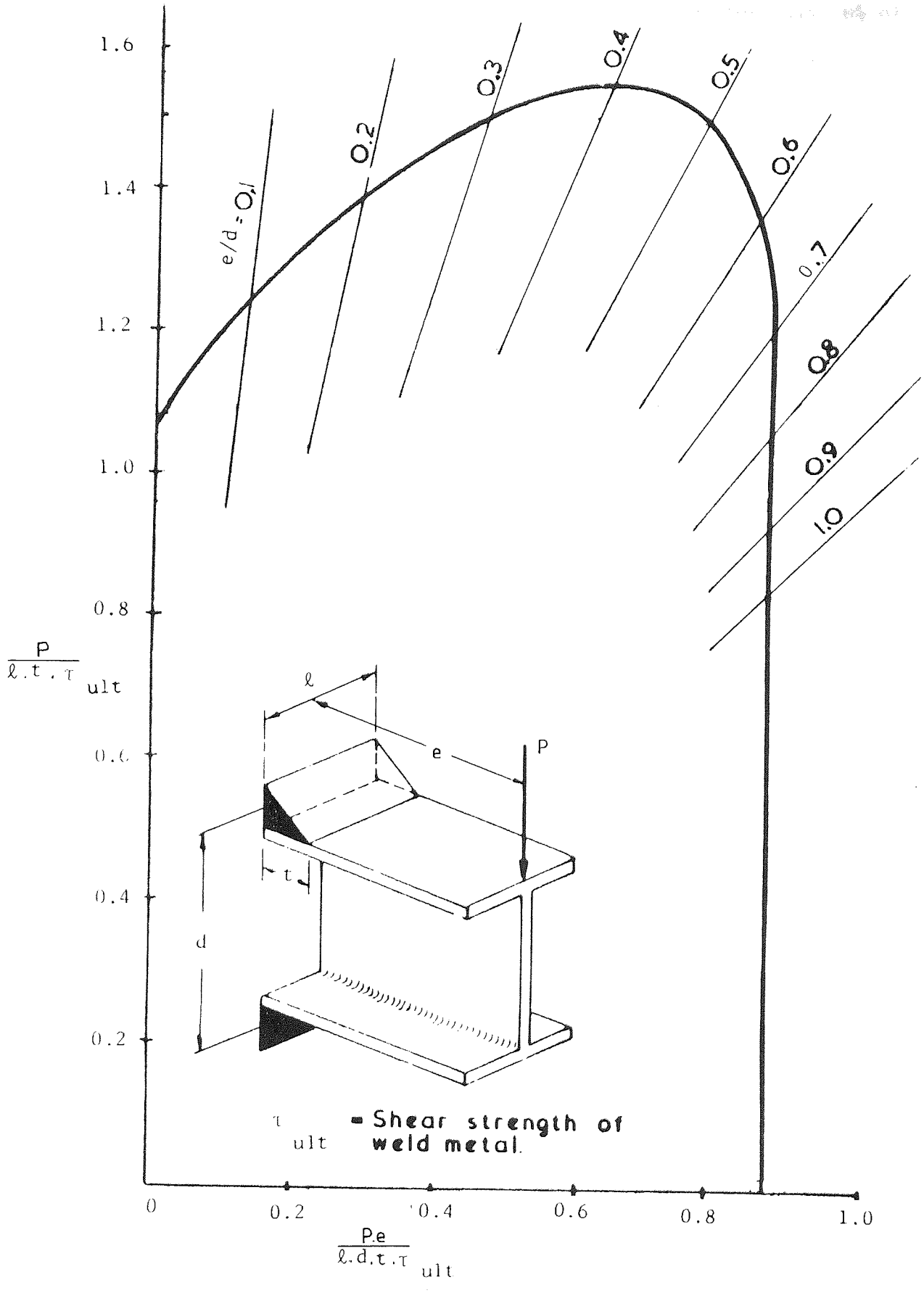

Fig.28 Design Graph for Beam-Column Connection

Archer did make some attempt to assess the position of the actual failure plane, and quoted angles to the nearest 5° but for only 50% of the tests. It is surprising that he made no attempt to compare these actual with his theoretical positions of the critical plane.

Archer et al then went on to consider a connection with web welds only, see fig. 13, which had been tested by Archer et al[19] in 1959. Twenty-one tests were conducted at that time with various lengths of welds in various positions on the web-plate. Weld length, including stops and starts, varied from 3.00 to 4.00 inch; leg length from 0.198 to 0.233 inch and load eccentricity from 0.25 to 4.06 inch. All these results have been grouped together and are represented in fig.29 as a nominal stress $P/\ell.t$.

Since the maximum shear stress criterion was so successful for the flange welded connections (at least, it was for Jensen's[5] results), they decided to apply it to the longitudinal web welds, arguing that a web weld under combined bending and shear was basically a flange weld with a longitudinal shear stress imposed upon it.

For the theoretical analysis, the following was assumed:

1. the neutral axis passed through the weld centroid; logically, considering the physical constraints imposed upon the connection, rotation is very unlikely to be about the assumed neutral axis, and the I.I.W.[21] did suggest rotation about the end of the weld,
2. weld above and below the neutral axis behaved in an identical manner,
3. entire length of weld was plastic at failure.
4. the normal force on the weld leg produced by the applied bending moment was uniformly distributed along the length of the weld,

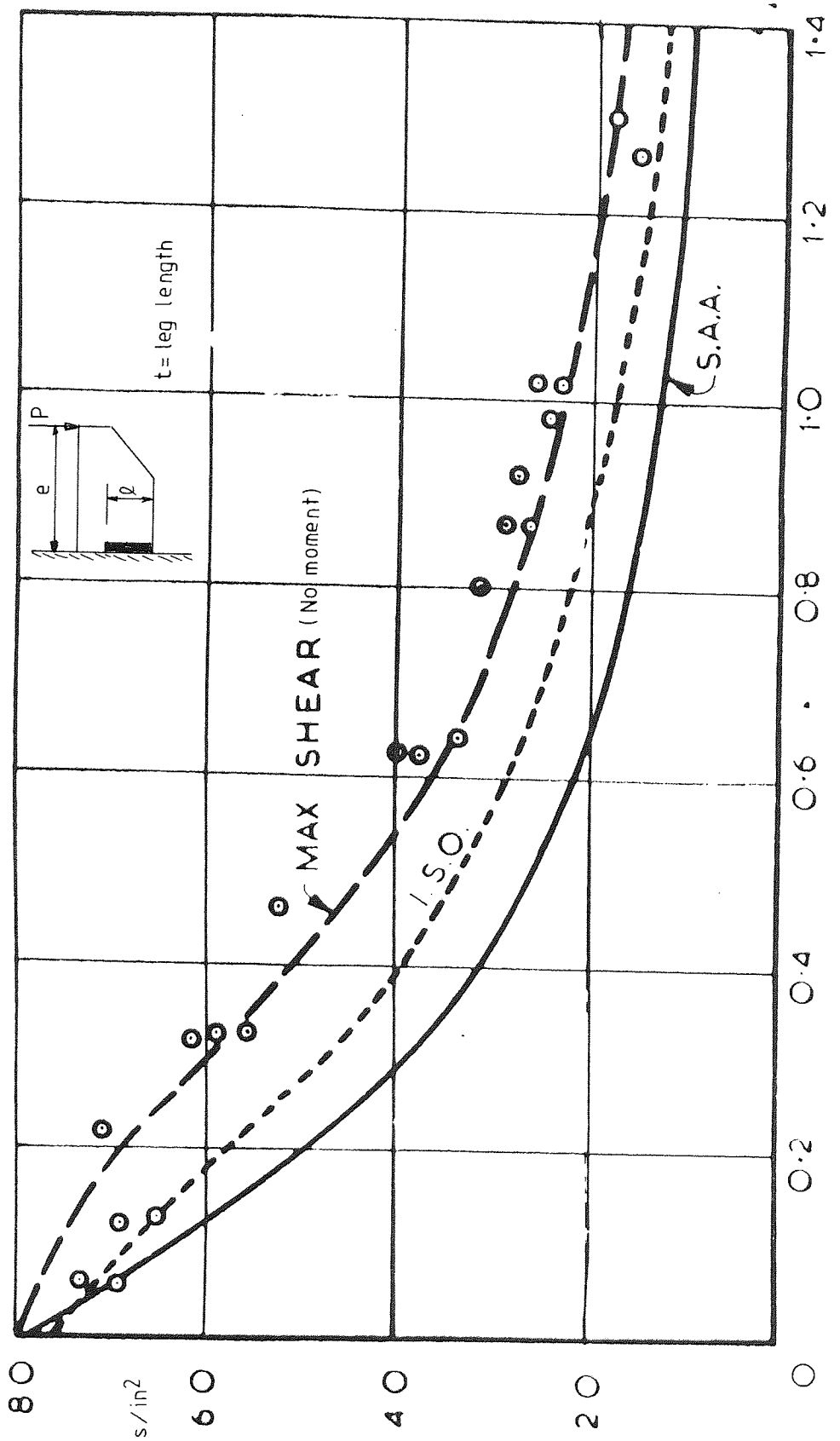

Fig.29 Relationship between (P/ℓt) and (e/ℓ)

5. the couple produced by this normal force was balanced by an equal normal force acting on the other leg of the weld,

6. the critical plane was uniform for the complete length of the weld.

The resulting force equilibrium diagram is shown in fig. 30 and the free-body diagram with reference to the critical plane AA, in fig.31.

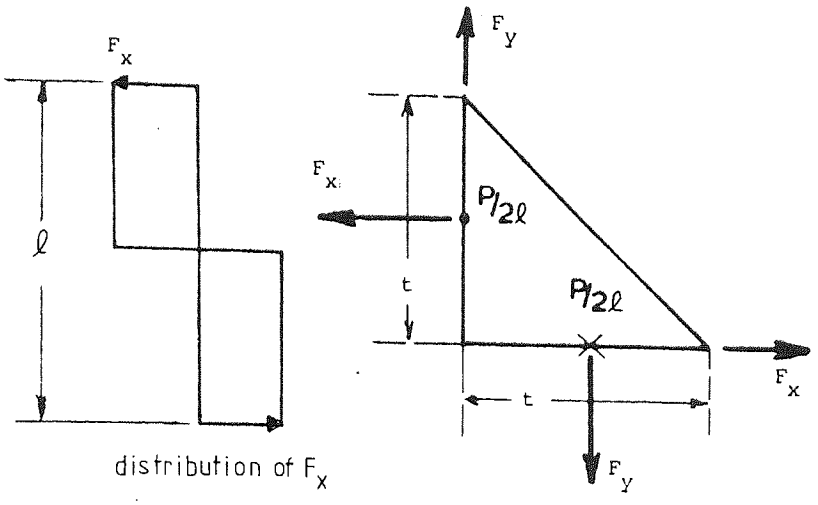

Fig. 30 Force Equilibrium Diagram.

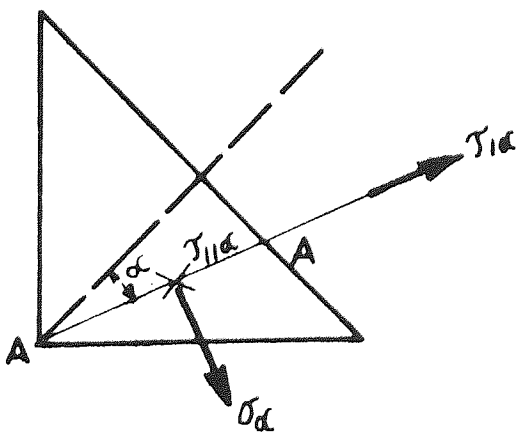

Fig. 31 Free-Body Diagram

The maximum shear stress criterion was derived in a similar manner to the previous analysis, and is shown below:

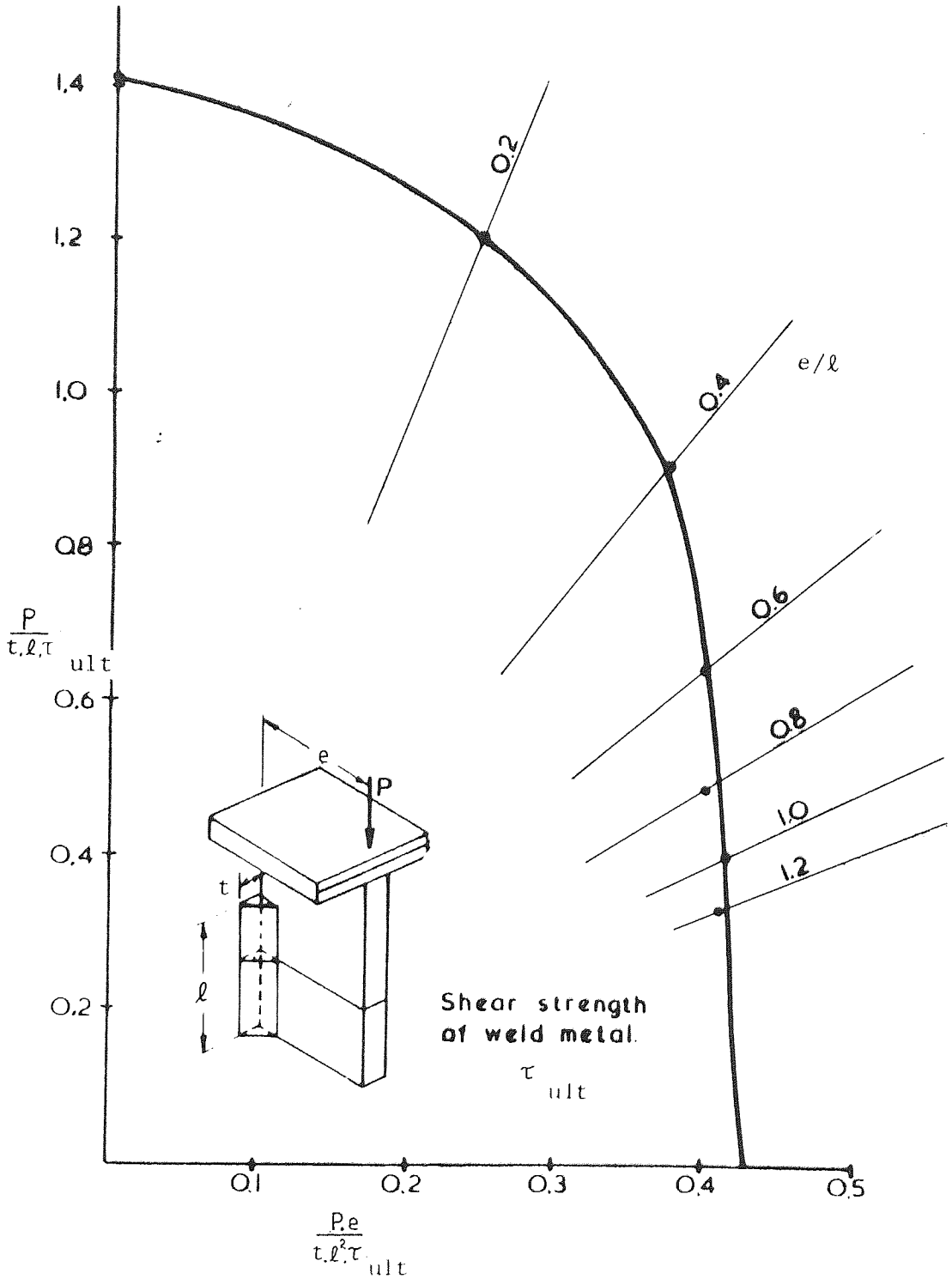

Fig.32 Design Graph for Beam-Column Connection

$$\text{Maximum shear stress} = \frac{P\cos\alpha}{2\ell t}\left[2 + \{40-24\cos 2\alpha\}\left(\frac{e}{\ell}\right)^2\right]^{\frac{1}{2}}$$

Once again an iterative solution is required to establish the position of the critical plane, for a given value of (e/ℓ) in order to maximise the shear stress. This criterion is compared with the experimental results in fig. 29 along with the I.S.O. and S.A.A. criteria. Once again, Archer et al have shown the maximum shear stress criterion compares extremely well with their experimental results, and that both the I.S.O. and S.A.A. criteria are very conservative (as expected). Again, the criterion has been presented in the form of a design curve, and is shown in fig. 32.

Flange deformation in beam-column connections obviously has an effect upon the load distribution along the length of the flange welds. A study of this effect was made by Elzen [23], in 1966, who conducted tests on column connections, fig. 33, in order to determine the effective weld length when the applied force was perpendicular to the face of the column. Elzen's interest was in how the column section influenced the effective weld length, and he looked at stiffened and non-stiffened H and box-section columns.

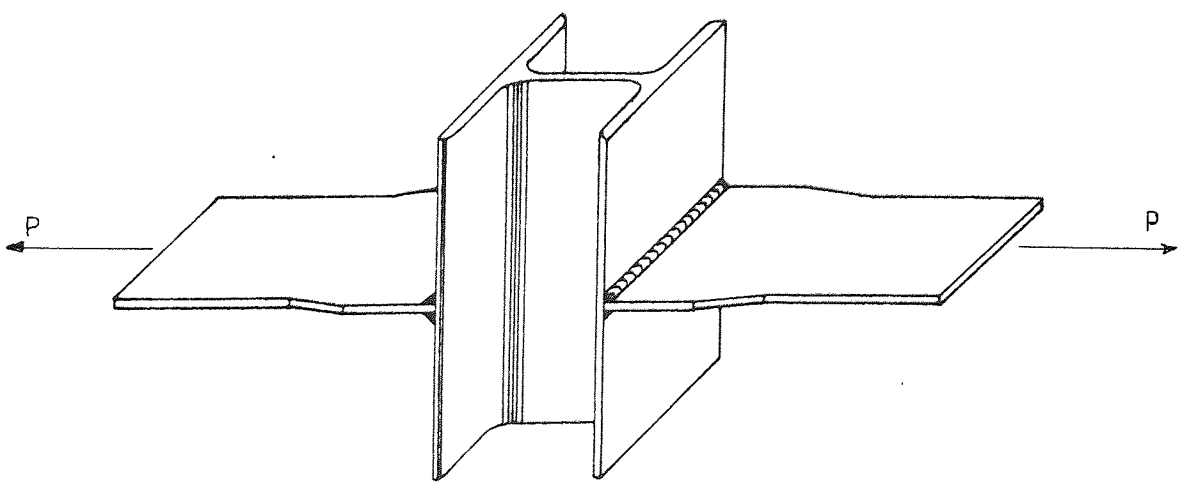

Fig.33 Column Connection

These tests simulate a beam-column connection under pure bending and also possibly under a condition of pure shear.

Deformation of the column flanges was measured, and also the stress distribution in the "beam flange" just above the welds by means of strain gauges. The "beam flanges" were 12 mm thick and 180 mm wide.

The importance of Elzen's work to the author's proposed research into beam-column connections is that it has shown the dramatic effect of column face flexibility on the weld length. This effect is illustrated in fig.34, which shows the stress distribution in kg/cm^2 across the "beam flange", adjacent to the weld, for an increasing applied load P in tonne.

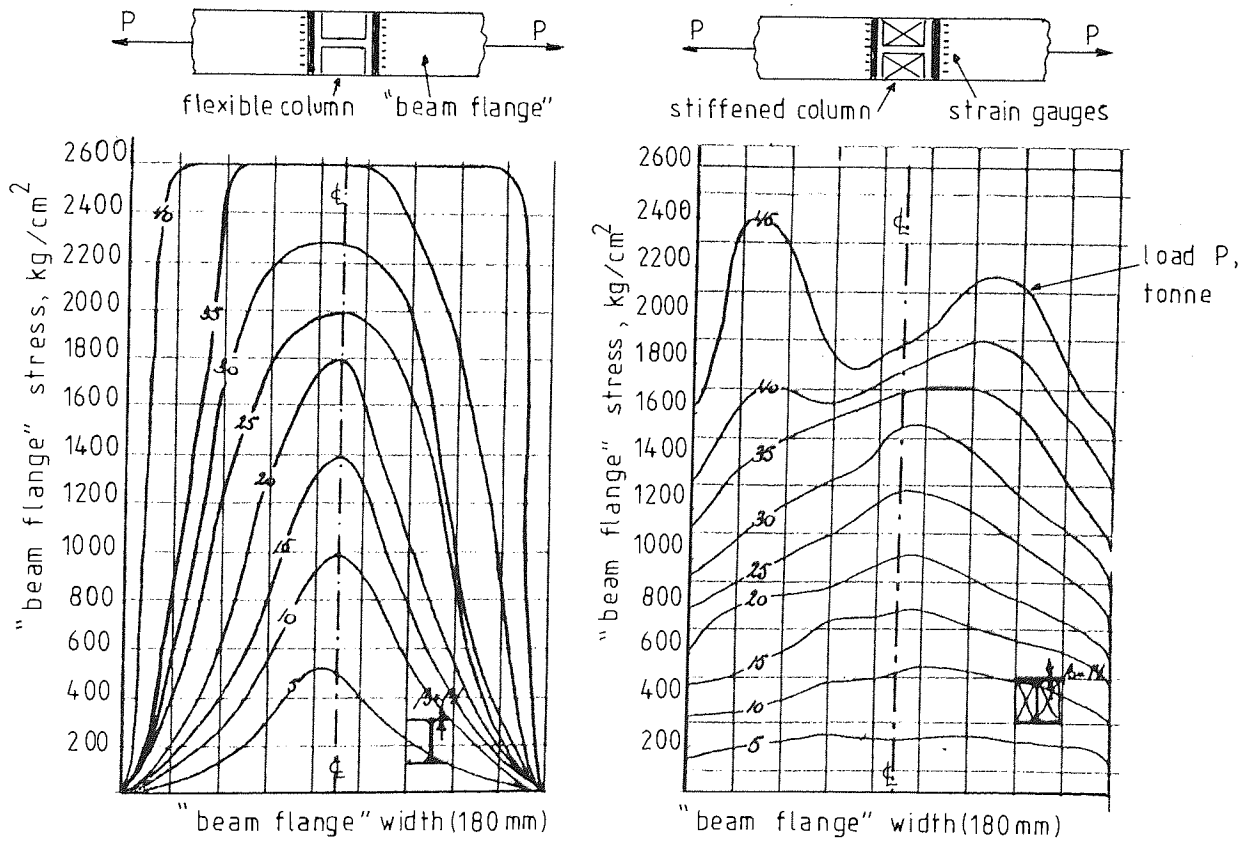

(a) (b)

Fig.34 Effect of Column Flexibility

Fig. 34(a) is for the unstiffened H section column, and (b) is for the same column with stiffeners. Elgen assumed for the stiffened column the effective weld length was 100% and by comparison of ultimate loads, the unstiffened column gave an effective weld length of 69%. It can be seen from fig.34 (b) that for the stiffened column the stress distribution is not quite uniform, but it is probable that for a rigid column the weld length would be fully effective with a uniform stress distribution.

Attention to a realistic value of safe working stress was given by Higgins and Preece[24] in 1968.

This report is of no great importance to the development of a limit state design method since their concern was for working stresses rather than ultimate stresses. Until a limit state design method has been adopted, however, working stresses are of course important. It was felt that as a result of improved welding techniques and material the value of working stress should be revised. One hundred and sixty-eight tests were conducted on lapped specimens of both longitudinal and transverse welds with variables, weld size, base metal, and electrode classification. The welds were machined to length but not to profile. A lack of complete root penetration was reported in one or two cases.

Concern about the effects of dilution of the weld metal has been expressed, but it was found that there was surprisingly little change in expected strengths of weld metal when combined with incomparable base metals.

The following conclusions were drawn:

1. steels having a tensile strength roughly comparable to that required of an electrode classification could be regarded as "matching" steel.

2. a safe working stress, to be applied to the throat as usual, of 0.3 x tensile strength of electrode classification was fully justified,

Once again, longitudinal and transverse welds are to be treated equally although it is now a well known fact that the transverse weld has a greater strength by a factor ranging through 1.272, Jensen[5]; 1.333, Freeman[4]; 1.45, Schreiner[7]; 1.563, Archer[19], and 1.5 by the investigators.

The final report of the international test series, on lapped specimens under tension, carried out under the guidance of Commission XV of the I.I.W. was presented by Ligtenberg[25] in 1968. One of the conclusions drawn was that the greater strength of the transverse weld in tension was attributed to the restricted deformation parallel to the lapped plates. It was suggested that this greater strength would not be realized if the same lapped specimens were loaded in compression. It is being suggested here that restricted deformation leads to the greater strength. Now, further doubt has been cast upon Vreedenburgh's[16] prediction regarding the strength of welds in compression. Ligtenburg's strength factor for the transverse weld, under a tensile load, was found to be 1.6.

With regards the comparative stress, σ_c, of the I.S.O. criterion, it was stated that a better estimate of strength could be made if σ_c was equated to $\frac{\sigma_p + \sigma_w}{2}$.

2.7 In 1971 Clark[26] reviewed recent research work and some foreign codes relating to the estimation of the strength and performance of fillet-welded joints. He pointed out the limitations of theoretical stress analysis and suggested that the load-strain characteristic for the weld could provide the basis for a more rational approach.

He suggested the internal stress system of a fillet weld was highly complex being a combination of residual stresses and stresses resulting from the applied load. Simplifying assumptions had to be made before theoretical solutions could be presented. Each solution presented a particular permutation of assumptions. Clark remarked that principle stress, maximum shear stress, and strain energy criteria were more properly used to predict material yield. This is obviously correct and such criteria take no account of work hardening and plastic behaviour. All the theories were based upon the throat section, with the exception of Archer et al[22], and all underestimate the true weld strength.

Clark acknowledged the limit curve of Vreedenburgh[16] and pointed out that by the introduction of empirical coefficients to the theoretical results, various curves had been produced which approximated to the experimental limit curve of Vreedenburgh[16]. The latest of such criteria was presented by Douwen and Witteveen[27] in 1966 and based upon the results of 620 tests carried out at the Steven Laboratory of the Delft Technological University. The criterion was based upon the von Mises equation and took the form

$$\sigma_e = \beta\sqrt{\sigma_1^2 + 3\,(\tau_1^2 + \tau_{11}^2)}$$

where β is a constant dependent upon the strength of the base material, and σ_e is the equivalent, or comparative stress. This criterion was later to be approved by Commission XV of the I.I.W. in 1975 and eventually adopted by the I.S.O. This and other criteria are compared to Vreedenbergh's[16], experimental results in fig. 35.

The value of β of 0.7 was that chosen for the base metal St 37 and it can be seen from fig. 35 the criterion using this constant over-estimates the weld strength.

The other criteria are shown to under-estimate weld strength.

With regard allowable design values it was suggested the most logical approach would be to use one of the I.S.O. criteria in conjunction with suitable load factors and a specified weld deposit strength.

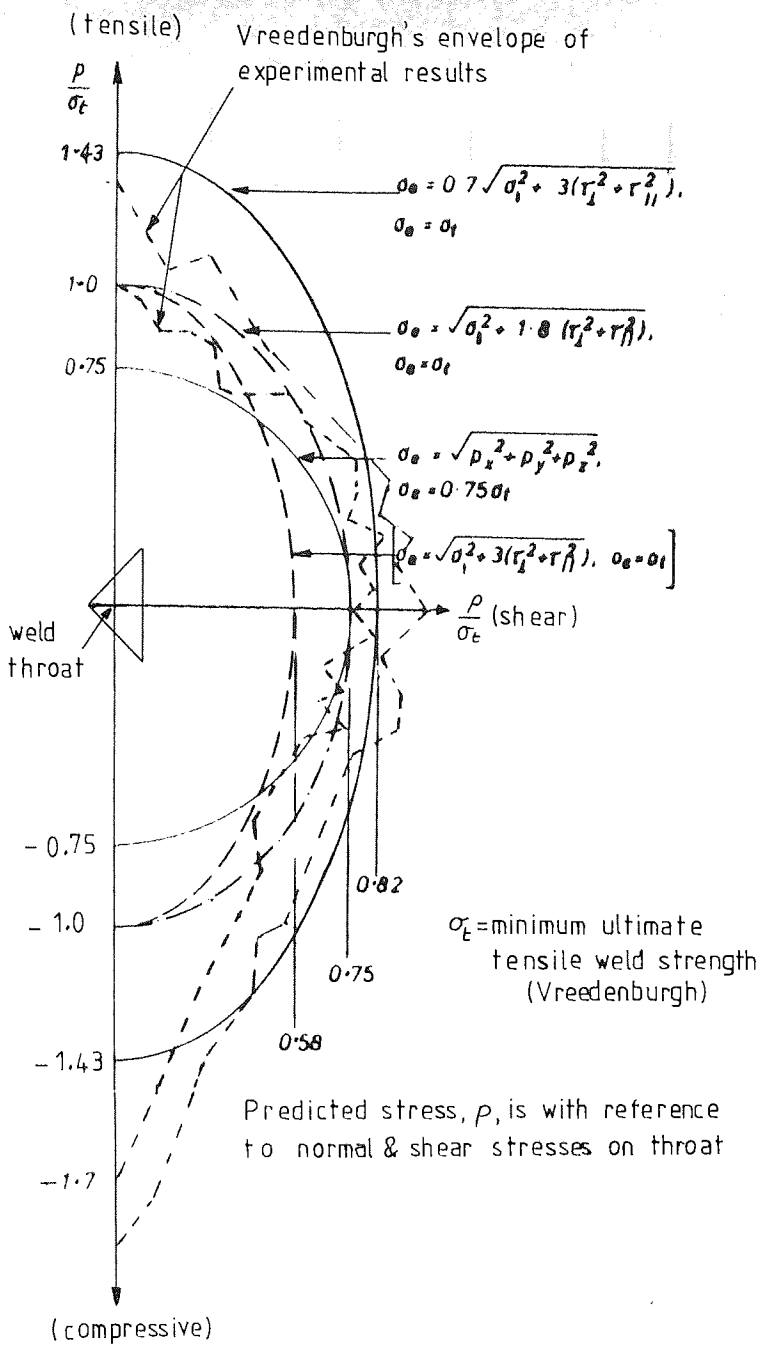

Fig. 35 Comparison of Failure Criteria

Clark extracted information from various design codes and presented it as in fig. 36. The load factors in columns 6, 7 and 8 were based upon an assessment of true weld strength using the 1975 I.S.O. criterion. With regard to fig. 36, the following comments were made:

1. relatively high load factors were used which reflected the wide scatter in weld properties which could result from variations in material, workmanship, and welding conditions.

Fig. 36 Typical design values for fillet welds on mild steel, taken from selected design codes for structural steelwork

1	2	3	4	5	6	7	8	9	10	11
Steel design rules	Rule for combination of loads on the throat for load in any direction (see also Fig. 4)	$\frac{p}{\sigma_t}$ 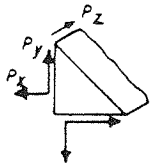			Load factor against failure for 'normal' load conditions			Reduced design strength for long longitudinal fillets	Reduced strength for combined end and side welds, or increased throat size	Guidance on design calculation
		Side fillet $p_x = p_y = 0$	End fillet $p_y = p_z = 0$	$p_x = p_y$ $p_z = 0$	$p_x = p_y = 0$	$p_y = p_z = 0$	$p_x = p_y$ $p_z = 0$			
France	$\sigma_e = \sqrt{\sigma_i^2 + 1.8(\tau_\perp^2 + \tau_{//}^2)}$	0.75	0.85	1.0	3.04	3.30	3.98	No	Yes	Yes
Netherlands	where	0.75	0.85	1.0	3.04	3.30	3.98		Yes	Yes
Belgium	$\sigma_e = \frac{\sigma_y \text{ (plate)}}{1.5} = \sigma_t$	0.75	0.85	1.0	3.04	3.30	3.98		Yes	Yes
buildings Germany - bridges	$\sigma_e = \sqrt{p_x^2 + p_y^2 + p_z^2}$	0.84	0.84	0.84	2.72	3.34	4.73	Yes	No	Yes
		←	0.65	→	3.52	4.32	6.10			
UK	$\sigma_e = \sqrt{p_x^2 + p_y^2 + p_z^2}$ (+ Von Mises)	←	0.74	→	3.92	4.83	6.85	No	No	No
buildings USA - bridges	$\sigma_e = \sqrt{p_x^2 + p_y^2 - p_z^2}$	←	0.72*	→	3.88	4.78	6.77	No	No	
		←	0.62	→	5.08	6.25	8.90			
eq. 3	$\sigma_e = 0.7\sqrt{\sigma_i^2 + 3(\tau_\perp^2 + \tau_{//}^2)}$	0.82	1.01	1.43	2.82	2.82	2.82			

Key: $p_{x,y,z,} = \frac{\text{applied load in specified direction}}{\text{throat area}}$

$p = \frac{\text{allowable load}}{\text{throat area}}$

σ_t = allowable tensile stress in a simple mild steel tie

*where there is a choice of electrode strengths the stronger has been taken

2. two distinct approaches to design were presented:

   (i) lower safety factors were combined with relatively comprehensive rules for designing welds, and in some cases restrictions on the effective lengths of welds for long joints,

   (ii) somewhat higher safety factors to cover the approximation implicit in very simple rules for design,

3. the method of vector addition, which takes no account of the load or ent ation to the throat and hence gives a variable safety factor, could be justified to some extent by the fact that the greatest safety factor occur with the transverse weld which was known to have only a limited deformation before abrupt failure.

With regard to joint design and load transfer Clark pointed out that the distribution of load throughout the joint would depend upon the load-deformation characteristics of the separate welds of the joint.

It was suggested that given a reasonable knowledge of the properties and an approximate analysis, an estimation of the ultimate capacity could be made.

This idea was put forward by Ligtenberg[20] in 1959, and represents the other side of the coin with respect to the methods of Archer[22], and Koenigsberger[15], who assumed full plasticity of the weld group in the joint. The full plasticity concept is of course much more convenient than a combination of individual load-deformation characteristics. Clark made reference to previously published load-deformation characteristics[28], and pointed out that these did not go beyond the peak value of load.

A series of tests were conducted on small specimens which Clark regarded would not cover the less ductile welds that might be expected from heavy plates in colder conditions. This is another reference to residual stress and obviously Clark believed it plays a significant role. There is a school of thought which believes residual stresses are relieved as soon as yielding begins, and hence have no further effect upon weld strength. The issue is yet to be decided.

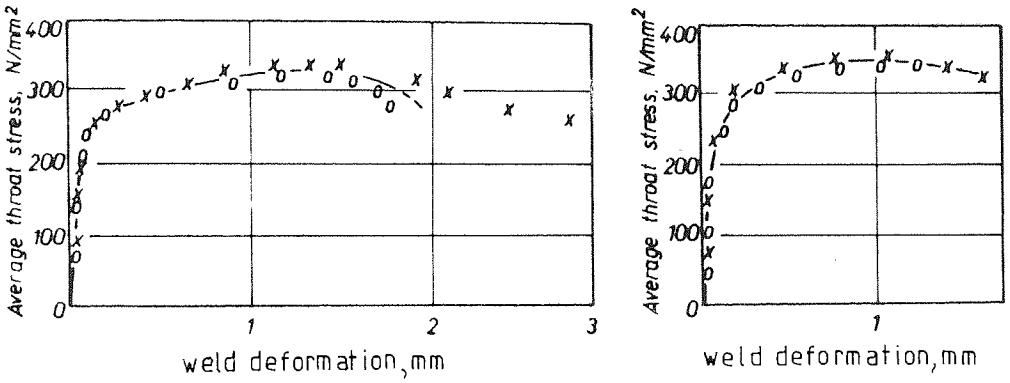

(a) 50 mm Side Weld (b) 254 mm Side Weld

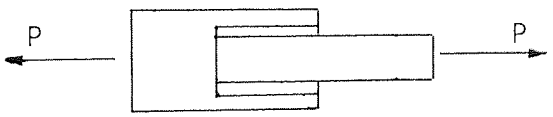

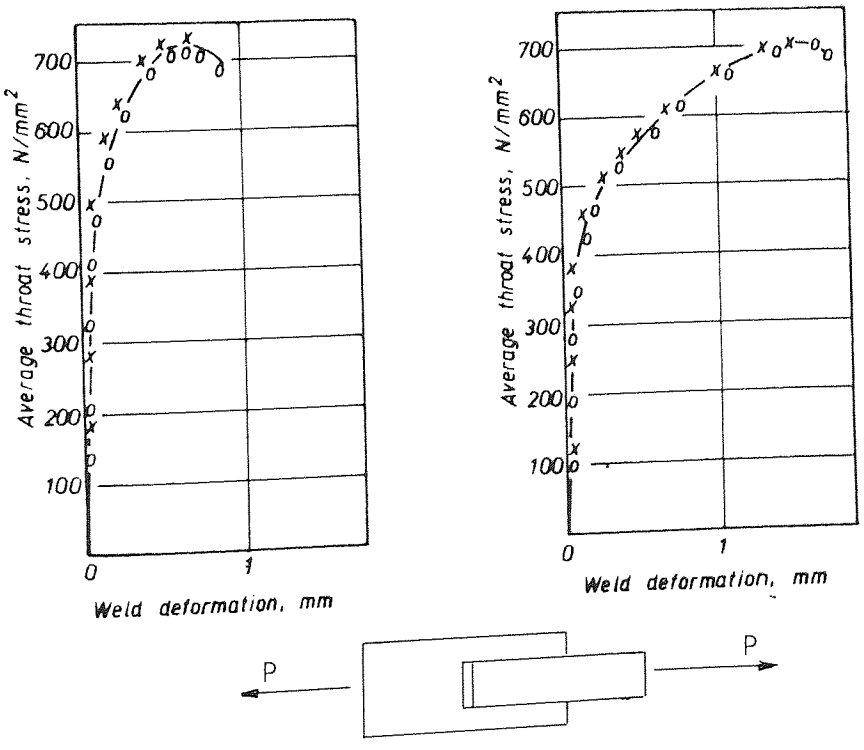

(c) 50 mm End Weld (d) 50 mm End Weld

Fig.37 Load-deformation Characteristics.

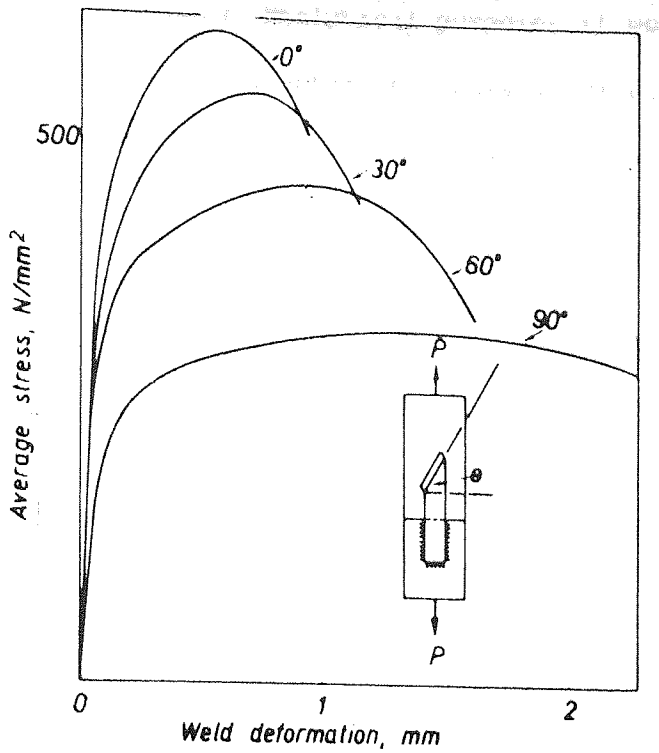

Fig.38 Safe Load-deformation Characteristics.

Typical examples of Clark's test results are shown in fig. 37, where deformation has been compared with average throat stress.

Clark admitted the strengths obtained were consistently lower by 20 - 25% than those obtained in the I.I.W. international test series.

He tries to explain this by suggesting that his welds must have been more ductile than those of the I.I.W. Clark is suggesting here a relationship, which has no foundation, between ductility and strength. Perhaps poor root, penetration accounts for the lower strength.

There is a fair scatter in his results; for side welds, ultimate deformation ranges from 1.03 to 2.8 mm, and for end welds from 0.71 to 1.42 mm. These show that some of his end welds were more ductile than some of his side welds.

He suggested for general analytical purposes it would be more convenient to have a series of 'safe' characteristic curves corresponding to a lower bound of expected ductility. These are shown in fig. 38.

With regard to the combination of end and side welds in one joint Clark suggested that no restriction would be necessary provided the end welds were not subjected to deformation in excess of 1 mm. Such deformation he maintained would only occur in exceptionally large joints. He has based this judgement on his poor test results which he averaged to produce the 'safe' curves in fig. 38.

Clark went on to propose a design method for brackets subject to torsional moment and shear which he likened to the 'plastic approach' which Abolitz[29] used in connection with bolted joints.

In fact it is very similar to the method proposed by Koenigsberger[15], the difference being in the assumption regarding the strength of the elemental weld. Koenigsberger[15] assumed the unit resistance of the elemental weld to be constant whereas Clark assumed it to be a variable dependent upon the amount of deformation and the inclination of the element to the instantaneous centre of rotation.

Because of the complexity of analysis, Clark presented his design method in the form of design interaction curves.

Like Koenigsberger[15], Clark did not extend his design method to beam-column connections.

Fundamental to Clark's method are the load-deformation characteristics

which he admits are dependent to a large extent on residual stress level which in turn is dependent upon such variables as joint size, welding parameters and fit-up. The difficulty arises now of designing test specimens, from which to obtain the load-deformation characteristics, which will simulate full-sized joints made under field conditions.

2.8 At the same time as Clark[26], Butler and Kulak[30] were investigating load-deformation characteristics of fillet welds, on the grounds that little was known of such characteristics, and that such information would be useful in assessing the validity of current design methods. As did Clark[26], Butler and Kulak assumed a fixed relationship between weld strength and ductility, i.e. the lower the ductility the higher the strength.

No doubt this is true with regard to a material in isolation but, in the situation of a fillet weld the mode of failure is very much dependent upon the ductility of the weld metal since it is very likely that failure is initiated at the weld root. It is quite possible that an increase in ductility would be accompanied by an increase in strength. Furthermore, it is well known that residual stresses reduce ductility of a fillet weld and that such a state can cause brittle fracture, i.e. a reduction in ultimate weld strength.

Twenty-three tests were conducted on small lapped specimens, fig. 39, with θ having values of 0, 30, 60 and 90°. Only tensile tests were done as with all previous investigators, and deformation was not measured after maximum load had been attained.

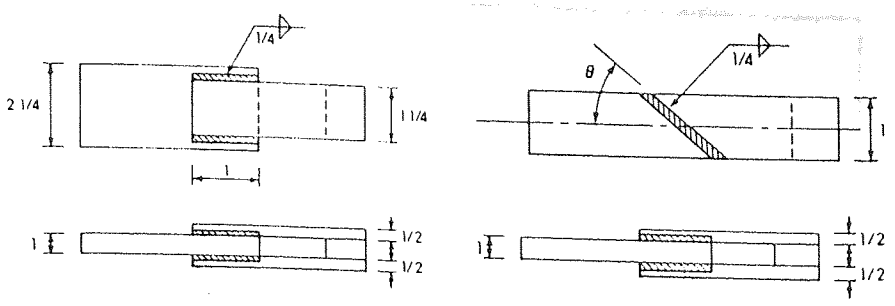

Fig.39 Test Specimens.

The results of these tests are shown in fig.40

A theoretical method of load-deformation response was then developed starting from Fisher's[31] expression for load-deformation response for mechanical fasteners:

$$R = R_{ult}(1 - e^{-\mu\Delta})^{\lambda}$$

where R = fastener load resistance at any given deformation,

R_{ult} = ultimate load resistance attainable by fastener,

Δ = deformation of fastener plus connected plates,

μ, λ = regression coefficients

e = base of natural logarithms.

By a trial-and-error curve fitting procedure expressions for the variables in the above equation were determined as follows:

$$R_{ult} = \frac{10 + \theta}{0.92 + 0.0603\theta}$$

$$\Delta_{max} = 0.225(\theta + 5)^{-0.47}$$

$$\mu = 75e^{0.0114\theta}$$

$$\lambda = 0.4e^{0.0416\theta}$$

By substitution into Fisher's[31] equation Butler and Kulak were able to predict the load-deformation characteristic for any value of the [illegible] particular test specimens.

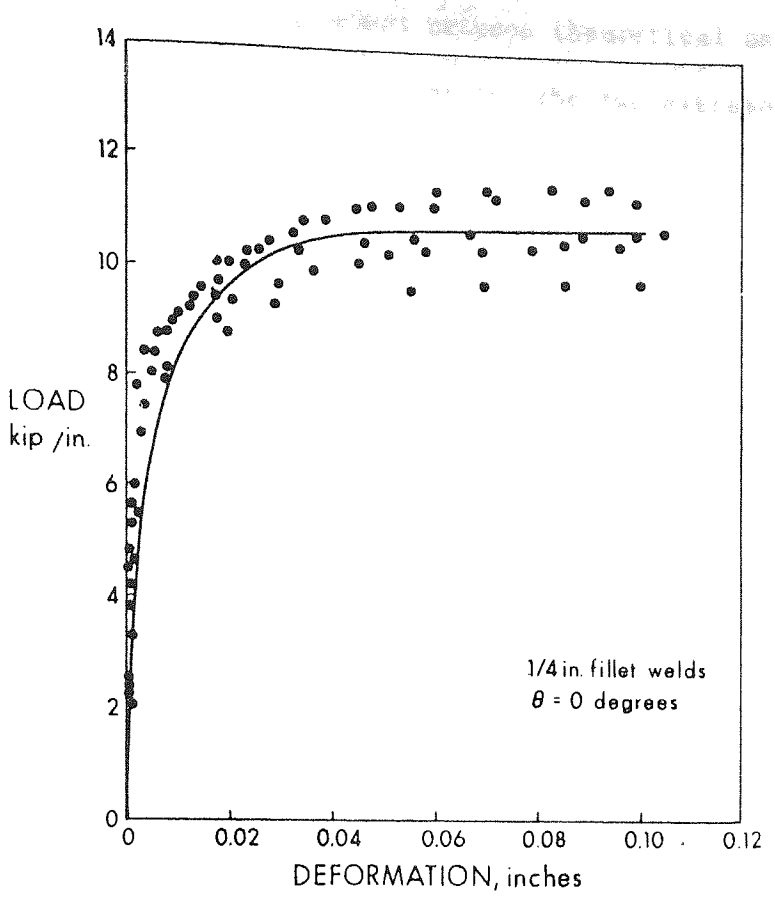

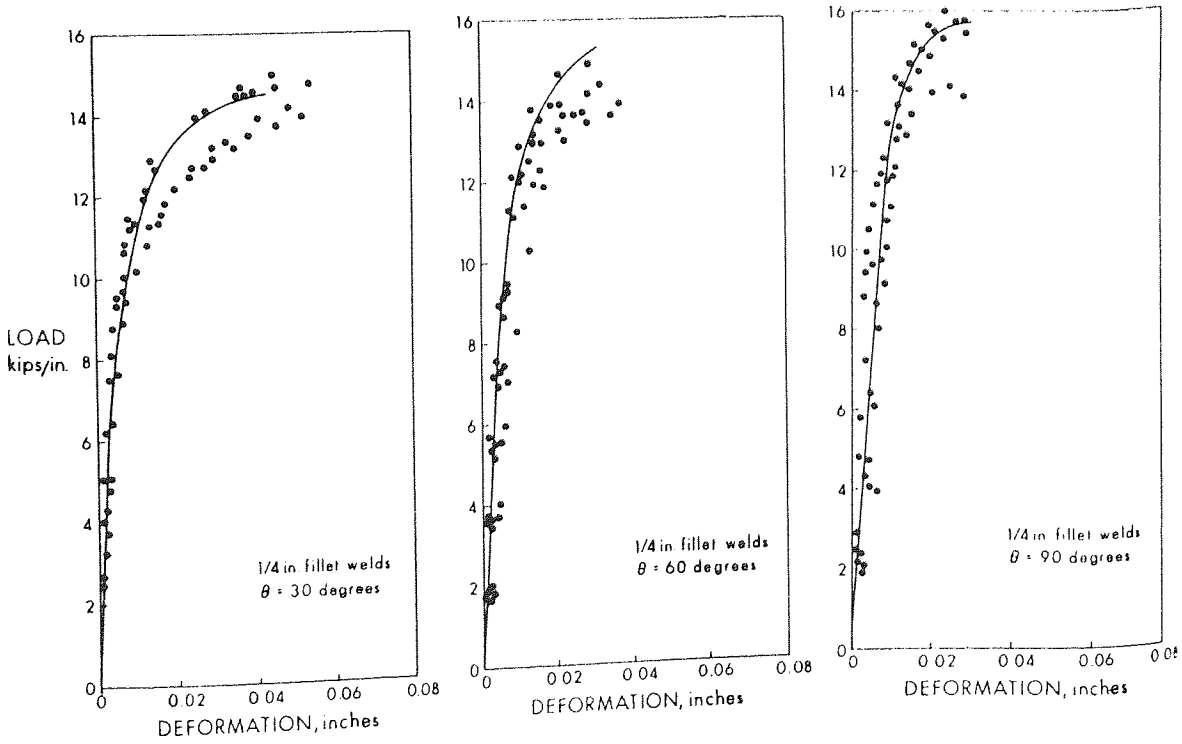

Fig. 40 Load-Deformation Characteristics

It was concluded that agreement between theoretical and experimental load-deformation response was excellent for the two extremes, i.e. side, and end welds and adequate for values of θ of 30° and 60°.

An important point was made by Butler and Kulak namely; deformation could be expected to be independent of the weld leg size. There is some verification of this supposition if a comparison is made with the load-deformation characteristics, see fig. 37 (a), (b) and (c), obtained by Clark[26] whose welds were of 8 mm leg as opposed to 6.35 mm. The test specimens of Clark[26] are slightly larger than those of Butler and Kulak, both being small relative to real beam-column connections.

It is very clear from the characteristics presented here that the side weld has a greater ductility and a lesser strength than the end weld. This fact does not necessarily lend credibility to the assumed relationship between strength and ductility since the greater strength of the end weld must be due, at least in part, to the greater area of the critical plane. Higgins and Preece[24] commented that the critical plane was close to the plane of the weld leg in their test specimens. The ratio of weld strengths from results presented here is 1.422. The maximum ratio of areas is obviously 1.4142.

Kato et al[32], summarized the work which had been done in Japan by Naka & Saito[33], Miki et al[34], Igarashi and Sakamoto[35] and Hoshino et al[36] on joint efficiency of beam-column connections. This work was similar to that done by Elzen[19], de Geeter[37] and Rollos[38] in Holland, but the Japanese interest was in the strength of the complete joint as opposed to the weld strength. Their joints were so designed to produce failure in either the flanges or column web. Their results were expressed in terms of joint efficiency with reference to the strength of the beam flange only. Groove welds were used instead of fillet welds.

This work is at present of no direct interest to the author.

In 1972, Strating et al[39] pointed out the I.S.O. weld strength criteria was based upon the yield hypothesis of Huber-Hencky-von-Mises;

$$\sigma_c = \sqrt{\sigma_{11}^2 + \sigma_1^2 - \sigma_{11} \cdot \sigma_1 + 3(\tau_{11}^2 + \tau_1^2)}$$

In 1957 the I.S.O. proposed that the σ_{11} stress, this is a tensile/compressive stress on the longitudinal axis of the weld, had little influence on the strength of the weld and it was not included in the I.S.O. criterion.

Their objective was to establish unambiguously that neglecting this σ_{11} stress had no unfavourable effects.

A series of tests was conducted in which the σ_{11} stress was induced by an external load. It was found that this longitudinal stress, σ_{11}, either tensile on compressive, had no effect on the strength of the weld even if it was non-equally distributed.

Neumann and Ziethe[40], conducted similar tests in which the longitudinal stress σ_{11} was induced as a residual stress. Again, these tests showed the presence of the stress had no influence on weld strength.

The load deformation response which Butler and Kulak[30], had developed in 1971 was employed by Butler et al[41] in a proposed method of predicting the ultimate capacity of column brackets under torsional moment and shear. This is remarkably similar to the method proposed by Clark[26] in 1971.

Clark[26] presented his design method in the form of design interaction curves whereas Butler et al have presented theirs in the form of ultimate load tables.

Both methods assume an instantaneous centre of rotation on an axis through the weld centroid, and equality of behaviour by welds under tension and compression. The method of Butler et al is obtained through an iterative solution of the equilibrium and compatibility equations in conjunction with the load-deformation characteristic.

Both investigators have employed load-deformation characteristics derived from relatively small and simple test specimens. No regard has been given to the different parameters which are bound to exist in real connections. Ductility of the weld and hence ultimate strength, is greatly influenced by residual stress levels which in turn are dictated by joint geometry and welding conditions.

A series of thirteen tests conducted on column brackets showed that the error in the predicted ultimate capacity ranged between +9.3% to -9.5% of the actual ultimate capacity.

It was concluded that the magnitude of error was acceptable on the grounds of the inevitable non-uniformity of a length of weld

This popular explanation for the occurrence of error, may or may not have any foundation and clearly the onus is with the investigator to ensure as far as possible, uniformity of welds.

The experimental results were compared with safe load predictions using the current vector method, and safety factors were found to range between 5.0 and 7.55.

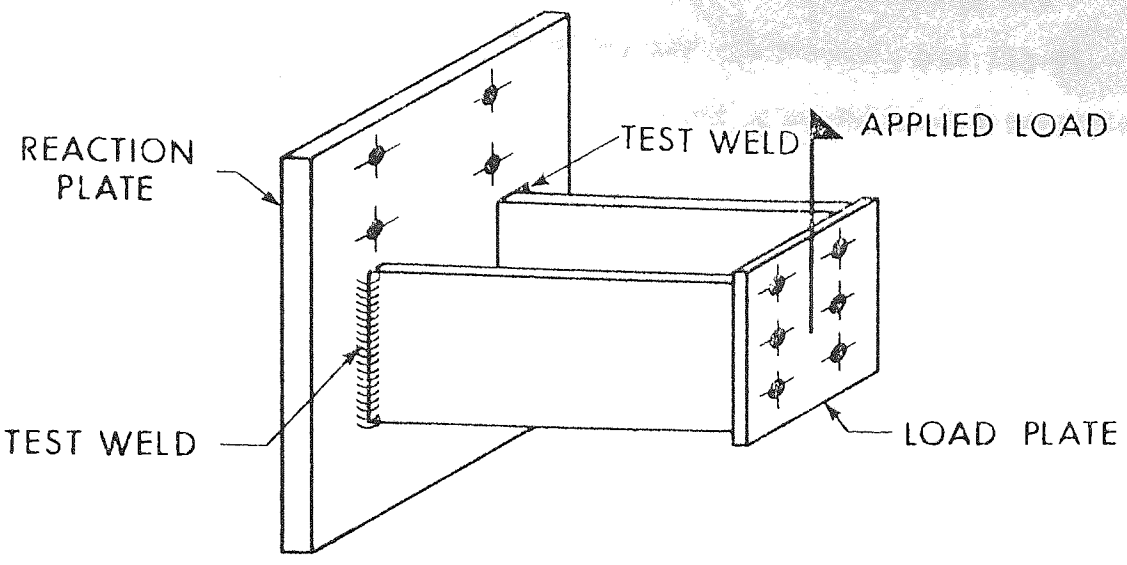

(a) Web-welded Connection

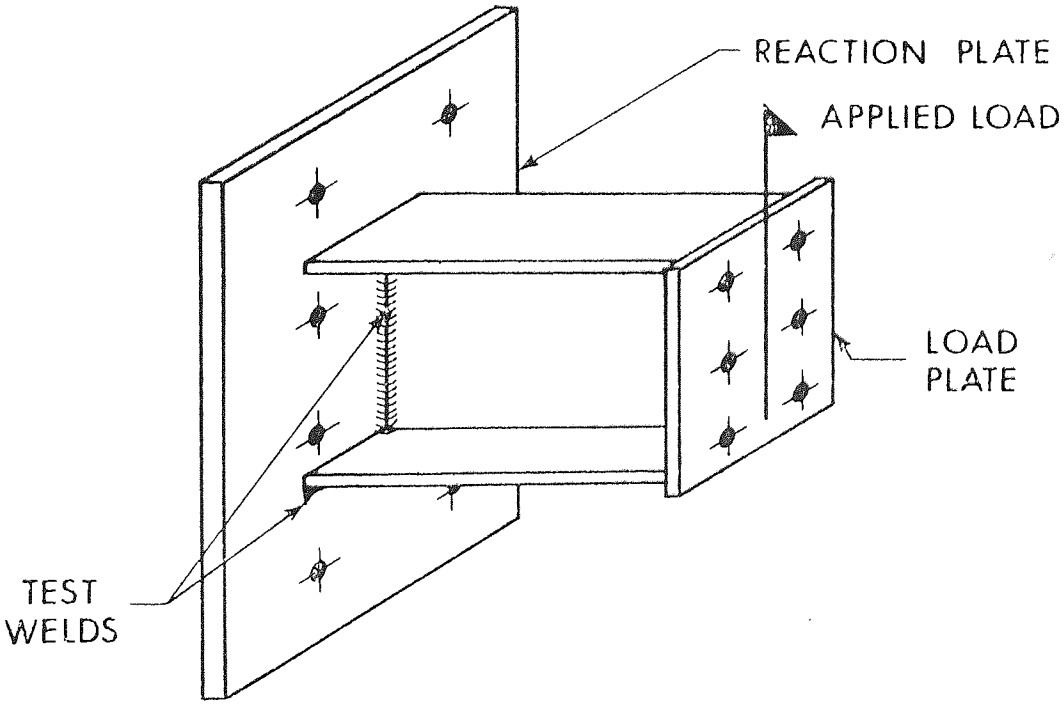

(b) Web and single flange-welded Connection

Fig. 41 Beam-column Connections (with plate-bearing)

2.9 Dawe[42] extended the work of Butler et al[41] by investigating beam-column connections in which plate-bearing was present, see fig.41. The method of ultimate load prediction was based upon the load-deformation characteristic proposed by Butler and Kulak[30].

The basic assumptions that were made are as follows:

1. the ultimate capacity of the connection is reached when the weld element farthest from the instantaneous centre reaches its ultimate deformation,
2. the load-induced resisting force of each weld element acts through the centre of gravity of that element,
3. the deformation of each weld element varies linearly with its distance from the instantaneous centre and takes place in a direction perpendicular to its radius of rotation,
4. the overall resisting capacity of the weld group is obtained by summing the individual resisting capacities,
5. the weld group rotates about an instantaneous centre located on an instantaneous neutral axis.

For the web welded connection, fig.41(a), the proposed condition for static equilibrium is represented in fig.42.

Particular assumptions were made as follows:

6. plate bearing exists below the neutral axis and it produces a triangular stress distribution of maximum value equal to the yield stress, σ_y, of the plate material. The resultant bearing force is represented by F_B.
7. the weld in compression below the neutral axis resists only shear force F_S,

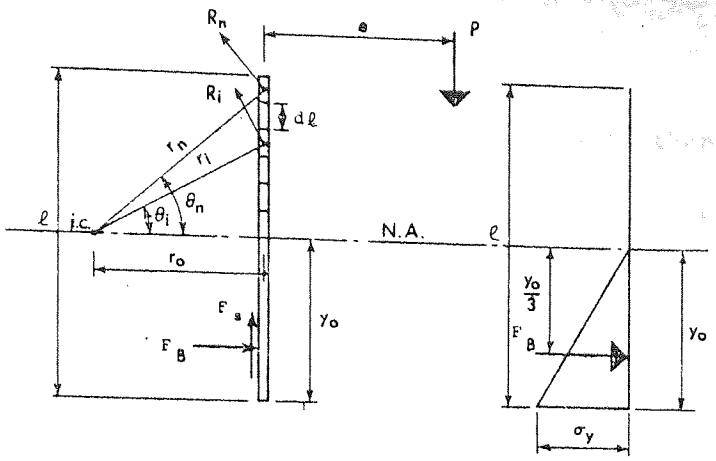

Fig. 42 Condition for Static Equilibrium

8. the weld in the tension zone, above the neutral axis is subdivided into elements of equal length, $d\ell$, each element providing its own resistance, R_i, as defined by the load-deformation characteristic;

$$R_i = R_{ult} (1 - e^{-\mu\Delta_i})^{\lambda}$$

where

$$R_{ult} = \frac{10 + \theta_i}{0.92 + 0.0603\ \theta_i}$$

$$\mu = 75e^{0.0114\theta_i}$$

$$\lambda = 0.4e^{0.0146\theta_i}$$

9. the uppermost element, n^{th}, of weld in the tension zone will be critical, and subjected to the maximum deformation

$$\Delta_{max} = 0.225(\theta_n + 5)^{-0.47}$$

10. the resisting force, R_i, of each element will have vertical and horizontal components.

Solution of the static equilibrium equations is then obtained by an iterative procedure, beginning with trial values of the position of the instantaneous centre and neutral axis; the final outcome being the minimum value for the ultimate capacity of the weld group.

The above method was extended to the web and single flange welded connection shown in fig. 41(b) and the proposed condition for static equilibrium is represented in fig. 43.

The particular assumptions were made as follows:

11. the flange weld, which is in tension, is concentrated at one point and its resisting force R_n is equal to R_{ult}, where

$$R_{ult} = \frac{10 + \theta}{0.92 + 0.0603\theta}$$

where, $\theta = 90°$ since the weld is loaded at an angle of 90° to its longitudinal axis. It will not be loaded at 90° to the weld leg as in the tests of Butler and Kulak[30].

12. the flange weld will be critical and subjected to maximum deformation,

$$\Delta_{max} = 0.225\ (\theta + 5)^{-0.47} \quad \text{where } \theta = 90°$$

13. plate bearing exists below the N.A. and it produced a triangular stress distribution for the web section, and a rectangular distribution for the flange. The maximum stress being equal to the yield stress of the plate material, θ_y. The two resultant bearing forces are represented by F_{Bf} and F_B,

14. the weld in the compression zone, below the neutral axis, resists only shear force F_S,

15. the web weld above the neutral axis to be treated as before, see assumption (8).

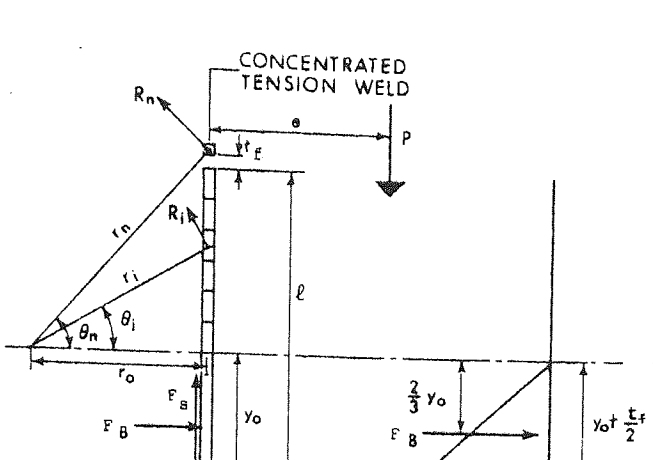

Fig. 43 Condition for Static Equilibrium

The extension of the method to the connection with web welds and both flange welds was not presented by Dawe, although it must have been employed for the prediction of ultimate capacity of such joints that were tested.

Three series of tests on full-sized connections were conducted. Average leg length for all tests was 0.3 inch.

Series I, fig.41(a) consisted of 8 tests with variables:

(i) weld length, 8 inch and 12 inch

(ii) ratio of e/ℓ, 1.03 to 2.56

(iii) 'web' thickness 0.52, 0.43, 0.62 and 0.76 inch

There are obviously too many variables for eight tests. The test set-up is shown in fig. 44.

Series II, fig. 41(b) consisted of only 4 tests with variables:

(i) weld length, 5.52 and 7.10 inch

(ii) ratio of e/ℓ, 2.11 to 3.62

(iii) flange, and web area.

Difficulties of obtaining uniform web welds was reported, however, it was felt the exact length would not be too critical since calculations showed that most of the capacity of the specimen was developed by the flange weld. Such calculations were not presented by Dawe and his claim lacks credibility.

Series III, similar to those of series II but with both flanges welded again only 4 tests, with the same variables as for Series II.

A number of tests were also conducted on small lapped specimens with longitudinal welds in order to establish the load-deformation characteristic, see fig. 45.

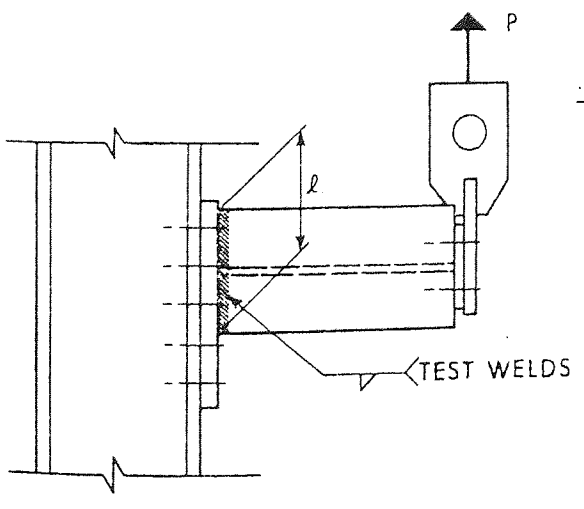

Fig. 44 Test set-up

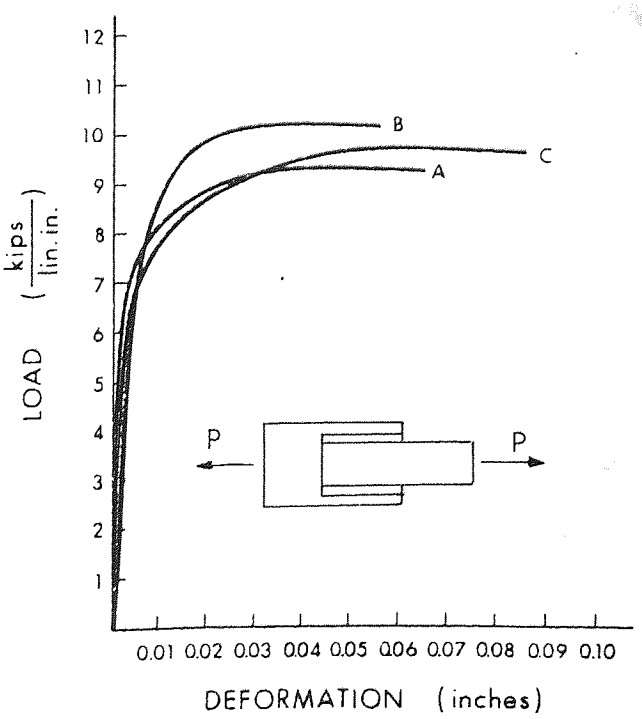

Fig. 45 Load-deformation Curves

This characteristic was used to modify the load-deformation relationships developed by Butler and Kulak[30].

As did Butler et al[41], Dawe assumed the load-deformation characteristic derived from small lapped specimens was directly applicable to full-sized beam-column connections.

For each test joint, rotation was measured and the results are shown in figs.46, 47 and 48.

Dawe made the following comments regarding the load-rotation curves:

1. range of rotations for specimens A2, A6, A7 and A8 was small, 0.015 to 0.017 radians, whilst the range of e/ℓ was from 1.26 to 2.02. The overall range of rotations was 0.015 to 0.025 radians whilst the corresponding ratio of e/ℓ varied from 1.03 to 2.03.

Dawe's theory assumes the uppermost element of the weld in tension to be critical, and hence, one would expect the joint rotation to decrease as the ratio e/ℓ decreased. Specimens A1, A7, A8 and A2 appear to comply with this logic but, the other three, especially A5 and A3, appear to behave in a reverse manner.

2. average ultimate rotations for series II & III were approximately 0.010 radians compared to 0.020 radians of series I. The smaller rotational capacity of series II and III was a result of the lower ductility of the transverse flange weld.

3. the effect of the additional weld on the compression of flange series III was to make the connection initially more rigid than the series II connections.

The most interesting observation to be made from the comp arison of

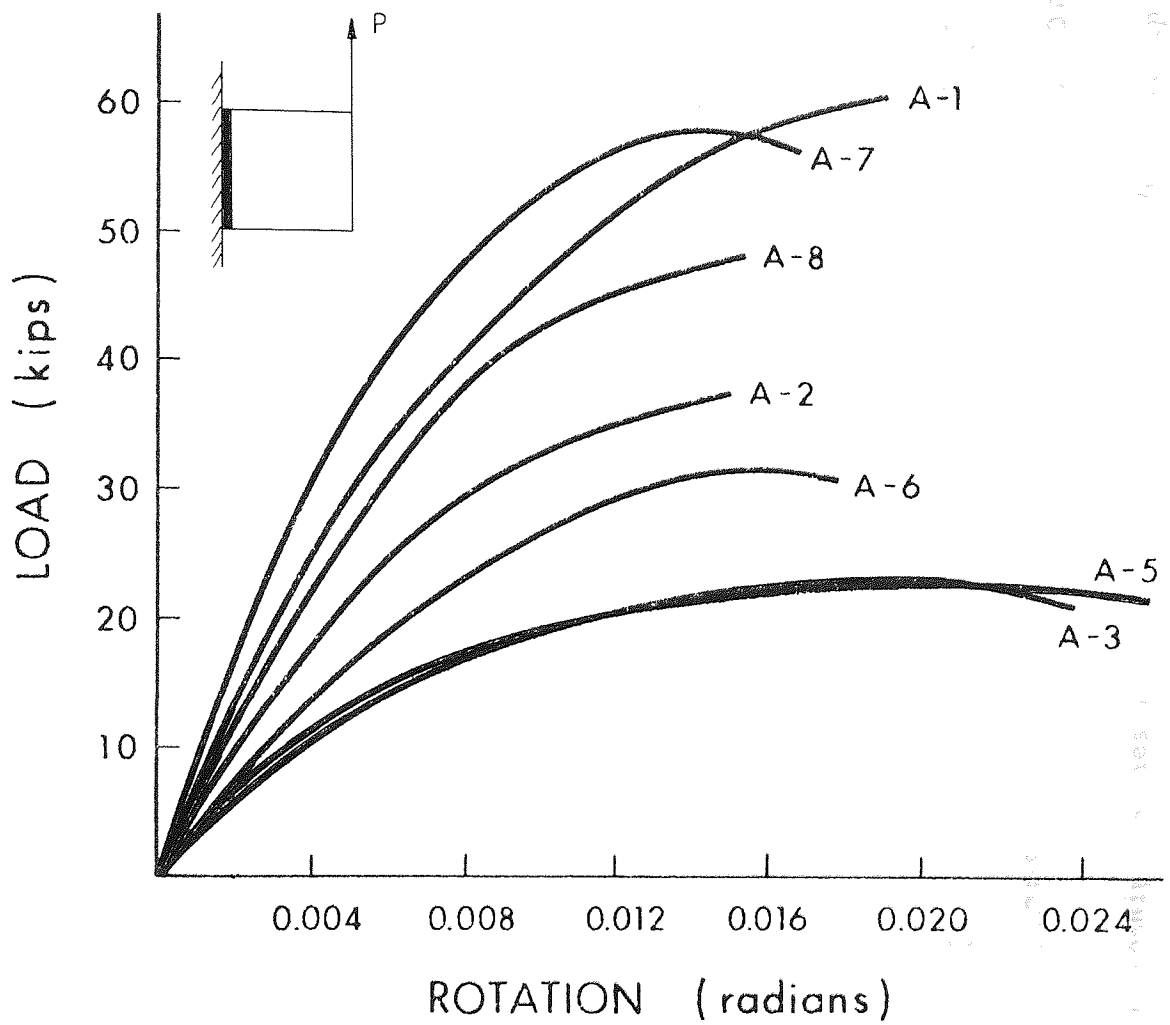

Fig.46 Load-rotation Relationship - Series I

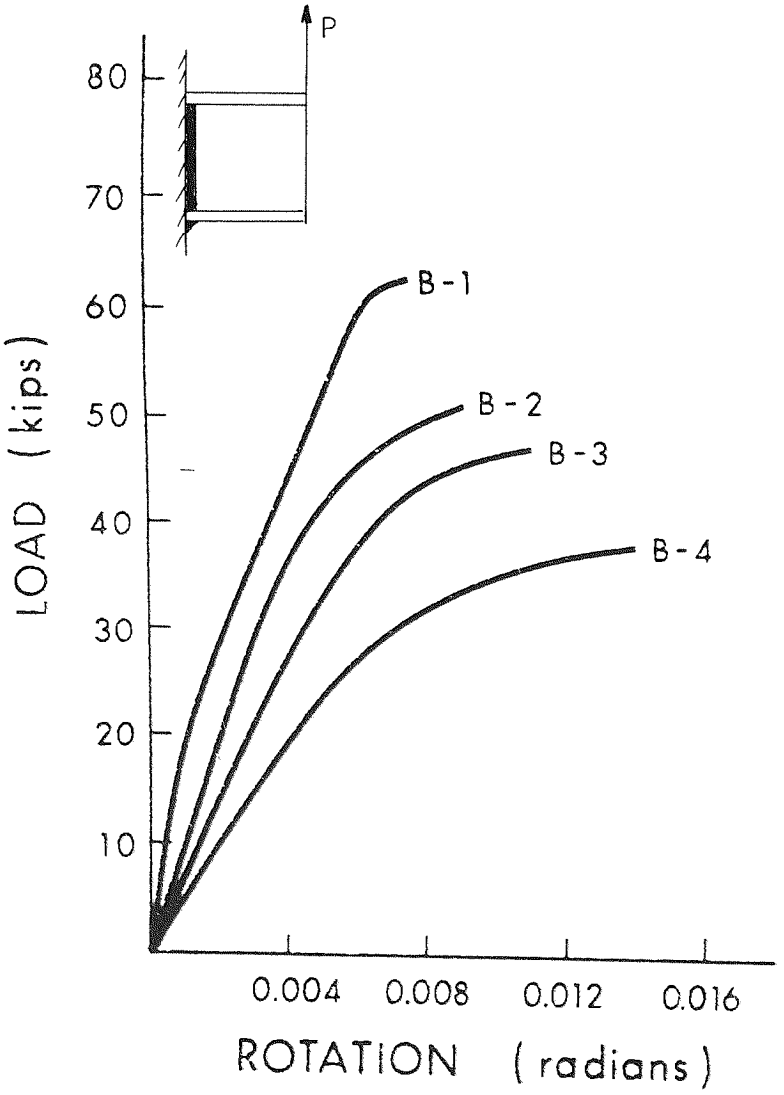

Fig.47 Load-rotation Relationship - Series II

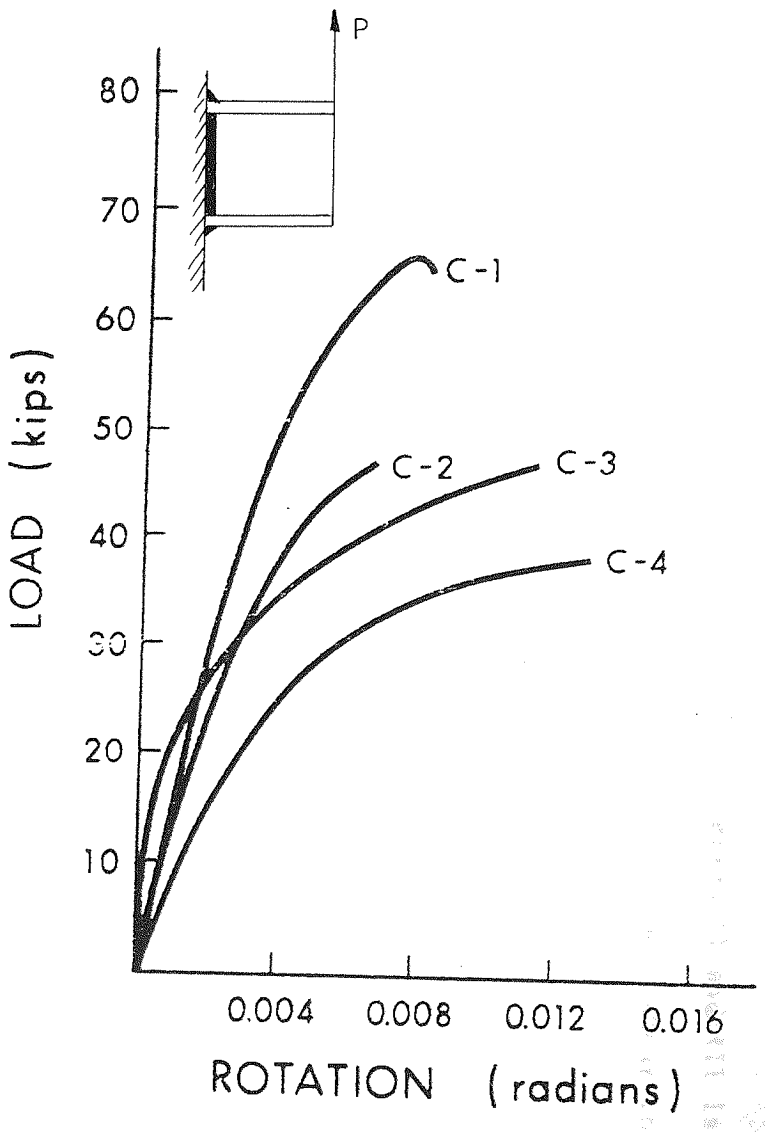

Fig.48 Load-rotation Relationship - Series III

series II and III is that the additional compression flange weld has not increased the ultimate capacity of the connection. This is not really surprising since the smallest ratio of e/ℓ for series II and III is 2.1, i.e. the connections are resisting only a relatively small shear load. The compression flange weld is unlikely to offer any resistance to bending owing to the presence of plate-bearing, but it is more than likely to offer resistance to shear as the ratio of e/ℓ approaches zero.

A comparison was made between predicted and actual ultimate capacities. For series I the error was random, ranging from -16% to +12.1%; for series II the error was conservative ranging from 1.8 to 16.9%, and for series III the error was also conservative ranging from 8.7 to 17.4%.

With regard to these errors, Dawe suggested possible sources:

1. no account was taken of the frictional forces which must have existed between the plates in bearing and likely to increase the ultimate capacity of the connection,
2. non-uniform size of web welds,
3. wrongly assumed stress distribution in the bearing zone,
4. imperfect centering and alignment of the sections on the column plate,
5. load measuring device (possible error ±2%)

With regard to the stress distribution in the bearing zone, Dawe computed the errors again using parabolic and rectangular distributions. He found that for series I the triangular block gave the minimum error and for series II and III, the rectangular block. He concluded that the triangular block was the one best suited to the connections in general.

Any choice of stress block is purely arbitary unless perfect fit-up can be guaranteed.

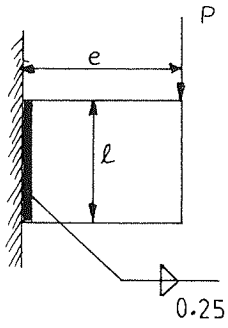

ℓ (inches)	e(inches)								e(inches)						
	2	4	6	8	10	12	14	16	18	20	22	24	26	28	30
2.00	13.26	6.64	4.47	3.35	2.66	2.22	1.95	1.70	1.54	1.41	1.30	1.12	1.03	0.96	0.90
4.00	51.88	26.37	17.61	13.23	10.54	8.82	7.56	6.62	5.88	5.29	4.81	4.40	4.06	3.76	3.51
6.00	110.70	58.90	39.47	29.68	23.73	19.79	16.86	14.86	13.21	11.89	10.80	9.90	9.12	8.45	7.86
8.00	173.80	103.51	69.92	52.57	42.11	35.11	30.16	26.34	23.43	21.00	19.15	17.53	16.23	15.06	14.05
10.00	231.93	158.05	108.54	81.99	65.69	54.81	46.98	41.10	36.55	32.88	29.94	27.37	25.30	23.51	21.98
12.00	286.75	218.57	154.93	117.57	94.38	78.76	67.57	59.17	52.60	47.32	43.02	39.46	36.38	33.86	31.59
14.00	339.36	280.78	207.71	159.16	128.16	107.12	91.93	80.48	71.64	64.42	58.57	53.63	49.49	45.99	42.96
16.00	390.20	342.28	265.36	206.30	166.77	139.59	119.90	105.03	93.37	84.08	76.53	70.10	64.71	60.05	56.10
18.00	439.84	402.11	325.67	258.14	210.06	176.15	151.49	132.73	118.08	106.35	96.77	88.68	81.86	76.04	70.97
20.00	488.59	459.80	387.36	313.69	257.57	216.72	186.57	163.69	145.69	131.23	119.39	109.44	101.09	93.86	87.66

Fig. 49 ULTIMATE LOAD TABLES (P, kips)

Ultimate capacities were compared with predicted ones using the current vector method with an allowable stress of 18000 lbf/in^2. Resulting safety factors ranged from 4.7 to 8.4.

Dawe concludes that his proposed theoretical method has been validated by his experimental results. Such a claim is hardly justifiable considering the small number of tests, the very limited ranges of e/ℓ, and the random error.

Dawe did not recommend the direct use of his proposed theoretical method, but instead presented ultimate load tables as shown in fig.49. These tables are applicable only to web welded connections with welds of 0.25 inch leg length and an ultimate shear strength of 360 N/mm^2.

It is unfortunate that Dawe did not report the theoretical predictions for the positions of the neutral axis and instantaneous centre.

Dawe's work was later summarized and presented by Dawe and Kulak in 1974[43].

2.10 The main objective of Crofts' work was to investigate the full plasticity idea proposed by Koenigsberger[15] in 1951. Koenigsberger[15] suggested that the entire length of weld in a joint subjected to torsion and shear was plastic at the moment of failure.

Two series of tests were conducted, the first to determine the ultimate torsional capacity of elemental lengths of weld, and the second to determine the ultimate capacity of full lengths of weld.

It was hoped to show that the sum of the capacities of the elemental welds was equal to the capacity of the full length weld. The elemental length was chosen at 15 mm and it was assumed that a weld of such length would be fully plastic at failure.

Crofts concluded that the experimental results verified Koenigsberger's[15] assumption of full plasticity.

The experimental technique used by Crofts is notable for the fact his test welds were machined to exact lengths and to an exact profile of 45° (4.1 mm leg), thus eliminating the size variable which has resulted in large scatter reported by previous investigators. Unfortunately, Crofts welds suffered from lack of root penetration and as a result some of the benefit gained by machining was lost. His average ultimate shear stress was 340 N/mm^2. A further, more important advantage gained by machining is a fairly uniform fracture surface which approximates a plane. Crofts' type of specimen is not really of a design which would give a fracture surface as a plane because of the twisting action of the torsional moment. Nevertheless, Crofts was able to make the first meaningful quantitative assessment of fracture 'plane' angles.

This quantitative assessment was made use of by Crofts and Martin[45], for the development of a failure criterion based upon the actual critical plane. With the exception of Archer[19] and Butler[30], all criteria have been based upon the throat section.

With regards the Crofts and Martin criterion, the forces acting on the test welds have been resolved into directions parallel and normal to the actual fracture plane. Normal and shear stresses have been computed

on the basis of uniform distribution over the critical plane area. It was pointed out the stress distribution was not likely to have been uniform, but for the sake of simplicity it was assumed so. These calculated failure stresses are shown in fig. 50.

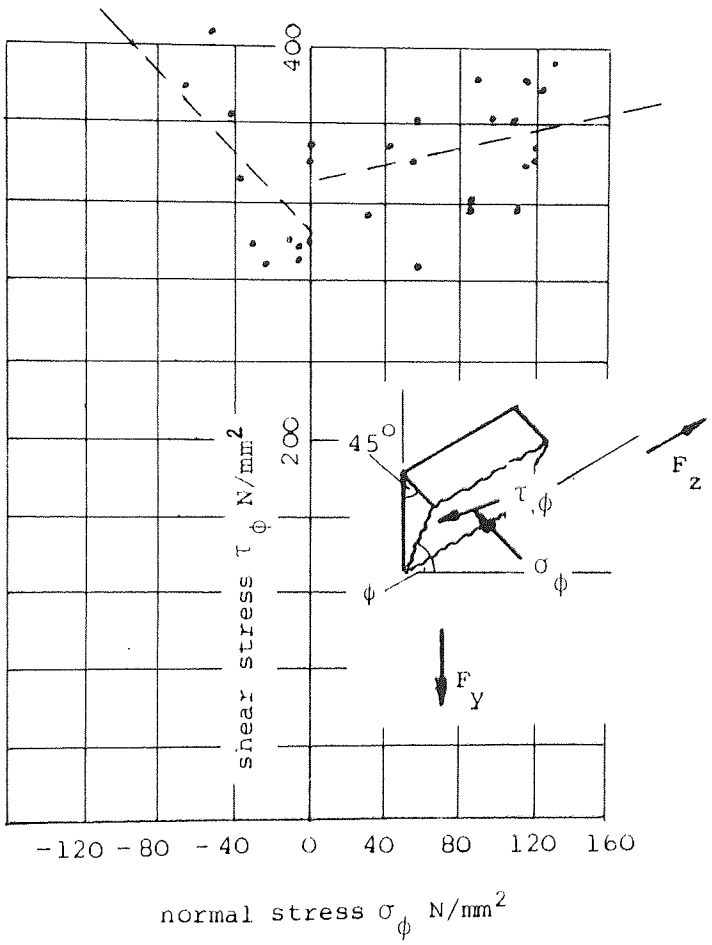

Fig. 50 Stresses on the Failure Plane (short welds)

The failure criterion proposed by Vreedenburgh[16], was based not on the actual failure plane, but on the theoretical throat, and its shape cannot be simply represented arithmetically. Crofts and Martin

propose here a linear relationship which is much simpler and hence more attractive. The criterion was expressed as follows:

$$\tau_{\phi} = A\sigma_{\phi} + \tau_{ult} \qquad (1)$$

where A = slope of line.

Values of A and τ_{ult} were obtained by regression analysis of the experimental results and were,

(i) tension/shear zone, A = 0.21 & τ_{ult} = 331 N/mm^2

(ii) compression/shear zone, A = 1.06 & τ_{ult} = 305 N/mm^2

A theoretical method was then proposed for the prediction of ultimate capacity of short welds when subjected to forces on the x, y and z plane:

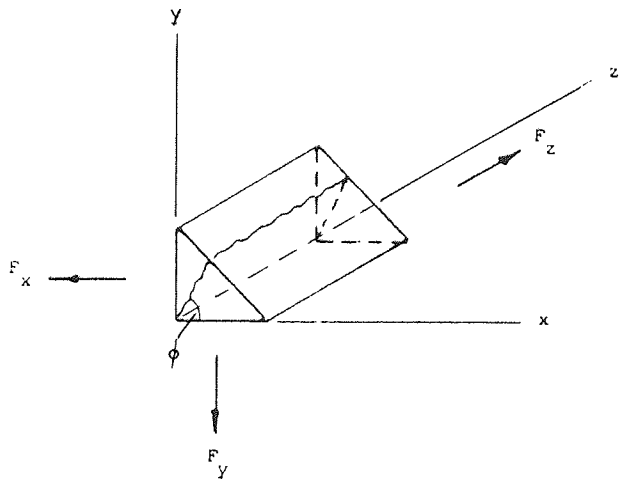

Fig. 51 Forces on a Weld

With reference to fig. 51 by resolution of forces the shear stress on the theoretical critical plane at angle ϕ is

$$\tau_{\phi} = \frac{\sqrt{[(F_x \cos\phi + F_y \sin\phi)^2 + (F_z)^2]}}{t/(\sin\phi + \cos\phi)} \qquad (2)$$

and the normal stress:

$$\sigma_{\phi} = \frac{F_y \cos\phi + F_x \sin\phi}{t/(\sin\phi + \cos\phi)} \qquad (3)$$

Equations (1), (2) and (3) were then combined to give an expression relating F_x, F_y and F_z with the critical plane angle ϕ as a variable.

For Crofts' test specimens, $F_x = 0$ and F_y and F_z were expressed in terms of the torsional resistance. The value of ϕ giving the torsional resistance a minimum value, was obtained by iteration and hence the theoretical values for both ϕ and torsional resistance were obtained.

Crofts and Martin admitted the method of solution was too laborious for use in design and suggested that it might be possible to present the solution in tabular or graphical form.

It is difficult to assess the accuracy of the method proposed because the experimental results for both torsional resistance and fracture angle show a fair degree of scatter and naturally this scatter is more acute on the failure criterion plot, fig. 50. Because of the degree of scatter it is difficult to justify a linear relationship between the normal, and shear stresses acting on the critical plane. Having chosen to fit a straight line it becomes more difficult to accept since the two straight lines cut the shear axis at two different levels, implying the weld metal has two values of ultimate shear strength - with F_y equal to zero, then the ultimate shear strength is dependent upon the direction of F_z. This is inexplicable and Crofts and Martin offered no explanation. However, in spite of all the scatter there is reasonable correlation between theoretical and experimental results.

Up until this time no investigator has reported a study of the specific effects of plate-bearing on the ultimate capacity of welded beam-column connections. Dawe[42] did present an analytical method for predicting the ultimate capacity of welded connections with plate bearing but, did not assess the actual contribution by the plate-bearing to the ultimate capacity.

2.11 In 1975 Higgs[46] conducted a series of tests with the objective of assessing the specific contribution of plate-bearing. Two series of simple beam-column web-welded connections, one in which the plates were in direct contact, and the other with grooved back-plates so that direct bearing was avoided, fig. 52. Both series were thermal stress relieved at 600 °C so that the results could be directly compared.

Higgs developed a welding technique which produced 100% root penetration, and an ultimate shear strength of 440 N/mm^2, this being approximately 25% greater than strengths so far reported.

Like Crofts[44], Higgs machined his welds to a given length and exact profile of 45°. The leg length was 4 mm. Ten tests were made on specimens with plate bearing and nine tests without, range of e/d was from 0.13 to ∞. This is the first time that a full range has been tested.

Higgs found that for his connections the effect of plate bearing was to increase the ultimate capacity as follows: increased shear resistance at a given moment by an average of 31% or, increased moment resistance at a given shear load by an average of 14.25%. The increase in ultimate capacity was attributed to the presence of friction at the point of bearing and the change in the position of the point of rotation of the connection.

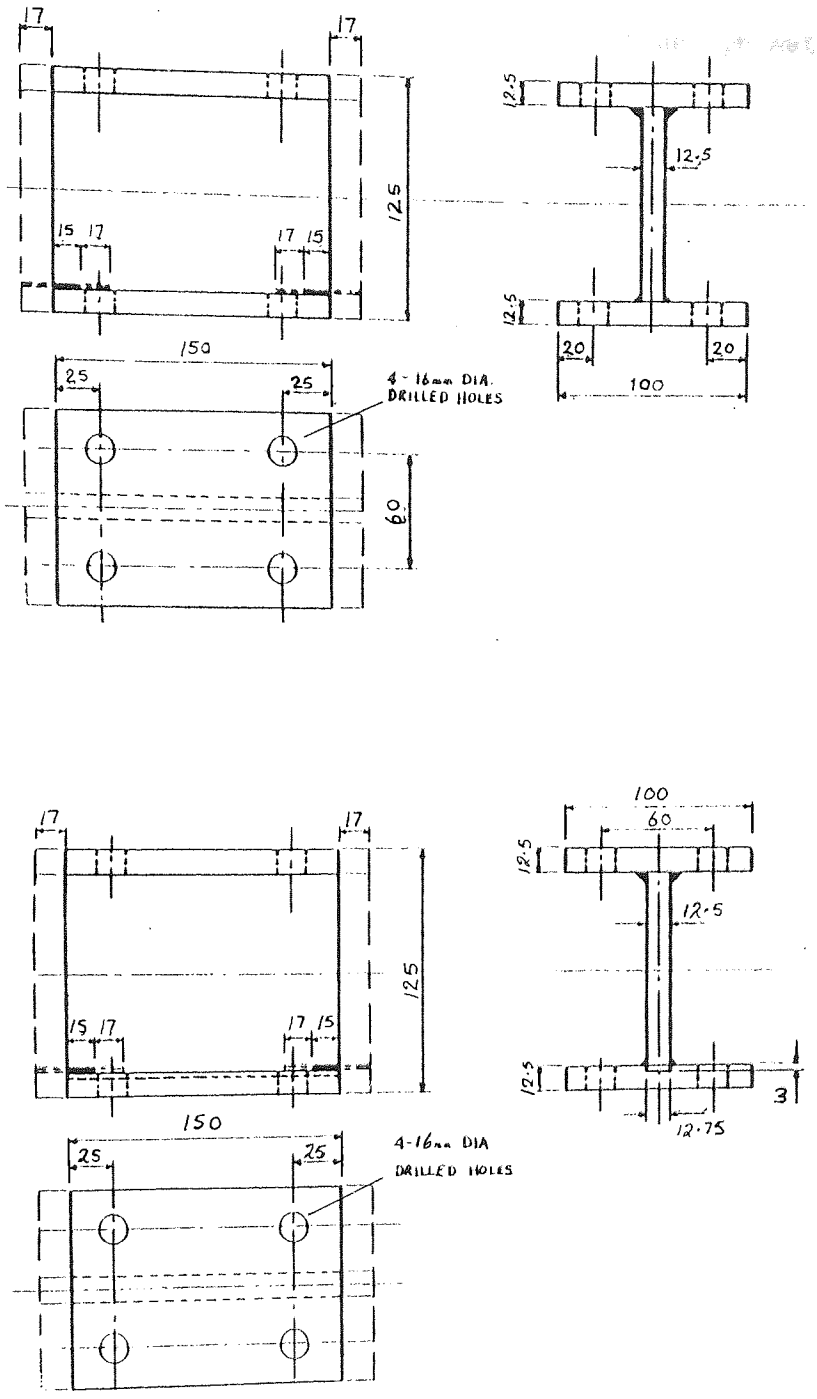

Fig. 52 Beam-column Test Specimens

These figures, as Higgs points out represent a significant increase in the ultimate capacity. None of the current design methods take any account of plate bearing.

Higgs then went on to examine the failure criteria proposed by Crofts and Martin[45], though in Higgs' case he could only look at the tension/shear field.

His assessment of the fracture plane angles appears to be more accurate than Crofts'[44] and he reports more uniform surfaces. The angles were measured on a shadow-graph at a magnification of x20. The failure plane stresses were computed in a similar way to Crofts and Martin[45], and produced a failure criterion for the tension/shear field for both series of connections:

(i) series with plate bearing

$$\tau_\phi = 0.2\sigma_\phi + 420 \text{ N/mm}^2$$

and

(ii) series without plate bearing

$$\tau_\phi = 0.0\sigma_\phi + 420 \text{ N/mm}^2$$

i.e. an ultimate shear strength criterion.

It must be pointed out that Higgs' specimens were stress relieved before testing. It is difficult to see why there should be two criteria for the welds under tension/shear since the effect of removing the bearing in the compression zone could have no effect upon the strength of the tension weld which would still be loaded in the same way. It is true that the connection will be stronger but, it is not the slope of the criteria that causes this, but the presence of friction and the change in the

position of rotation. It was reported there was only an insignificant difference between the fracture angles of comparable specimens of the two series.

Fitting a single criterion by linear regression, to the complete set of results gives

$$\tau_\phi = 0.1342\sigma_\phi + 417.65 \text{ N/mm}^2$$

compared to Crofts and Martin[45],

$$\tau_\phi = 0.21\sigma_\phi + 331 \text{ N/mm}^2$$

The difference in the ultimate shear strength is attributed basically to root penetration. One would not expect the slopes of the above criteria to be equal because of the stress relieving by Higgs, however, bearing this in mind they are comparable and some credibility has been given to the work of Crofts and Martin[45].

2.12 In 1976 Commission XV of the I.I.W. published a document[47] setting out general design rules for welded connections submitted to static loads. The recommendations, which were based upon a decade of international co-operation, did not commit the I.I.W. as a whole and were merely meant as guide lines rather than definitive rules.

Changes were made to the I.S.O. stress criterion, i.e. from

$$\sigma_c = \sqrt{\sigma_1^2 + 1.8(\tau_1^2 + \tau_{11}^2)}$$

to

$$\sigma_c = \beta\sqrt{\sigma_1^2 + 3(\tau_1^2 + \tau_{11})^2}$$

where σ_c was to be taken as equal to the permissible tensile stress in the base material, provided the workmanship and welding techniques were satisfactory, and

$\beta = 0.7$ for base metal F_e 360

$\beta = 0.85$ " " " F_e 510

Other values of β were to be determined by linear interpolation proportional to the guaranteed yield strength of the steel.

With regard the distribution of load among the individual welds of a joint, two approaches were suggested:

1. the load in the weld to be assumed to depend directly on the stress in the adjacent parent metal, or
2. the joint is to be considered to constitute a separate unit in the structure and the loading of the individual welds was derived from the load of the entire joint.

With regards beam-column connections it was recommended to allocate the moment as a couple of forces to the flange welds and the shear force to the web. Where columns were not stiffened an effective width factor was to be applied to the beam flange width (assuming column and beam have equal flange widths):

$$\text{effective flange width} = C_1 . t_1 + 2.t_2$$

where t_1=the flange thickness of the column

t_2=the web " " " "

Factor C_1 to be selected from the following table:

C_1			
7	5	tensile flange	F_e 360
10	7	compressive flange	
5	4	tensile flange	F_e 510
7	6	compressive flange	
I section column	box-section column		

For stiffened columns the flange width was assumed to be 100% effective.

Once again, the analysis assumes the neutral axis to be at half-beam height, and takes no account of the plate-bearing.

The proposed method is bound to involve a variable, conservative safety factor.

2.13 Large numbers of static tests of butt-welded structures have been made with the object of determining the condition under which residual stresses may contribute to fracture. Some of these would seem to justify the opinion held by many that residual stresses have little or no influence. Nevertheless, many failures have occurred in practice during and after welding of engineering structures that could only be explained by assuming that residual welding stresses contributed to the failure. Failures have occurred in both the welded plate and the weld itself and many of the plate failures were initiated by prior failure of the weld.

Correlation between laboratory results and known field conditions has not been very fruitful. Greene[48] suggested this was due in part to the characteristically small size of laboratory test specimens. He commented it could not be expected that residual stresses would obtain to appreciable levels in the small specimens prepared for tensile and other tests. Greene believed, as other investigators before him,the effects of residual stresses were nullified as soon as yield state had been reached. Greene's interests were in the behaviour of the plate rather than the weld itself and he assumed that as soon as a state of yield had been reached in the plate the residual stresses were relieved.

Tests were conducted on butt-welded plates approximately one metre square. During welding, defects such as notches and triaxial stress

raisers, were included in the welds. Bend tests were then conducted at various temperatures from -25 to 40°F and all specimens failed in a brittle manner with little or no deflection, at bending stresses from 0 to 17,000 lbf/in^2, i.e. well below yield stress of the plate. Another series of tests was conducted, on specimens which had been stress relieved by the low temperature method, i.e. at 350°F, and all sustained loads well above the yield point. It is difficult to gain any information about the behaviour of the actual weld from Greene's tests. The actual modes of failure were not described.

Similar tests have been conducted by other investigators[49,50,51] and it has been shown that both preheating, and post thermal stress relieving of butt welded steel plates greatly reduces the tendency to brittle fracture. The interest in the above tests was centred on the behaviour of the plate, and failure was centred on some deliberately introduced stress raiser such as a vee-notch. Parker[52], pointed out that experimental evidence appeared to indicate that residual stresses had little effect unless defects such as a crack were present. In the case of the fillet weld, however, the geometry is sufficient to guarantee a stress raiser at the root, and this coupled with a generally eccentric load on the weld will create a very unfavourable condition. It was further pointed out that although the longitudinal residual stress of butt-welds frequently reached the base metal yield point, the stress in the transverse direction was normally much less. This reasoning is of course only applicable to unrestrained plates. With regard to welded structures it was suggested the residual stress was a combination of two types of stress:

(i) direct welding stress as a result of weld shrinkage, and

(ii) reaction stress as a result of the restraint offered by the structure to thermal deformations in the joint.

It must be the case that the residual stresses are generally elastic, and will store elastic strain energy. The direct welding stress energy is contained in only a small volume and consequently the amount of energy stored is small. On the other hand, the reaction stresses are stored in the large volume of the structure but they may develop their effects in any part of this volume, however small. This stored energy is bound to have its effects at defects and stress raisers such as a fillet weld root. It is only the direct welding stresses that may necessarily be relieved during plastic deformation.

Parker did report on the effects of thermal stress relieving on the physical properties of mild steel weld metal. After stress relieving for 2 hours at 600°C the following changes were noted:

6.25% reduction in tensile strength

16% increase in elongation

7.5% reduction in yield strength.

He attributed these changes largely to alterations in the microstructure of the weld metal.

Wheatley and Baker [53,54] conducted tests on weld specimens machined from deposits of 6XX, basic coated electrodes, on mild steel plate. These specimens were reheated to various temperatures and changes in mechanical properties were investigated. The following deductions may be drawn from their results:

(i) there is no appreciable reduction in yield or tensile strength unless the weld metal is heated above the eutectoid temperature,

(ii) there is slight increase in the yield and ultimate tensile strengths on heating at temperature in the range 500° - 650°C and,

(iii) there is no appreciable change in either the reduction in area on the elongation until the eutectoid temperature is reached.

In view of the above findings it may be concluded that the changes in mechanical properties reported by Parker[52] are probably due entirely to the relaxation of residual welding stresses. It follows then that residual welding stressses are not entirely elastic in their behaviour and not fully relieved during plastic deformation.

Higgs[46] reported a reduction of 4.5% in the ultimate shear strength of longitudinal fillet welds of lapped test specimens as a result of stress relieving at 600°C. These are the only reported tests of stress relieving of fillet welds.

2.14 Current methods used for the prediction of ultimate strength of fillet welds have been shown to be very conservative, and produce variable and unknown safety factors. This is hardly surprising since there is ample evidence to show that the position of the critical plane is variable and rarely at the throat where it is assumed to be for the current methods.

Various empirical, and theoretical limiting criteria have been examined, the first of these, proposed by Vreedenburgh[16], has been largely discredited because it was based upon the throat section, and predicted unrealistic strength for welds in compression. There is evidence to suggest the fillet weld under compression may in fact be weaker than when under tension.

The theoretical maximum shear stress criterion proposed by Archer et al[22], is of interest since it is based upon a theoretically variable critical plane. This proposed criterion was not convincingly verified by the twenty-one test results provided by Jensen[5], in 1934.

An alternative to the limiting stress envelope criterion, namely a limiting weld deformation, has been proposed by both Clark[26], and

Butler et al[30]. This takes the form of empirical load-deformation characteristics which in the case of Butler et al[30] have been expressed mathematically. Use of these criteria involves a very lengthy iterative procedure which is going to be very difficult to simplify for design office use, unless the method is presented in a series of ultimate load tables.

The empirical limiting stress envelope proposed by Crofts and Martin[45] which is based upon the actual critical plane, takes a linear form and shows suitability for use by designers. It is obviously far better to have a generally applicable strength criterion than large numbers of interaction curves and tables.

The current design procedures used for beam-column connections are based on the procedures formerly used to analyze riveted joints. The neutral axis is assumed to be at half beam-depth and no account is taken of plate-bearing.

Alternative methods have been proposed, but these have been compared, in general, with only a few, and unreliable experimental results having appreciable scatter. Ligtenberg's work[25] was really of an exploratory nature and served its purpose by indicating the importance of column flexibility, flange stiffness and weld size.

Archer et al[22] proposed a method of prediction of ultimate capacity based upon their maximum shear stress criterion. Effects of friction and plate-bearing were ignored and the neutral axis was assumed to be at half beam-height. Their difficulty was the distribution of the shear load between top and bottom flange welds. This was solved by the choice of an arbitary shear load sharing relationship which accounted for the effects

of flexibility of the web and the flanges. No attempt was made to explain or assess these effects.

The presence of plate-bearing was taken into account in the method proposed by Dawe[42], and also the position of the neutral axis and the centre of rotation, both of which were assumed to be instantaneous. Dawe's method is based upon the load-deformation criteria proposed by Butler and Kulak[30], and its solution requires an iterative procedure. The flexibility of the beam web and flanges was not considered. Dawe attempted to verify his method with three series of tests, totalling 16 individual specimens, and covering too many variables.

The main interest in residual stress has been concentrated on its effects upon brittle fracture of the base material, and the effect upon the ultimate strength of fillet welds has not been investigated. There is a common belief the effects of residual stresses are nullified as soon as yield point has been reached owing to the purely elastic nature of the stresses. However, changes in physical properties of weld metal resulting from thermal stress relieving have been reported by Parker[52], who attributed such change to changes in microstructure of the weld metal. Wheatley and Barker[53,54], on the other hand showed that microstructural changes resulting from stress relieving at 600°C did not produce the changes Parker found.

CHAPTER 3

EXPERIMENTAL OBJECTIVES

Current design practices attribute welds under compression with a strength of at least equal to that attributed to welds under tension - such a treatment has been fostered by the experimental results of Vreedenburgh[16]. Evidence contrary to that of Vreedenburgh was presented by Bibber[1] and Schreiner[7].

It is generally assumed that relief of residual stresses results in increased ductility and a consequent decrease in ultimate capacity of the weld metal. This reduction in ultimate capacity is certainly applicable to butt welds and weld metal in isolation. It is not necessarily applicable to fillet welds in sitio, since failure of such welds is probably initiated at the weld root and an increase in weld ductility could well be accompanied by an increase in ultimate weld strength.

There is a wealth of evidence[5, 16, 22, 45, 46 and 55] to show that the actual fracture plane of a fillet weld is rarely at the throat section as it is assumed to be by existing codes and design procedures, however, only two methods[22, 46] of ultimate load prediction based upon a variable fracture plane have been presented.

Very little work has been reported on the ultimate capacity of beam-column connections, and only Ligtenburgh[25] made any attempt to assess the effects of beam flange flexibility.

As a consequence of the above and the summary of the Historical Review the following objectives were judged to be pertinent:

1. To determine the ultimate strength of fillet welds in compression relative to those in tension.

2. To ascertain the effect and significance of residual stress upon the ultimate capacity of fillet welds.

3. To investigate the validity of the maximum shear stress criterion proposed by Archer et al.

4. To extend the failure criterion of Crofts and Martin.

5. To develop a method, based upon an extended Crofts and Martin criterion, for the prediction of ultimate capacity of beam-column connections.

CHAPTER 4

EXPERIMENTAL PROCEDURE

The experimental work was divided up into two phases:

(i) design and testing of small specimens for the development of the Crofts and Martin[45], failure criterion.

(ii) design and testing of full-sized beam-column connections for the development of a method for ultimate load prediction based upon a developed Crofts and Martin[45] failure criterion.

4.1 Failure Criteria Specimens

The obvious thing to do was to endeavour to continue work with the Crofts and Martin[45], style of test specimen, fig.53, with the hope of extending the field of the failure criterion in both the compression/shear and tension/shear quadrants. It was felt the field of the criterion was too limited, see fig.50, and would not cover all loading situations applicable to fillet welds. It must be noted that Crofts and Martin

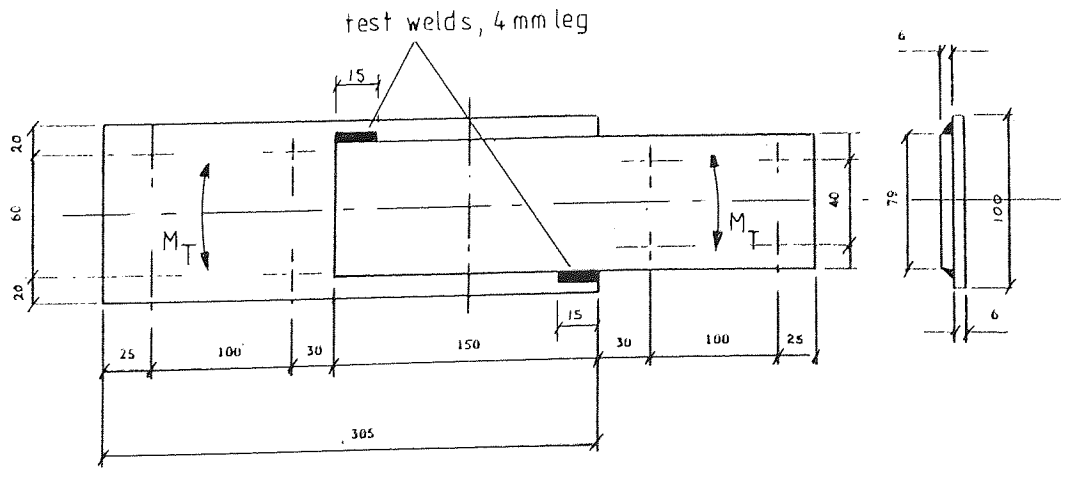

Fig.53 Crofts and Martin Style Test Specimen

test specimen, fig.53, was not designed primarily for the investigation of stresses acting on the critical plane, but for an investigation of the concept of full plasticity proposed by Kroenigsberger[15]. However, since the failure criterion had been derived from this style of specimen it was decided to at least undertake a preliminary testing programme to establish the suitability of the style for the development of the criterion.

Twenty-six specimens were manufactured with the welds being machined to a length of 15 mm and to an exact profile of 45° with leg depth of 4 mm. The improved welding technique of the author[46], was used, and can be summarized as follows:

Angle of inclination to root:	20°
Open circuit potential:	100 volts r.m.s.
Polarity:	work positive
Welding speed	fast enough to prevent spluttering or arc extinction
Electrodes:	Mirrospeed S.W.G.8, Class E.217
Current:	ranged from 227 to 190 ampere depending upon temperature of plates.

Contact between electrode-tip and the root was always maintained.

Fifteen of the specimens were tested in the as welded condition and the remainder after thermal stress relieving at 600°C for 30 minutes (air cooled). The test variable was the distance between the elemental welds, this ranged from 0 to 150 mm. The fractured specimens were cut up and the angle of the fracture 'plane' was measured on a shadow-graph at a magnification of x20. The fracture surfaces were not very planar as a result of the rotation of the weld metal during their failure, and this made meaningful fracture angle measurement rather difficult. Evidence of this rotation can be seen in Plate 1.

It was decided to abandon the Crofts and Martin style specimen in favour of one without rotation. A double lap-joint was considered, like that shown in fig.39, in which the angle of the longitudinal axis of the weld to the line of action of the applied load could be varied. The required test variable is the ratio F_x/F_z, see fig. 51, and in order to extend the field of the failure criterion, this ratio was required to vary between zero and infinity.

Thirty specimens were made up from *B.D.M.S. bar 125 x 19 mm and 75 x 12.7 mm, using the welding technique already mentioned. Before welding the plates were de-greased, scratch-brushed and linished. The welds were machined to size as before. Half of the specimens were tested under a tensile load and the other half under a compressive load.

It was soon apparent the required range of the ratio F_x/F_z was not going to be achieved without great difficulty and changing of the plate thicknesses. It was considered that changing of the plate thickness during a testing programme would invalidate the results owing to the attendant charges in residual stress - the double lap-joint was abandoned. A fractured specimen of this style is shown in plate 2, along with a typical microstructure of the machined weld showing the quality produced by both the welding and machining techniques. All the welding and machining was done by the author.

A great deal of thought was given to the style of specimen with which the required ratios of F_x/F_z could be achieved by the application of a single external load. Jensen's[5] test specimen was considered, but rejected because of the difficulty of achieving compression of the weld

---

* B.D.M.S. - Bright drawn mild steel.

Plate 1 Fractured Crofts Style Specimens

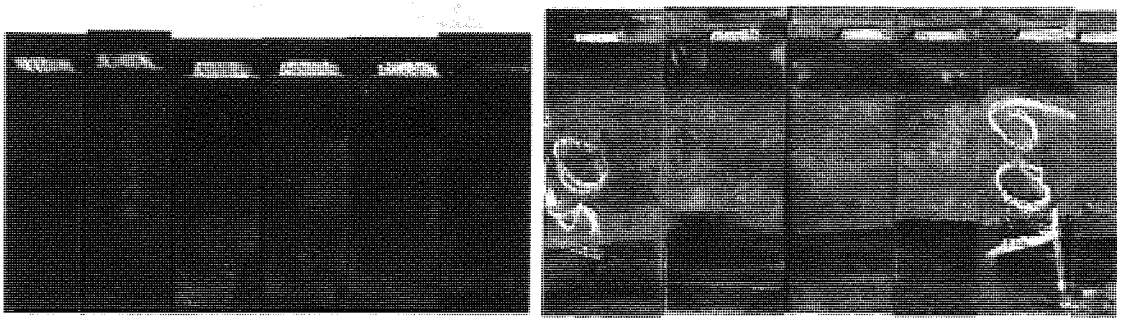

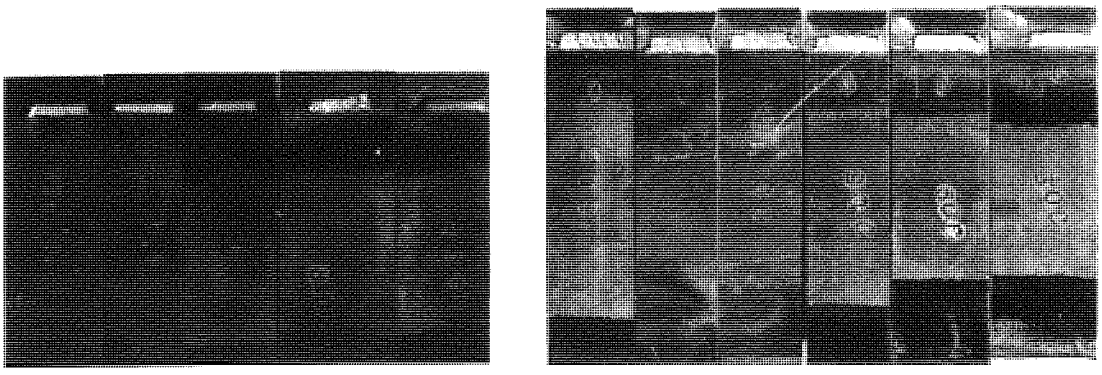

(b) stress relieved (a) as welded

Plate 2 Fractured Failure Criterion Specimens

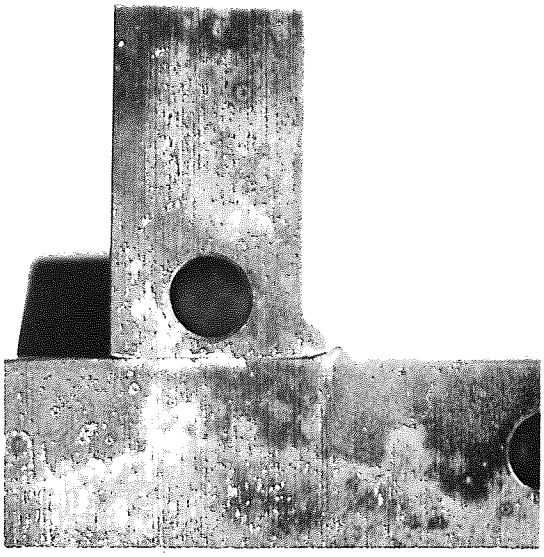

Style L Specimen, L8

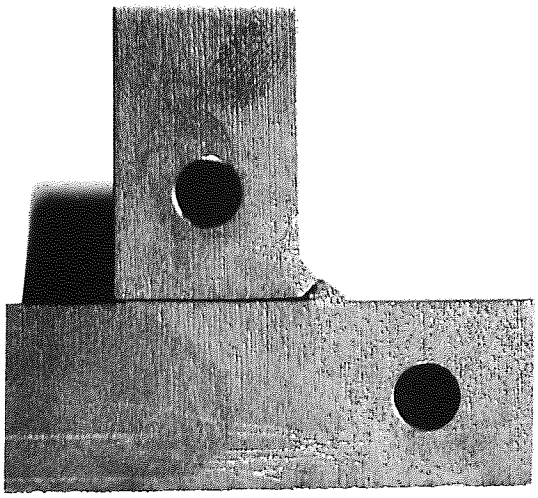

Style L Specimen, L33

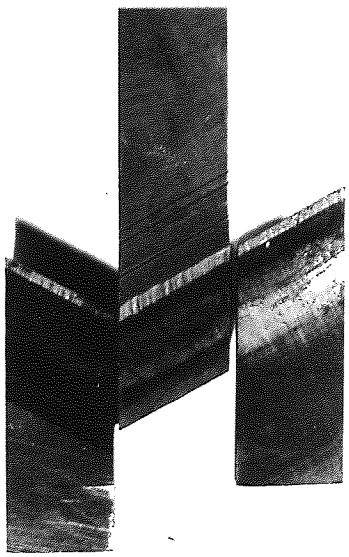

Double Lap-Joint, SC7

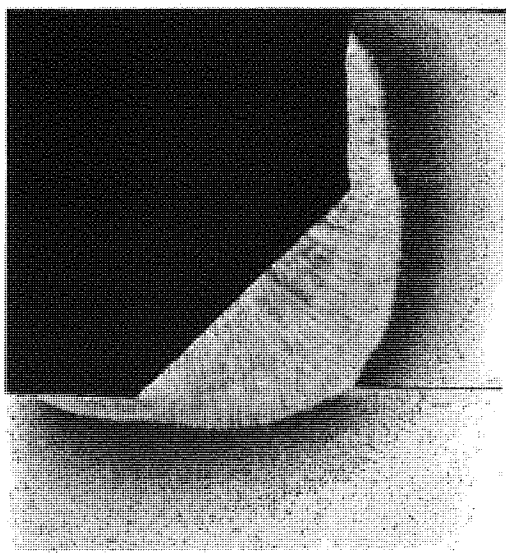

Microstructure of Machined Test Weld

without simultaneously producing plate bearing. This style of specimen is suitable only for investigation of the ratio F_x/F_y since no force in the F_z direction is implied.

Eventually it was concluded the necessary conditions were best achieved using a double external load system - one load applying the F_z force, and the other the F_x force, tensile or compressive. The test set-up envisaged was a 50 tonne Denison Testing Machine, to apply the F_z force, in conjunction with a hydraulic ram to apply the F_x force. Such a system of loading is represented in fig.54 (a) and (b). By use of bearings it was hoped to obtain uninhibited relative movements, in both vertical and horizontal directions, of the two parts of the test specimens during failure thus eliminating weld rotation. The biaxial loading jig was designed by the author and detailed drawings can be found in the Appendices.

The test specimens were manufactured by the author using the materials and techniques already described, and are shown in figs. 55 and 56. The biaxial loading rig, test specimens and test set-up are shown in plates 3 and 4.

Ninety-six specimens were tested in the as welded condition, and fifty-nine after thermal stress relieving at 600°C for one hour. The ratio of F_x/F_z ranged from zero to infinity.

The hydraulic ram and pressure gauges used were calibrated against the Denison Testing Machine and data can be found in the Appendices.

Although the tests of styles T and C specimens conducted covered the complete range of F_x/F_z little extension of the field of the

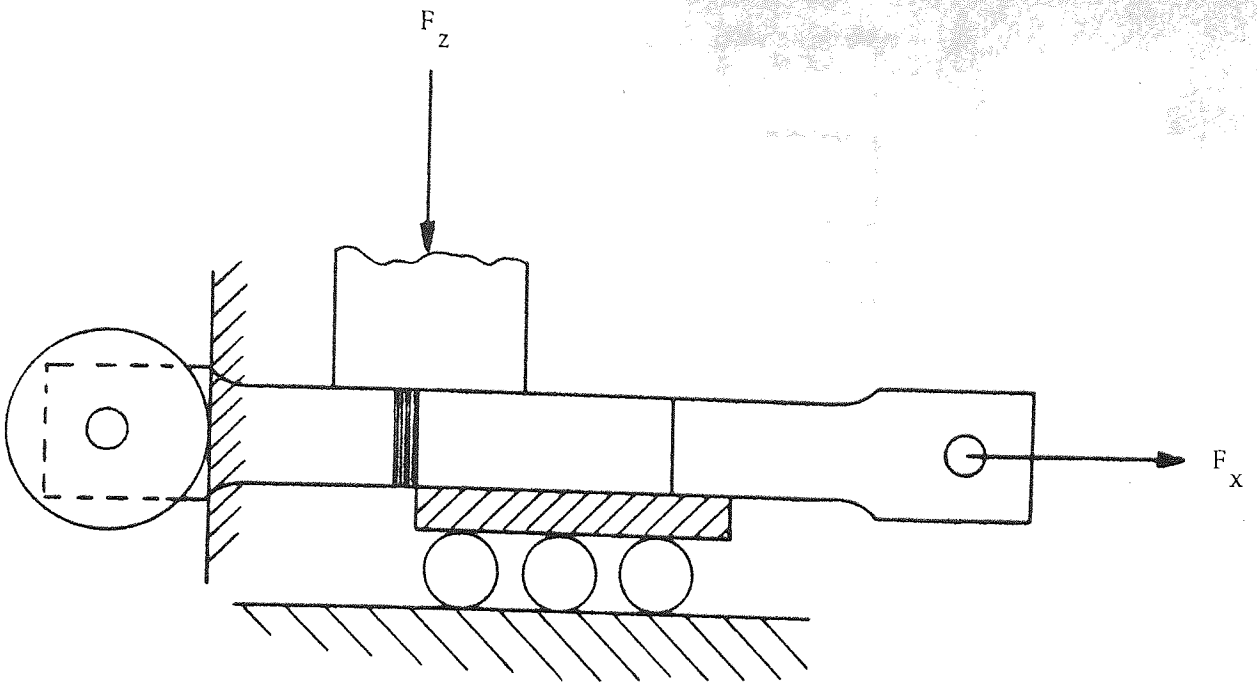

(a) Loading of Style T Specimen

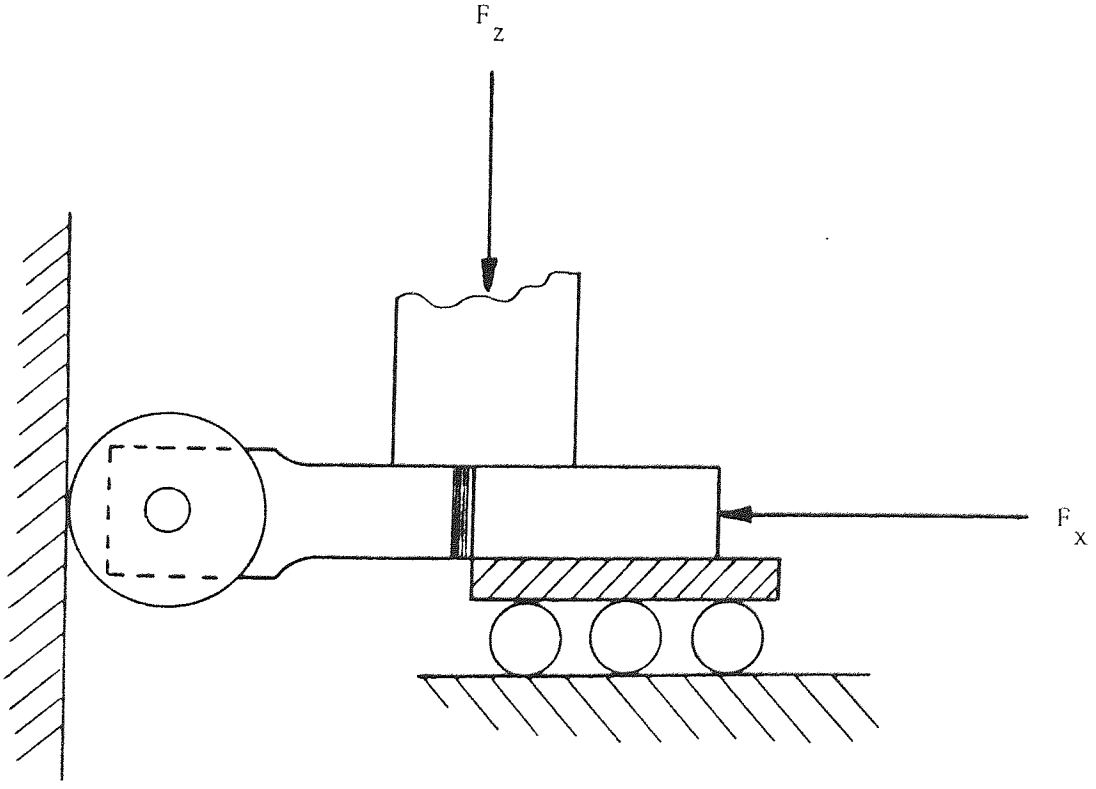

(b) Loading of Style C Specimen

Fig.54 Method of Loading Failure Criterion Specimens T and C

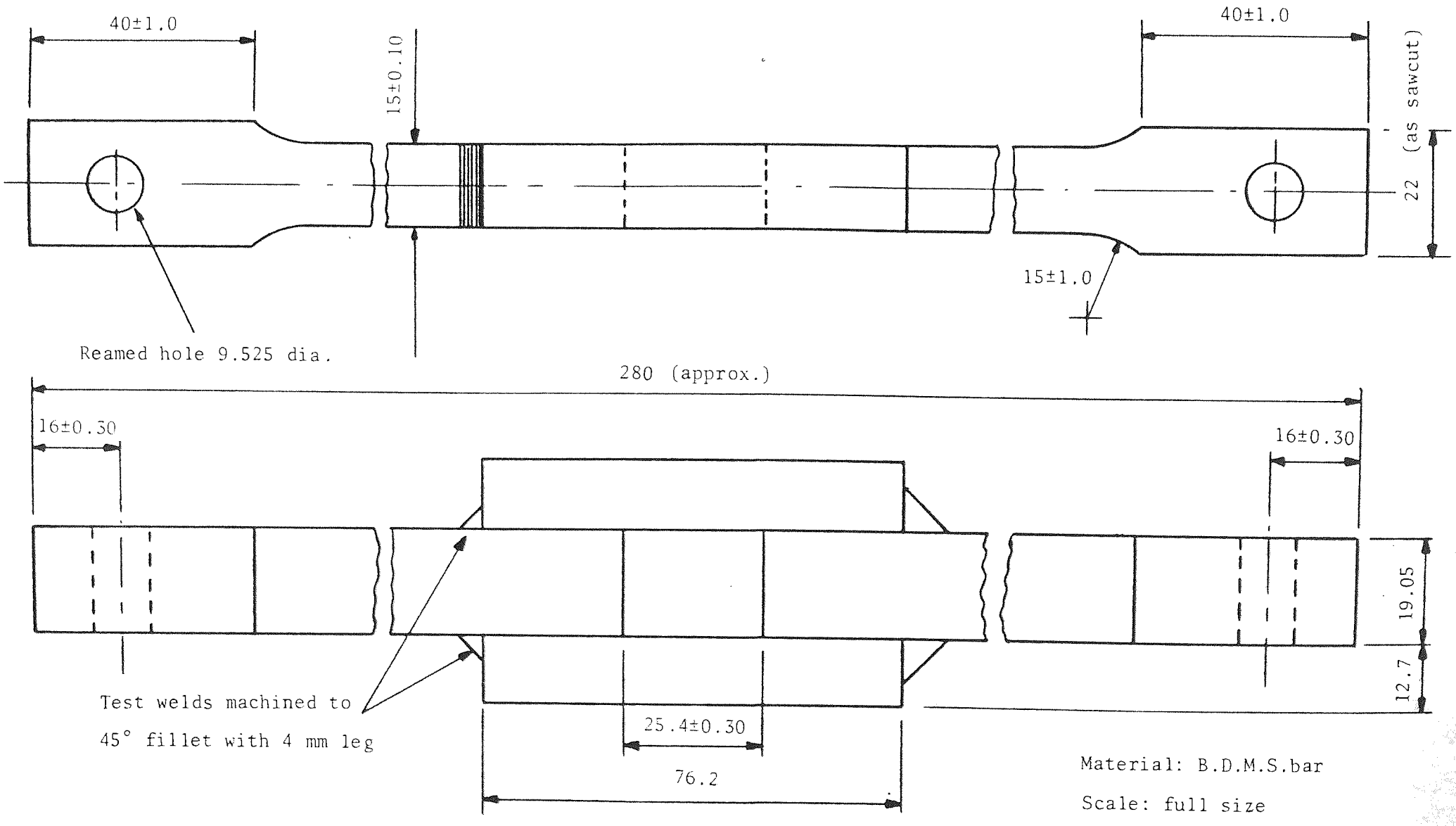

Fig.55 Failure Criterion Test Specimen, Style T

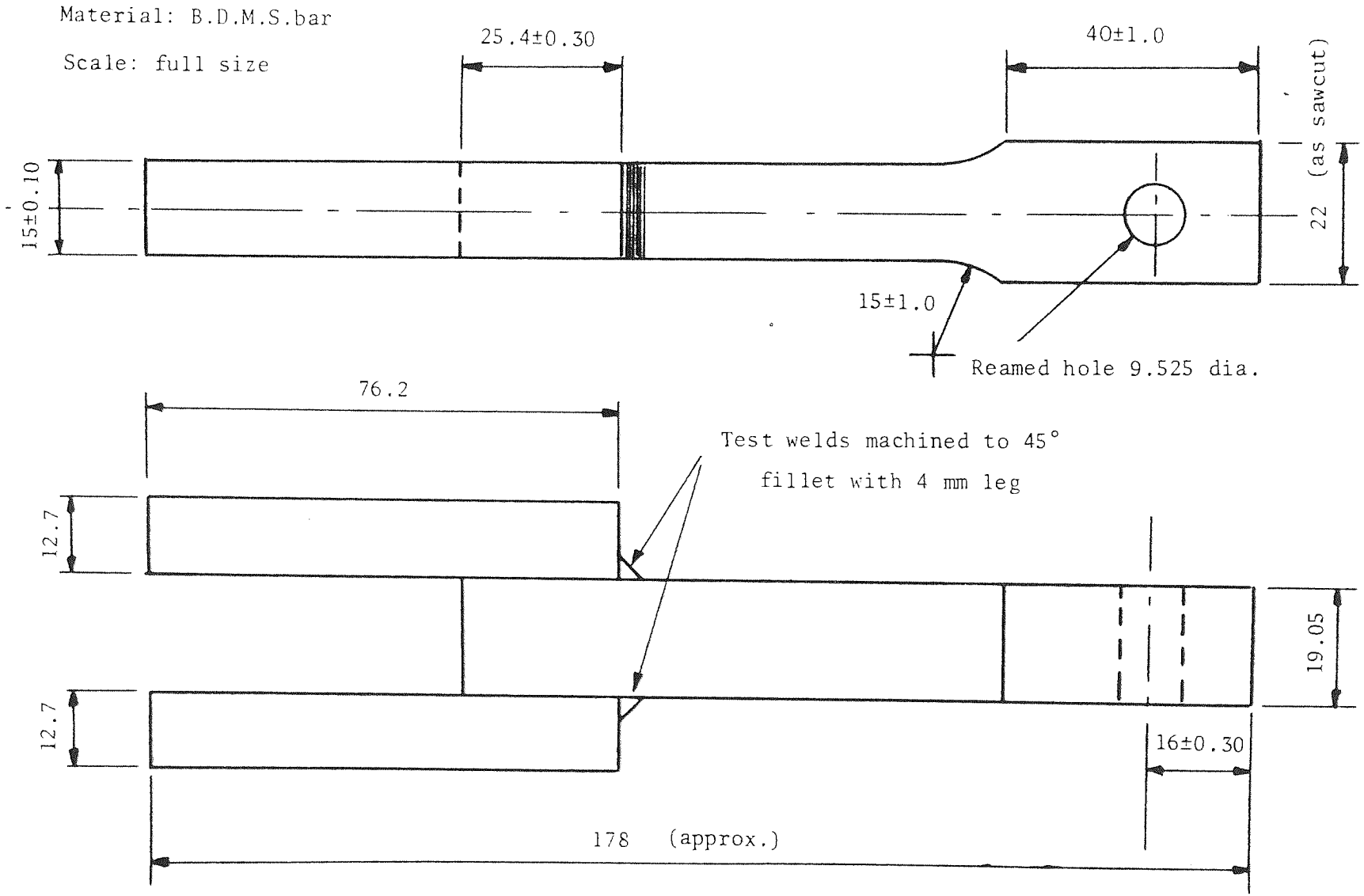

Fig.56 Failure Criterion Test Specimen, Style C

failure criterion in either quadrant was obtained. It was obvious then that in order to obtain the required extension, tests on welds subjected to F_x and F_y would have to be made.

A very simple test specimen was conceived, style L shown in fig. 57, which would give the required range of F_x/F_y with a single external load application, see fig.58. By altering the positions of the holes the angle of the applied load to the throat section could be varied. It was assumed the reaction to the externally applied load would be acting at the mid-point of the throat section. This was obviously not strictly true since the stress distribution on the critical plane was unlikely to be uniform, and the actual critical plane unlikely to have been at the throat. However, for the proposed range of F_x/F_y it was expected the actual critical plane to have been close to the throat section. The external load was applied with the Denison Testing Machine, see plate 4.

It was appreciated that the level of residual stress in the style L specimen would not be the same as that in the styles T and C specimens, which in themselves were likely to have been different owing to the lack of reaction stress in style C specimen.

The plates of the style L specimens were tack-welded, prior to the test weld being laid in an attempt to reduce distortion resulting from weld shrinkage. The holes in the legs of the specimen were drilled after welding in such a position that after initial loading of the specimen the distortion would have been corrected, and both shrinkage and reaction stresses reimposed. With the distortion corrected the legs would then have been perpendicular and the line of action of the external load would have been passed through the mid-point of the throat section.

Plate 3 Testing Arrangements for Failure Criterion Specimens

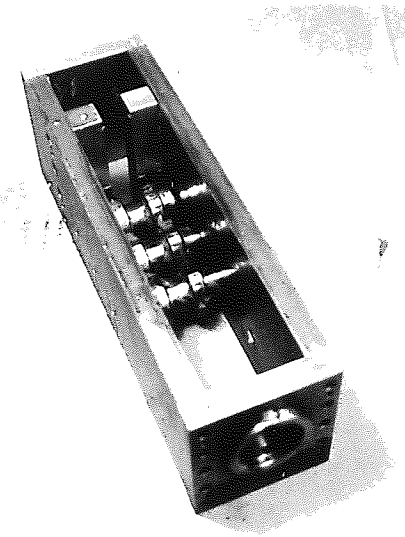

Biaxial Loading Jig

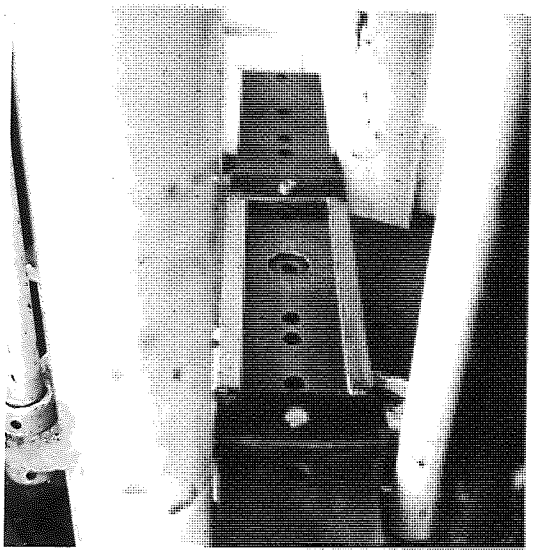

Denison Machine - Location Frame

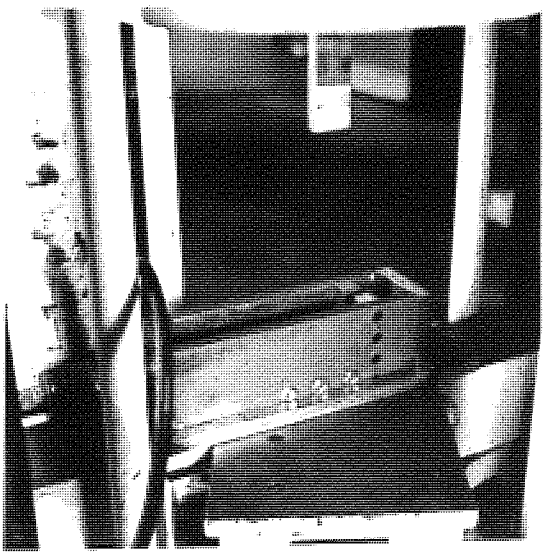

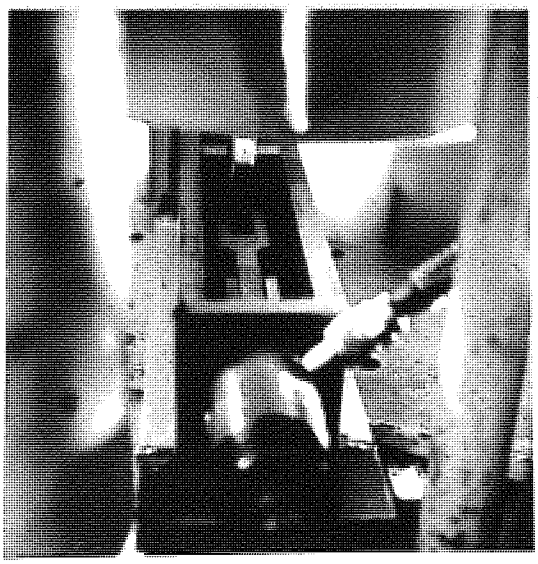

Biaxial Loading Jig & Denison Machine Ready for Test

Plate 4 Loaded Failure Criterion Specimens

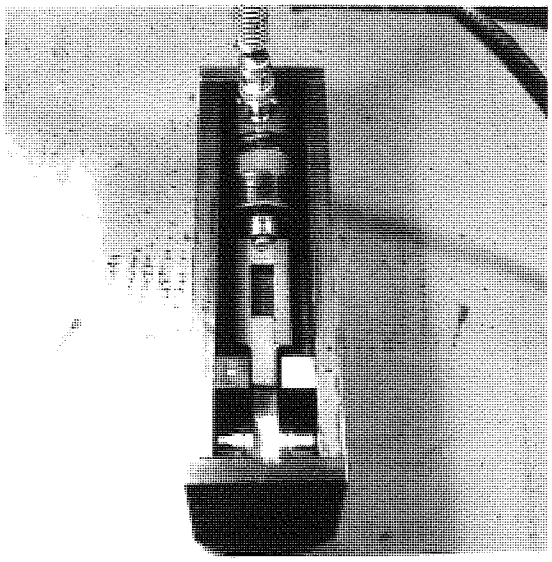

Loaded Jig - Style C

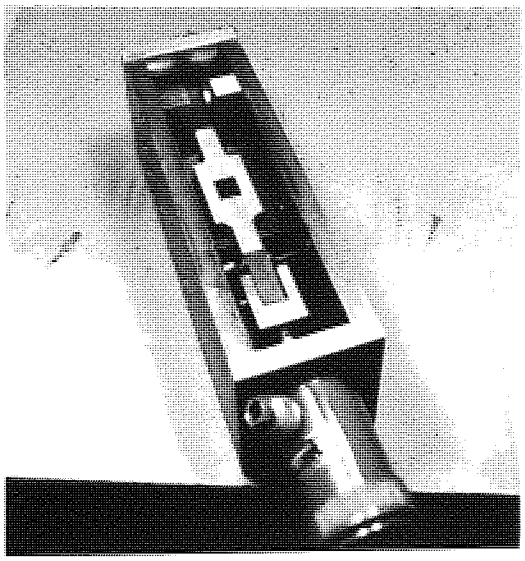

Loaded Jig-Style T

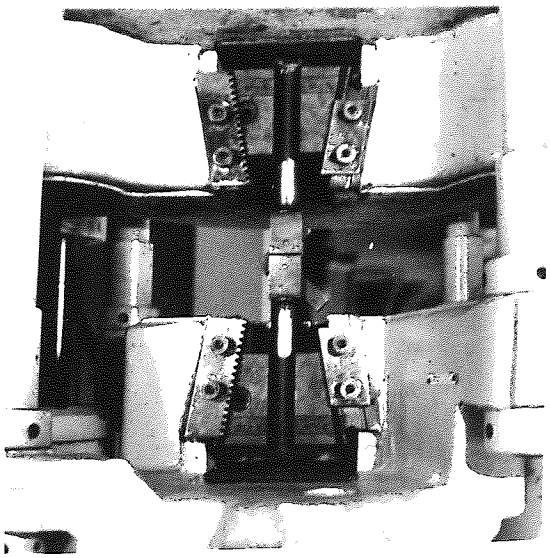

Style L Specimen Under Test

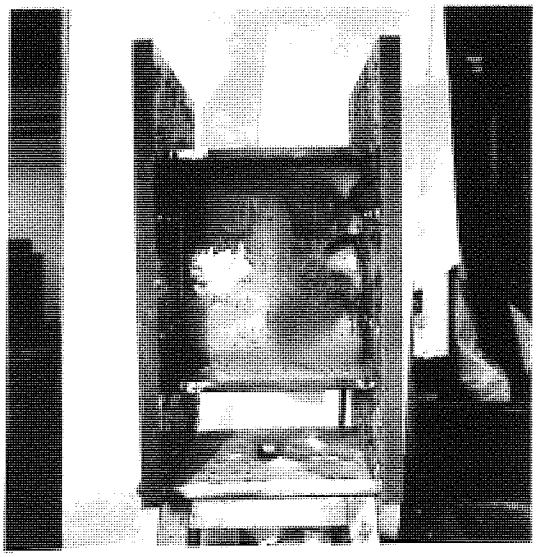

Typical Beam-Column Test Connection

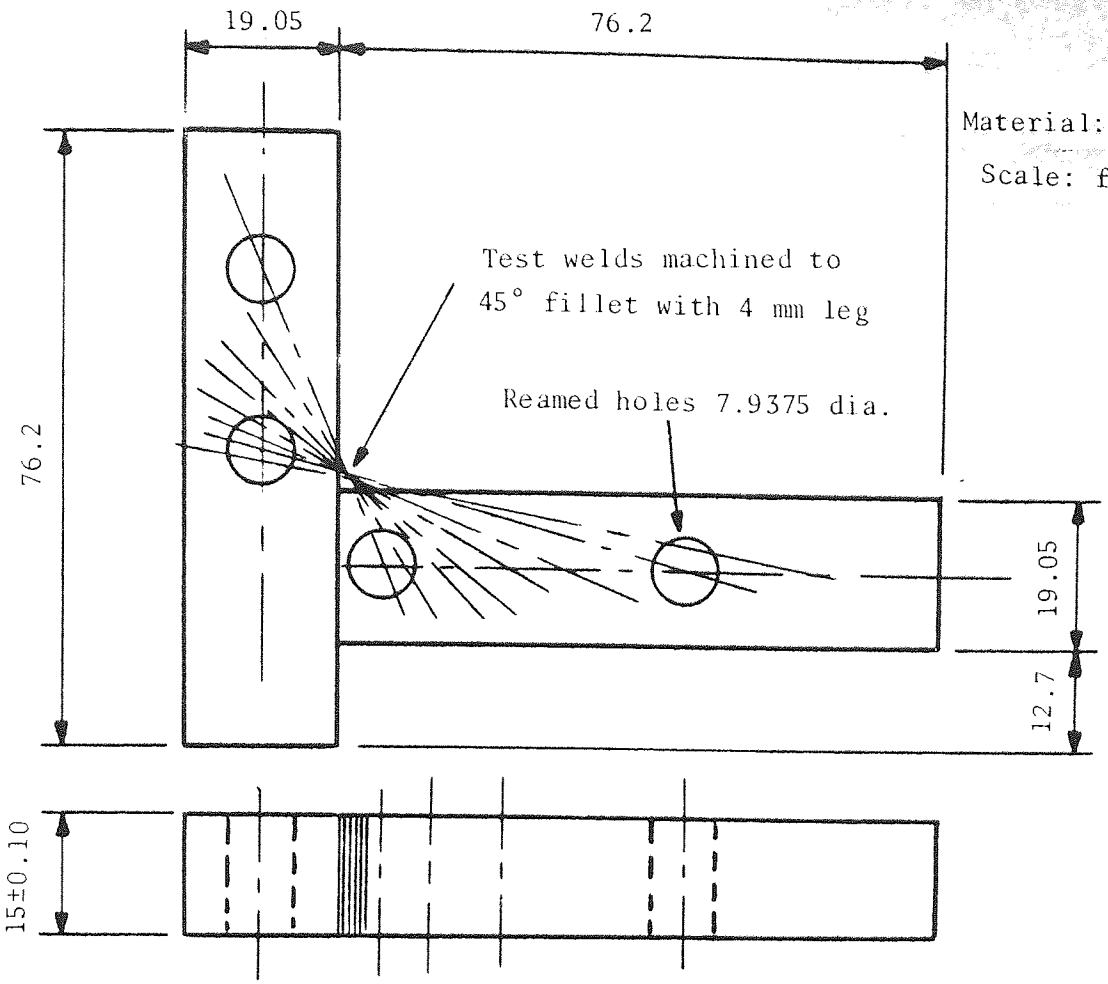

Fig.57 Failure Criteria Test Specimen, Style L.

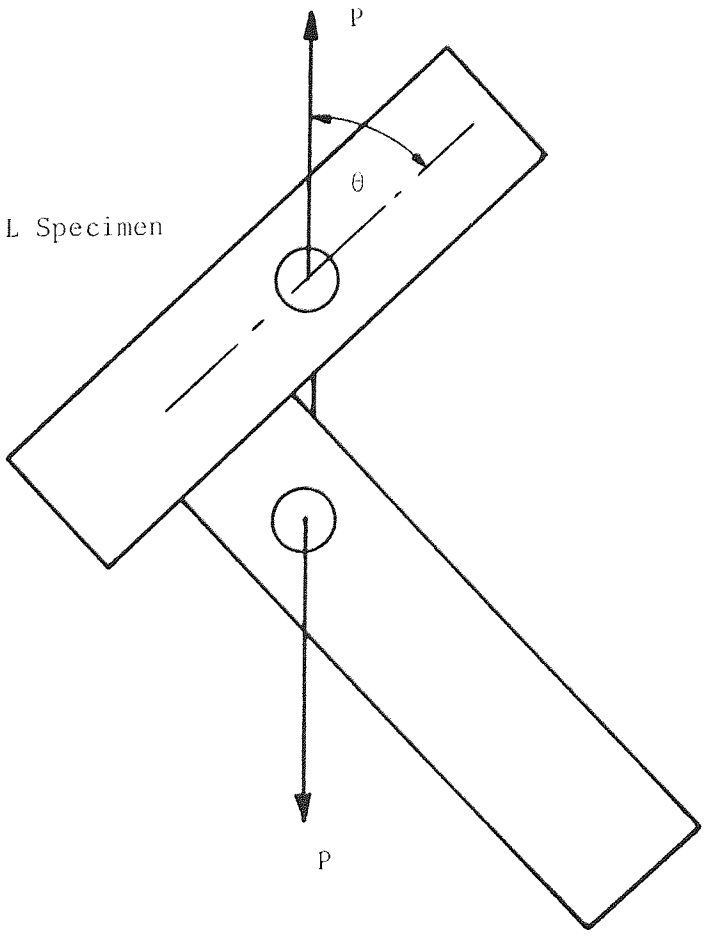

Fig. 58 Loading of Style L Specimen

Forty-one specimens were tested in the as welded condition, and twenty-one after thermal stress relieving at 600°C for 30 minutes.

4.2 Beam-column Connections

The ultimate capacity of a beam-column connection may, or may not be influenced by the loading configuration. Certainly, the deflection pattern of a beam is influenced by the condition at the supports and the distribution of the load. The question arises as to whether the ultimate capacity of a given connection under a given load ratio of shear load/bending moment is affected by the beam deflection behaviour. The flexibility of the column has been shown by Ligtenberg[20], Elzen[23], and others to have an effect upon the ultimate capacity of the connection, but no study has yet been reported regarding the effect of beam deflection behaviour. It was decided to test beam-column connections under the conditions of a point-loaded cantilever to a rigid column. For the sake of economy and handling it was decided to use short beams for the test connections, and incorporate them into a loading beam with which the required conditions could be achieved. The envisaged test set-up is shown in fig. 59 with the actual test connection bolted inbetween the two halves

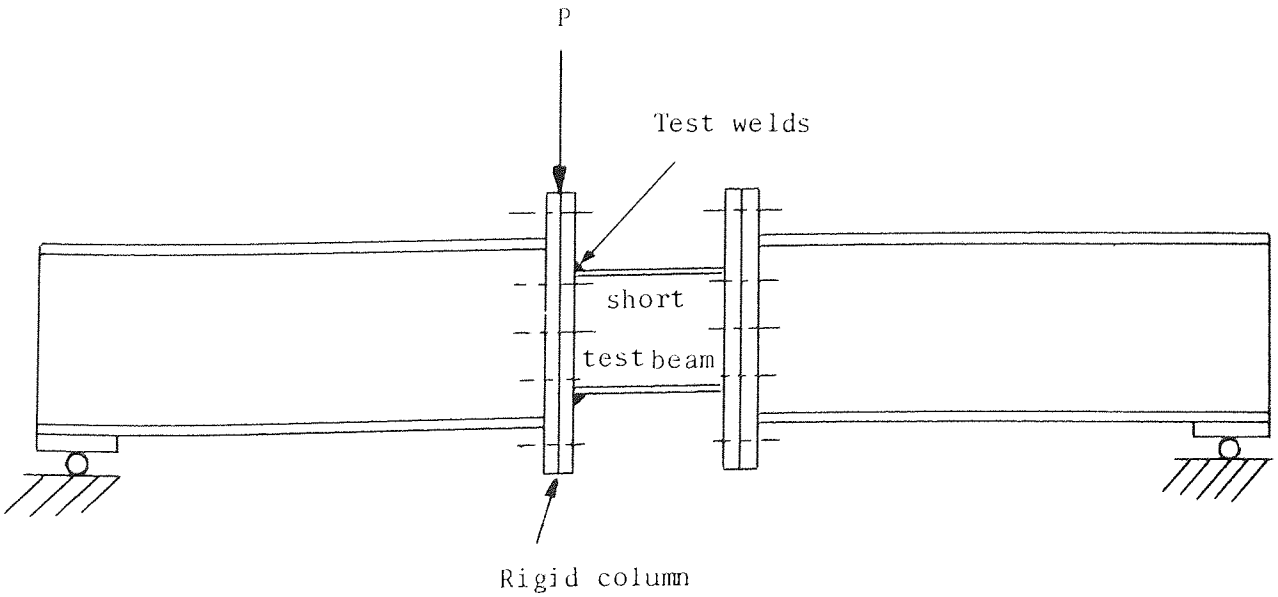

Fig.59 Simply Supported Composite Loading Beam

of the loading beam. With this kind of arrangement a pure bending moment load may be achieved by using a double-point load through a spreader.

The external load P, was to be applied using a 1000 kN hydraulic ram, and the required ratios of shear load, V/bending moment, M to be achieved by movement of the right-hand support towards the test welds. From the author's previous work[46], it was realized that in order to obtain a complete range of e/d it would be necessary for the tests to cover a range of V/M from 0.5 to 60 m^{-1}. Previous investigators had used very limited ranges; Ligtenburg[20], 0 to 6.7 m^{-1}, Archer et al[22], 6.6 to 79, and Dawe[42], 2 to 5 m^{-1}. With regard the beam I-section of the beam-column connections, the interest was to be centred upon flexibility of the web, and the effective width of wide flanges. Ligtenberg's work[20] has shown that flange deformation greatly affected the shear load distribution along the flange welds. The I-section sizes he tested were 200 x 200 mm and 280 x 119 mm. Archer et al[22] had tested only narrow flanges, section size of 150 x 50 mm, and showed that web flexibility greatly affected the shear load distribution between the two flange welds. Little information could be extracted from Dawe's results[42], owing to his very limited range of V/M.

The maximum flange width of a test beam-column connection with flange outer welds only was estimated to be 320 mm. This figure was based upon the maximum shear load available, i.e. 1000 kN, and 4 mm welds having an ultimate shear strength of 440 N/mm^2. The maximum bending moment corresponding to a flange width of 320 mm was estimated to be 500 kNm, assuming a maximum beam depth of 1 m.

The calculations that were done in order to determine the required I-section of the loading beam arms were in accordance with BS 449[6]. The

design criteria considered were,

(i) a maximum bending moment of 500 kNm,

(ii) a " shear load of 1000 kN,

(iii) web crushing

(iv) web buckling with bearing plates of thickness 50 mm and length 150 mm

The shear load was found to be the limiting factor and required a minimum I-section of 610 x 305 mm at 179 kg/m of grade 50 steel, BS 4360,[57]. This section would resist a safe maximum bending moment of 1130 kNm.

The number and size of bolts was determined in accordance with BS 449[6], the bolts selected being M24, of grade 6.8 as specified in BS 3692[58].

Full details of the 1130 kNm, 1000 kN testing beam can be found in the Appendices along with charts giving safe bolt loads. The design and the manufacture of the testing beam were undertaken by the author.

The full test programme envisaged was to cover three flange widths and three section depths of connections; flange welds only, web welds only, and combination of flange and web welds.

It was obviously not possible to cover this full programme and it was decided to concentrate on flange welded connections only, leaving the remainder of the programme for a later date.

As already mentioned, the areas of interest were as follows and it was hoped to make quantitative assessments using dial gauge indicators:

(i) flange deformation under the vertical shear load.

(ii) possible web buckling

(iii) position of the axis of rotation

(iv) amount of joint rotation, and

(v) degree of deformation in the plate-bearing zone.

After connection fracture, critical plane angles were to be measured so that the failure criterion, derived from the first phase of the experimental work, could be applied with the objective of developing a method for prediction of connection ultimate capacity.

The sizes of the test connection beam section were limited to the available capacity of the loading beam, i.e. 1130 kNm and 1000 kN, and were chosen with a combination of web and flange welds in mind although it was planned to test connections with flange welds only. This was done in order that the full test programme, already mentioned, could be carried out using the same beam sections for all tests, i.e. flange welds only, web welds only, and combination of flange and web welds. The chosen sections to BS 449[6] were as follows:

(i) 356 x 171 @ 67 kg/m

(ii) 305 x 127 @ 48 kg/m

(iii) 305 x 305 @ 97 kg/m.

Sections (i) and (ii) are Universal Beam, and section (iii) a Universal Column. Steel, grade 43 to BS 4360[59].

The connection end-plates were designed in accordance with BS 449[6], and the safe bolt load charts drawn up by the author. Details of the end-plates, grade 43 BS 4360[59], may be found in the Appendices.

The test connections were prepared by the author in the following sequence:

1. the test beams were saw-cut to a standard length of 300 mm.
2. beam-ends were squared off using file and hand-grinder,
3. flange faces at the beam-ends were flash ground to remove oxide and mill-scale,
4. run-on and run-off tags were welded to flange ends,
5. end-plates were drilled, and flash ground to remove mill-scale,
6. end-plates and beam-ends were de-greased.
7. end-plates and beams were paired-off and additional grinding done as necessary to ensure perfect fit-up,
8. end-plates bolted to a flat welding-table,
9. beam was tacked into position to ensure exact fit-up before test welding.
10. test welds were laid, by the author, using the welding technique already described at a fixed current of 235 ampere,
11. run-on and run-off tags were removed,
12. test welds were machined to an exact 45° profile with a 4 mm leg using a form tool on a shaping machine,
13. end-plates were welded to the other end of the beam,
14. inner-flange and web tack welds were removed by hand grinding,
15. dial gauge mounting brackets were welded to the end-plate and beam flange.

A typical test connection is shown in plate 4, (after fracture). For the purpose of testing, the test connection was bolted inbetween the two halves of the loading beam, and the dial gauges were attached as shown in figs. 60, 61 and 62. Although great care had been taken to minimize distortion of the end-plates during welding it did occur and as a result packing shims were used to prevent pre-loading of the test welds upon tightening of the end-plate bolts.

Fig. 60 Dial Gauge Positions, Series 305 x 127

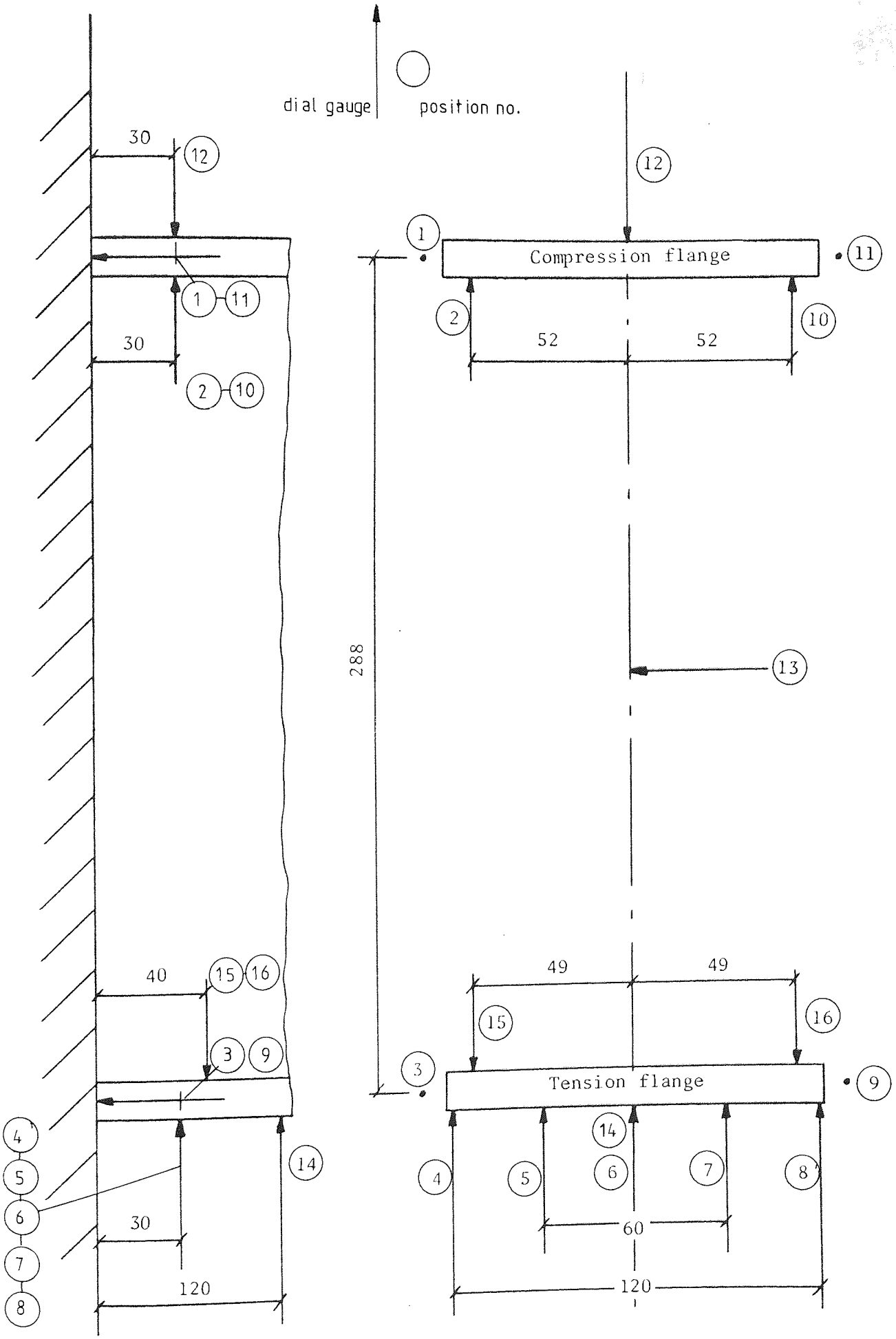

Fig. 61 Dial Gauge Positions, Series 305 x 305

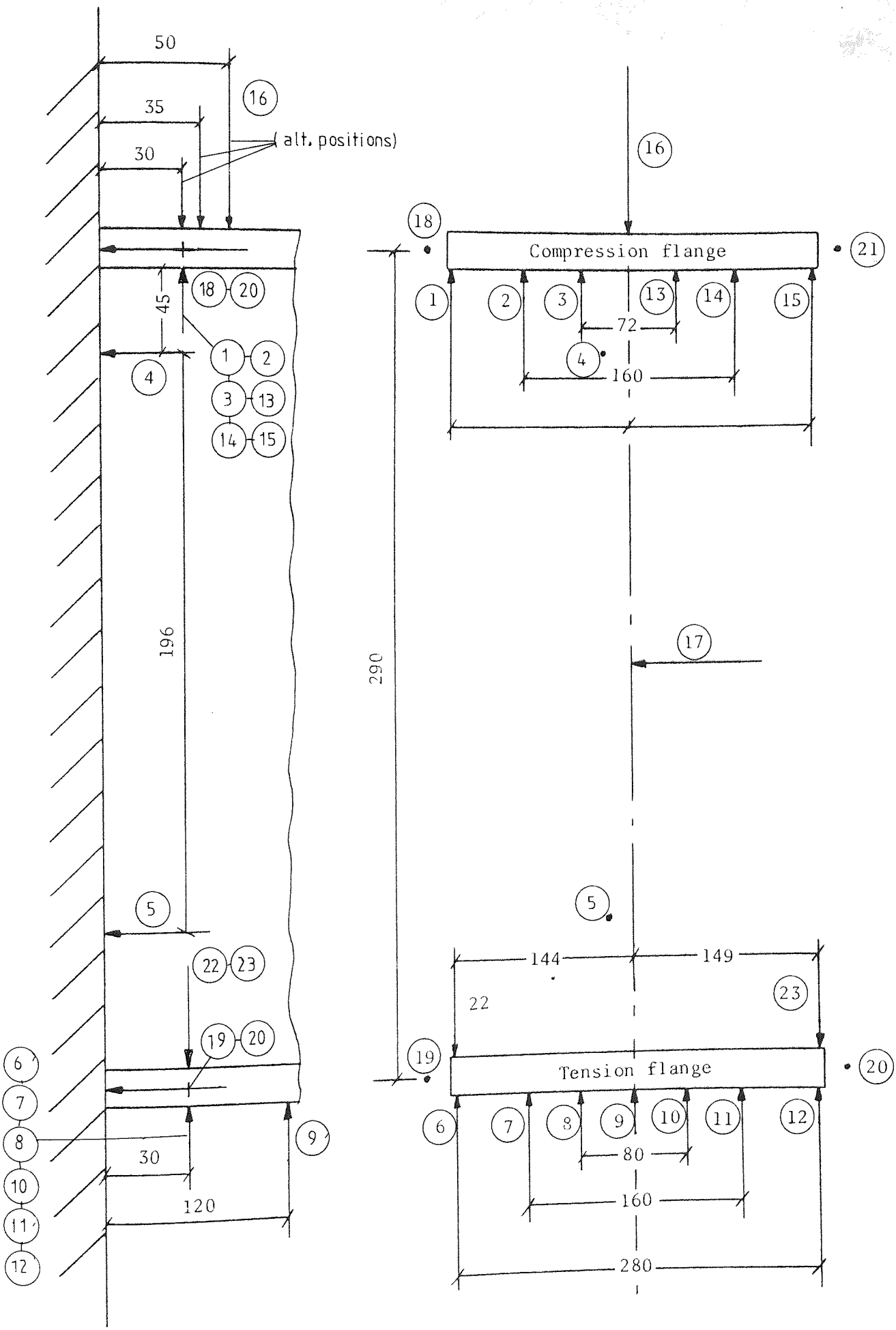

Fig. 62 Dial Gauge Positions, Series 356 x 171

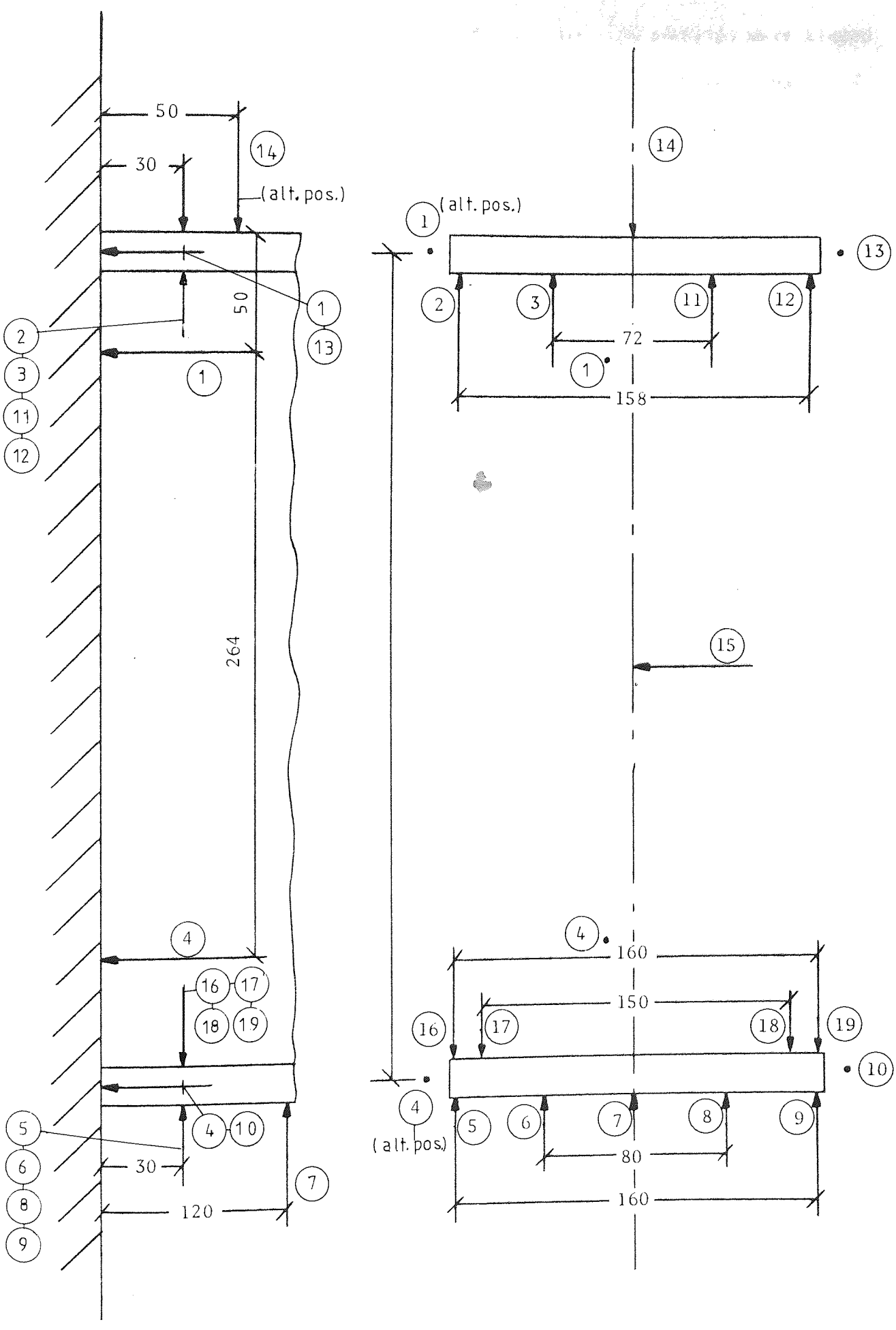

Before the connections were welded up, the beam profiles were traced so that an accurate pattern of flange deformation and web buckling could be obtained from profiles that were traced after fracture. These profiles may be found in Chapter 6.

CHAPTER 5

RESULTS AND DISCUSSION - FAILURE CRITERIA

5.1 Crofts Style Specimens

Twenty-six tests were conducted before it was decided to abandon the style of specimen because of the weld rotation during failure. This rotation led to irregular failure 'planes' which made meaningful assessment of fracture plane angles difficult.

The following assumptions were made regards the behaviour of the joint, and the forces acting, see fig. 63:

1. the centre of rotation of the joint was midway between the two welds on a line joining the weld centroids. This assumption assumed the resistive forces of both welds were equal,
2. resistive weld element forces, F, acted at right angles to the line joining the weld centroids,
3. the resistive force could be represented by rectangular components acting parallel, F_z, and normal, F_x, to the longitudinal axis of the weld,
4. the normal component, F_x, could be resolved parallel and normal to a critical plane acting at an angle ϕ to the horizontal leg of the weld,
5. the resultant shear force acting on the critical plane was the vectorial sum of the shear forces produced by F_x and F_z,
6. the forces acting on the critical plane acted uniformly and produced uniform shear stress, τ_ϕ, and normal stress, σ_ϕ. The stress distribution is obviously not uniform, but it was assumed to be so for the sake of simplicity,
7. effects of the couple due to the eccentricity of force F_x were negligible.

The critical plane stresses were computed as follows:

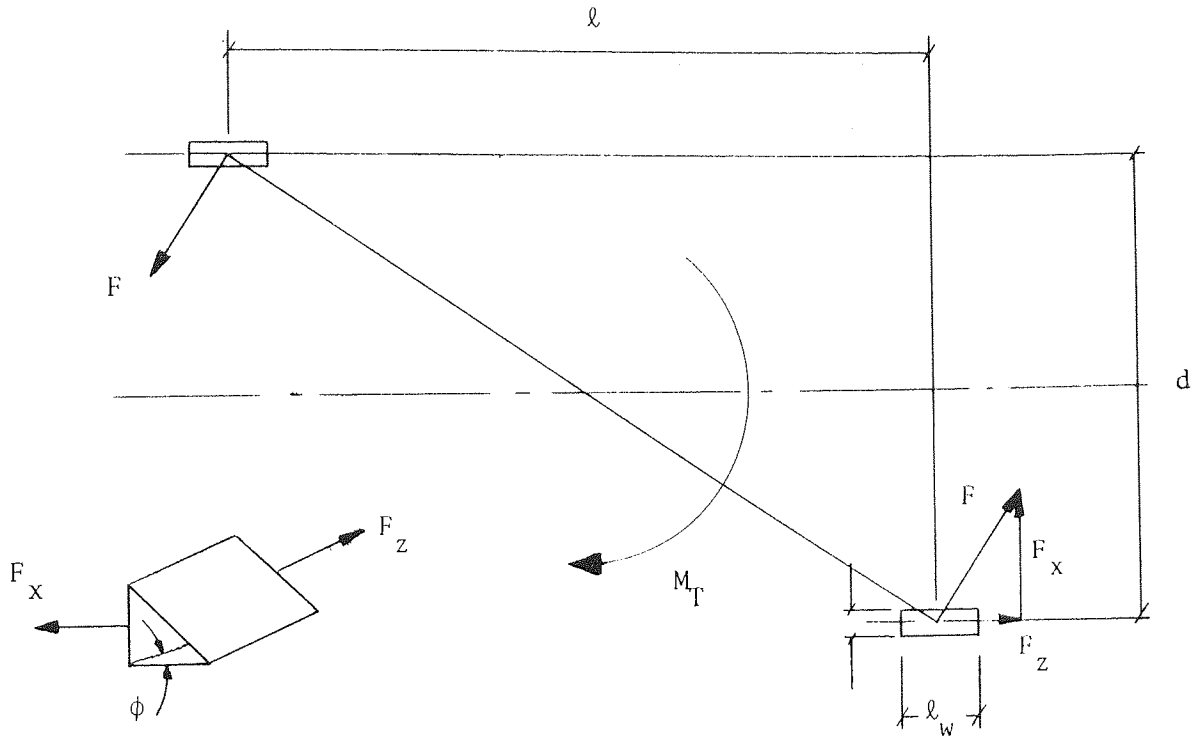

Fig. 63 Forces Acting - Crofts Style Specimens

Resistive force, $F = M_T/(\ell^2 + d^2)^{\frac{1}{2}}$

Rectangular components,

$$F_x = \ell \ M_T/(\ell^2 + d^2)$$

$$F_z = d \ M_T/(\ell^2 + d^2)$$

Normal stress on critical plane,

$$\sigma_\phi = F_x \sin\phi(\sin\phi + \cos\phi)/t \ \ell_w$$

Shear stress on critical plane,

$$\tau_\phi = [F_z^2 + (F_x \cos\phi)^2]^{\frac{1}{2}}(\sin\phi + \cos\phi)/t \ \ell_w$$

Specimen No.	Distance ℓ mm	Moment M_T kNmm	Fracture angle ϕ deg.	Stress σ_ϕ N/mm^2	Stress τ_ϕ N/mm^2
TO	0	1657	45	476	0
T1	150	4310	18	510	144
T2	137	3949	20	505	155
T3	120	3206	21	454	141
T4	90	2782	26.5	482	168
T5	60	2379	33	511	174
T6	30	1870	38	490	106
C1	150	3418	2	345	11
C2	137	3228	5	364	27
C3	120	2930	2	347	10
C4	90	2570	3.5	372	17
C5	60	2061	7	376	27
C6	30	1636	16	385	37
T7R	150	4437	21	531	176
T8R	120	3970	17.5	553	142
T9R	90	2634	20	447	117
T10R	60	2082	20	429	88
T11R	30	1721	32	445	82
C7R	0	1477	46	425	0
C8R	150	3291	1.5	329	8
C9R	120	2931	3	353	15
C10R	90	2400	1.5	337	7
C11R	60	1997	3	344	11
C12R	30	1721	10	380	23

Table 1. Experimental Results - Crofts Style Specimens.

Four series of tests were conducted;

(1) with F_x tensile, code T)
) as-welded
(2) with F_x compressive, code C)

(3) with F_x tensile, code TR)
) stress relieved at 600°C
(4) with F_x compressive, code CR)

and the results are shown in Table 1.

Additional information.

$d = 82$ mm

$\ell_w = 15$ mm

$t = 4$ mm

5.2 Double-lapped Style Specimens

This style of specimen was abandoned because it would have been very difficult to cover the required range of F_x/F_z. Furthermore, like the Crofts style specimens, failure is greatly constrained to take place in the direction of the applied load. In the case of the Biaxial Loading Jig failure can take place in two directions.

The following assumptions were made regards the forces acting, see fig. 64:

1. the external load, P, is resisted equally by the two welds,
2. the resistive force, P/2, could be represented by rectangular components acting parallel, F_z, and normal F_x, to the longitudinal axis of the weld,
3. the normal component, F_x, could be resolved parallel and normal to a critical plane acting at an angle ϕ to the direction of the applied load P,
4. the resultant shear force acting on the critical plane was the vectorial sum of the shear forces produced by F_x and F_z,
5. The forces acting on the critical plane acted uniformly and produced uniform shear stress, τ_ϕ, and normal stress, σ_ϕ,
6. effects of the out of balance couple were negligible.

Specimen No.	Load P kN	Angle θ deg.	Weld length ℓ_w mm	Fracture angle ϕ deg.	Stress τ_ϕ N/mm^2	Stress σ_ϕ N/mm^2
T1	108	90	32	15.5	498	138
T3	110	83	32.5	14.5	497	128
T7	99	76.5	33.7	17.25	439	132
T9	106	69.5	33.5	18.5	479	149
T11	108	62.5	33.5	22.25	494	176
T13	82	55.5	35	31	366	171
T14	51	90	17.3	17.5	498	159
T15	47	76.5	14	19	486	159
T16	51	67.5	14.2	22.5	455	174
C1	82	83	32	3	336	17.5
C3	82	76.5	32.3	5.5	343	32
C5	88	69	33.7	6.25	358	37
C7	86	62	33.5	9	364	51
C9	94	56	35.5	6.5	365	34
C11	88	56	34	5.75	353	29
C13	101	48.5	36	5	378	25
C14	87.3	90	28	3	420	34
T2R	124	90	31.2	14.5	584	151
T4R	124	83	32	15.5	573	158
T5R	112	76.5	32	15.5	519	140
T6R	126	76.5	31.7	16.5	591	170
T8R	126	69.5	33	-	-	-
T10R	129	62.5	34.5	17.5	566	157
T12R	115	55.8	34.5	17.5	506	129
C2R	76	83	32	7.75	329	44
C4R	76	76.5	32	9	336	52
C6R	82	69	33	10	355	58
C8R	84	62	32.8	8	358	44
C10R	83	56	34.5	9	340	44
C12R	91	48.5	36	8.5	358	40

Table 2. Experimental Results - Double-lapped Specimens

The critical plane stresses were computed as follows:

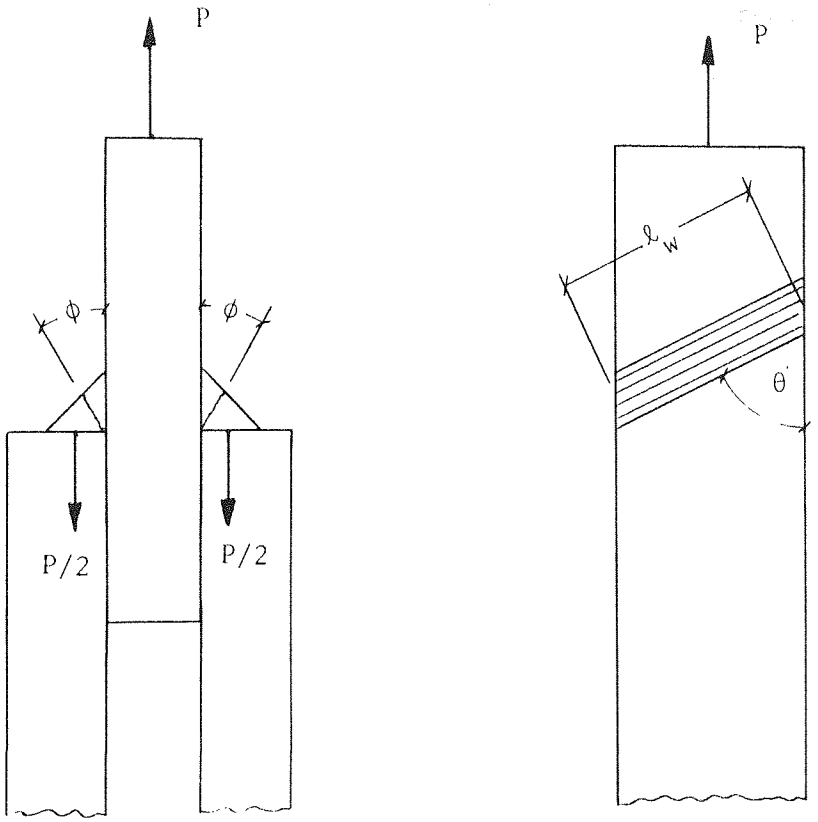

Fig. 64 Forces Acting - Double-lapped Specimens

Shear Stress, $\tau_\phi = [(P\cos\theta)^2 + (P\sin\theta\cos\phi)^2]^{\frac{1}{2}}(\sin\phi + \cos\phi)/2t\ell_w$

Normal Stress, $\sigma_\phi = P\sin\theta\sin\phi(\sin\phi + \cos\phi)/2t\ell_w$

Four series of tests were conducted similar to those of the Crofts style specimens, and the results are given in Table 2.

5.3 Biaxially-loaded Specimens

These specimens in conjunction with the style L specimens provided the bulk of the results which were used to establish a failure criterion. The biaxially-loaded specimens produced the same weld forces as both the Crofts style and the double-lapped specimens, but in this case the forces F_x and F_z were applied directly and not as rectangular components. The weld was free to deform in either of the two directions of applied forces.

The following assumptions were made regarding the behaviour of the joints and the forces acting, see fig. 65:

1. the external forces, F_x and F_z were resisted equally by the two welds,
2. the effects of the unbalanced couples produced as a result of eccentricities of both F_x and F_z were negligible,
3. the external force, F_x, could be resolved parallel and normal to a critical plane acting at an angle ϕ to the direction of the force,
4. the resultant shear force acting on the critical plane was the vectorial sum of the shear forces produced by F_x and F_z.
5. the orientation of the resultant shear stress to the axis of the weld did not effect the ultimate capacity of the weld (this also applied to the previous specimens),
6. the stresses acting on the critical plane were uniform,
7. the welds were 'free' to deform rather than be constrained to fail in one direction only,
8. the aforementioned applied equally to specimens under compression, style C and those under tension, style T.

The critical plane stresses were computed as follows:

Table 3 - Experimental Results - Biaxially-loaded Specimens

Specimen	Force F_x kN	Force F_z kN	Fracture Angle ϕ deg.	Stress σ_ϕ N/mm^2	Stress τ_ϕ N/mm^2
T1	17.0	26.88	33	106.7	350.7
T2	0	28.45	43	0	335.1
T3	11.0	30.6	42	86.6	372.8
T4	14.0	29.6	38	100.9	371.7
T5	17.0	30.55	31.5	101.8	387.6
T6	1.5	32.89	47	12.7	387.6
T7	3.8	34.9	46.5	32.5	412.3
T8	7.3	32.4	46	61.9	386.4
T9	6.1	32.85	45.5	51.3	390.4
T10	14.0	33.0	38	105.7	407.4
T11	8.45	30.4	40.5	64.5	365.0
T12	46.5	0	21	127.5	459.6
T13	9.6	28.74	39	70.8	348.0
T14		scrapped			
T15	11.0	30.9	44	90.0	375.8
T16	23.0	30.2	29	126.3	411.1
T17	42.0	21.96	15.25	113.0	471.8
T18	9.6	31.7	42	75.6	382.4
T19	17.0	29.3	39	125.4	376.7
T20	29.35	27.4	24	131.4	421.8
T21	35.7	20.9	17.5	112.2	417.6
T22	5.0	29.8	43	40.2	353.6
T23	9.6	33.05	43	77.1	397.4
T24	42.0	17.65	16	119.3	454.2
T25	17.0	32.1	43.5	137.9	404.6
T26	6.1	30.3	38.5	44.5	359.2
T27	43.2	0	13.5	101.3	422.1
T28	2.6	34.9	47	22.4	411.6
T29	0.46	32.7	39	3.4	383.3
T30	1.5	35.45	40	11.3	416.4
T31	2.6	31.2	42.5	20.7	368.0
T32	3.8	32.3	42.5	30.2	381.7
T33	5.0	34.72	43.2	40.3	411.2
T34	6.1	32.6	43.5	49.5	387.6
T35	7.3	30.27	44.7	60.52	361.9
T36	8.45	33.0	41.7	66.1	395.3
T37	11.0	32.8	41.5	85.7	397.8
T38	12.25	32.0	39.5	91.4	391.4
T39	20.0	31.3	34.5	131.3	409.9
T40	26.25	27.0	31	154.6	401.9
T41	32.5	25.2	20.5	122.1	423.8
T42	38.75	18.6	22.5	161.5	439.3
T43	42.0	21.0	18.5	140.6	474.9
T44	43.1	11.78	18.5	144.3	448.6
T49R	0.46	42.5	37	3.25	496.0
T50R	1.5	45.6	38.5	10.94	534.1
T51R	2.6	39.8	41	20.1	468.5
T52R	3.8	49.75	42	29.9	586.5
T53R	5.0	40.2	42.5	39.8	475.3
T54R	6.1	40.95	43.7	49.7	485.3
T55R	7.3	41.25	45.5	61.4	489.8
T56R	8.45	39.3	43	67.9	468.6
T57R	9.6	38.53	41	74.1	460.9
T58	11.0	44.4	38	79.2	529.2

cont'd

Table 3 continued...

T59R	12.25	35.4	40.5	93.5	430.1
T60R	14.2	46.35	38.5	103.5	558.1
T61R	17.0	35.2	36	116.3	439.9
T62R	29.3	29.7	27.5	152.1	443.6
T63R	20.0	39.0	38.5	145.8	492.1
T64R	23.0	38.5	37	161.6	497.8
T65R	26.25	32.83	36	179.6	455.1
T66R	32.5	34.31	25	152.1	500.8
T67R	35.7	31.0	23.5	156.1	494.4
T68R	38.75	31.9	26	189.3	526.3
T69R	42.0	24.72	20	153.5	497.4
T70R	43.1	28.43	22	175.2	532.0
T71R	60.0	0	17	182.6	597.1
T72R	46.5	16.35	19.5	165.1	467.6
T73R	49.65	17.02	18.5	166.2	528.1
T74R	51.5	0	17.5	161.9	513.4
T75R	45.9	0	16.5	scrapped	
T76R	43.8	20.7	21	169.0	493.4
T77R	47.1	17.8	23.5	206.0	512.3
T78R	48.5	13.35	19.5	172.2	506.6
T79R	50.0	18.65	21.5	198.1	541.7
T80R	51.0	14.52	18	165.5	531.7
T81R	43.8	0	16	127.9	445.9
C1	5.0	25.4	N.R.	-	-
C2	4.4	34.5	41.5	34.3	402.8
C3	7.3	32.0	N.R.	-	-
C4	2.6	33.07	N.R.	-	-
C5	35.7	27.4	11	66.6	434.6
C6	11.0	31.0	N.R.	-	-
C7	35.7	19.75	7.5	43.6	379.0
C8	32.5	22.8	6.5	33.9	364.6
C9	42.8	0	5.5	37.3	387.4
C10	26.25	27.8	N.R.	-	-
C11	1.5	35.0	38	10.8	409.6
C12	2.6	33.62	37	21.5	396.8
C13	2.06	34.34	41	15.9	404.1
C14	38.8	14.72	4.5	27.3	370.9
C15	17.0	32.85	32	110.0	413.5
C16	29.35	28.45	18	95.3	418.5
C17	23.0	28.43	N.R.	-	-
C18	42.0	0	5	33.1	377.7
C19	23.0	32.0	35	119.4	426.6
C20	29.35	30.9	33	89.3	434.4
C21	17.0	33.45	34	110.0	420.0
C22	26.25	31.6	24	117.5	436.5
C23	0.45	34.4	44	3.68	405.4
C24		scrapped			
C25	41.4	0	6	39.6	377.1
C26	5.0	35.7	44	40.9	422.8
C27	9.6	31.0	N.R.	-	-
C28	6.1	33.62	42	49.0	399.5
C29	6.1	34.2	40	46.0	405.3
C30	7.86	36.1	44	61.9	430.4
C31	3.8	35.6	35	31.1	420.7

Table 3 continued

C32	11.0	35.4	40.5	83.9	427.4
C33	6.1	33.6	41.5	47.6	398.9
C34	20.0	33.5	25	117.8	430.3
C35		scrapped			
C36	2.6	29.42	N.R.	-	-
C37	14.2	34.0	38.5	99.8	418.3
C71	0.46	37.9	33.5	2.9	437.7
C72	1.0	33.81	38	7.2	395.6
C73	2.05	33.0	36	14.0	384.6
C74	2.6	35.4	34	16.8	410.3
C75	3.2	33.28	38.5	23.3	390.8
C76	4.4	35.0	37	30.9	410.5
C77	6.1	33.5	27	31.0	380.4
C78	7.3	35.2	31.5	43.7	409.6
C79	8.45	33.28	26	41.3	380.4
C80	32.0	30.1	0	0	366.0
C81	33.1	23.58	0	0	338.7
C82	34.5	25.5	0	0	357.5
C83	36.9	22.39	0	0	359.7
C84	39.4	20.9	0	0	371.7
C85	40.6	6.86	5	31.9	370.4
C38R	0.46	42.4	36.5	3.2	494.2
C39R	1.0	46.5	30.5	5.8	530.7
C40R	1.5	44.85	34.5	9.8	519.9
C41R	2.05	42.45	37	14.4	495.8
C42R	2.6	46.25	33	16.3	533.8
C43R	3.2	49.0	32	19.5	563.5
C44R	3.8	52.85	22.5	15.8	576.7
C45R	5.0	52.0	31	29.5	596.7
C46R	6.1	48.0	27	31.0	541.5
C47R	7.3	48.05	28.5	39.4	547.8
C48R	8.45	50.0	26	41.3	563.6
C49R	9.6	41.23	20.2	35.5	451.5
C50R	11.0	41.26	22	44.7	461.1
C51R	14.2	43.1	17	43.2	470.2
C52R	17.0	47.83	18.2	55.9	531.1
C53R	20.0	48.8	10.7	36.2	512.2
C54R		scrapped			
C55R	26.25	42.95	N.R.	-	-
C56R	29.3	26.0	0	0	326.4 *
C57R	32.0	23.4	2	9.6	341.6 *
C58R	33.1	35.4	N.R.	-	-
C59R	34.5	24.15	0	0	350.9 *
C60R	35.7	17.27	11	66.6	381.7 *
C61R	36.9	2.99	9	53.0	348.7 *
C62R	38.1	25.1	0	0	380.2 *
C63R	39.4	3.63	6.5	41.1	362.6 *
C64R	40.0	3.2	7	45.3	369.9 *
C65R	40.6	0	6	38.9	369.8 *

Table 4. Experimental Results - Style L Specimens

Specimen	Force F_x kN	Force F_y kN	Fracture Angle ϕ deg	Stress σ_ϕ N/mm^2	Stress τ_ϕ N/mm^2
L1	19.94	19.59	46	658.7	5.7
L2	21.61	21.24	34	687.0	139.8
L3	20.54	20.90	44.5	690.6	0
L4	21.24	21.61	40	709.3	55.8
L5	22.39	22.01	45	740.1	6.5
L6	20.79	21.90	46.5	710.6	37.2
L7	22.61	23.83	47	772.4	47.2
L8	19.41	20.45	48	661.7	52.1
L9	19.12	20.86	45	651.3	87.8
L10	20.07	21.89	57	662.9	171.5
L11	21.71	23.69	49	750.6	85.5
L12		scrapped			
L13	18.74	22.33	53	662.9	153.1
L14		scrapped			
L15	17.34	20.30	55	600.0	155.2
L16	19.40	23.53	48	710.0	106.1
L17	18.93	23.79	62	628.3	273.3
L18	20.86	20.50	35	689.4	6.0
L19	17.80	22.38	70	520.9	319.2
L20	17.6	22.93	72	500.1	343.8
L21	17.39	23.08	56	632.2	217.7
L22	18.99	27.11	68	602.2	391.1
L23	19.18	28.43	65	651.1	391.3
L24	18.48	27.40	66.5	611.2	389.4
L25	17.92	28.13	69.5	571.2	430.5
L26	16.46	26.86	70	526.5	418.9
L27	17.31	29.38	68	586.9	450.4
L28	17.08	29.57	67	596.0	449.2
L29	15.93	28.73	66	577.2	435.0
L30	14.93	28.08	62	594.2	400.9
L31	13.34	26.76	66	507.6	418.5
L32	14.90	31.23	65	591.3	487.5
L33	13.02	27.91	70	465.2	465.2
L55	9.24	25.37	60	470.8	395.2
L56	11.39	27.30	66	471.6	447.8
L57	6.83	25.50	60	424.9	425.0
L58	4.52	25.60	55	426.7	426.8
L59	1.88	19.53	53	309.3	337.7
L60	2.61	21.27	54	340.2	364.9
L61	2.99	21.29	57	325.1	374.1
L62	3.29	20.74	57	323.9	359.8
L34R	21.92	21.92	25	645.2	234.9
L35R	23.20	24.44	25	707.8	236.9
L36R	21.69	23.25	34	726.7	115.1
L37R	22.15	24.60	30	737.1	156.7
L38R	22.37	25.73	45	801.8	56.1
L39R	20.61	25.0	50	748.0	138.7
L40R	18.95	24.70	75	504.0	386.8

cont'd

Table 4 continued

L41R	18.95	24.70	75	504.0	386.8
L42R	21.23	28.70	73	596.8	441.7
L43R	18.67	26.17	73	530.7	407.3
L44R	18.44	26.33	70	562.5	393.9
L45R	17.72	26.77	68	573.9	394.5
L46R	16.96	27.14	70	538.6	420.9
L47R	14.81	24.64	70	477.2	386.5
L48R	15.40	26.67	71.5	486.5	430.5
L49R	15.61	27.59	72.5	484.6	452
L50R	14.19	26.70	72	456.6	441.0
L51R	14.19	27.85	71	476.3	460.0
L52R	13.72	28.13	70	480.9	464.5
L53R	13.23	28.37	75	410.6	489.4
L54R	13.63	27.93	73	441.0	473.0

* Failure occurred in the side wall

N.R. not recorded

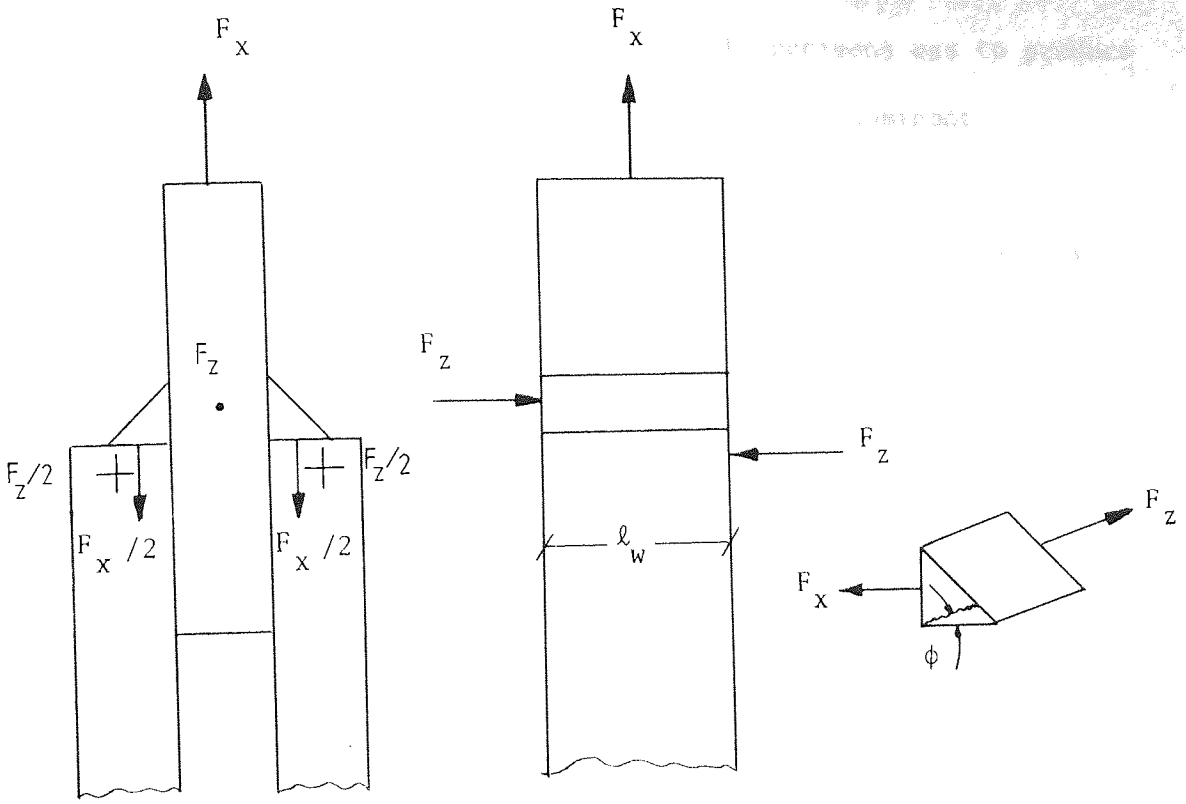

Fig. 65 Forces Acting - Biaxially-loaded Specimens.

Normal stress, $\sigma_\phi = F_x \sin\phi(\sin\phi + \cos\phi)/2t\ell_w$

Shear stress, $\tau_\phi = [F_z^2 + (F_x\cos\phi)^2]^{\frac{1}{2}}(\sin\phi + \cos\phi)/2t\ell_w$

Four series of tests were conducted similar to those of before and the results are given in Table 3.

5.4 Style L Specimens

Although the ratio of F_x/F_z was varied from zero to infinity, the results of the biaxially loaded specimens only covered a limited field of the failure criterion - the maximum normal stress computed was 206 N/mm^2.

It appeared that in all tests conducted the dominant stress was the shear stress, τ_ϕ. The purpose of the style L specimens was to produce a situation in which the normal stress, σ_ϕ, would be dominant.

The following assumptions were made regarding the forces acting, see fig. 66:

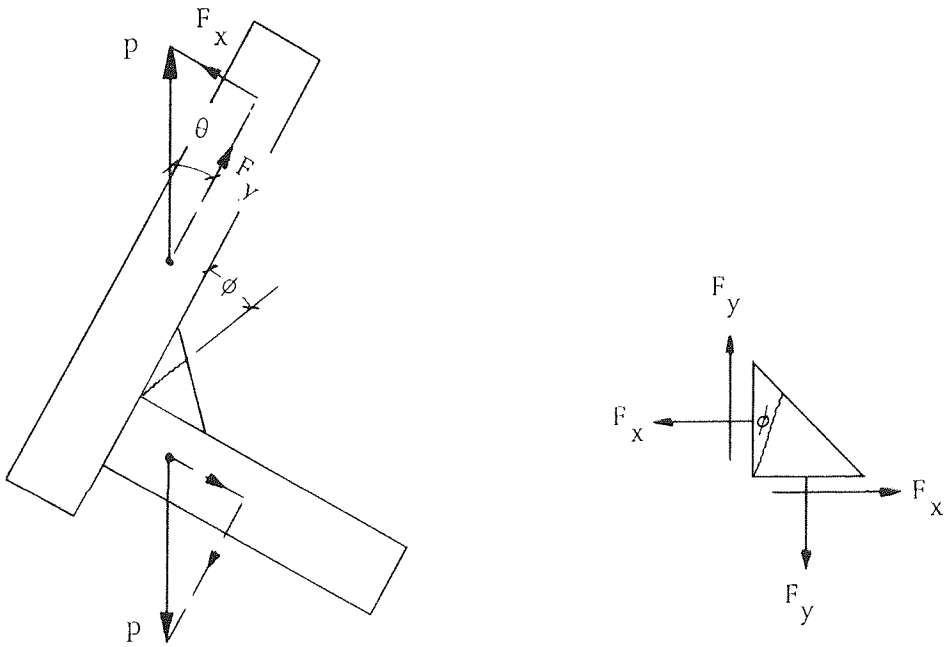

Fig. 66 Forces Acting - Style L Specimens

1. the external load, P, could be represented by rectangular components F_x and F_y acting normally to the legs of the weld,
2. the rectangular components, F_x and F_y could be resolved parallel and normal to a critical plane at an angle ϕ to the line of action of the upwards component F_y,
3. the resultant shear and normal forces acting on the critical plane were the algebraic sum of the forces produced by F_x and F_y,
4. stresses acting on the critical plane were uniform,
5. the effect of the residual couple was negligible,

6. the bending moments produced by the rectangular components were negligible. For the range of θ considered the loading pin holes were reasonably close to the weld. Obviously as the angle θ was decreased the bending moment produced by component F_x increased, and that by component F_y decreased.

The critical plane stresses were computed as follows:

$$\text{normal stress, } \sigma_\phi = (F_x\cos\phi + F_y\sin\phi)(\sin\phi + \cos\phi)t\ell_w$$

$$\text{shear stress, } \tau_\phi = (F_y\cos\phi - F_x\sin\phi)(\sin\phi + \cos\phi)t\ell_w$$

where $F_x = P\sin\theta$, and $F_y = P\cos\theta$.

Two series of tests were conducted, one with specimens in the as-welded condition, and the other with specimens after stress relieving at 600°C. The results are shown in Table 4.

5.5 Relative Strength of Welds under Compression

It is a common belief that welds under compression are stronger than when under tension, and it is common practice to treat the welds equally for design purposes. The limit curve proposed by Vreedenburgh[16] showed for the ratio F_x/F_y equals 1,

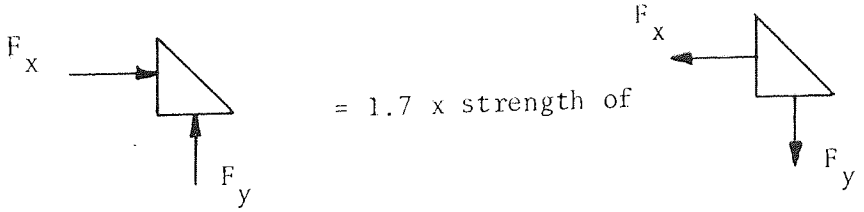

This implies the weld ultimate compressive strength is 1.7 times greater than the ultimate tensile strength. There is no evidence to corroborate this, in fact, Bibber[1] suggested the ultimate strengths were approximately equal.

Jensen[5] showed that

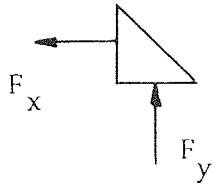

was weaker for the full range of F_x/F_y than (see fig.12)

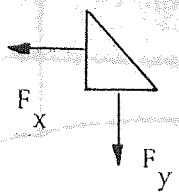

Vreedenburgh's results also showed this when they were presented as in fig.12.

Schreiner[7] found superficial evidence indicating

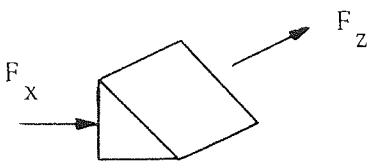

was weaker than

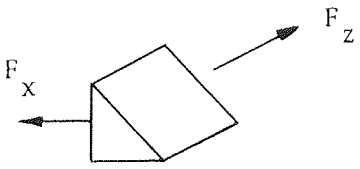

The author's results were presented in figs. 67, 68, 69 and 70 which show the relationship between the ultimate weld forces F_x and F_z, and F_x and F_y for the various styles of test specimens.

The following facts can be noted (with reference to as-welded specimens):

(a) for biaxially-loaded specimens, fig.67, for the range of F_x/F_z 0 to 1.6, welds under compression, and tension appear to be of equal strength, whereas for the range 1.6 to ∞, the compression weld appears to be weaker. When F_z equals zero

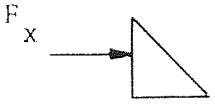

= 0.94 x strength of

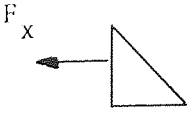

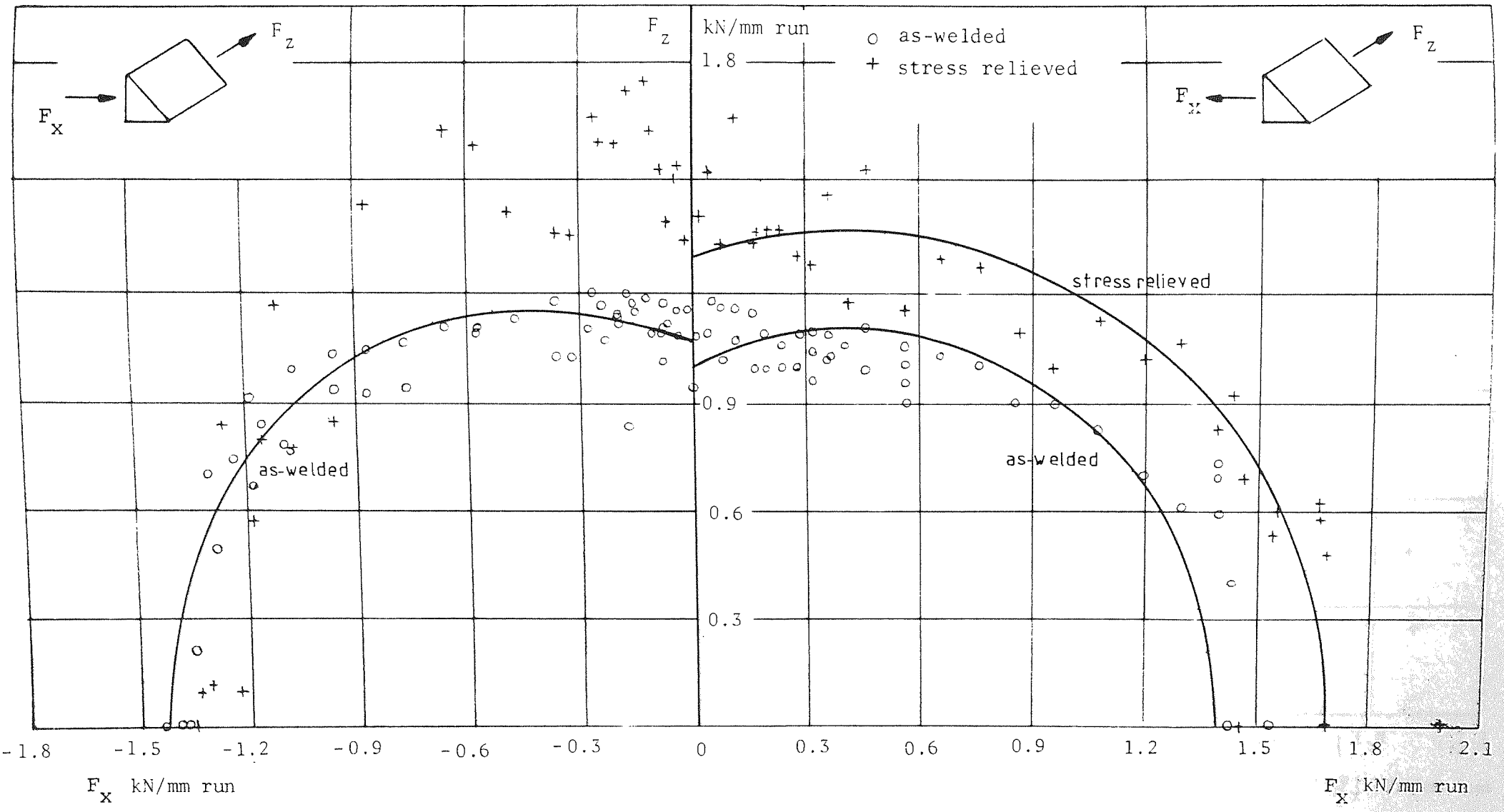

Fig.67 Relationship between F_x and F_z for Biaxially-loaded specimens

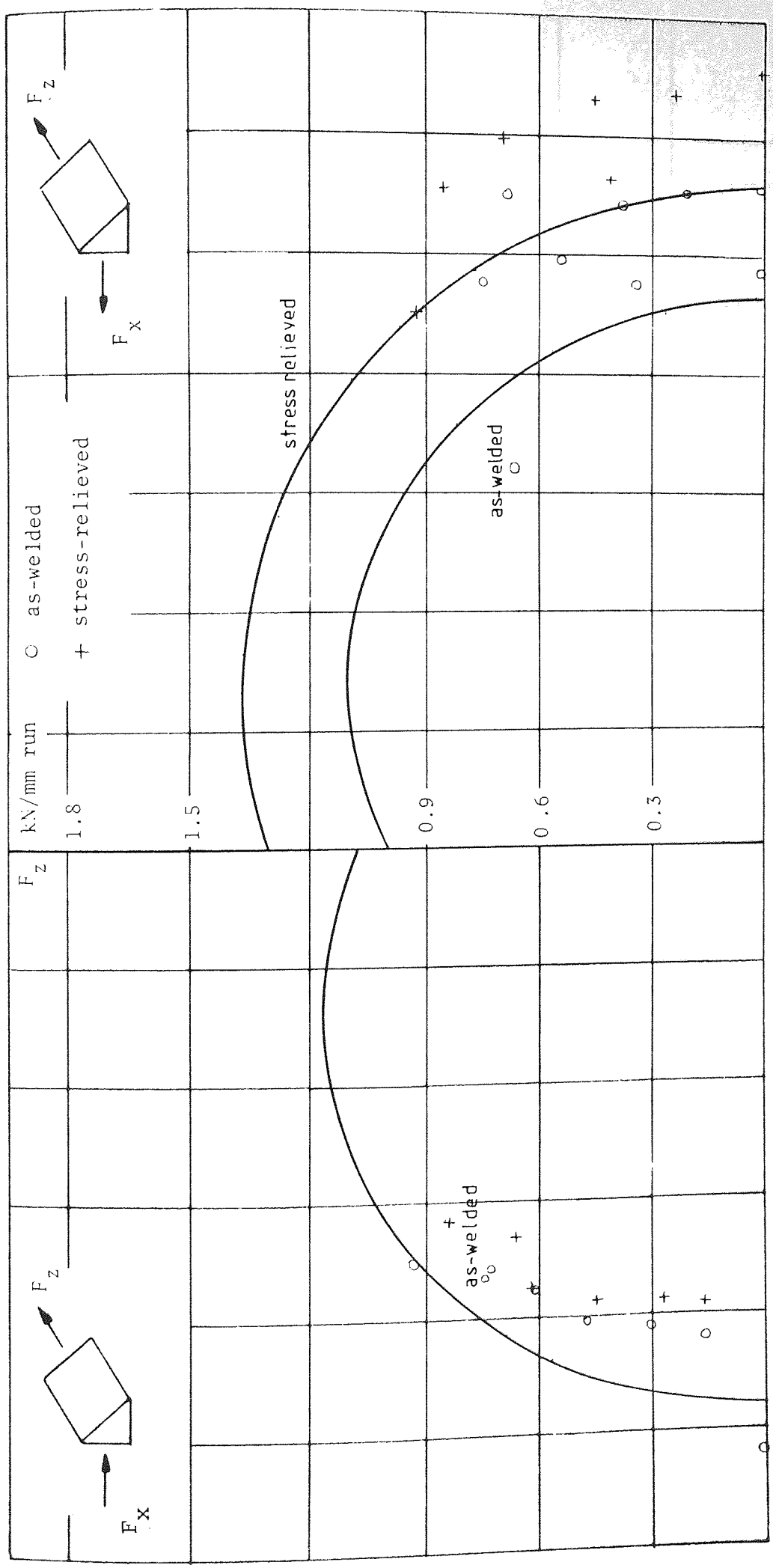

Fig.68 Relationship between F_x and F_z for Double-lapped specimens

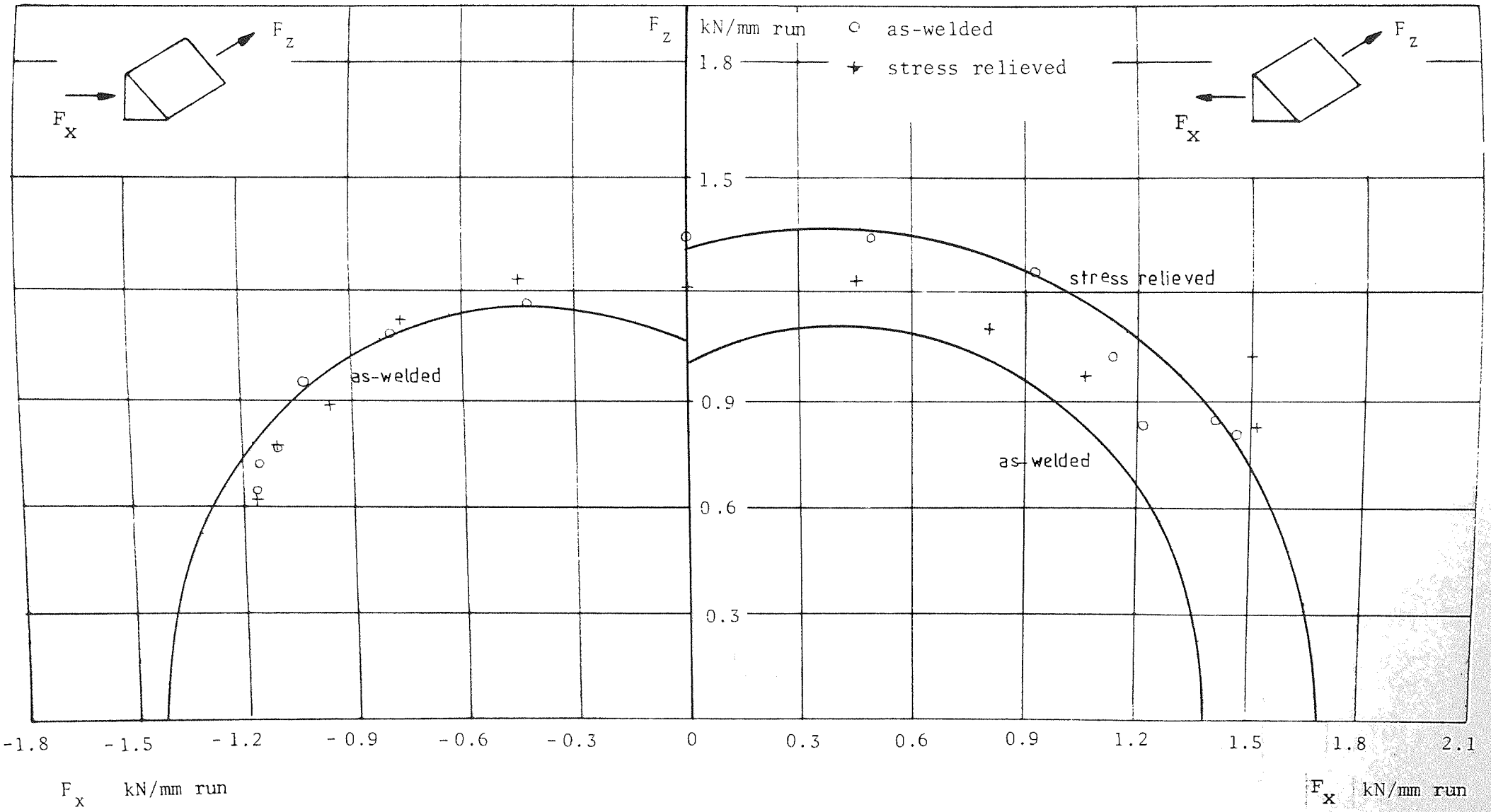

Fig.69 Relationship between F_x and F_z for Crofts Style specimens

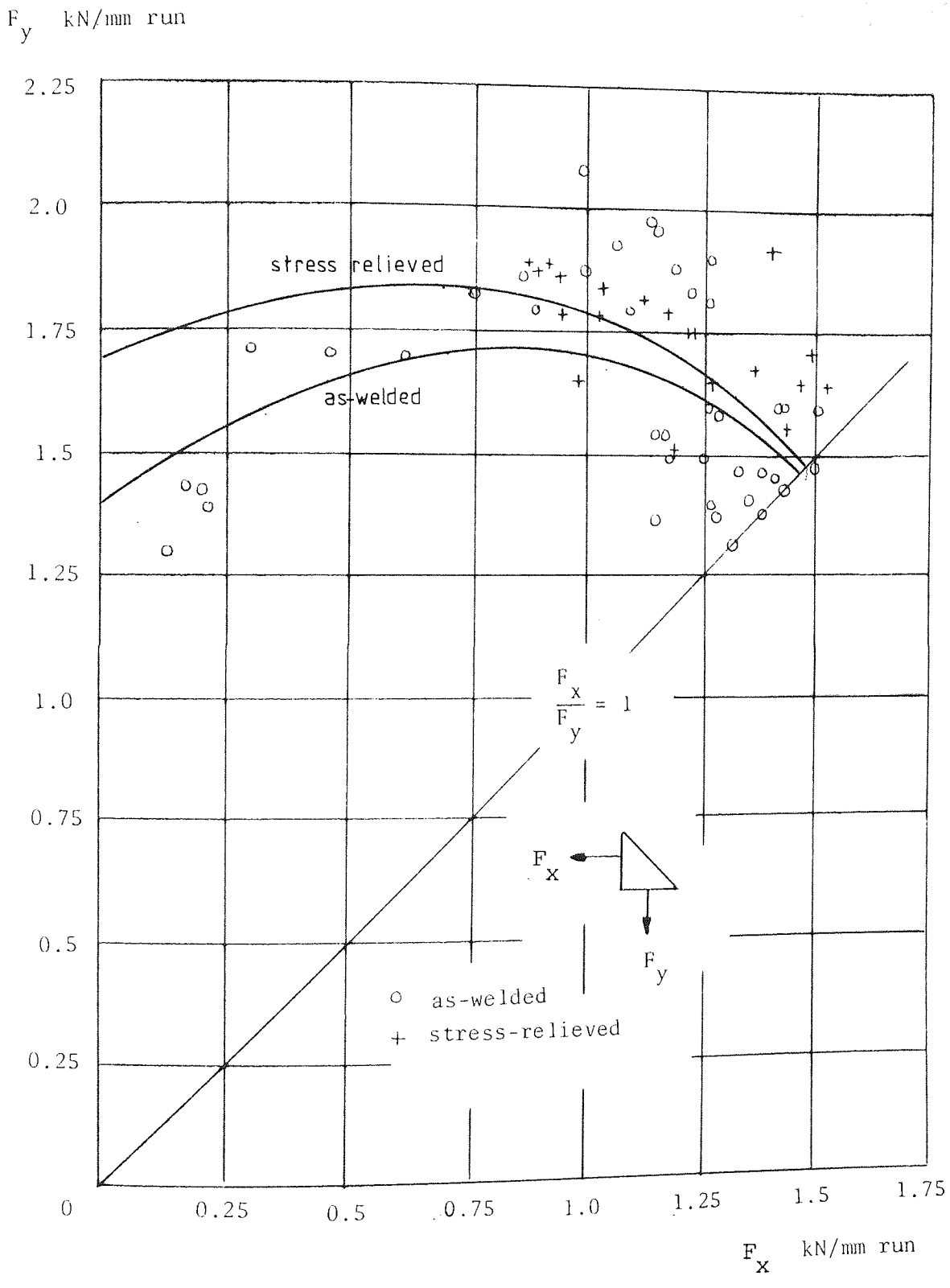

Fig.70 Relationship between F_x and F_y for L Style specimens

Specimen No.	Force F_x kN/mm	Force F_z kN/mm
T1	1.682	0
T3	1.667	0.205
T7	1.441	0.346
T9	1.492	0.549
T11	1.436	0.747
T13	0.973	0.669
T14	1.482	0
T15	1.636	0.378
T16	1.655	0.686
C1	1.270	0.156
C3	1.229	0.295
C5	1.220	0.468
C7	1.134	0.603
C9	1.097	0.740
C11	1.072	0.723
C13	1.049	0.928
C14	1.559	0
T2R	1.978	0
T4R	1.922	0.236
T5R	1.704	0.409
T6R	1.913	0.459
T8R	1.788	0.669
T10R	1.642	0.855
T12R	1.358	0.933
C2R	1.171	0.144
C4R	1.555	0.277
C6R	1.159	0.445
C8R	1.129	0.601
C10R	0.992	0.669
C12R	0.949	0.840

Table 5. Experimental Results - Double-lapped Specimens

Specimen No.	Force F_x kN/mm	Force F_z kN/mm
T0	0	1.347
T1	1.475	0.806
T2	1.415	0.847
T3	1.214	0.830
T4	1.126	1.026
T5	0.922	1.260
T6	0.490	1.341
C1	1.170	0.640
C2	1.157	0.693
C3	1.110	0.758
C4	1.040	0.948
C5	0.798	1.090
C6	0.429	1.173
T7R	1.518	0.830
T8R	1.504	1.027
T9R	1.066	0.971
T10R	0.806	1.102
T11R	0.452	1.234
C7R	0	1.201
C8R	1.126	0.616
C9R	1.110	0.758
C10R	0.971	0.885
C11R	0.774	1.057
C12R	0.452	1.234

Table 6. Experimental Results - Crofts Style Specimens

(b) for the double-lapped specimens, fig.68, it is clear the compression weld is weaker than the tension weld for the entire limited range of F_x/F_z tested, i.e. 2 to ∞. When F_z equals zero the average compression weld strength is 0.892 of that for the tension weld.

(c) for the Crofts style specimens, fig.69, both welds appear to be of approximately equal strength for the range of F_x/F_z tested, 0 to 2.

The results definitely show that the weld under compression is weaker than the weld under tension when the force in the F_x direction is dominant. When the F_z force is dominant the welds appear to be of equal strength.

There are four factors which might explain this phenomenon:

1. joint constraint: there is obviously a high physical constraint when F_x is tensile, the lapped plates being forced to move parallel to each other and in contact under a reactionary normal force - this is likely to give rise to a frictional force between the sliding plates which will be measured as in increase in weld strength. When F_x is compressive the constraint is not present and as a result there may not be plate contact, and relative movement may not be parallel. Ligtenberg[25] referred to this constraint and suggested that its absence when F_x was compressive would probably result in the weld being weaker - which the author's results have shown to be the case. Of course the constraint is not operative with F_z is the dominant force.

The effects of joint constraint on the failure of the weld can be seen in plate 5. Plate 5(1) shows a compression specimen in which the whole weld has deformed with consequent loss of weld profile. The separated parts do not fit together as they do for the tension specimen shown in plate 5(4) which shows a sharp contrast with an almost perfect weld profile.

Plate 5 Fractured Failure Criterion Specimens

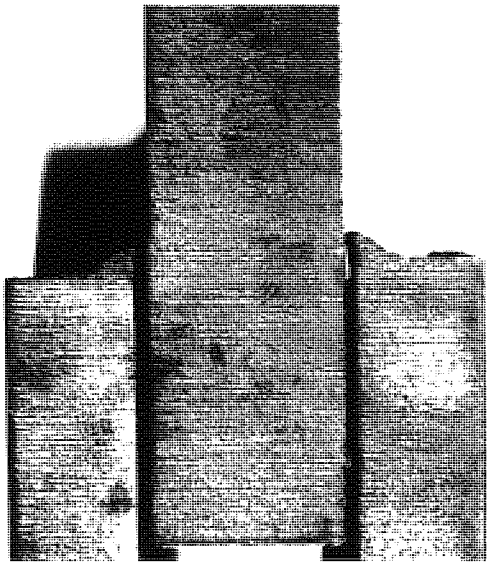

1 Speciman C9

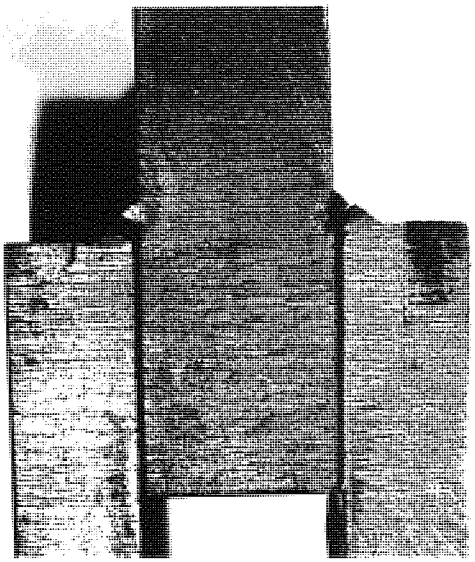

2 Specimen C74

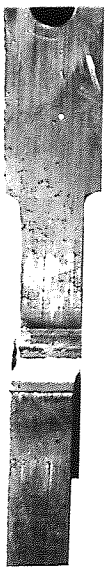

3 Specimen T29

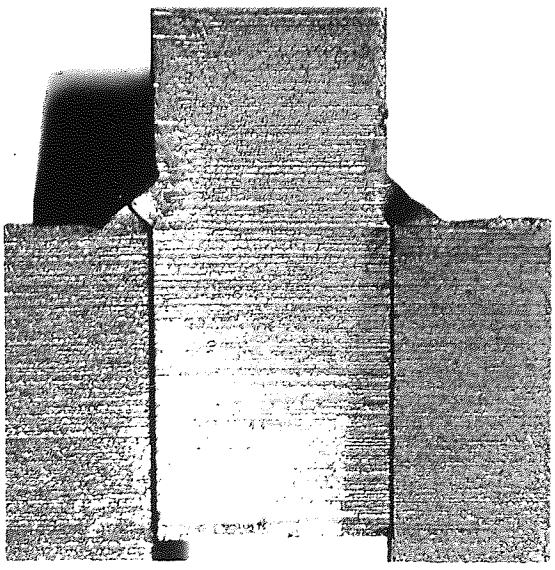

4 Specimen T30

2. fracture plane angle: it can be seen from fig. 70a, which shows the relationship between the fracture plane angle and the load ratio, for values F_x/F_z greater than unity, fracture angles for welds under compression are approximately half those for welds under tension,

3. Crofts and Martin[45] failure criterion: smaller fracture plane angles imply larger fracture plane surfaces and this could be expected to result in greater weld strength if it were not for the failure criterion proposed by Crofts and Martin[45], see fig. 50. As the fracture angle decreases the ratio of failure plane stresses, τ_ϕ/σ_ϕ must increase and this represents a movement down the slope of the failure criterion. If this slope is greater than some critical value then movement down the slope means reducing weld strength even though the fracture plane area is increasing,

4. mode of failure of weld: although uniform stress distributions have been assumed, it is reasonable to assume that weld failure is initiated at either the weld root or toe. It is likely that the direction of the weld force F_x will affect the mode of failure of the weld. It was observed during testing that failure was initiated at the weld root in the case of the tension specimens. No such clear evidence was obtained during testing of the compression specimens.

5.6 Effects of Stress Relieving

Wheatley and Baker[53,54] have shown that reheating of mild steel weld metal in isolation from the joint at a temperature of 600°C produced no appreciable change in mechanical properties of the weld metal. On the other hand, Parker[52] reported reduction in both tensile and yield strength, and a large increase in ductility of butt welds in situ after thermal stress relieving at 600°C. No tests on stress relieved fillet welds have been recorded. The purpose of the author's tests was simply to

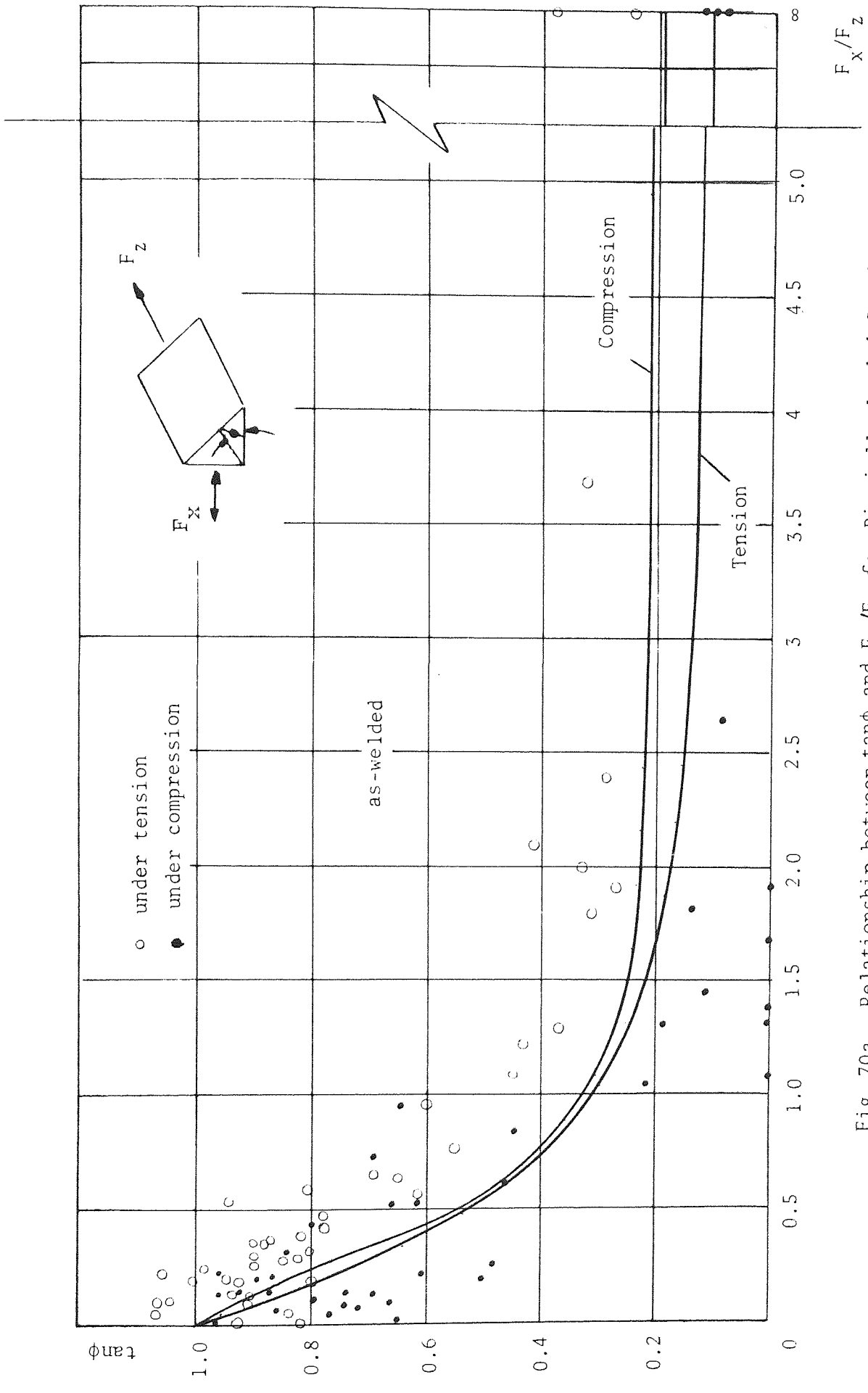

Fig. 70a. Relationship between tanΦ and F_x/F_z for Biaxially-loaded Specimens

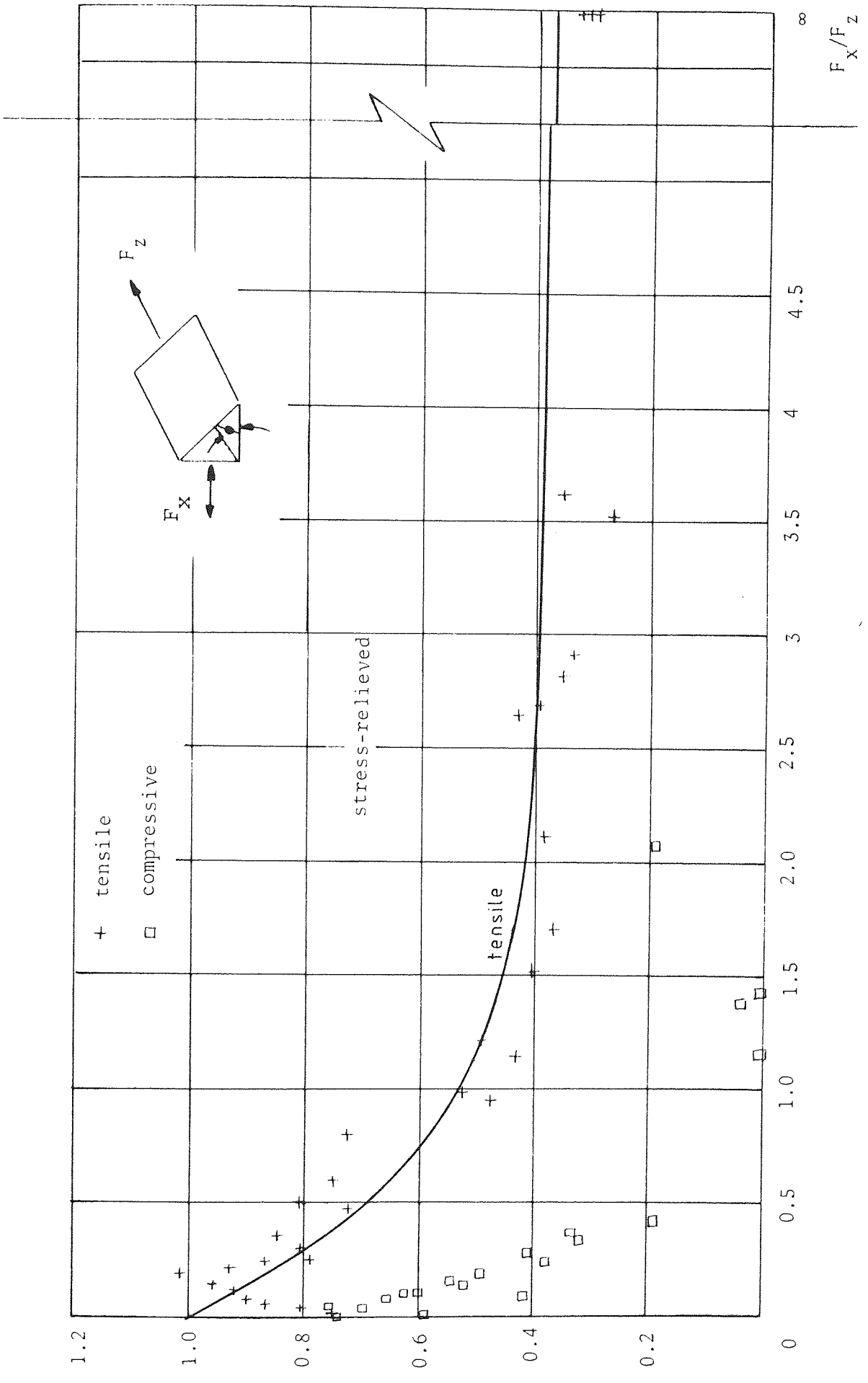

Fig.71. Relationship between tanϕ and F_x/F_z for biaxially-loaded specimens

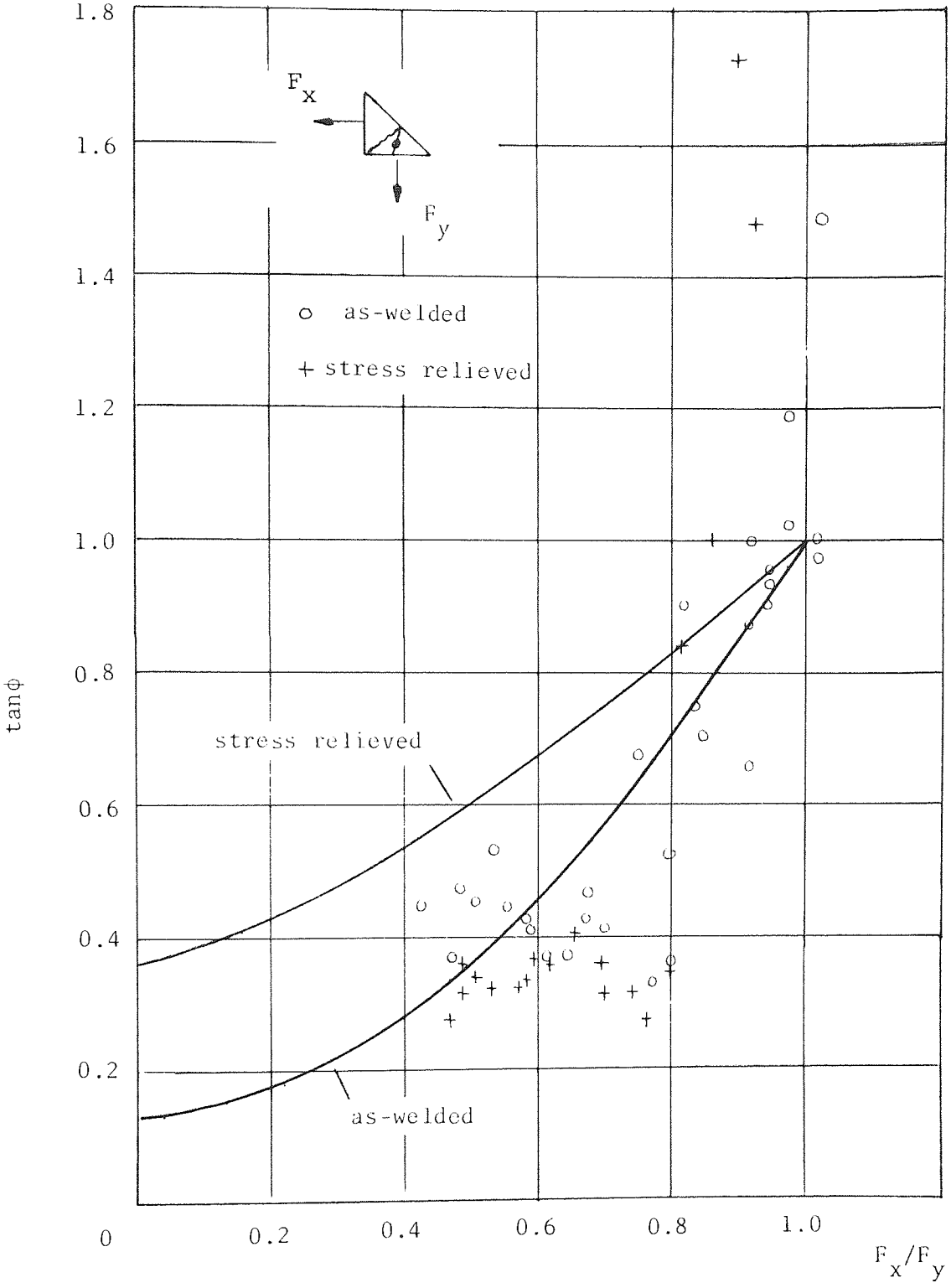

Fig. 72. Relationship between tanϕ and F_x/F_y for L style specimens

establish whether or not residual stresses in fillet welded joints affected the ultimate strength of the welds. Results of the stress relieved test specimens are shown alongside the results of the as-welded specimens in figs. 67, 68, 69 and 70.

For the biaxially-loaded specimens, fig. 67, for the load condition $F_x = 0$, weld force F_z has been increased by approximately 30%. The weld strength has been increased for the entire range of F_x/F_z of the weld under tension with an approximate increase of 12% for the condition of F_z equals zero. For the compression weld there appears to be a slight reduction in weld strength in the range of F_x/F_z of 2 to ∞.

The trend indicated by the double-lapped specimen results, fig.68, is in agreement with the trend outlined above. This cannot be said of the results of the Crofts style specimens,fig. 69, which show little or no differences in weld strength as a result of stress relieving. This would indicate a low level of residual stress in the as-welded condition. This is quite feasible since the Crofts style specimens were made up from relatively thin plate to a design which is very flexible when compared to the biaxially-loaded and double lapped specimens. The same reasoning can be applied to the L style specimens, the results of which are shown in fig. 70, these indicate little or no difference in the weld strength as a result of stress relieving, except for a small increase as the ratio F_x/F_y approaches unity.

It follows, that since the Crofts style specimens had a lower residual stress in the as-welded condition then the biaxially-loaded specimens, the welds should display a greater strength. If a comparison is made between figs. 69 and 67 it can be seen that the Crofts style

specimens were indeed stronger, but only under tension. Under compression equal strength is indicated.

The double-lapped specimens are of a similar design and construction to the biaxially-loaded specimens, and hence they would be expected to have approximately equal strengths. A comparison of figs. 67 and 68 will confirm this expectation.

The question now arises as to how fillet weld strength is increased by a reduction in residual stress level. The author does not intend to answer this question in depth, but merely to point out a possible avenue down which a solution may be found. It has already been suggested that failure of the fillet weld is initiated at the weld root. This is due to two factors, firstly the weld root must necessarily undergo a finite displacement and secondly, as a direct result of the weld geometry the root acts as a severe stress raiser. Weld ductility could well be the limiting factor in root crack initiation, and an increase in ductility would probably produce an increase in weld strength. Parker[52] reported an increase in weld ductility of 16% after thermal stress relieving at 600°C. When the F_z force is dominant the weld root is called upon to accommodate a greater displacement than when the F_x force is dominant thus, an increase in weld ductility would bestow a greater increase in weld strength when the F_z is dominant then when F_x is dominant - this has been shown to be the case, see fig. 67. The importance of weld ductility as the ratio of F_x/F_z tends to zero is well illustrated in plate 6(1), (2) and (3). The ratios of F_x/F_z are 0.61, 0.072, 10.85 respectively for these stress relieved specimens. No such contrast was found in the as-welded specimens.

Plate 6 Fractured Failure Criterion Specimens

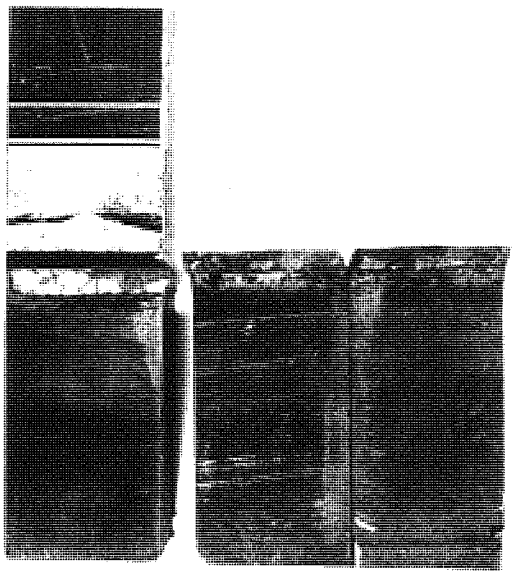

1 Specimen C 55 R

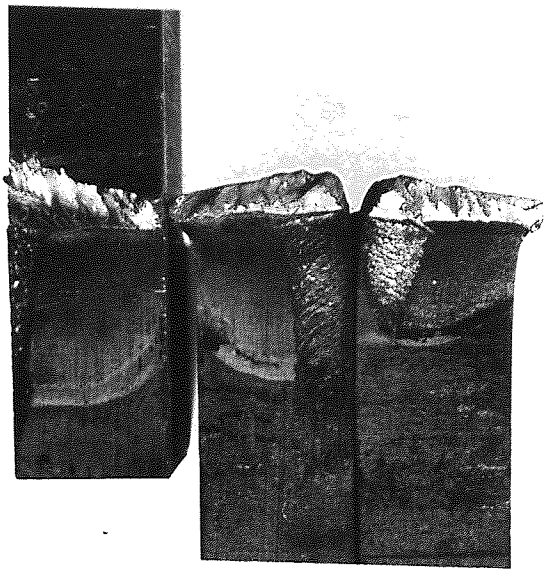

2 Specimen C44R

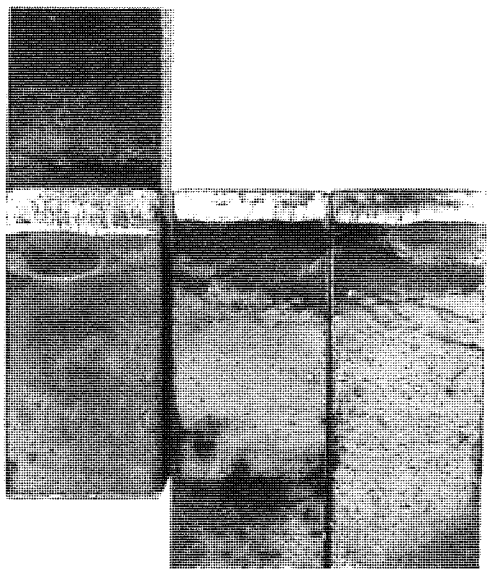

3 Specimen C63R

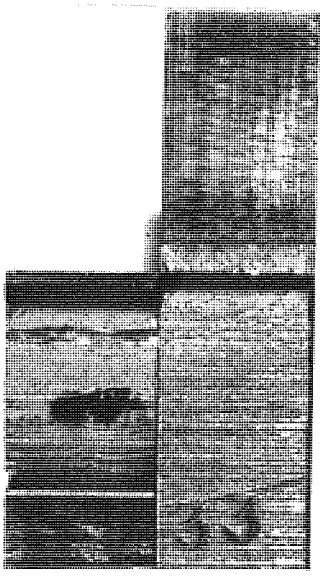

4 Specimen L33R

5.7 Compatibility of Styles of Test Specimens

It is common practice to make comparisons between results produced by different investigators using different styles of test specimen without giving due regard to the importance of such differences. The results presented so far have shown that the biaxially-loaded, and the double-lapped specimens can be directly compared since they have similar residual stress levels. The Crofts style specimen is not comparable because of its relatively low residual stress level and high flexibility. The L style is loaded with F_x and F_y, and cannot be directly compared with the other specimens which are loaded with F_x and F_z. It is intended to combine the results of the L style and biaxially-loaded specimens to produce a failure criterion. It is realized that these two different designs of specimen may not be compatible owing to differing residual stress levels.

5.8 Linear Failure Criterion

The linear failure criterion was presented by Crofts and Martin[45] and is shown in fig. 50. It is much more attractive than the Vreedenburgh[16] limit curve because of its simplicity. It contains an anomaly by giving two values of the ultimate shear strength of the weld metal, namely 331 N/mm^2 from the shear/tension zone, and 305 N/mm^2 from the shear/compression zone.

The field of the criterion as it stands is rather limited since it only covers loading situations which produce a predominant shear stress on the critical plane. Obviously there are loading situations which produce predominantly normal stresses rather than shear stresses, such a situation is not catered for by the existing linear criterion.

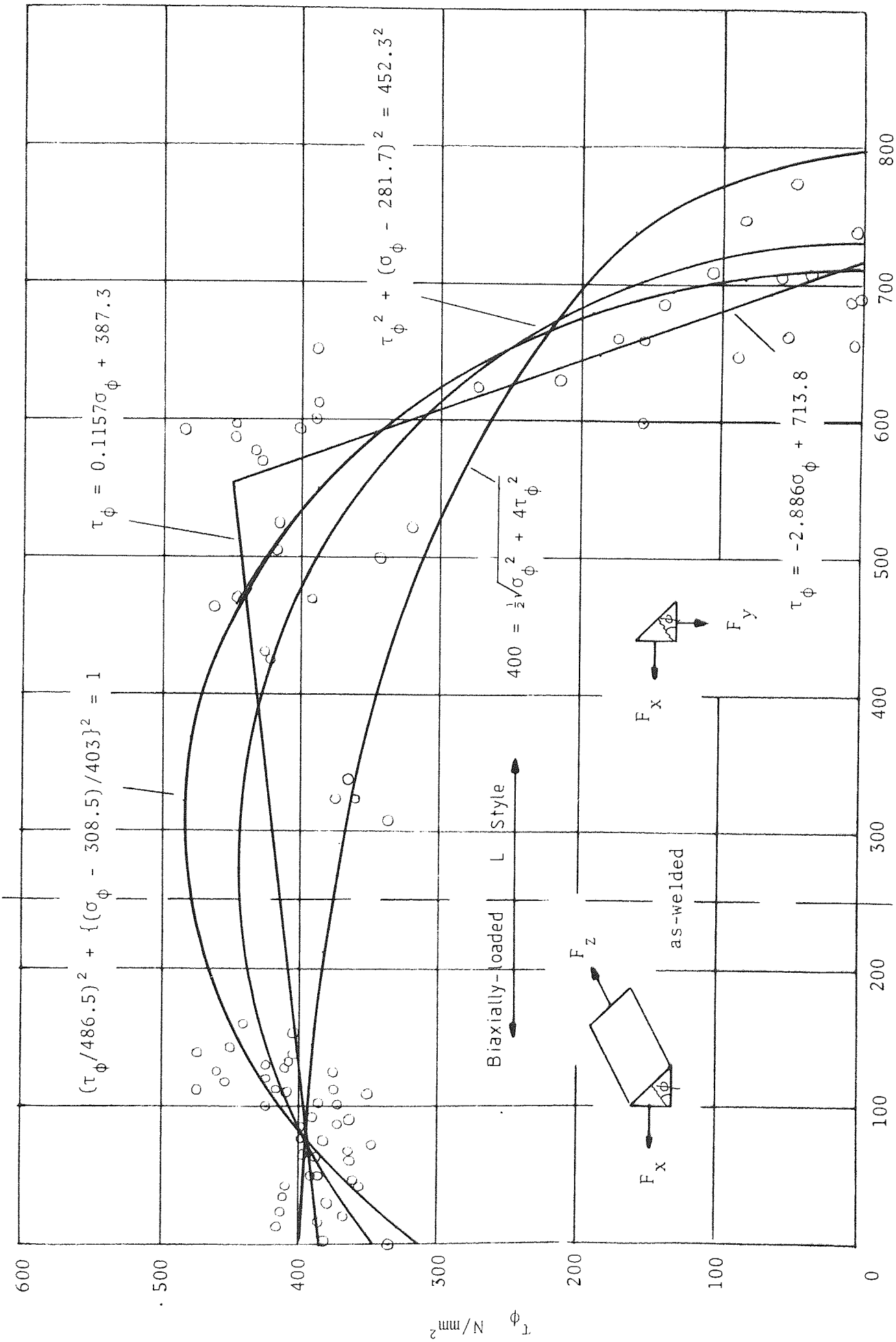

Fig.73 Relationship between Critical Plane Stresses τ_ϕ and σ_ϕ

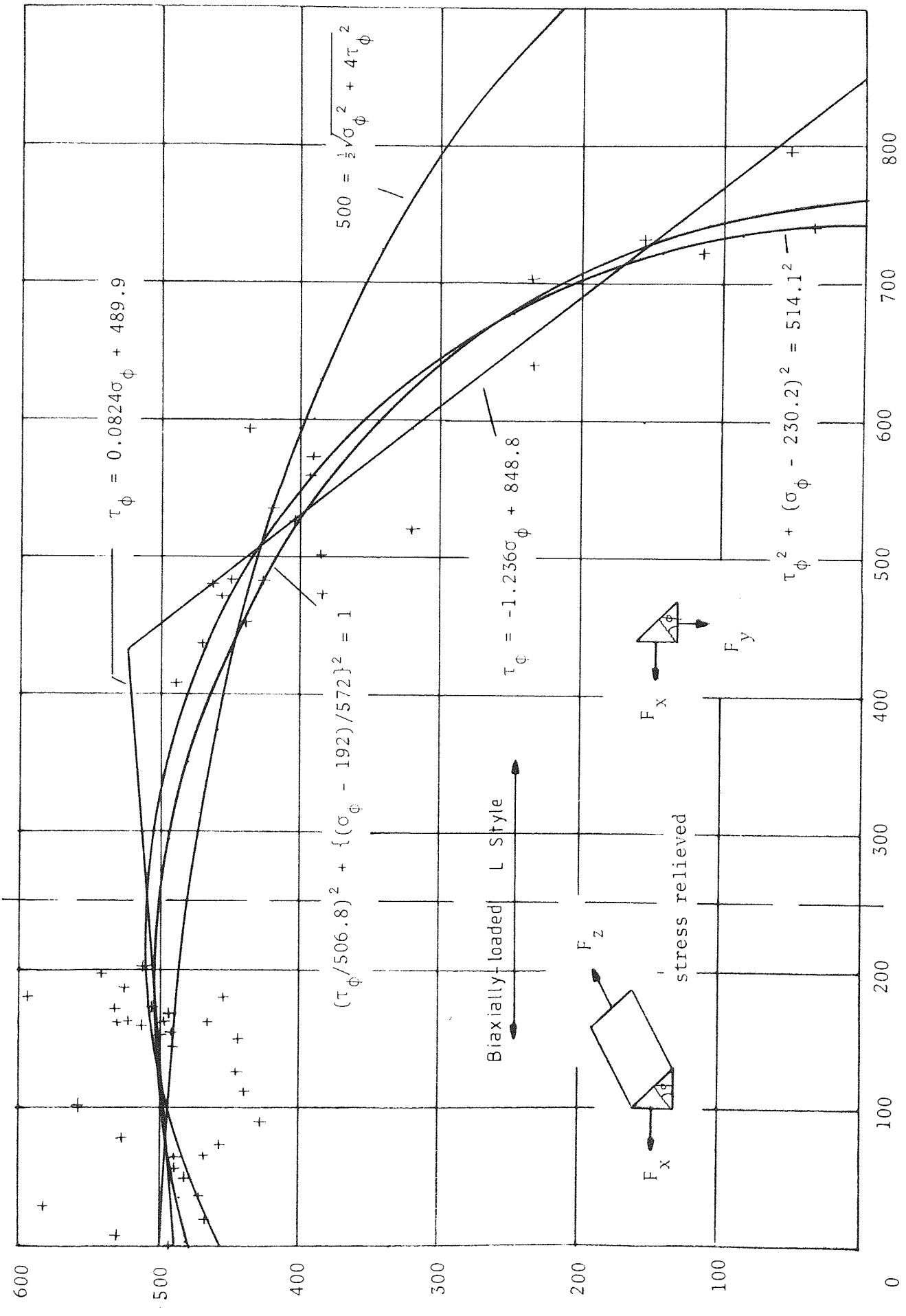

Fig.74 Relationship between Critical Plane Stresses τ_ϕ and σ_ϕ

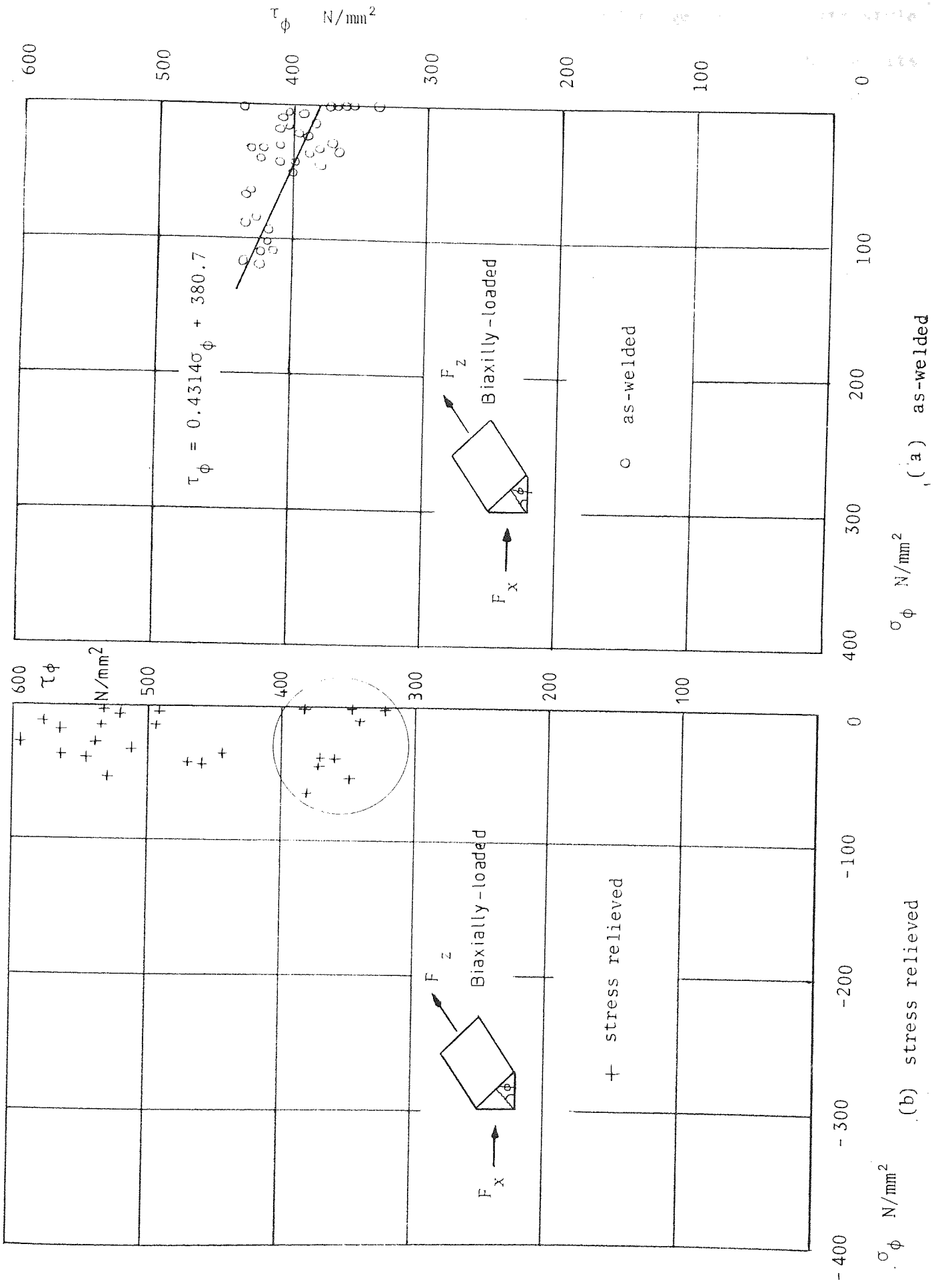

Fig.75 Relationship between Critical Plane Stresses τ_ϕ and σ_ϕ

Because of the limited number of tests and range of the Crofts style and double-lapped specimens, it was decided to concentrate on the results from the biaxially-loaded and L style specimens. The critical plane stresses have been computed from these results and are shown plotted in figs. 73, 74 and 75. It will be noted that the shear/tension zone, figs. 73 and 74, is denoted by two styles of test specimen, the biaxially-loaded, and the L style. It is the author's contention that neither of the two styles can give results covering the complete shear/tension zone, and therefore by necessity if a complete coverage is required, more than one style of specimen must be tested. This raises the question of test specimen compatibility and the expectation of a single continuous rather than a bi-part linear criterion. Although it is not possible for either of the two styles of specimen to give complete coverage of the shear/tension zone, it is possible to obtain overlapping results. Unfortunately overlap has not been achieved in the results shown because of the limited range of F_x/F_y tested - a full range of F_x/F_z was tested.

Linear regression analysis was carried out on the results and the findings are tabulated below. These best-fit straight lines have been plotted on the failure criterion field shown in figs. 73, 74 and 75. In the case of the shear/tension zone, complete coverage has been achieved (except for the gap already discussed), but in the shear/compression zone, no advance has been made beyond that achieved by Crofts and Martin[45]. If a direct comparison is made between the Crofts and Martin and the authors' criterion it would be seen that the slopes of the former were approximately twice those of the latter. Compatibility of styles of test specimens has already been discussed - the differences in the aforementioned slopes are probably due to the

Loading Situation	Slope of line m	Intercept τ_ϕ axis N/mm^2	Intercept σ_ϕ axis N/mm^2	Regression correlation factor
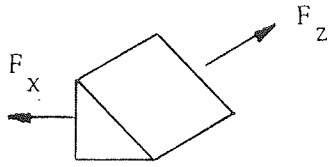 as welded	0.1157	387.3	-	0.3969
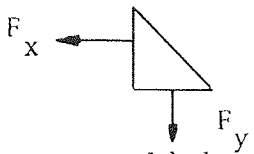 as welded	-2.886	-	713.8	-0.8023
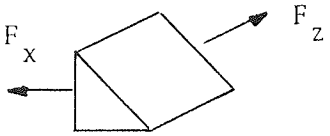 stress relieved	0.0824	489.9	-	0.1245
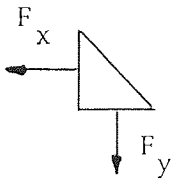 stress relieved	-1.236	-	848.8	-0.9383
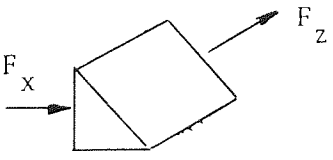 as welded	0.4314	380.7	-	0.6314
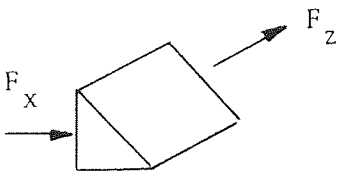 stress relieved	too much scatter in the results to give any meaningful assessment			

greater ductility of welds in the Crofts style specimens. The difference in the average values of ultimate shear strength is due to the improved welding technique (already described) used by the author.

The role of residual stress and the effects of stress relieving have already been discussed with reference to figs. 67, 68, 69 and 70. The increase in strength of the weld under the F_x/F_z loading situation, see fig. 67, is represented in fig. 74 by an apparent increase in the ultimate shear strength (the intercept of the τ_ϕ axis) of approximately 28%. The slight reduction in the weld strength indicated in fig. 67 when the F_x force was dominant and compressive is reflected in fig. 75(b) by nine points in the shear/compression zone which are ringed. These specimens did not fail in the normal manner i.e. along a planar surface within the 45° fillet shape, but in the side wall region of the welded plates in a non-planar mode. Owing to these anomalous failures a straight line has not been fitted to the results of the stress relieved shear/compression specimens.

With reference to the L style specimens and fig. 70, it was noted that little or no increase in weld strength was apparent as a result of stress relieving, except for ratios of F_x/F_y approaching unity. At the ratio of F_x/F_y equals unity the critical plane is assumed to be at 45° to the weld leg and under a purely tensile stress. The slight increase in weld strength, as a result of stress relieving, indicated in fig. 70 should be reflected by a slight increase in the ultimate tensile strength of the weld (intercept of the σ_ϕ axis) as indicated by figs. 73 and 74. In fact the predicted increase is relatively large, from 713.8 to 848.8 N/mm^2, approximately 19%. This unrealistic increase in tensile strength is a manifestation of the poor fit provided by the straight

line criterion, especially with regard to the σ_ϕ intercept in fig. 74. The generally poor fit of the linear criterion is reflected in the regression correlation factors, ±1 denoting a perfect fit. Further, it is most unlikely that the meeting of the straight lines represents the actual situation in that part of the shear/tension zone. Some sought of curve joining the two straight lines is much more realistic. The original simplicity of the Crofts and Martin[45] failure criterion is no longer present in this suggested tri-part criterion of the shear/tension zone.

The purpose of establishing a failure criterion is to gain a position from which a general method for the prediction of the ultimate capacity of welded beam-column connections could be developed.

The welds of an all-round welded beam-column connection are subjected to five different loading situations;

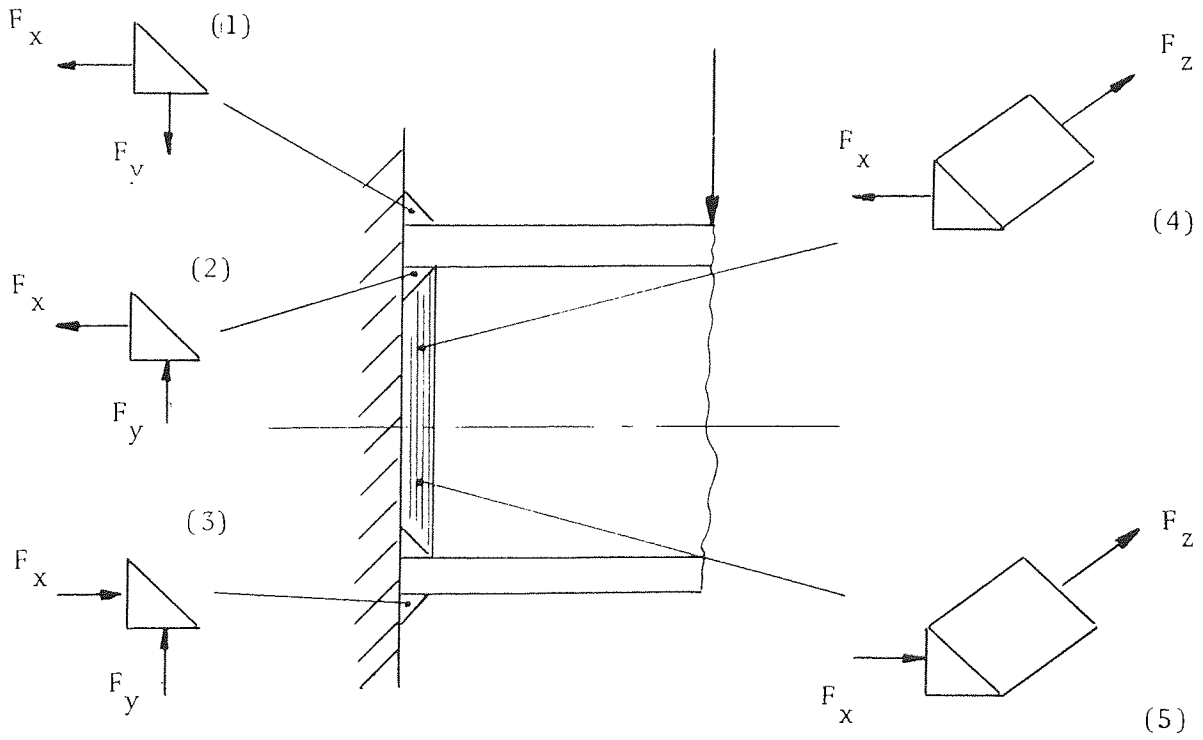

Use of a tri-part, or even a bi-part failure criterion would cause serious problems because prior judgements would have to be made with regard to which part of the criterion was applicable to which loading situation. Obviously a uni-part criterion applicable to all loading situations is the ideal situation. This is probably not attainable because welds under compression have been shown to behave differently to those under tension - though the difference is small and a slight approximation might allow for a single uni- part all-embracing criterion.

No results were obtained by the author for the loading conditions (2) and (3) shown above, and so efforts will be concentrated on establishing a uni-part failure criterion for the shear/tension zone.

5.9 Elliptic Failure Criteria

The general spread of the plotted points of the shear/tension zone are suggestive of an ellipse with one of its axes coincident with the σ_ϕ axis. A regression analysis was carried out using the technique of minimising the sum of the normal errors squared, in order to find the best-fit ellipse for both as-welded, and stress relieved specimens. The equation of the ellipse is as follows:

$$\left[\frac{\tau_\phi}{a}\right]^2 + \left[\frac{\sigma_\phi - c}{b}\right]^2 = 1$$

where a and b are half-axes, and c is the axis shift from the τ_ϕ axis. The computer results are given below:

Specimen condition/ number of points	a N/mm^2	b N/mm^2	c N/mm^2	$\sum(\text{error})^2$
as-welded 78	486.5	403.0	308.5	106339
stress-relieved 53	506.8	572.0	192.0	70695

Regression was also done for the circle, the results as follows:

as-welded 78	452.3	452.3	281.7	136911
stress-relieved 53	514.1	514.1	230.2	73894

The failure criterion proposed by Archer[22] is based on the maximum shear stress,

$$\text{maximum shear stress} = \tfrac{1}{2}\sqrt{\sigma_\phi^{\,2} + 4\tau_\phi^{\,2}}$$

this being related to the ultimate shear strength of the weld as determined by side-weld, or torsional control tests. The side-weld test of the double-lapped specimen is likely to give an overestimate of the ultimate shear strength because of the very high constraint controlling the relative movement of the plates (this point has already been discussed).

Side-weld tests carried out by the author gave an ultimate shear strength of 440 N/mm^2 for the as-welded specimens, and 420 N/mm^2 for the stress relieved specimens. Neither of these two values makes a good comparison with those values suggested by figs. 73 and 74, namely 400 N/mm^2 (approx.) for as-welded and 500 N/mm^2 (approx) for stress relieved specimens. This comparison serves to highlight the possible dangers of relating standard control tests to the field situation.

The Archer[22] criterion (based upon 400 N/mm^2 and 500 N/mm^2) along with the bi-part linear, ellipse, and circle are shown in figs. 73 and 74. With the exception of the Archer criterion a rising characteristic from the τ_ϕ axis is displayed in keeping with the general trend of the results. The full explanation of this rising characteristic is not known to the author, but it is thought to be allied to the behaviour of an

Table 7. Failure Criteria Calculated Results

$\frac{F_x}{F_y}$	F_x kN/mm run	F_y kN/mm run	tan ϕ
0.0	0.0	1.701	0.3668
0.1	0.177	1.770	0.3948
0.2	0.363	1.817	0.4328
0.3	0.552	1.838	0.4810
0.4	0.734	1.834	0.5387
0.5	0.904	1.808	0.6049
0.6	1.058	1.762	0.6778
0.7	1.192	1.704	0.7556
0.8	1.309	1.636	0.8364
0.9	1.407	1.563	0.9183
1.0	1.489	1.489	1.0000

(a) Best-fit circle criterion, stress relieved specimens

0.0	0	1.399	0.1192
0.1	0.150	1.504	0.1354
0.2	0.319	1.594	0.1648
0.3	0.498	1.661	0.2093
0.4	0.680	1.700	0.2708
0.5	0.856	1.712	0.3501
0.6	1.018	1.696	0.4475
0.7	1.161	1.659	0.5626
0.8	1.284	1.605	0.6942
0.9	1.386	1.540	0.8406
1.0	1.468	1.468	1.0000

(b) Best-fit circle criterion, as-welded specimens

cont'd

(c) Best-fit circle criterion, stress relieved, and as-welded

$\frac{F_x}{F_z}$	as-welded			stress relieved		
	F_x	F_z	tanϕ	F_x	F_z	tanϕ
	kN/mm run	kN/mm run		kN/mm run	kN/mm run	
0	0.0	1.001	1.0000	0.0	1.300	1.0000
0.1	0.105	1.052	0.8883	0.134	1.339	0.9296
0.2	0.218	1.088	0.7819	0.273	1.363	0.8618
0.3	0.333	1.109	0.6846	0.411	1.371	0.7986
0.4	0.446	1.115	0.5990	0.545	1.363	0.7414
0.5	0.553	1.106	0.5257	0.671	1.342	0.6909
0.8	0.817	1.021	0.3703	0.983	1.228	0.5778
1.0	0.944	0.944	0.3063	1.134	1.134	0.8279
1.5	1.139	0.759	0.2190	1.372	0.914	0.4561
2.0	1.236	0.618	0.1797	1.493	0.746	0.4219
2.5	1.289	0.516	0.1594	1.560	0.624	0.4037
3.0	1.320	0.440	0.1477	1.599	0.533	0.3931
4.0	1.353	0.338	0.1356	1.642	0.410	0.3820
7.0	1.384	0.198	0.1247	1.681	0.240	0.3719
14.0	1.395	0.100	0.1206	1.696	0.121	0.3680
1000.0	1.399	0.001	0.1192	1.701	0.002	0.3668

cont'd

$\frac{F_z}{F_x}$	F_x kN/mm run	F_z kN/mm run	$\tan\phi$
0.0	1.441	0.0	0.1942
0.1	1.433	0.143	0.1983
0.2	1.410	0.282	0.2032
0.3	1.372	0.412	0.2114
0.4	1.325	0.530	0.2217
0.5	1.269	0.635	0.2309
0.75	1.116	0.837	0.2679
1.25	0.837	1.046	0.3979
2.0	0.566	1.133	0.5543
3.5	0.326	1.140	0.7536
5.0	0.226	1.128	0.8391
∞	0.0	1.074	1.0000

(d) Linear criterion for compression/shear (as-welded) specimens

elastically-strained crystal lattice. There must obviously be a peak to this rise, that predicted by the best-fit ellipse is thought to be too far reaching, especially so, since there is no experimental data in the peak zone. The peak of the circle criterion appears more realistic. With regard to the τ_ϕ axis intercept, the ellipse gives the lowest value, approximately 314 N/mm^2 and the Archer criterion the highest, 400 N/mm^2 (this is chosen realistic value). Use of the ellipse criterion would lead to very conservative estimates of strength in loading situations in which the F_z force was very dominant. Similar values of the σ_ϕ axis intercept are predicted by the circle, and ellipse criteria, whereas that predicted by the Archer criterion is overestimated, especially for the stress relieved specimens. It is fair to say that although the circle is not the best-fit, it is the most realistic fit of those examined. The ellipse fit gives smaller average errors than the circle, but the differences are not significant;

37/42 N/mm^2 - as-welded;

36.5/37.3 N/mm^2 - stress welded

No doubt a high-powered polynomial could provide a better fit both statistically and realistically, but would create enormous difficulties in the development of a method for prediction of ultimate capacity of beam-column connections - which must be simple enough for use in the design office. The circle criterion seems the most suitable for this purpose.

Owing to the restricted scope and number of experimental results in the shear/compression zone, only the best-fit linear criterion has been applied, see fig. 75.

The linear criterion is represented by the equation

$$\tau_\phi = m\sigma_\phi + \tau_{ult}$$

where, m = slope of criterion

$\tau_{ult} = \tau_\phi$ axis intercept

The weld in the shear/compression zone is subjected to loading condition (5) and by resolution of the forces F_x and F_z onto the critical plane at angle ϕ to the horizontal leg:

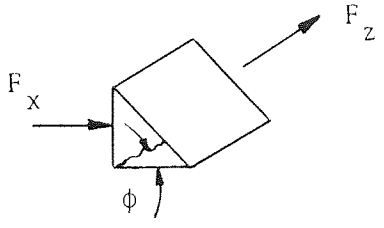

$$\frac{t\tau_{ult}}{F_x} = (\sin\phi+\cos\phi)\left[\sqrt{\cos^2\phi+(F_z/F_x)^2} - m\sin\phi\right]$$

where t equals weld leg length, and weld forces are per unit length.

By an iterative procedure, the angle ϕ can be evaluated, for a given ratio of F_z/F_x, to give F_x a minimum value, i.e. a minimum weld strength. The results of this iterative procedure are given in Table 7(d), and the predicted weld strengths, and critical plane angles have been plotted in figs. 67 and 70a respectively. It can be seen from fig.70a that when F_x is dominant the predicted fracture angles are slightly greater than the actual angles. The greater the angle, the higher up will be the condition on the linear criterion, and greater will be the weld strength. Fig. 67 does show a slightly greater predicted weld strength when F_x is the dominant force.

The circle criterion is represented by the equation

$$\tau_\phi^2 + (\sigma_\phi - c)^2 = a^2 \qquad (1)$$

where, a is the radius, and c the centre shift. The weld in the shear/tension zone can be subjected to a combination of loading conditions (1) and (4) and by resolution of the forces F_x, F_y and F_x onto the critical plane, with reference to unit leg and length:

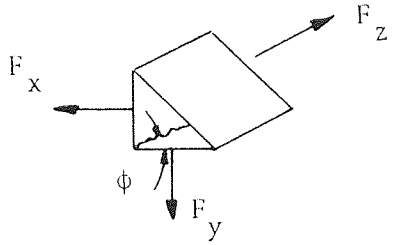

$$\sigma_\phi = (F_x \tan\phi + F_y)\frac{(1 + \tan\phi)}{(1 + \tan^2\phi)} \qquad (2)$$

and, $$\tau_\phi = \sqrt{F_z^2(1 + \tan^2\phi) + (F_x - F_y\tan\phi)^2}\ \frac{(1 + \tan\phi)}{(1 + \tan^2\phi)} \qquad (3)$$

where forces F_x, F_y and F_z referenced to unit weld length.
By substitution into the circle criterion the following relationship is obtained

$$(F_x^2 + F_y^2 + F_z^2)\frac{(1 + \tan\phi)^2}{(1 + \tan^2\phi)} - 2c(F_x\tan\phi + F_y)\frac{(1 + \tan\phi)}{(1 + \tan^2\phi)} = a^2 + c^2 \qquad (4)$$

By differentiating equation (4), the value of tan ϕ for which F_x is a minimum for a fixed ratio of F_y/F_x and F_z/F_x is

$$\tan \phi = \left[(A + B)/(C + B)\right] - \sqrt{\left[(A + B)/(C + B)\right]^2 + \left[(C - B)/(C + B)\right]} \qquad (5)$$

where $$A = (1 - F_y/F_x)^2/\left[1 + (F_y/F_x)^2 + (F_z/F_x)^2\right] \qquad (6)$$

$$B = (b/c)^2 - 1 \qquad (7)$$

$$C = \left[1 - (F_y/F_x)^2\right]/\left[1 + (F_y/F_x)^2 + (F_z/F_x)^2\right] \qquad (8)$$

Equations (2) to (8) are applicable to fillet welds loaded under tension on both legs and under longitudinal shear, i.e. subjected to forces F_x (tensile), F_y (tensile) and F_z.

For loading condition (1), $F_z = 0$ and equations (4), (6) and (8) become

$$(F_x^2 + F_y^2)\frac{(1 + \tan\phi)^2}{(1 + \tan^2\phi)} - 2c(F_x\tan\phi + F_y)\frac{(1 + \tan\phi)}{(1 + \tan^2\phi)} = a^2 + c^2 \qquad (4a)$$

$$A = (1 - F_y/F_x)^2/\left[1 + (F_y/F_x)^2\right] \qquad (6a)$$

$$C = \left[1 - (F_y/F_x)^2\right]/\left[1 + (F_y/F_x)^2\right] \qquad (8a)$$

For loading condition (4), $F_y = 0$ and equations (4), (5), (6) and (8) become

$$(F_x^2 + F_z^2)\frac{(1 + \tan\phi)^2}{(1 + \tan^2\phi)} - 2c\,F_x\tan\phi\,\frac{(1 + \tan\phi)}{(1 + \tan^2\phi)} = a^2 + c^2 \qquad (4b)$$

$$\tan\phi = 1 - \sqrt{1 + \left[(C - B)/(C + B)\right]} \qquad (5b)$$

$$A = C = 1/\left[1 + (F_z/F_x)^2\right] \qquad (6b), (8b)$$

The minimum values of weld strength have been obtained from the above equations for load conditions (1) & (4) and are shown in Table 7(a), (b) and (c), and the predicted weld strengths and critical plane angles have been plotted in figs. 67, 70, 70a, 71 and 72.

It can be seen from fig. 67 that the predicted weld strength, using the circle criterion, for the shear/tension zone compares very well with the experimental results, both as-welded and stress relieved. There is slight under-estimation of strength as F_x/F_z approaches zero - this is expected because the circle criterion predicts a slightly low value of the 'ultimate shear strength' (the τ_ϕ axis intercept). The same strength prediction is compared with the results from the Double-lapped, and Crofts style specimen in figs. 68 and 69 respectively - it is not possible to draw any firm conclusions owing to the limited number of experimental results.

There is slight scatter in the experimental results obtained from the Style L specimens, see fig. 70, however, it can be said the strength predictions of the circle criterion compare reasonably well - there is a lack of experimental results, especially for the stress relieved specimens, for low values of the ratio F_x/F_y.

The author's theory for weld strength prediction requires the weld to have a critical plane at the theoretical position corresponding to minimum weld strength.

This implies that the two parts of the weld, at the time of failure, are able to move without restriction and in a direction related to the dominant stress acting on the critical plane. If this is not allowed to

happen then failure could well be by a tearing-mode. The biaxial-loading jig was designed to give as much freedom of movement as possible in an attempt to reduce the possibility of failure by tear. A tearing-mode failure would obviously affect the position and shape of the critical plane as well as the strength of the weld.

For the loading condition F_z dominant, the testing arrangements did allow for the necessary freedom of movement, but not so for the loading condition F_x dominant since the plates were more or less constrained to move parallel to the weld leg (typical critical plane angle for this condition is 18°). The theoretical, and actual critical plane angles are compared in figs. 70a and 71. For the as-welded specimens the predicted angles are somewhat smaller than the actual. For the stress relieved specimens, the correlation is very good, probably as a result of the increased weld ductility which would allow for greater flexibility regarding the relative movement of the failing parts of the weld.

For the majority of the style L specimens the actual fracture angles were greater than 30° which signifies a predominantly normal stress on the critical plane, and a direction of failure generally in the direction of the applied load. Fracture plane angles are compared for these specimens in fig. 72. Despite the scatter in results, good correlation is evident for the as-welded specimens.

The predicted weld strength and critical plane angles for the shear/compression biaxially-loaded specimens (as-welded) are shown in figs. 67 and 70a.

The author feels that the circle criterion and the method of weld strength prediction have been sufficiently justified by the experimental results.

CHAPTER 6

RESULTS AND DISCUSSION - BEAM-COLUMN CONNECTIONS

6.1 Flange Profiles

Ligtenberg[20] had shown that flange stiffness was an important factor in determining the shear load distribution along the flange weld, and in the proportioning of the applied shear load between the two flange welds. Dawe[42] had attempted to measure flange deformation during testing, but did not report his findings.

Flange width was one of the variables considered by the author and it was felt that flange deformation patterns could display certain behavioural characteristics regarding shear load distribution and sharing. It was anticipated that for low values of V/M flange deformation would be relatively small. It was intended to compare flange profiles of before and after failure, and so it was considered necessary to record the profiles before testing. These recorded profiles are shown in figs. 76, 77, 78, 79 and 80. It will be seen that in many cases the flanges are neither perpendicular to the web, nor parallel to each other. Flanges of series 305 x 127 and 356 x 171 were reasonably flat, but not those of series 305 x 305. For all test specimens the flanges which were most perpendicular to the web were chosen to be the tension flanges, i.e. to be the flanges which would carry the weld under a shear/tension load(loading condition (1)). This was done in order to ensure, as far as possible, the shear/tension weld would be loaded symmetrically and without twisting. It was anticipated that the shear/tension weld would fail first and hence, was considered the more important of the two welds.

Fig. 76 Flange Profiles Before Testing, Series 305 x 127

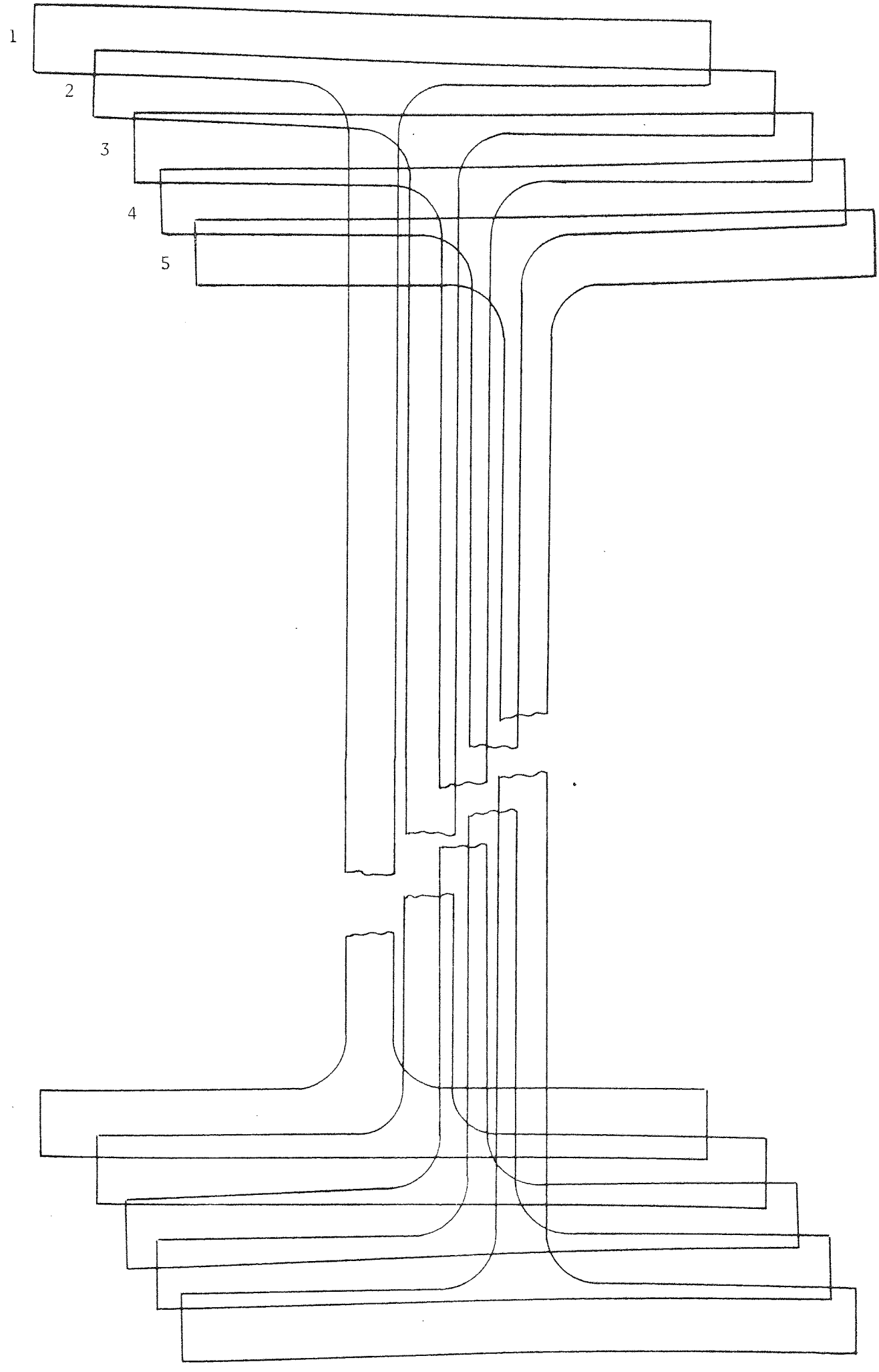

Fig. 77 Tension Flange Profiles Before Testing,

Series 356 x 171

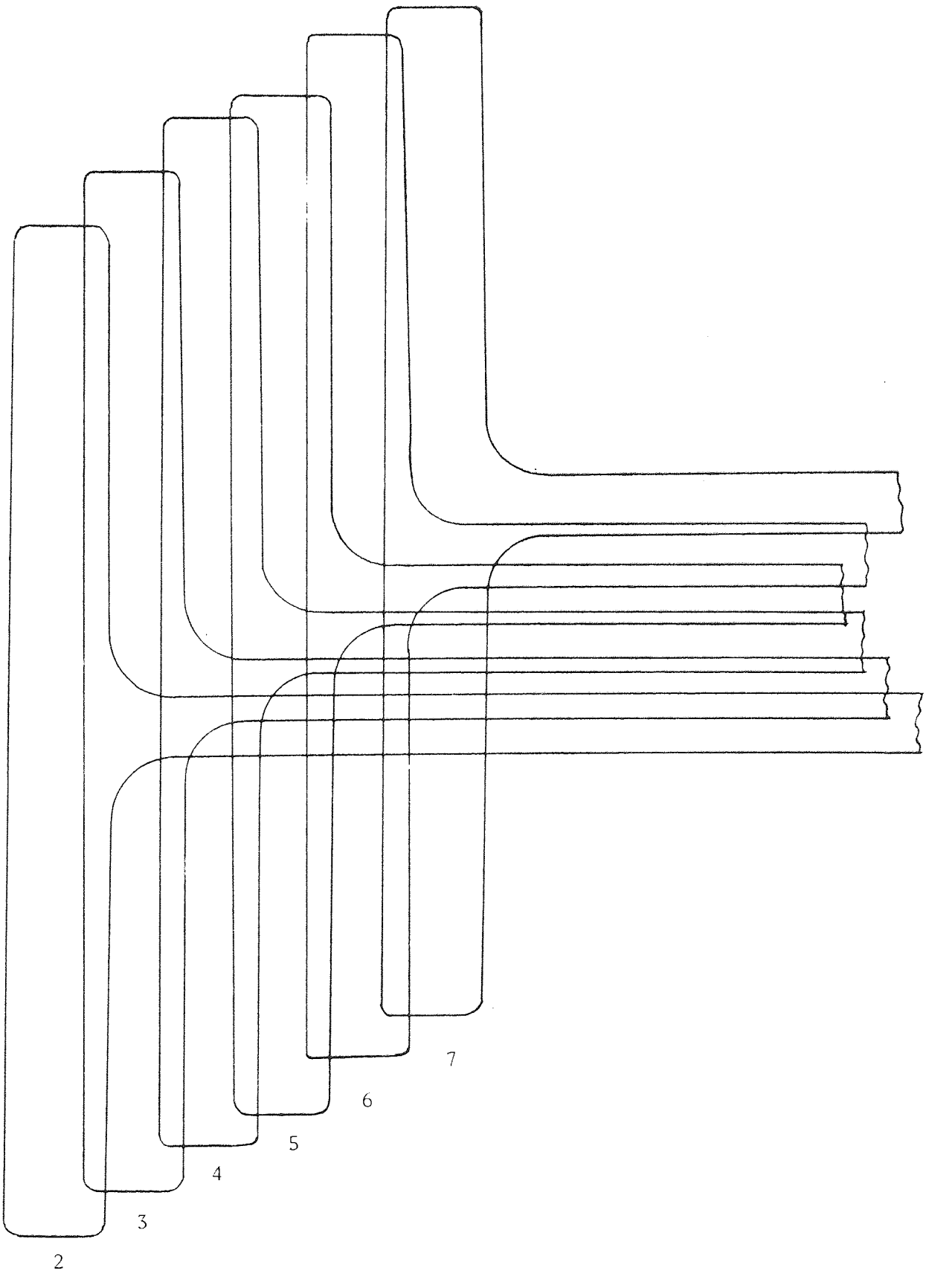

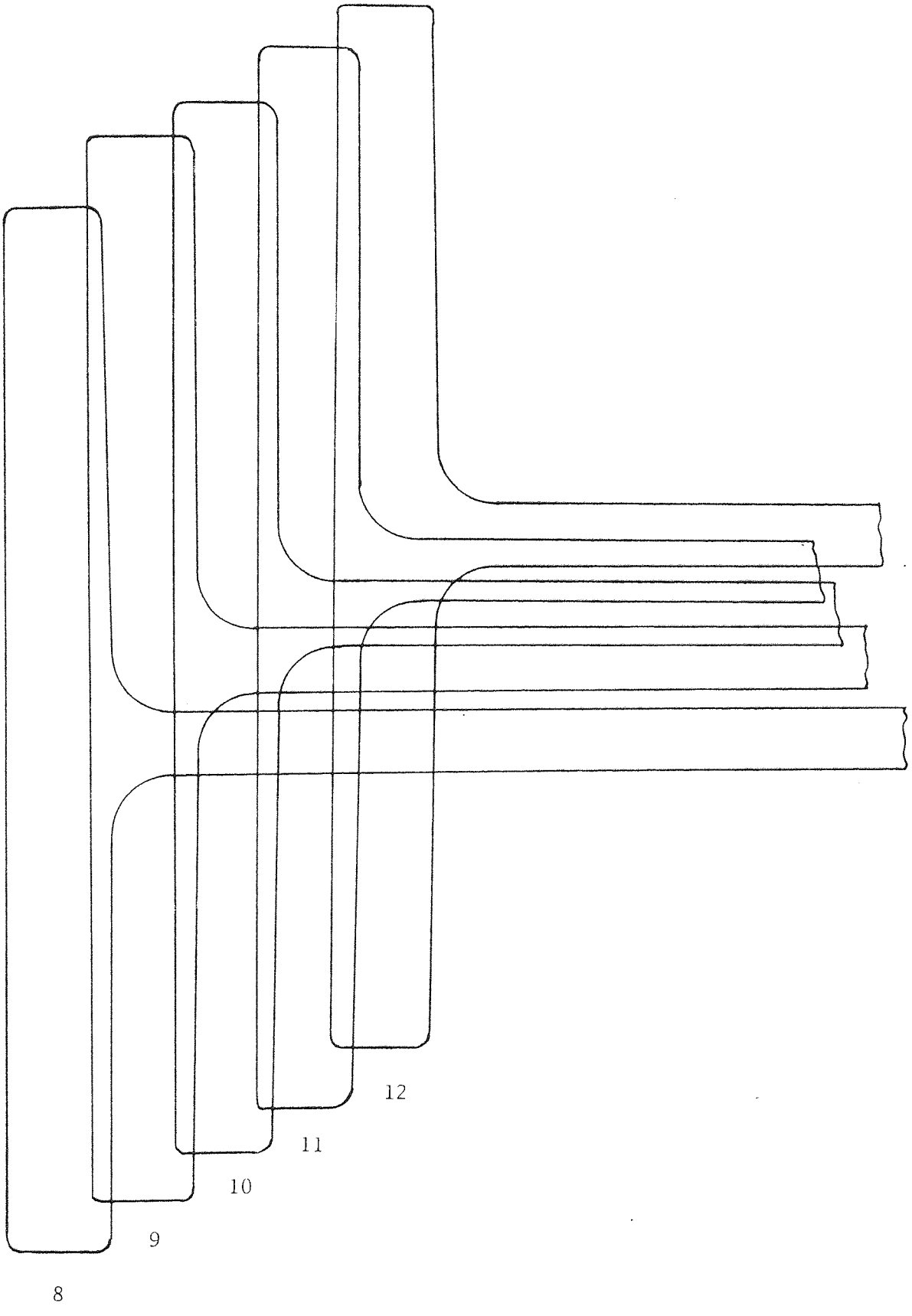
12
11
10
9
8

Fig. 78 Compression Flange Profiles Before Testing,
Series 356 x 171

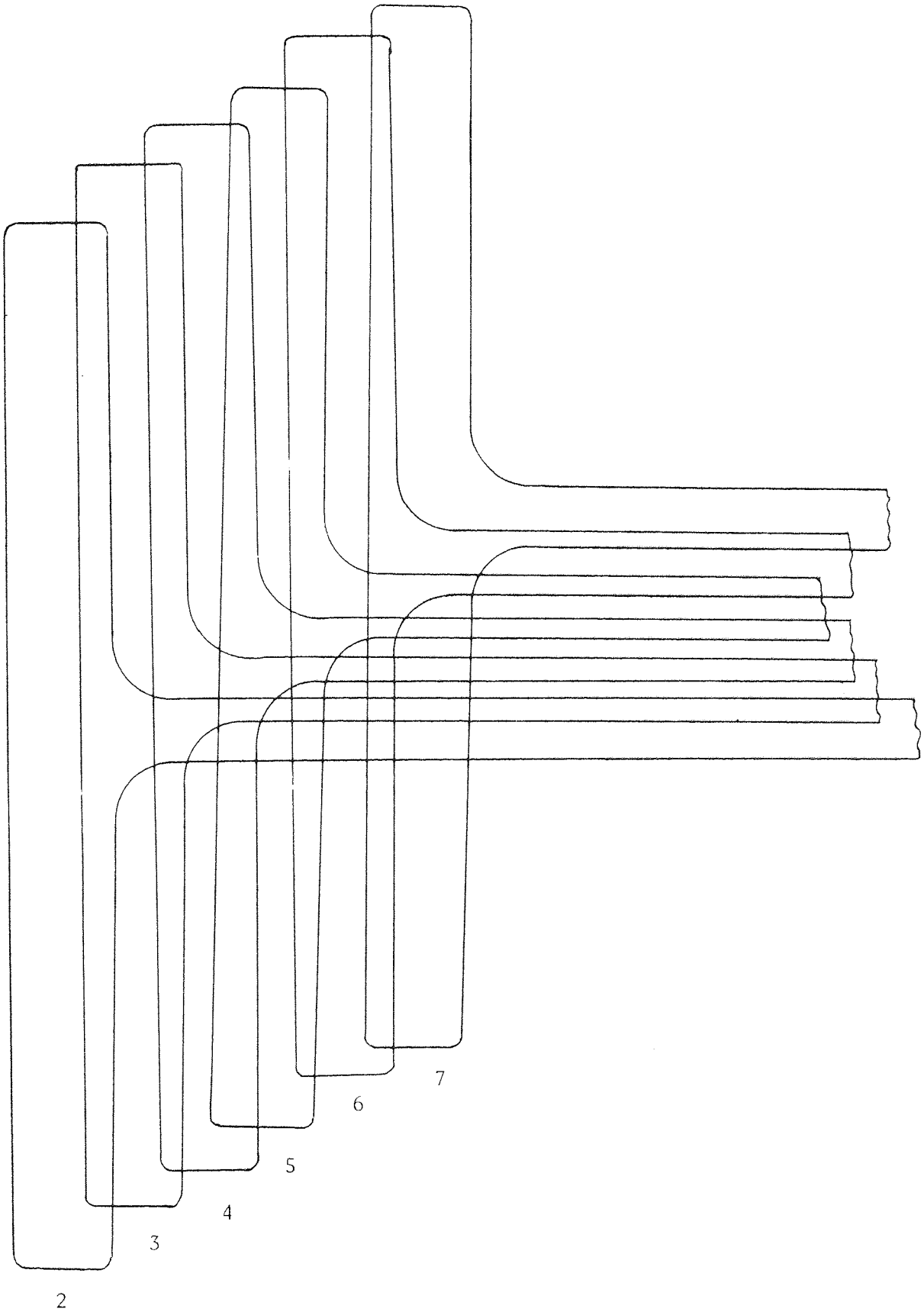

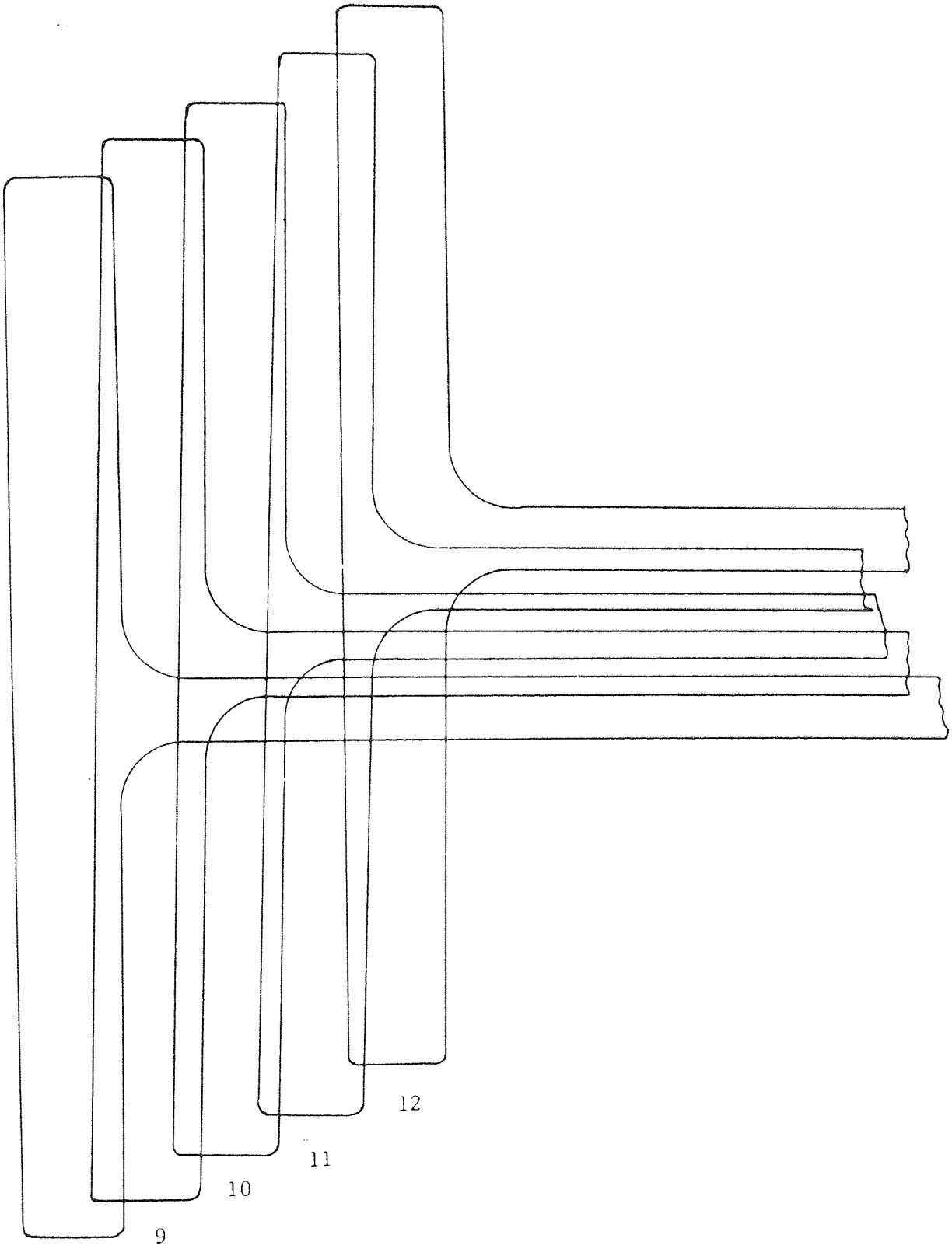
12
11
10
9
8

Fig. 79 Tension Flange Profiles Before Testing , Series 305 x 305
(scale: 2/3 full size)

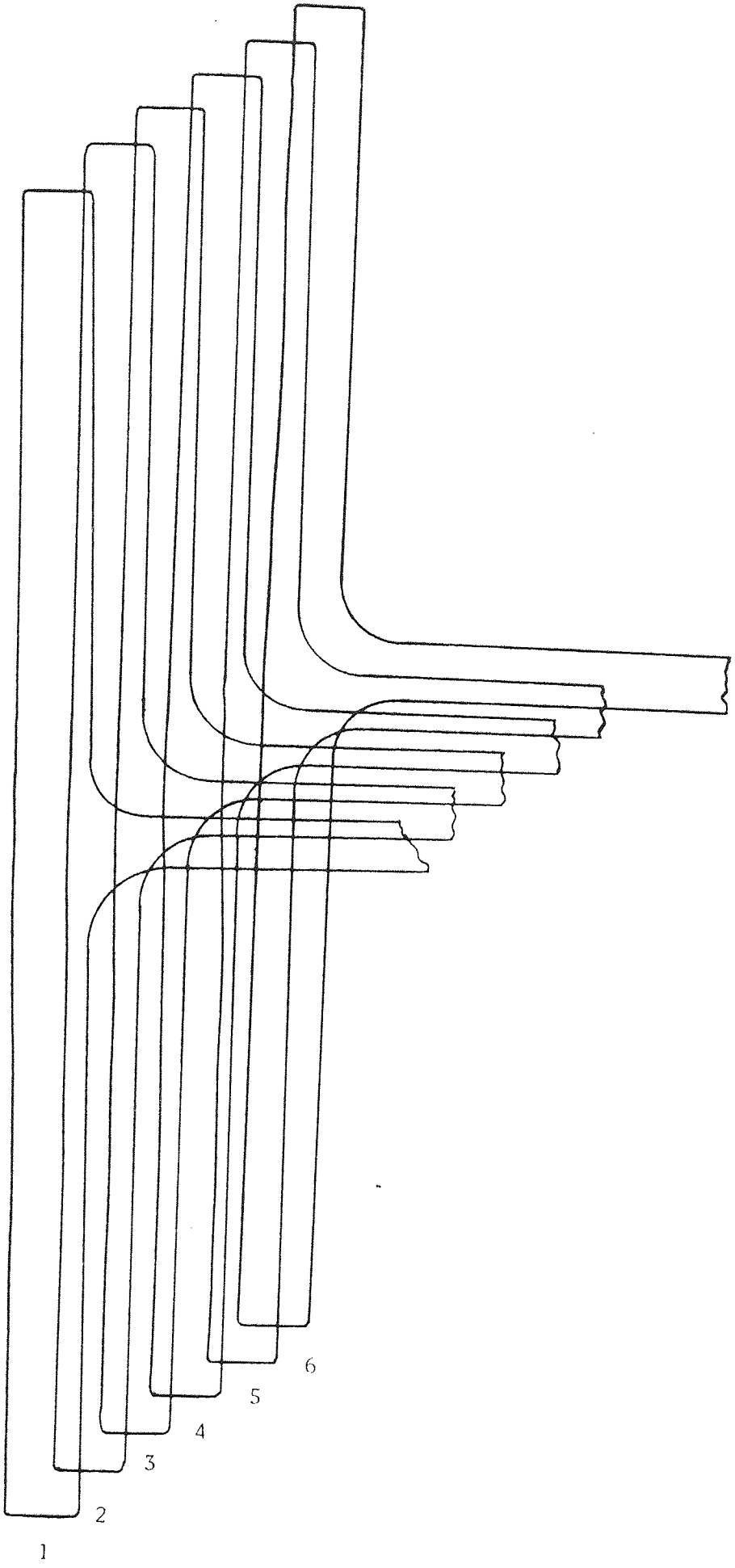

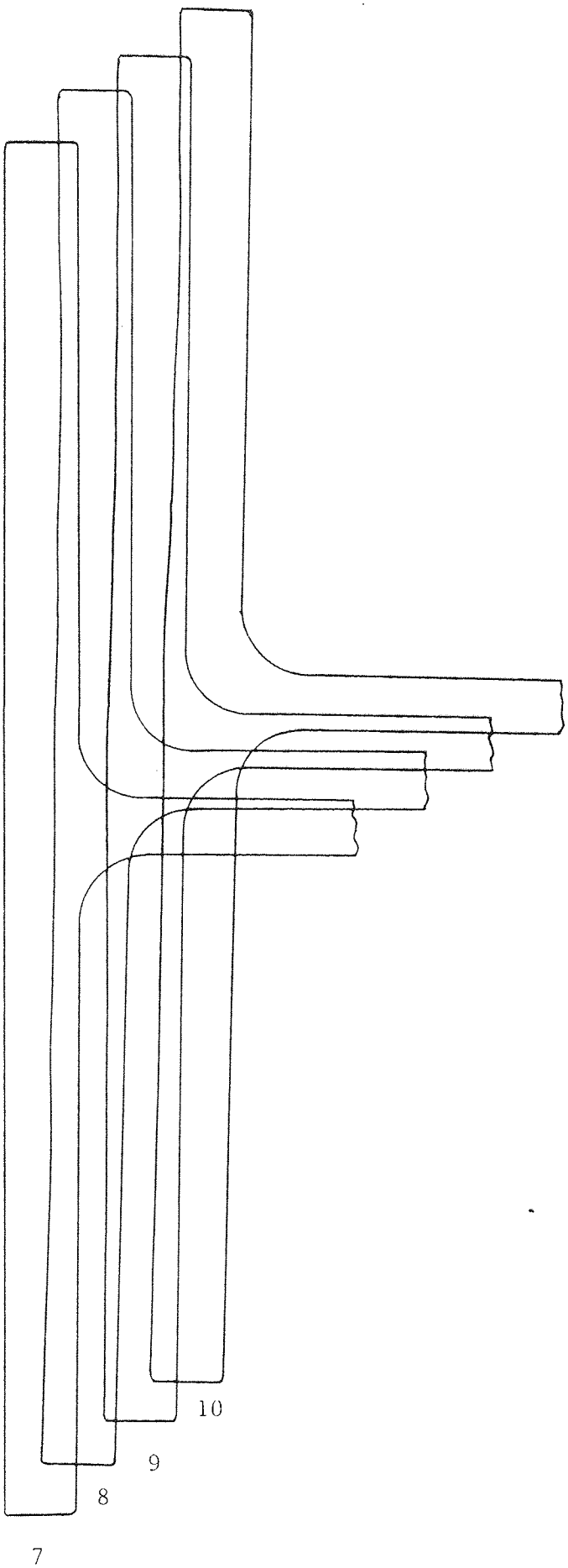
10
9
8
7

Fig. 80 Compression Flange Profiles Before Testing , Series 305 x 305

(scale: 2/3 full size)

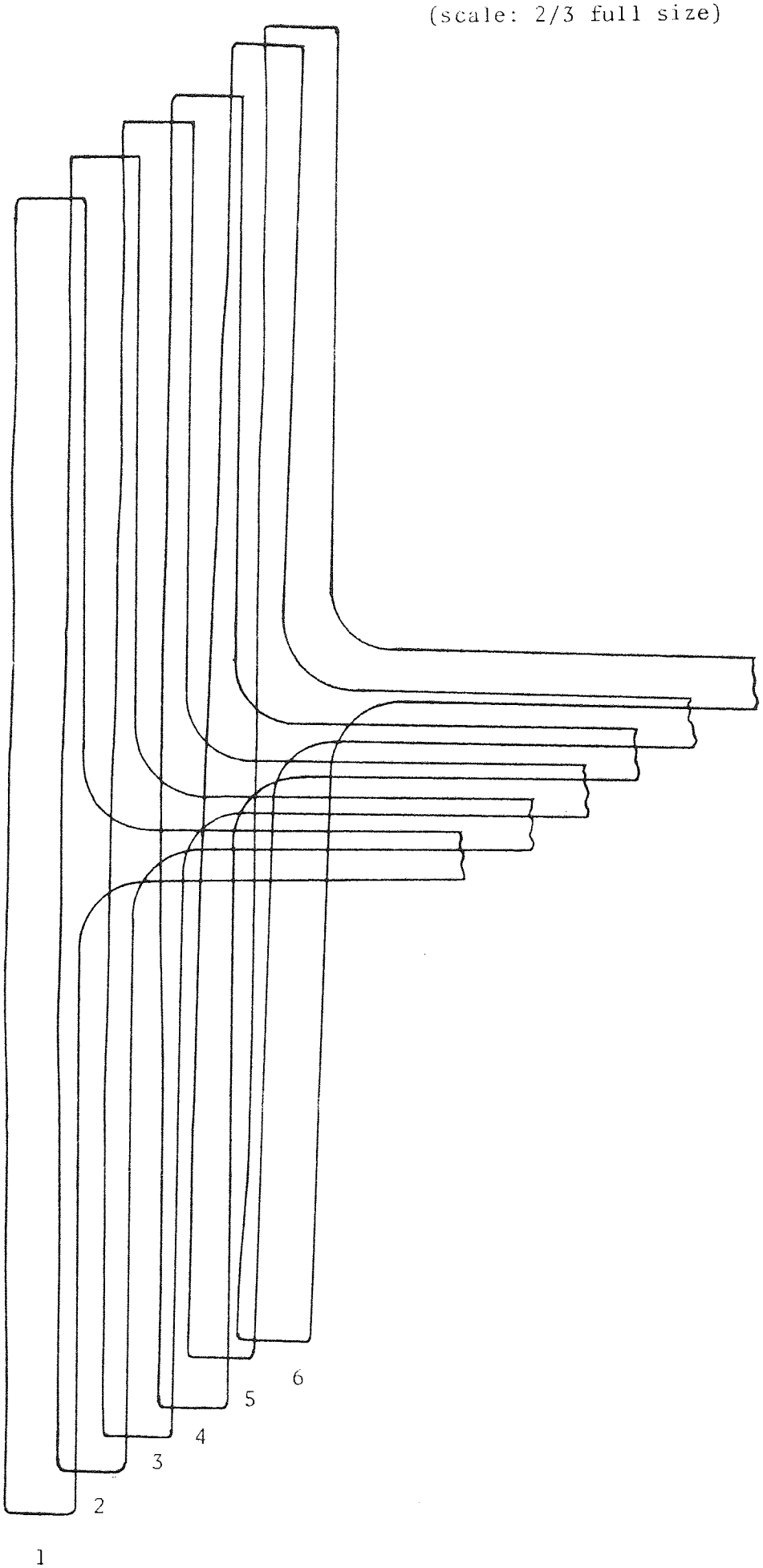

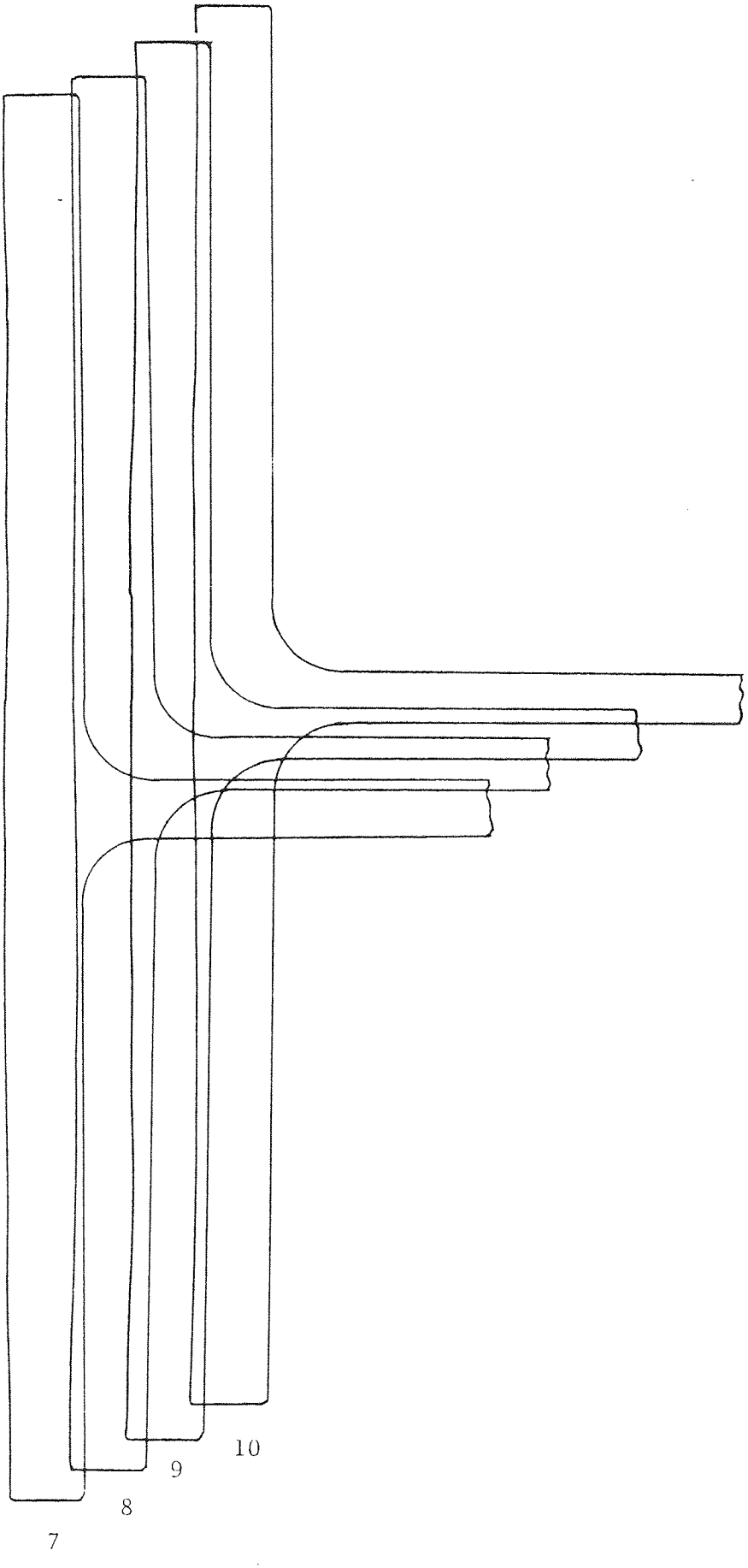
10
9
8
7

The uneveness of the flanges of the 305 x 305 series caused some concern because it would inevitably lead to slight non-uniformity in the leg size of the machined weld. The flanges which gave the greater uniformity in the web region were chosen as the tension flanges - it was anticipated that for high values of V/M failure would be initiated in the tension weld above the web.

6.2 Dial Gauge Readings

Three series of tests were conducted, and prior to each test the ultimate shear load capacity of the test connection was estimated so that load scales and increments could be decided upon. Dial gauge readings were taken at each load increment until failure occurred - in most cases dial gauge readings were recorded at, or very slightly below the failure load. Only in two tests were the dial gauges removed before failure took place - these were with load sharing plates inbetween the flanges. With these two specimens very high loads were involved, and for reasons of safety gauges were not read prior to failure.

Dial gauge readings for each test, along with various notes recorded during the testing, are given in Tables 8 to 33 inclusive. The final dial gauge readings are given in units of 10^{-3} inch.

For several of the tests it was necessary, in order to obtain a high value of V/M, to locate the right-hand loading-beam support directly underneath the test connection. The presence of the 50 mm width support underneath the test connection obviously affected the tension flange deformation and this is reflected in the dial gauge readings. Its other affects will be discussed later.

TABLE 8

Specimen No: 305127/1 — Distance Between Supports: 5.5 m
Dial Gauge Correction: 0.0018 inch

Load tonne	Dial Gauge Position 1 10^{-3} inch	2 10^{-3} inch	3 10^{-3} inch	4 10^{-3} inch	5 10^{-3} inch	6 10^{-3} inch	7 10^{-3} inch	8 10^{-3} inch	11 10^{-3} inch	10 10^{-3} inch	9 10^{-3} inch	12 10^{-2} mm
Dead Weight	11.5	3	89	0	96	90	90	93	17	6.5	92	1.5
0.3	13.5	3	87	1	96	88	88	92.5	19	7.5	90.5	1.8
0.6	15	3	85.5	1	95.5	87	87	92.5	20.5	8	89	2.05
0.9	17	4	83.5	1	95	85	85.5	92	23	8	86.2	2.4
1.2	19	4	81.5	0.5	94	83	84.5	92	25.5	8.5	83.5	2.7
1.5	21	5	79.5	0.5	93	81.5	83.5	92.5	28	9	80.5	3
1.8	23	6	77	0.5	92	80	83	93.5	30.2	9.5	77	3.3
*2.1	25	6	74.5	0	91.5	78	82.5	95	32.5	10	69	3.6
2.4	28	6.5	72	99.5	90	76	81.5	97	34.8	10.5	56.5	3.9
2.7	30	7	65	99.5	89	75.5	80.5	98.2	37	11	46	4.2
3.0	32.5	7.5	52	99.5	88	73.5	78.5	99.5	40	11.5	33.5	4.6
**3.2	33	8	31	0	88	72.5	78.5	3.5	42	11	17	5
3.3	35	8	10	2.5	88	72	78.5	7	43.5	11	1	5.1
3.4	35	8	77	8.5	88	72	80	13	45.5	10	81	5.3
3.4	35	8	62	10.5	88	72	80	15.5	45.5	9.5	70	5.35
3.5	Failure											
Indicated Deflections 0.001 inch	3.5	0.8	13.8	1.05	1.2	2.8	2.0	1.55	4.55	0.95	13.0	2.1
Corrected Deflections 0.001 inch	3.5	2.6	13.8	2.85	0.6	1.0	0.2	2.35	4.55	2.75	13.0	0.3
Direction of Deflection Rel. Datum	←	↑	→	↑	↑	↓	↓	↑	←	↑	→	↓

* Deflection at position 9 has started to move ahead of deflection at position 3 indicating a failure from right-hand end of tension weld.

** Definite creep indicated at positions 9 and 3. Small crack at left-hand end of tension weld.

TABLE 9

Specimen No: 305127/2 Distance Between Supports: 3.815 m
Dial Gauge Correction: 0.0018 inch

Load tonne	Dial Gauge Position 1 10^{-3} inch	2 10^{-3} inch	3 10^{-3} inch	4 10^{-3} inch	5 10^{-3} inch	6 10^{-3} inch	7 10^{-3} inch	8 10^{-3} inch	9 10^{-3} inch	10 10^{-3} inch	11 10^{-3} inch	12 10^{-2} mm
Dead Weight	3	0	93	97	94.5	94	96	97	97	0	8	0.8
1.2	6.5	0	90	96.5	92.5	91	92	95.5	95	0	11	1.8
3.0	12.5	0	82.5	94.5	87	84.5	86	92	90	0	16	3.2
4.0	16	0	76	92	81.5	79.5	82.5	90	87	0	19	4.1
5.0	19	0	69	91.5	78	75	78.5	87	85	99.5	22.5	5.1
6.0	22.5	0	60	91	74	69	74	83	82	99	26	6.0
7.0	25.5	0	48	92	71	63.5	70	81	78	98	29.5	7
7.5	27	0	37	94	69	61	68.5	82	72.5	98	31	7.4
8.2	29	98.5	20	96.5	67.5	57.5	67	83	63.5	97	34	8.1
8.6	30	98.5	7	99	67	55	66.5	86	55.5	96	35.5	8.6
8.8	31	98.5	96	0	66	54	66.5	87	48	96	36	8.8
9.0	32	98	88	3	66	51	66	88	42	95.5	37	9.1
9.2	32.5	98	78	5	66	49	66	89	35	95	38	9.4
9.4	33	97.5	67	7	65	47	66	90	26.5	95	39	9.2
9.6	34	97	45	8	64	46	66	92.5	10	94.5	40	10
9.7	35	96	25	14	64	46	66	95	95	93	41	10.5
9.8	Failure											
Indicated Deflections 0.001 inch	3.5	0.4	17.5	1.4	3.6	5.4	3.4	0.5	10.5	0.7	4.1	4.14
Corrected Deflections 0.001 inch	3.5	1.4	17.5	3.2	1.8	3.6	1.6	1.3	10.5	1.1	4.1	2.34
Direction of Deflection Rel. Datum	←	↑	→	↑	↓	↓	↓	↑	→	↑	←	↓

Notes: Although deflections at positions 3 and 9 were not comparable throughout the test, failure was not initiated at one end but appeared to be plastic along the entire length of the tension weld.

TABLE 10

Specimen No: 305127/3 Distance Between Supports: 3.32 m

Dial Gauge Correction: 0.0012 inch

Load	Dial Gauge Position											
tonne	1 10^{-3} inch	2 10^{-3} inch	3 10^{-3} inch	4 10^{-3} inch	5 10^{-3} inch	6 10^{-3} inch	7 10^{-3} inch	8 10^{-3} inch	9 10^{-3} inch	10 10^{-3} inch	11 10^{-3} inch	12 10^{-2} mm
Dead Weight	3	99	98.5	97	97	95	97	97	99	0	3	0.7
2	5.5	98	97	94	92.5	90	93	94.5	96.5	0.5	6	1.7
4	9	97.5	95.5	91	89	85.5	89	91.5	94.5	0.5	9	3.0
6	13.5	96	94	88	85	80	84.5	88.5	93	0	12	4.4
8	17.5	93	91	82.5	77	72	77.5	83.5	90	98	15	6.1
10	21.5	90	87.5	75	68	62	69	77	87.5	96	18	8.2
12	25	87	83	67.5	57.5	51	59.5	69.5	84	93	21	10.2
14	30	84	78.5	59	45.5	38.5	48.5	61.5	80	90	23.5	12.7
16	34	80	74	50.5	34	25.5	37	54	75	87	26.5	15
17	36	77	71.5	46	28	18.5	31	49.5	72	85	27.5	16.3
18	38	75	68.5	41	19.5	9.5	23.5	44.5	67.5	83	29.5	17.8
19	40	72.5	65	35	12.5	2	17	41	62	80	31	19.5
20	43	70	58.5	31	4	90	6	35	55	77	32.5	1.6
21	45	66	49	28	95	80.5	97.5	30.5	45	73	34.5	3.8
22	48	61	29.5	28	88	68	87	27	26.5	68	36.5	6.3
23	Failure											
Indicated Deflections 0.001 inch	4.8	3.9	7.05	7.2	11.2	13.2	11.3	7.3	7.35	3.2	3.65	10.35
Corrected Deflections 0.001 inch	4.8	2.7	7.05	6.0	10.0	12.0	10.1	6.1	7.35	2.0	3.65	9.15
Direction of Deflection Rel. Datum	←	↓	→	↓	↓	↓	↓	↓	→	↓	←	↓

TABLE 11

Specimen No: 305127/4 Distance Between Supports: 3.123 m
Dial Gauge Correction: 0.00012 inch

Load	Dial Gauge Position												
tonne	1 10^{-3} inch	2 10^{-3} inch	3 10^{-3} inch	4 10^{-3} inch	5 10^{-3} inch	6 10^{-3} inch	7 10^{-3} inch	8 10^{-3} inch	9 10^{-3} inch	10 10^{-3} inch	11 10^{-3} inch	12 10^{-2} mm	13 10^{-3} inch
Dead Weight	1.5	99	1	99	98	95	98	96	0	99	0.5	0.6	0
5	6.5	98	98.5	95	93.5	87	84	85	1	96.5	3	2.8	0.75
10	9	91.5	98	89	83	74	70	73	2	91.5	5.5	5.7	1.25
15	12.5	82	98	75	62	49	47.5	56	2.5	83	8	10.8	1.25
20	15	69	98	60	37	15	13	32	2	72.5	11.5	17.1	1.5
25	16.5	43	97	38	0	61	62	96	1.5	46	12	9.1	2.5
26	16	35	97	32	88	43	47	83	1.5	38	12	13.0	2.5
27	16	27	97	26	77	28	33	74	1	30	11	16.5	2.5
*28	15	12	98	15	58	0	9	57	1	16	10	3.1	2.5
28.5	15	1	99	6	43	77	91	47	1	5	9	8.2	2.5
29	14	86	99	95	20	43	62	31	0.5	88	7	17.1	2.5
29.5	Failure												
Indicated Deflections 0.001 inch	1.4	11.4	0.1	10.5	18	25.7	24.8	16.9	0.05	11.2	0.7	22.4	2.5
Corrected Deflections 0.001 inch	1.4	11.28	0.1	10.4	17.9	25.6	24.7	16.8	0.05	11.1	0.7	22.3	2.5
Direction of Deflection Rel. Datum	←	↓	→	↓	↓	↓	↓	↓	←	↓	←	↓	→

* Creep was indicated at positions 5, 6 and 7 suggesting yielding of the tension weld around the web. Load applied through a 50 mm bearing at the tension flange.

TABLE 12

Specimen No: 305127/5 Distance Between Supports: 3.043 m

Dial Gauge Correction: — inch

Load tonne	Dial Gauge Position					
	2 10^{-3} inch	15 10^{-3} inch	14 10^{-3} inch	16 10^{-3} inch	10 10^{-3} inch	12 10^{-3} inch
Dead Weight	99	1	50	2	99	2
5	96	45*	0	57*	96	5
10	93	60	48	83	92	11
15	88	82	46	16	86	25
20	81	11	43	53	78	42
25	74	45	39	0	67	66
26	58	62	37	21	60	75
27	54	69	37	30	58	79
28	48	76	36	44	55	86
28.5	44	82	35	52	53	90
29	41	88	34	61	51	95
29.5	37	95	33	72	48	1
29.75	33	2	32	78	46	6
30	30	4	32	82	44	8
30.25	28	8	32	87	44	11
30.5	25	13	31	93	42	15
30.75	20	20	30	2	40	21
31	15	30	30	14	36	30
31.25	Failure					
Indicated Deflections 0.001 inch	8.5	23	20	31.4	6.4	13.0
Direction of Deflection Rel. Datum	↓	↓	↓	↓	↓	↓

* These large deflections are due to the 50 mm bearing being so close to the tension weld and the tension flange not being flat.

Rotation is assumed to be negligible.

TABLE 13

Specimen No.356171/2 Distance Between Supports 5.5 m

Dial Gauge Correction: 0.00085, 0.0014 inch

Load tonne	Dial Gauge Position 2 10^{-3} inch	3 10^{-3} inch	1 10^{-3} inch	4 10^{-3} inch	5 10^{-2} mm	6 10^{-2} mm	7 10^{-2} mm	8 10^{-2} mm	9 10^{-2} mm	11 10^{-3} inch	12 10^{-3} inch	14 10^{-3} inch
Dead Weight	0	0	0	0	0	0	0	0	0	0	0	0
0.5	0	0	1	99	0	99	19.5	0	19.6	0	0	2
1	0	99.5	2	98.5	0	96	18.5	95	19.1	0	0	6
1.5	0	99	3	98.5	19.8	93.5	17.5	90.5	18.4	99.5	0	10
2	0	98.5	4	98.5	19.5	91	16.5	86	17.5	99	0	13.5
2.5	0	98.5	5	98.5	19.5	89	15.5	82	16.8	98.5	0	18
3	0	98	6	77.5	19.5	87	14.4	77	16	98	0	22
3.5	99.5	97.5	6.3	72	19.5	85	13.4	71.5	15	97.5	0	26.5
4	99.5	97	6.5	72	19.6	83	12.1	65	14.1	97	0	30
4.5	99.5	96.8	6.5	69.5	0	81.5	11	60	13.1	96.5	0	34
5	99.5	95	5	30	1.4	81.5	10	54	11.8	95.5	99.5	38.5
5.15	Failure											
Indicated Deflections 0.001 inch	0.05	0.5	0.5	7.0	0.56	1.5	4	3.7	3.3	0.5	0.05	3.85
Corrected Deflections 0.001 inch	0.9	0.35	0.5	7.0	1.4	0.65	3.15	2.85	2.45	0.3	0.9	2.43
Direction of Deflection. Rel. Datum	↑	↑	←	→	↑	↓	↓	↓	↓	↑	↑	↓

TABLE 14

Specimen No: 356171/3 Distance Between Supports: 3.12 m

Dial Gauge Correction 0.0004, 0.00066 inch

Load	Dial Gauge Position											
tonne	2 10^{-3} inch	3 10^{-3} inch	1 10^{-3} inch	4 10^{-3} inch	5 10^{-2} mm	6 10^{-2} mm	7 10^{-2} mm	8 10^{-2} mm	9 10^{-2} mm	11 10^{-3} inch	12 10^{-3} inch	14 10^{-3} inch
Dead Weight	0	0	0	0	0	0	0	0	0	0	0	0
2	0	0	0	98.5	18.2	98	19.6	93	16.8	0	0	0
4	0	99.5	0	97.5	16	94	19.5	87	13.8	99.5	0	0
6	99.5	99	0.5	96.7	14.4	90	18.7	80	11.2	98.5	99.5	3
8	99	98	0.7	96	13.6	86	17.8	73	9.2	97.5	99	5
10	98	97	1	95.4	12.5	82	16.6	67	7.4	96	98	10
12	97	95	1.2	94.5	11.7	77	15.3	61	5.8	94.5	97	14
14	95.5	92.5	1.5	93.7	11	72	13.8	53	41	92	96	19
16	94	90	1.8	93	10.5	67	12	44	2.0	98	94	23
18	92	86	2	92.2	10.1	62	10.1	32	19.7	86	92	27
20	90	81.5	2.5	91.5	9.6	55	8.4	21	17.4	81.5	90	31
22	87	76.5	3	90.2	9	47	6	10	15	76.5	86.5	36
24	84.5	71	3.2	89	8.3	40	3.6	9.7	12.6	72	83	41
26	81	65	3.5	87	7.6	31	1	84	10	65	80	46
28	78	59	4	85.3	7.1	23	18.2	69	7.5	60	75	53
30	74	51.5	4.3	83	6.5	12	13.8	51	4.2	51	70	65
32	71	45	4.8	81	6.2	4	11.8	35	1.2	45	64.5	78
34	66	35	5.2	78	5.7	90	6.8	12	17.1	33.5	56	95
38	49	99	6.3	71.5	3.7	41	9.4	44	5.3	96	26	44
41.9	Failure											
Indicated Deflections 0.001 inch	5.1	10	0.63	2.85	6.5	12.8	20	20.5	21.8	10.4	7.4	14.4
Corrected Deflections 0.001 inch	4.7	9.6	0.63	2.85	6.1	12.4	19.6	20.1	21.4	10.0	7.0	13.8
Directions of Deflection	↓	↓	←	→	↓	↓	↓	↓	↓	↓	↓	↓
Rel. Datum												

Test was conducted with a 50 mm bearing at the tension flange

TABLE 15

Specimen No. 356171/4 Distance between Supports 3.342 m

Dial Gauge Correction: 0.00145, 0.00087 inch

Load	Dial Gauge Position											
	2	3	1	4	5	6	7	8	9	11	12	14
tonne	10^{-3} inch	10^{-3} inch	10^{-3} inch	10^{-3} inch	10^{-2} mm	10^{-2} mm	10^{-2} mm	10^{-2} mm	10^{-2} mm	10^{-3} inch	10^{-3} inch	10^{-3} inch
Dead Weight	0	0	0	0	0	0	0	0	00	0	0	0
2	99.5	99	1	0	0	99	19.8	99.5	0	0	1	2
4	98	97.5	3	96	0	97.5	19.2	99	0	0	3	5
6	97	97	5	94.5	0	96	18.4	97	0	0	5.5	8
8	96.5	96	7	93	0	93.5	17.6	94.5	0	0	5.5	11
10	95.5	94.5	9	91	0	90	16.3	90	19.4	99	6.5	14.5
11	95	93	9.5	90.5	0	88	15.5	86.5	19.1	98.5	6.5	17
12	94	92.5	10	89	0	85	14.5	82.5	18.7	98	6.5	20
13	93	90.5	11	87	19.8	82	13.4	79	18.3	97	6	22.5
14	92	89	11	85	19.7	78.5	12.2	75	17.8	96	5.5	25
15	90.5	87	11.5	83	19.4	75	10.9	70	17.2	94	5	29
16	89	85	12	80	19.1	70.5	9.5	66	16.7	92.5	4	32.5
17	88	83	12	77.5	19	66	8.1	61	16.2	90.5	3	36
18	86	80	12.5	74	18.8	62.5	6.6	56	15.4	88.5	2	40
19	84.5	77	13	69.5	18.7	58.5	5	50	14.7	86	1	44.5
20	83	74	13	65	18.7	53	3.3	44	13.8	84	99.5	49
21.25	81	70	13	58	18.9	47.5	1	36	12.8	80	97.5	55
22.5	78	66	13	50	19	41	18.7	27.5	11.5	77	85	61
23.75	75	61	11.5	35	19.6	33.5	15.5	15.5	9.8	71.5	93	68.5
24.6	Failure											
Indicated Deflections 0.001 inch	2.5	3.9	1.15	6.5	0.16	5.3	9.8	6.8	4.1	2.85	0.7	6.85
Corrected Deflections 0.001 inch	1.6	3.0	1.15	6.5	0.7	4.4	8.9	5.9	3.2	1.95	0.17	5.4
Direction of Deflection Rel. Datum	↓	↓	←	→	↑	↓	↓	↓	↓	↓	↑	↓

TABLE 16

Specimen No. 356171/5 Distance Between Supports 3.815 m

Dial Gauge Correction: 0.00147, 0.00083 inch

Load	Dial Gauge Position											
	2	3	1	4	5	6	7	8	9	11	12	14
tonne	10^{-3} inch	10^{-3} inch	10^{-3} inch	10^{-3} inch	10^{-2} mm	10^{-2} mm	10^{-2} mm	10^{-2} mm	10^{-2} mm	10^{-3} inch	10^{-3} inch	10^{-3} inch
Dead Weight	0	99	1	98.5	0.2	99.5	19.8	98	19.3	0	0	3
1	0	99	2	97.5	0.3	99.5	19.8	98	19.3	0	0	4.5
2	0	99	3	96	0.4	98	19	95.5	18.9	0	0	8
3	1	98	4.5	95	0.8	97	18.5	94	18.6	99.5	0	11.5
4	1.5	98	5	93	1	96	18	92.5	18.4	99	99.5	14.5
5	2	98	7	91	1.2	95	17.6	91	18	98	99	18.5
6	1.5	97.5	8.5	87	1.3	93.5	17	88	17.6	97.5	99	23
7	2	97	9	83.5	1.5	92	16.3	86	17.3	96.5	98.5	27
8	2	96.5	10.5	80	1.6	91	15.8	84	17.3	95	97.5	32
9	2.5	96	12	77	1.7	89	15	82	17.2	95	97.5	37
10	2.5	95	13	73.5	1.7	87	14.3	80	17.2	94	96.5	42
10.5	2.5	94.5	14	71.5	1.7	86	14	78	17.1	94	96.5	45
11	2.5	94	14.5	69.5	1.8	84.5	13.8	77.5	17.1	93.5	96	47.5
11.5	2.5	93.5	15	68	1.8	83.5	13.1	76	17	92.5	95.5	50
12	2.5	93	15.5	63	2	82.5	12.5	74	16.9	92	95	53
12.5	2	93	16	60.5	2	80	12	72.5	16.8	91.5	95	56
13	2	92.5	16	57	2	79.5	11.4	71	16.7	91	94	59
13.5	2	91.5	16.5	53	2	78	10.7	68	16.5	90	93.5	62.5
14	2	90	17	50	2	75	10.7	66	16.5	89	93	66
14.5	1	89	17.5	44	2.1	73.5	9.2	63	16.4	87.5	92	70.5
15	Failure											
Indicated Deflections 0.001 inch	0	1.1	1.75	5.6	0.84	2.12	4.3	2.96	1.44	1.25	0.8	7.05
Corrected Deflections 0.001 inch	0.83	0.27	1.75	5.6	1.67	1.3	3.47	2.13	0.61	0.42	0	5.58*
Direction of Deflection Rel. Datum	↑	↓	←	→	↑	↓	↓	↓	↓	↓		↓

* It is not possible for this deflection to be greater than that at position 7 - gauge must have slipped

TABLE 17

Specimen No: 356171/6 Distance Between Supports: 3.21 m

Dial Gauge Correction : 0.00058 inch

Load	Dial Gauge Position													
tonne	1 10^{-3} inch	2 10^{-3} inch	3 10^{-3} inch	4 10^{-3} inch	5 10^{-3} inch	6 10^{-3} inch	7 10^{-3} inch	8 10^{-3} inch	9 10^{-3} inch	10 10^{-3} inch	11 10^{-3} inch	12 10^{-3} inch	13 10^{-3} inch	14 10^{-2} mm
Dead Weight	2	1	98	99	1	0	97	97	98	0	98	98	99	19.2
5	6	99	92	97	97	93	92	89	93	0	92	95	1.5	16.8
10	10	95	85	95	91	84	76	79	88	0	86	93	5.5	13
15	13	92	79	93	86	73	63	68	84	98	80	90	9.5	10
20	16	88	72	89	80	60	47	56	78	97	72	86	12.5	6.4
25	19	84	62	78	71	41	27	41	72	96	60	80	15	2.2
30	23	78	49	65	60	18	13	19	62	95	43	71	18	16
31	24	77	45	63	58	14	9	16	60	95	40	69	18	15.2
32	24	75	42	61	56	9	2	11	58	95	36	66	18.5	13.2
33	25	73	39	57	3	95	95	5	55	95	32	64	19	11.6
33.5	26	73	37	56	52	0	93	3	54	95	29	62	19	11.1
34	26	71	35	54	50	97	88	99	52	95	26	60	19.5	10
34.5	28	70	33	52	49	94	85	96	51	95	23	58	19.5	9.2
35	27	69	30	50	47	90	79	92	49	95	20	56	19.5	7.9
35.5	28	68	27	47	45	86	73	88	46	95	15	54	20	6.6
36	28	65	22	43	43	79	65	81	44	96	10	50	20	4.9
36.5	28	65	20	41	42	76	61	78	42	96	8	49	20	3.6
*37	29	63	17	38	41	72	55	73	40	97	5	56	20	2.8
37.5	29	60	9	27	39	62	42	61	35	98	95	41	20	1.2
38	30	57	3	20	38	54	31	53	32	99	90	37	21	0
38.5	Failure													
Indicated Deflections 0.001 inch	3.0	4.3	9.7	8.0	6.2	14.6	16.9	14.7	6.8	0	11.0	6.3	2.1	15.8
Corrected Deflections 0.001 inch	3.0	3.7	9.1	8.0	5.6	14.0	16.3	14.1	6.2	0	10.4	5.7	2.1	15.2
Direction of Deflection Rel. Datum	←	↓	↓	→	↓	↓	↓	↓	↓		↓	↓	←	→

* Signs of yielding of tension weld around the web and at left-hand end.

Test conducted with a 25 mm bearing at tension flange

TABLE 18

Specimen No: 356171/7 Distance Between Supports: 6.0 m
Dial Gauge Correction: 0.00063 inch

Load	Dial Gauge Position													
tonne	1 10^{-3} inch	2 10^{-3} inch	3 10^{-3} inch	4 10^{-3} inch	5 10^{-3} inch	6 10^{-3} inch	7 10^{-3} inch	8 10^{-3} inch	9 10^{-3} inch	10 10^{-3} inch	11 10^{-3} inch	12 10^{-3} inch	13 10^{-3} inch	14 10^{-2} mm
Dead Weight	10	8	3	97	98	98	95	97	99	92	1	3	8	18.5
* 1	18.5	13	6	95	95	93	90	93	98	70	3	5	97	17
2	23	15	7	94	93	91	88	91	0	71	4	7	99	16.2
2.5	26	17	8	94	91	89	85	91	1	61	5	8	1	15.8
3	30	19	9	94	88	86	83	90	4	50	6	9	3	15.2
3.5	34	20	10	93	85	83	81	89.5	8	36	6.5	10	4.5	14.6
4	38	22	11	93	82	80	79	89.5	12	22	7	11	6	14
4.5	42	24	12	93	79	77	75	90	7	30	8	12	7	13.4
5	48	25	13	92	73	73	71	90	26	75	8.5	13	8.5	12.6
5.3	50	26	13	91	70	70	69	90	30	58	8.5	14	9	12.2
5.5	54	27	13	89	68	68	68	91	44	70	8.5	14	7.5	11.6
5.5	Failure													
Indicated Deflections 0.001 inch	5.4	2.7	1.3	1.1	3.2	3.2	3.2	0.9	4.4	23.0	0.85	1.4	0.75	3.3
Corrected Deflections 0.001 inch	5.4	3.3	1.9	1.1	2.6	2.6	2.6	0.3	5.0	23.0	1.5	2.0	0.75	2.7
Direction of Deflection Rel. Datum	←	↑	↑	→	↓	↓	↓	↓	↑	→	↑	↑	←	↓

* Unusually large horizontal deflection as the compression weld - possibility of poor fit-up prior to welding

TABLE 19

Specimen No: 356171/8 Distance Between Supports: 3.32 m

Dial Gauge Correction: 0.00087 inch

Load	Dial Gauge Position														
	1	3	2	4	5	6	7	8	9	10	15	11	12	13	14
tonne	10^{-3} inch	10^{-3} inch	10^{-3} inch	10^{-3} inch	10^{-3} inch	10^{-3} inch	10^{-3} inch	10^{-3} inch	10^{-3} inch	10^{-3} inch	10^{-3} inch	10^{-3} inch	10^{-3} inch	10^{-3} inch	10^{-3} inch
Dead Weight	3.5	97.5	99.5	99	98	98.5	97.5	99	98	0.5	0.5	98	99	98.5	97
5	9	93	98	97	91	87	86	90	93.5	99	0.5	94	97	2	6.5
10	15	89	97	96	86	80	77	81.5	90	97	0.5	90	95.5	5.5	16
15	21	83	95	93	77	67	61	70	84.5	93.5	0	84.5	92.5	9.5	29
20	27	76	92	89	65	51	42	55	77.5	89	0	77.5	89	14	44
25	34	66	89	82.5	53	31	19	38	69.5	82	49.8	68	84.5	18	61
26	35	65	88	81	51	27	14	34	67.5	81	49.8	66	83.5	19	64
27	36.5	62	87	80	48	23	8	29.5	65.5	79	49.8	63	82	20	69
28	38	60	86	78	56	18	3	25	64	77	49.8	61	81	21	73
29	39	57	85	76	44	14	97	21	62	75	49.8	58	80	22	77
30	40	54	84	74	41	10	90	16	60	73	49.8	55	78	22	82
31	42	50	82	70	39	2	82	9	57	70	49.8	51	76	23	89
32	43	47	80	63	38	97	75	4	57	63	49.5	47	74	24	95
33	45	41	77	49	38	88	64	96	58	50	49.5	41	70	26	3
33.5	46	38	75	38	39	81	57	91	61	40	49.2	36	68	27	9
33.75	Failure														
Indicated Deflections 0.001 inch	4.6	6.2	2.5	6.2	6.1	11.9	14.3	10.9	3.9	6.0	0.8	6.4	3.2	2.7	10.9
Corrected Deflections 0.001 inch	4.6	5.3	1.6	6.2	5.2	11.0	13.4	10.0	3.0	6.0	0.8	5.5	2.3	2.7	10.0
Directions of Deflections Rel. Datum	←	↓	↓	→	↓	↓	↓	↓	↓	→	→	↓	↓	←	↓

Specimen No: 356171/9 Distance Between Supports: 3.043 m

Dial Gauge Correction: ——

Load	Dial Gauge Position					
tonne	2 10^{-3} inch	17 10^{-3} inch	7 10^{-3} inch	18 10^{-3} inch	12 10^{-3} inch	14 10^{-3} inch
Dead Weight	0	10	50	11	0	1
5	99	37	49	37	99.5	5
10	98	59	48	60	96.5	9
15	96	76	47	77.5	92.5	14
20	95	91	45.5	92	88.5	20
25	92	2	44	3.5	84.5	25
30	90	14	43	16	80	30
35	82	40	40	42.5	66.5	39
40	71	68	36.5	77	52	50
*43	66	81	34.5	93	44	55
50.5	Failure					
Indicated Deflections 0.001 inch	3.4	18.1	15.5	19.3	5.6	5.5
Direction of Deflections Rel. Datum	↓	↓	↓	↓	↓	↓

* Gauges were removed at this load.

Test conducted with spreaders welded in position directly beneath the welds. A 50 mm bearing was used.

TABLE 20

TABLE 21

Specimen No: 356171/10 Distance Between Supports: 3.19 m
Dial Gauge Correction: Negligible

Load	Dial Gauge Position													
tonne	1 10^{-3} inch	2 10^{-3} inch	3 10^{-3} inch	4 10^{-3} inch	5 10^{-3} inch	6 10^{-3} inch	7 10^{-3} inch	8 10^{-3} inch	9 10^{-3} inch	10 10^{-3} inch	11 10^{-3} inch	12 10^{-3} inch	13 10^{-3} inch	14 10^{-2} mm
Dead Weight	0	0	99	0	98	98	96	95	99	0	98	99	0	1
10	2	95	90	99	88	86	80	83	89	3	87	90	0	24
20	3	88	80	98	83	70	59	68	84	1	74	80	1	48
30	3	80	65	97	73	52	35	50	75	99	60	69	2	74
35	3	75	54	96	67	40	22	40	72	98	50	62	2	88
*37	4	71	50	96	62	28	4	26	66	97	40	52	2.5	5
37	5	68	45	96	60	22	95	21	64	96	34	50	2.5	10
37.5	5	66	42	95	59	15	87	14	59	96	31	44	2.5	18
37.75	Failure													
Indicated Deflections 0.001 inch	0.5	3.4	5.8	0.5	4.1	8.5	11.3	8.6	4.1	0.4	6.9	5.6	0.25	11.8
Directions of Deflections Rel. Datum	←	↓	↓	→	↓	↓	↓	↓	↓	→	↓	↓	←	↓

* Gauges indicated yielding of the tension weld near the web.

Test was conducted with flange spreaders (not welded in location) located 80 mm from welds and, a 50 mm bearing.

Specimen No: 356171/11 Distance Between Supports: 3.043 m

Dial Gauge Correction: —— inch

Load	Dial Gauge Position							
	3	2	16	7	19	11	12	14
tonne	10^{-3} inch	10^{-3} inch	10^{-3} inch	10^{-3} inch	10^{-3} inch	10^{-3} inch	10^{-3} inch	10^{-3} inch
Dead Weight	0	0	15	0	12	0	0	0
5	98	99	58	49.5	62	99	99	2
10	96	97	95	48.5	1	96	98	5
15	92	96	13	47.5	22	94	96	9
20	88	93	33	46	50	89	93	15
25	82	89	52	44	82	82	89	23
30	74	85	72	41.5	20	74	84	33
35	65	80	94	38.5	68	64	77	47
36	63	79	98	38	75	62	76	49
37	62	78	0	38	82	60	75	51
38	60	77	4	37	93	58	73	54
39	57	75	9	36.5	6	55	72	58
40	54	73	14	36	20	52	70	62
*41	51	72	19	35	35	48	68	65
41.5	50	70	21	34.5	42	46	66	69
42	46	68	24	33.5	60	42	64	73
42.5	Failure							
Indicated Deflections 0.001	5.4	3.2	22.4	16.5	36.0	5.8	3.6	7.3
Directions of Deflections Rel. Datum	↓	↓	↓	↓	↓	↓	↓	↓

* Signs of yielding below position 19.

Test conducted with a 50 mm bearing at tension flange.

TABLE 22

TABLE 23

Specimen No: 356171/12 Distance Between Supports: 3.19 m

Dial Gauge Correction: 0.00033 inch

Load	Dial Gauge Position														
	1	3	2	4	5	6	7	8	9	10	15	11	12	13	14
tonne	10^{-3} inch	10^{-3} inch	10^{-3} inch	10^{-3} inch	10^{-3} inch	10^{-3} inch	10^{-3} inch	10^{-3} inch	10^{-3} inch	10^{-3} inch	10^{-3} inch	10^{-3} inch	10^{-3} inch	10^{-3} inch	10^{-3} inch
Dead Weight	1	97	0	1	95	99	96	98	97	1	0	97	98	1	0
5	6	92	98	1	92	93	88	88	90	2	0	92	95	3	1
10	10	86	96	1	87	84	77	78	84	2	49.8	86	92	6	2
15	13	80	93	0	79	72	63	66	77	2	49.8	80	88	8	11
20	17	71	89	98	70	59	45	51	68	0	0	72	84	12	22
25	21	61	84	96	60	40	22	32	57	99	0.5	62	78	15	37
30	25	48	78	94	45	17	95	9	44	97	0.8	48	71	18	58
32	26	43	75	93	42	10	83	0	39	96	0.8	42	68	19	66
34	28	34	70	92	36	98	68	89	32	95	1	33	64	20	79
35	29	30	68	91	32	90	59	82	28	95	1	27	61	21	86
*36	30	22	64	91	27	80	47	73	23	94	0.7	20	58	22	95
36.5	30	20	61	91	26	78	40	69	21	94	0.5	16	56	23	0
37	31	16	60	91	24	73	35	64	18	94	0.5	13	54	23	5
**37.5	31	12	57	91	21	66	26	58	15	94	0	8	51	23	11
38	32	5	53	90	16	55	10	47	10	93	0	0	48	24	21
38.25	32	0	50	90	14	50	2	41	8	93	0	96	44	24	26
38.5	32	96	48	90	11	43	93	36	6	92	0	92	40	24	31
***38.75	Failure														
Indicated Deflections 0.001 inch	3.2	10,4	5.2	1.0	8.9	15.7	20.7	16.4	9.4	0.8	0	10.8	6.0	2.4	13.1
Corrected Deflections 0.001 inch	3.2	10.1	4.9	1.0	8.6	15.4	20.4	16.1	9.1	0.8	0	10.5	5.7	2.4	12.8
Directions of Deflections Rel. Datum	←	↓	↓	→	↓	↓	↓	↓	↓	→		↓	↓	←	↓

* Signs of yielding in the tension weld beneath the web ** Very strong indication of yielding beneath the web.

*** Failure was preceded by very large creep directly beneath the web in the tension weld.

TABLE 24

Specimen No: 305305/1 Distance Between Supports 5.5 m

Dial Gauge Correction: 0.00126 inch

Load	Dial Gauge Position																
	1	2	3	4	5	6	7	8	9	10	11	12	13	14	15	17	16
tonne	10^{-3} inch	10^{-3} inch	10^{-3} inch	10^{-2} mm	10^{-2} mm	10^{-3} inch	10^{-3} inch	10^{-3} inch	10^{-3} inch	10^{-3} inch	10^{-3} inch	10^{-3} inch	10^{-3} inch	10^{-3} inch	10^{-3} inch	10^{-3} inch	10^{-3} inch
Dead Weight	3	2	2	0.9	19.3	1.5	97.5	95	97.5	97	98	98	2.5	2.5	2	0	0.5
0.5	5	3	3	1.2	18.9	2	96.5	94	97.5	95	95.5	96.5	3.5	3.5	3	0	2
1	6	4	3.5	1.4	18.5	2.5	95	92	97	93.5	94.5	96	4	5	4	0.5	3.75
1.5	7.5	4.5	4	1.5	17.9	3	94.5	90	98	92.5	93.5	94.5	5	6	5	0.5	5.75
2	9	5	5	1.6	17.2	5	94	88	3	90	91.5	92.5	6	7	6	0.5	7
2.5	10	6	5.5	1.7	16.5	7	94	86	1	88.5	90	91.5	6.5	8	7	0.5	8.25
3	11	6.5	6	1.75	15.6	9.5	93.5	85.5	99.5	87	89	90.5	7	9	8	0.75	9.75
3.5	12	7	7	1.8	14.7	12.5	93.5	82	98.5	84.5	87.5	89	8	10	9.5	0.75	11.5
4	13	8	7.5	1.8	13.9	14.5	93	81.5	97	83	86.5	88	9	11	10	1	12.5
4.5	14	8.5	8.5	1.8	12.9	17	93	80	95.5	80.5	85	87	9.5	12	11.5	1	14
5	15	9	9	1.8	11.6	20.5	93.5	79	93	77	83.5	85.5	10.5	13	12	1	15.5
5.3	15.5	10	10	1.7	10.4	26	94	77	92	74	81.5	84	11	14	13	1	16.5
5.6	16	10	10	1.7	9.8	27	94	76.5	90.5	72	81	83.5	11.5	14.5	13.5	1	17
5.9	17	10	10.5	1.5	8.5	31.5	94.5	75	89	70	79.5	82.5	12	15	14.5	1	17.5
*6.2	17.5	10.5	11	1.5	7.6	33.5	95.5	74	87.5	68.5	78.5	81.5	12.5	15.5	15.5	1.25	18.5
6.5	18	11	11.5	1.3	6.2	38	96	72.5	87	66.5	77	80	13	16.5	16	1.5	19.5
**6.8	18	11.5	12	1.2	5.3	40	97	71	86	65.5	76	79	13.5	17	17	1.25	20
7.1	19	12	12	0.8	3.2	49	0	70.5	84	64	74.5	75.5	14	17.5	17.5	1.5	21.5
7.4	19	12	12	19.8	19.2	59	1	70	83.5	62.5	72.5	73	14.8	18	18	2	22.5
7.7	Failure																
Indicated Deflections 0.001 inch	1.9	1.2	1.2	0.1	8.2	5.9	0.1	3.0	1.65	3.75	2.75	2.7	1.5	1.8	1.8	1	2.2
Corrected Deflections 0.001 inch	3.2	2.5	2.5	0.1	8.2	7.2	1.36	1.74	0.4	2.5	1.5	2.4	2.76	3.06	3.06	1	0.94
Direction of Deflection Rel. Datum	↑	↑	↑	←	→	↑	↑	↓	↓	↓	↓	↓	↑	↑	↑	→	↓

* Small crack appeared at left hand end of tension weld.

** The crack is propagating and will undoubtedly precipitate failure by tearing of tension weld.

TABLE 25

Specimen No: 305305/2
Dial Gauge Correction: 0.00034 inch

Distance Between Supports: 3.043 m

Load	Dial Gauge Position															
	1	2	3	6	7	8	4	5	13	14	15	10	11	12	17	16
tonne	10^{-3} inch	10^{-3} inch	10^{-3} inch	10^{-2} mm	10^{-2} mm	10^{-3} inch	10^{-3} inch	10^{-3} inch	10^{-3} inch	10^{-3} inch	10^{-3} inch	10^{-2} mm	10^{-2} mm	10^{-2} mm	10^{-3} inch	10^{-3} inch
Dead Weight	99	99.5	0	52	3.1	1	0	0	0	99	98	0	1.8	32	0	0
5	98	99	0	89	5.2	5	99	98	99	98.5	97.5	2	3.4	48	0	2
10	98	97	97	12	7	12	98.5	97	96	96.5	97	5	5	59	0	6
15	97	95	92	35	8.9	21	98.5	95	92	94.5	95.5	8.3	6.9	72	0	13
20	95	92	85	62	11.3	33	98.5	93.5	86	91	93.5	12.6	9	86	0	22
25	93.5	88	78	89	13.8	48	98	92	79	86	91	17.1	11.4	3	0	34
30	91	84	69	20	16.7	64	98	90	71	81	87.5	2.6	14.4	21.5	0	47
35	89	80	60	55	19.9	85	98.5	88	61	74	83	9	18.4	44	0	61
40	85	72	46	1	3.9	10	98.5	86	45	64	76.5	17.2	3.9	68	0	81
42	83.5	69	40	22	5.7	21	98.5	85.5	37	60	73	2.5	6.2	78	0	90
*44	81	65	32	53	8.2	37	98.5	84	27.5	53	69	5.2	9.2	91	1	6
45	78	61	25	81	10.3	51	98.5	83	19	48	65	9	11.4	97	1.5	15
**46	70	48	2	68	16.8	94	98	81	92	33	54	19.9	16.7	95	3	53
47	63	39	87	10	1.7	14	97	79	81	25	49	5.2	1.3	21	4.5	67
48	60	33	79	35	4.9	27	96.5	77	74	20	46	8.6	2.2	28	4	79
+ 49	55	27	68	70	10.2	45	96	75	62	14	41.5	14	5.2	40	4	95
50	49	18	54	20	17.2	70	95	73	50	6	38	19.2	8.6	49	5	15
51	Failure															
Indicated Deflection 0.001 inch	5.1	8.2	14.6	48.8	22.7	27.0	0.5	2.7	15.0	9.4	6.2	31.2	27.0	19.6	2.5	21.5
Corrected Deflections 0.001 inch	4.76	7.86	14.3	48.5	22.4	26.7	0.5	2.7	14.7	9.06	5.86	30.9	26.7	19.3	2.5	21.2
Direction of Deflection Rel. Datum	↓	↓	↓	↓	↓	↓	←	→	↓	↓	↓	↓	↓	↓	←	↓

* Small crack appeared in tension weld beneath web. ** Small crack appeared at left-hand end of tension weld.
\+ End crack is propagating at the same time as centre crack.
Test conducted with a 50 mm bearing at the tension flange.

TABLE 26

Specimen No: 305305/3 Distance Between Supports: 5.5 m
Dial Gauge Correction: 0.00057, 0.00093 inch

Load	Dial Gauge Position															
	1	2	3	4	5	6	7	8	9	10	11	12	13	14	15	16
tonne	10^{-3} inch	10^{-3} inch	10^{-3} inch	10^{-3} inch	10^{-3} inch	10^{-3} inch	10^{-2} mm	10^{-2} mm	10^{-2} mm	10^{-2} mm	10^{-2} mm	10^{-3} inch	10^{-3} inch	10^{-3} inch	10^{-3} inch	10^{-3} inch
Dead Weight	46	16.5	6	7.5	5.5	27	1.4	0	19.1	95.5	17.6	82	97	96	85.5	11
1	48	17	5	8	3.5	28	1.1	9.8	18.7	93.5	17.3	83	97	96	88	13.5
2	51.5	18.5	5.5	8.5	97.5	31.5	0.7	91.5	17	86	16.2	73	97	97.5	93	21
3	53.5	18	5	7.5	85	35	0.3	85	15.6	74	14	65.5	96.5	97.5	97	29.5
4	54	18	4	6.5	70	41.5	0	77	12	63	12.4	59	96	99	1	38
5	Failure															
Indicated Deflections 0.001 inch	4.6	1.8	0.4	0.65	3.0	4.1	0	1.81	3.15	2.9	2.9	4.1	0.4	0.1	0.1	3.8
Corrected Deflections 0.001 inch	5.2	2.4	1.0	0.65	3.0	4.7	0.6	1.24	2.6	2.3	2.3	3.5	0.2	0.5	0.7	2.9
Direction of Deflection Rel. Datum	↑	↑	↑	←	→	↑	↑	↓	↓	↓	↓	↓	↑	↑	↑	↓

Failure by crack propagation from one end of the tension weld.

TABLE 27

Specimen No: 305305/4 Distance Between Supports 3.195 m
Dial Gauge Correction: negligible

Load	Dial Gauge Position																
	1	2	3	4	5	6	7	8	9	10	11	12	13	14	15	16	17
tonne	10^{-3} inch	10^{-3} inch	10^{-3} inch	10^{-3} inch	10^{-3} inch	10^{-3} inch	10^{-2} mm	10^{-2} mm	10^{-2} mm	10^{-2} mm	10^{-2} mm	10^{-3} inch	10^{-3} inch	10^{-3} inch	10^{-3} inch	10^{-3} inch	10^{-3} inch
Dead Weight	1.5	99	0	99.5	3.5	98	0	98	19.6	98	18.7	86	1	98.5	97	1	0
2.5	2	99	0	99.5	4	96	19.8	97.5	19.4	97	18.4	84	1	98	98	1	0
5	2.5	98.5	0	99.5	4	94	19.4	95.5	19.1	95	18.1	83.5	0	98.5	99	3.5	0
7.5	3	98	99	0	4	91	19	93	18.3	93	17.7	82.5	99.5	98.5	99.5	5.5	0
10	3	97.5	98	0.5	5.5	89	18.5	91	17.5	09.5	17.3	81.5	98.5	98.5	0.5	7.6	0
12.5	3	96.5	97	1	5.8	86.5	18.1	88	16.8	88	16.8	81	97	98.5	1	11	0
15	3	96	95	1.5	6	84	17.6	85	16	84.5	16.2	79	95.5	98	1.5	14.75	0
17.5	3	95	93	2	7	81.5	17	80.5	14.5	79.5	15.3	77	93	97.5	2	19	0
20	2	93.5	90	3	6	78	16.2	74.5	12.8	73	14.4	74	90.5	96	2	25	
22.5	1	91.5	86	3.4	5.6	72.5	15	66	10.6	66	13.2	71	86.5	94	1.5	31.5	0
25	0	89.5	82	3.4	5.6	66	13.6	57	8.2	58	12.0	68	82	92	1	39	0
27.5	99.5	87	76	4	4	61	12.3	48	5.6	49.5	10.8	65	77.5	89.5	0	46.5	0
30	98.5	85	71	4	4	57.5	11	38	2.8	40	9.4	61	72	87	99	54.5	0
32.5	97.5	82	65	4	4	51.5	9.6	28	0	29.5	8	57	66.5	83.5	97.5	63.5	0
35	96	79	58	4	4	46	8.1	15	16.6	17.5	6.4	53	59.5	79.5	95.5	74.5	0
37.5	95	75	51	4	4	40	6.2	0	12.8	0.4	4.5	51	51	75	93	86.5	0
*38.75	94	73	45	4	4	36	5.2	91	10.2	95.5	3.4	50	47	71.5	91	94.5	0
40	92	70	40	4	4	32	4.1	81	7.3	86	2.3	49	40	68	89	3.5	0
**41.25	91	68	33	4	4	29	3	70	3.8	75	1	48	33	64	85.5	13.7	0
42.5	89	64	23	3.5	1	23	1.2	53	19	58	19.1	47	22	57	81	30	0
+ 43.75	72	41	74	97	1	35	17	76	0.4	85	14	45	55	16.5	41	0	1.5

CONTINUED...

43.75	Failure																
Indicated Deflections 0.001 inch	2.8	5.9	12.6	0.3	0.1	16.5	16.5	17.7	23.8	16.8	10.2	4.5	14.5	8.4	5.9	20	0.75
Corrected Deflections 0.001 inch	2.8	5.9	12.6	0.3	0.1	16.5	16.5	17.7	23.8	16.8	10.2	4.5	14.5	8.4	5.9	20	0.75
Directions of Deflections Rel. Datum	↓	↓	↓	→	→	↓	↓	↓	↓	↓	↓	↓	↓	↓	↓	↓	→

* Small crack appeared in the tension weld beneath the web.

** Crack is propagating

\+ Massive creep around the web-in the tension weld.

TABLE 28

Specimen No: 305305/5 Distance Between Supports: 3.3 m

Dial Gauge Correction: 0.0003 inch

Load	Dial Gauge Position															
	1	2	3	4	5	6	7	8	9	10	11	12	13	14	15	16
tonne	10^{-3} inch	10^{-3} inch	10^{-3} inch	10^{-3} inch	10^{-3} inch	10^{-3} inch	10^{-2} mm	10^{-2} mm	10^{-2} mm	10^{-2} mm	10^{-2} mm	10^{-3} inch	10^{-3} inch	10^{-3} inch	10^{-3} inch	10^{-3} inch
Dead Weight	0	0	0	0	0	0	0	98	19.9	99	20	0	99	0	0	1
5	1.5	99.5	98	1	0	1	19.8	96.5	19.1	96	19.3	97.5	98	99	1	4
10	3	97	95	2	94	1	19.4	90	17	87.5	18	93	95	98.5	4	17
15	0	93	87.5	98	63.5	9	19.1	80	12.7	70	15.2	79.5	89	96.5	9	40
*20	97	82	0	76	56	46	8.6	70	5	62	64	42	90	95	4	71
21.25	Failure															
Indicated Deflections 0.001 inch	0.3	1.8	10	2.4	4.4	4.6	4.5	2.36	5.9	3.8	5.35	5.8	1.0	0.5	0.4	7.1
Corrected Deflections 0.001 inch	0	1.5	9.7	2.4	4.4	4.9	4.2	2.06	5.6	3.5	5.05	5.5	0.7	0.2	0.7	6.6
Direction of Deflection Rel. Datum		↓	↓	→	→	↑	↓	↓	↓	↓	↓	↓	↓	↓	↑	↓

* Initial failure occurred at this load when a tear propagated from the left-hand end of the tension weld to about half its length. Load was sustained and dial gauges read.

TABLE 29

Specimen No: 305305/6 — Distance Between Supports: 3.41 m

Dial Gauge Correction: 0.001 inch

Load	Dial Gauge Position																
	18	1	2	19	6	7	8	9	10	11	12	20	17	14	15	21	16
tonne	10^{-2} mm	10^{-3} inch	10^{-3} inch	10^{-3} inch	10^{-3} inch	10^{-3} inch	10^{-3} inch	10^{-3} inch	10^{-3} inch	10^{-3} inch	10^{-3} inch	10^{-3} inch	10^{-3} inch	10^{-3} inch	10^{-3} inch	10^{-3} inch	10^{-2} mm
Dead Weight	0.2	0	0	0	0	98	99	96	98	99	98	0	0	99	99	1	19.4
5	0.9	0	98	97	98	92	90	86	89	93	94	90	0	99	98	5	18.6
10	2.6	0	96	94	94	81	75	68	74	82	85	96	0	98	99	11	14.2
15	3.8	0	95	90	90	75	67	57	65	76	80	94	0	97	0	14.5	12.8
20	5.4	99	92	84	85	63	51	39	48	65	71	92	0	95	0	20	7.8
25	6.8	98	89	73	80	50	32	16	29	54	67	90	0	93	0	25	3.6
27.5	7.6	97	87	65	74	42	21	3	17	47	55	88	0	91	0	26	1.4
30	8.4	97	85	55	75	34	8	88	4	39	48	87	0	90	0	30	19.2
31	8.6	96	84	49	74	31	3	82	98	36	45	87	0	89	0	31	18.2
32	8.8	96	83	46	74	28	0	78	94	33	43	86	0	88	0	32	17
33	9.1	96	82	40	73	25	95	70	88	29	40	86	0	87	99	33	16
34	9.4	95	81	32	73	22	88	61	80	24	36	85	0	85	98	34	15.2
35	9.7	96	80	24	75	20	83	53	74	20	32	85	0	85	98	35	13.2
*36	10	95	78	13	78	17	76	43	66	16	28	84	0	83	97	36	11.6
36.5	10	94	77	5	79	15	74	40	62	13	26	84	0	81	97	38	11
**37	10.2	93	75	95	80	14	70	34	57	10	23	83	0	81	96	39	10
37.5	10.3	93	75	85	83	13	67	29	53	8	21	83	0	80	96	40	9.2
38	Failure																
Indicated Deflections 0.001 inch	4.05	0.7	2.5	11.5	1.7	8.7	13.3	17.2	14.7	9.2	7.9	0.7	0	2.0	0.4	4.0	12.1
Corrected Deflections 0.001 inch	4.05	0.3	1.5	11.5	0.7	7.7	12.3	16.2	13.7	8.2	6.9	0.7	0	1.0	0.6	4.0	11.1
Directions of Deflection Rel. Datum	←	↑	↓	→	↓	↓	↓	↓	↓	↓	↓	→		↓	↑	←	↓

* A crack is propagating from the left-hand end of the tension weld. The entire length of the weld appears to be yielding.

** Definite creep at positions 19, 8, 9 and 10.

TABLE 30

Specimen No: 305305/7 Distance Between Supports 3.1 m
Dial Gauge Correction: 0.00035 inch

Load	Dial Gauge Position																
tonne	18 10^{-2} mm	1 10^{-3} inch	2 10^{-3} inch	19 10^{-3} inch	6 10^{-3} inch	7 10^{-3} inch	8 10^{-3} inch	9 10^{-3} inch	10 10^{-3} inch	11 10^{-3} inch	12 10^{-3} inch	20 10^{-3} inch	17 10^{-3} inch	14 10^{-3} inch	15 10^{-3} inch	21 10^{-3} inch	16 10^{-2} mm
Dead Weight	0.4	1.5	0	0	97	99	0	90	98	92	80	5	0	0	0	2	19.4
5	0.2	99	98	10	70	92	95	85	87	76	50	15	49	98	98	1	17.7
10	0.4	99	95	13	57	85	89	75	75	68	39	18	48.5	96	97	2	16.4
15	1.2	96	90	23	12	59	63	45	39	32	94	25	47	90	95	4.5	10.2
20	1.4	96	89	25	5	55	60	40	33	27	84	27	46	89	95	5	9.4
25	1.7	95	87	28	92	49	52	30	21	18	73	30	44	87	94	7	7.4
30	1.9	95	84	31	80	41	46	20	11	9	69	133	44	85	94	7	5.6
35	2.6	92	77	38	45	15	20	90	74	75	20	39	44	77	90	10	19
40	3	89	70	43	16	92	91	45	33	44	80	44	43	68	87	11	10.8
42	3.3	87	67	45	7	85	82	28	34	68	68	45	43	64	85	12	7.4
*44	3.6	85	60	48	90	70	58	95	84	12	43	47	43	55	81	13	0.2
45	3.9	83	55	49	81	60	57	75	67	0	32	48	43	49	78	13.5	16.0
45.5	Failure																
Indicated Deflections 0.001 inch	1.54	1.7	4.5	4.9	21.9	14.0	14.3	22.5	23.3	20	26.8	4.8	0.7	5.1	2.2	1.35	9.45
Corrected Deflections 0.001 inch	1.54	2.0	4.8	4.9	22.2	14.3	14.6	22.8	23.6	20.3	27.1	4.8	0.7	5.4	2.5	1.35	9.0
Directions of Deflection Rel. Datum	←	↓	↓	→	↓	↓	↓	↓	↓	↓	↓	→	→	↓	↓	←	↓

Test conducted with a 50 mm bearing at the tension flange.
* Signs of plasticity beneath the web in the tension weld.

Specimen No: 305305/8 Distance Between Supports: 3.043 m

Dial Gauge Correction: Negligible

Load tonne	Dial Gauge Position					
	1 10^{-3} inch	22 10^{-3} inch	9 10^{-3} inch	23 10^{-3} inch	15 10^{-3} inch	16 10^{-2} mm
Dead Weight	98	26	49	79	97	19.5
5	91	73	48.5	79	93	18.8
10	85	98	48	15	87	17.8
15	77	17	47	48	82	16.6
20	69	35	45.5	77	75	15.4
25	60	55	44	6	67	13.8
30	49	75	42	37	60	12
35	38	95	41	66	52	10
40	27	14	39	99	42	7.4
45	15	32	37	31	32	5
50	0	51	35	65	21	3.2
*55	86	69	33	4	7	19.8
60	70	89	29	49	92	16.2
**65	53	7	26	85	77	11.2
° 70	35	30	21	24	59	7.8
75	6	65	15	74	32	19.6
°° 77.5	80	91	10	15	23	13.2
+ 80						
82	Failure					
Indicated Deflections 0.001 inch	22.0	39.0	40.0	61.5	17.7	18.4
Direction of Deflection Rel. Datum	↓	↓	↓	↓	↓	↓

* A 12 mm crack appeared at the right-hand end of the tension weld.

** No propagation of above -rack although deflection at position 23 is well ahead of position 22.

° Evidence of small plastic region of tension weld beneath the web,

°° Creep now evident - platic region extending side-ways.

\+ Massive creep at all positions.

Test conducted with flange spreaders welded in position and, a 50 mm bearing.

TABLE 31

TABLE 32

Specimen No: 305305/9 — Distance Between Supports 3.32 m

Dial Gauge Correction: 0.000835 inch

Load	Dial Gauge Position																
tonne	18 10^{-2} mm	1 10^{-3} inch	2 10^{-3} inch	19 10^{-3} inch	6 10^{-3} inch	7 10^{-3} inch	8 10^{-3} inch	9 10^{-3} inch	10 10^{-3} inch	11 10^{-3} inch	12 10^{-3} inch	20 10^{-3} inch	14 10^{-3} inch	15 10^{-3} inch	21 10^{-3} inch	16 10^{-2} inch	17 10^{-2} mm
Dead Weight	0.4	0	0	99	98	97	95	94	98	97	98	99	99	0	1.5	19	0
10	2	99	95	94	87	81	72	71	75	84	87	97	96	98	9	13	0
20	3.8	98	88	87	73	57	38	31	42	65	75	94	90	97	17.5	5.8	0
25	4.7	96	84	83	64	41	15	8	21	53	63	92	87	96	22	2.4	0
27	5.1	96	83	80	61	8	8	99	14	49	60	91	85	95	23.5	0	0
29	5.5	95	81	78	56	28	96	86	3.5	42	58	90	82	94	26	17.6	0
31	6	94	79	74	51	19	84	73	93	37	49	89	80	93	27	15.2	00
33	6.3	93	77	70	47	11	72	60	81	30	45	89	77	92	30	12.8	0
35	6.7	92	75	65	42	2	58	46	68	24	40	88	75	91	32	10	0
37	7.1	90	72	58	37	92	41	27	55	15	33	87	71	89	34	6.2	0
38	7.4	89	70	51	34	8.5	31	15	46	10	28	87	69	88	35	3.9	0
*39	7.6	88	67	44	33	81	22	3	37	5	24	86	66	87	36	1.4	0.5
40	7.8	87	65	36	36	77	11	88	27	99	18	86	63	85	38	18.8	0.75
40.5	7.8	87	63	31	35	74	6	82	22	96	16	86	61	85	39	17.5	1
41	8	86	62	26	35	72	99	72	15	93	14	86	59	83	40	15.3	1
**41.5	8	85	59	15	37	68	86	56	2	87	8	86	54	81	41	11.3	1.5
42	Failure																
Indicated Deflections 0.001 inch	3.14	1.5	4.1	8.5	5.3	13.2	21.4	24.4	19.8	11.3	9.2	1.4	4.6	1.9	4.1	19.2	1.5
Corrected Deflections 0.001 inch	3.14	0.7	3.3	8.5	4.5	12.4	20.6	23.6	19	10.5	8.4	1.4	3.8	1.1	4.1	18.4	1.5
Direction of Deflection. Rel. Datum	←	↓	↓	→	↓	↓	↓	↓	↓	↓	↓	→	↓	↓	←	↓	→

* Signs of yielding of the tension weld beneath the web

** Cross green of tension weld beneath the web

TABLE 33

Specimen No: 305305/10 Distance Between Supports: 3.814 m

Dial Gauge Correction: 0.0017 inch

Load tonne	Dial Gauge Position																
	18	1	2	19	6	7	8	9	10	11	12	20	17	14	15	21	16
	10^{-2} mm	10^{-3} inch	10^{-3} inch	10^{-3} inch	10^{-3} inch	10^{-3} inch	10^{-3} inch	10^{-3} inch	10^{-3} inch	10^{-3} inch	10^{-3} inch	10^{-3} inch	10^{-3} inch	10^{-3} inch	10^{-3} inch	10^{-3} inch	10^{-2} mm
Dead Weight	0.3	99	0	98	99	98	0	97	97	98	99	99	0	0	1	2	19.1
2	0.8	2	0	95	96	94	95	91	92	95	96	97	0	0	1	4.5	18
4	1.3	4	0	93	93	90	89	86	88	93	94	95	0	1	2	7	17
6	1.8	4	0	91	89	85	84	85	80	89	91	93	0	1	3	9.5	15.5
8	2.4	5	1	87	85	79	77	72	76	85	88	91	0	1.5	4	12	14.1
10	3.1	6	1	83	81	72	69	64	69	81	85	88	0	2	5	15.5	12.5
12	3.7	7	1	77	79	66	60	55	61	76	81	85	0	2.5	6	19	10.9
14	4.2	8	1	65	79	61	53	45	53	70	77	83	0	3	7	22	9.3
16	4.7	9	1	38	87	60	45	34	43	62	70	81	0	3	7	26	7.6
*17	4.9	8	0	20	92	60	42	29	37	59	67	80	0.5	3	7	29	6.8
18	5	8	0	99	99	60	38	21	31	55	64	79	0.5	3	7	31	6
18.5	5.1	8	0	87	3	59	35	17	28	53	62	78	0.5	3	6.5	32	5.7
**18.5	4.7	5	98	0	90	51	32	14	26	53	63	69	1	4.5	10.5	5.6	
19	4.7	5	97	98	90	50	30	12	24	52	63	68	1	5	10.5	36	5.7
19.5	4.8	5	97	95	91	49	28	9	22	50	62	67	1	5	10.5	36.5	5.3
20	5	5	97	92	92	48	26	6	19	48	61	65	1	5	10.5	37.5	5.1
+ 20.5	5.1	5	96	83	94	47	24	2	16	46	60	63	1	5	10.5	38.5	4.7
21	5.2	6	96	65	0	45	20	97	11	45	60	86	1	4	10.5	40	4.2
21.5	5.4	5	95	49	5	47	18	91	6	43	61	80	1	4	10.5	41	4
22	Failure																
Indicated Deflections. 0.001 inch	2.1	0.5	0.5	15.1	0.5	5.3	8.2	10.9	9.4	5.7	3.9	12.0	1	0.4	1.0	4.1	6.3
Corrected Deflections 0.001 inch	2.1	2.2	1.2	15.1	2.2	3.6	6.5	9.2	7.7	4.0	2.1	12.0	1	2.1	2.7	4.1	4.6
Direction of Deflection. Rel. Datum	←	↑	↑	→	↑	↓	↓	↓	↓	↓	↓	→	→	↑	↑	←	↓

* Deflection at position 19 is well ahead of position 20 - possible failure from left-hand end of tension weld.

** Bolts around the left-hand end of tension weld were slackened to relieve load and prevent a failure by crack

6.3 Calculation of Shear Load and Bending Moment

Details of the 1130 kNm, 1000kN Testing Beam, and the test connection end-plates may be found in the Appendices. Calculations were made in order to assess the deadweight effects of the testing beam, the following were taken into consideration;

1. U.D.L. of testing beam
2. semi-concentrated testing beam-end masses
3. bolt combination (each combination has mass 0.58 kg)
4. beam overhang
5. test connection.

The deadweight representation of the testing beam set up for test is shown in fig. 81. The masses of bolt combination and test connection end-plates have been included in the semi-concentrated beam-end mass. The external load P was applied at the position indicated in fig. 81.

The bending moment M and shear load, V, were determined as follows:

For Series 305 x 127

$$R_{rh} = \{2.889(P + 284) + 4296.8\}/x$$

$$R_{\ell h} = (P + 1622.2) - R_{rh}$$

$$M = 3R_{\ell h} - 0.111P - 836.5$$

$$V = P - R_{\ell h} + 811.5$$

For Series 356 x 171

$$R_{rh} = \{2.889(P + 284) + 4312.7\}/x$$

$$R_{\ell h} = (P + 1627.3) - R_{rh}$$

$$M = 3R_{\ell h} - 0.111P - 836.5$$

$$V = P - R_{\ell h} + 811.5$$

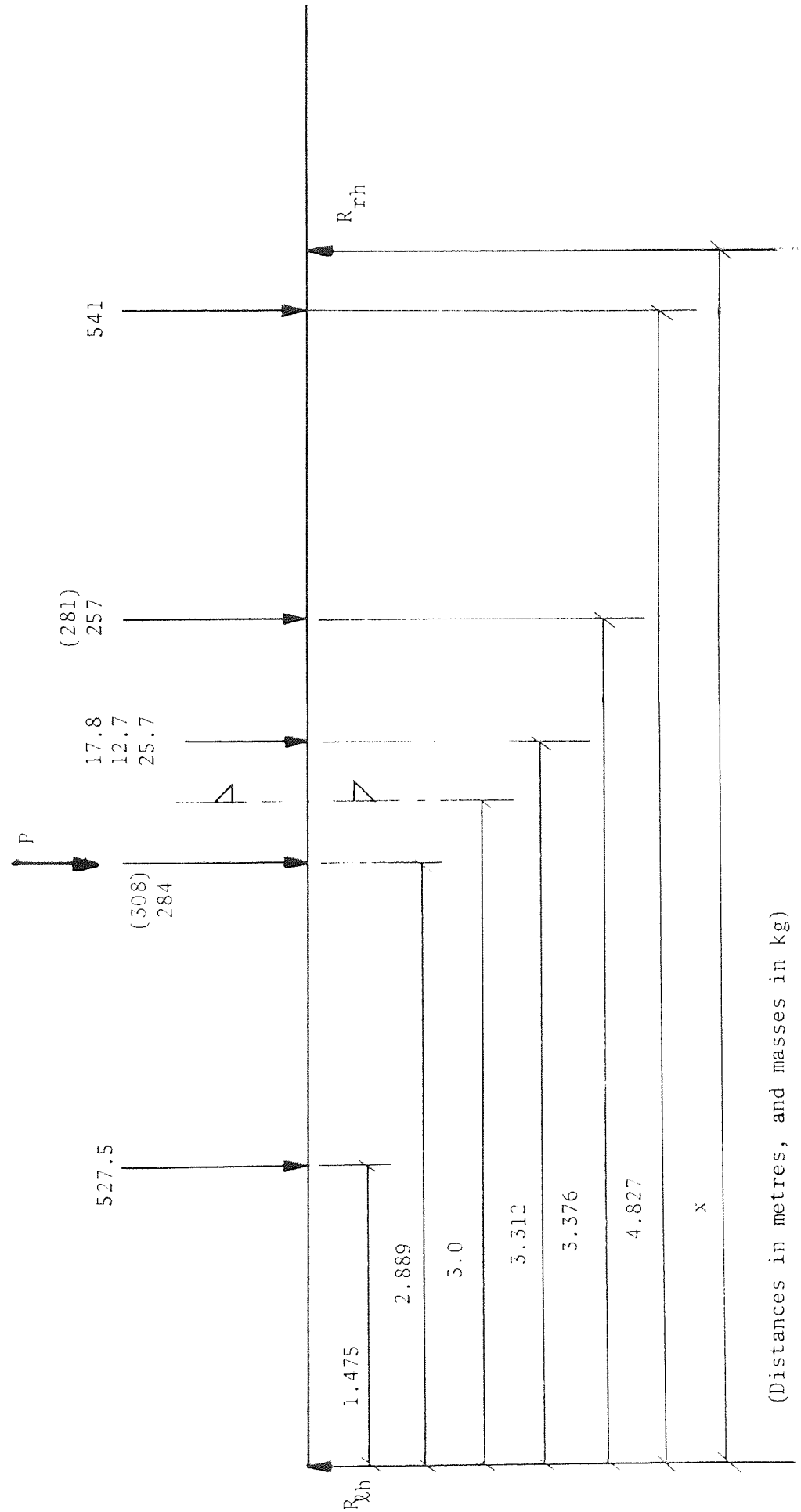

Fig. 81 Deadweight Representation of Testing Beam

For Series 305 x 305

$$R_{rh} = \{2.889(P + 308) + 4418.5\}/x$$

$$R_{\ell h} = (P + 1683.2) - R_{rh}$$

$$M = 3R_{\ell h} - 0.111P - 839.2$$

$$V = P - R_{\ell h} + 835.5$$

These calculated results are given in Table 34 and plotted in fig.82.

The first three test connections were welded up without using constrai to reduce distortion of the end-plates. Some distortion did result but its importance was not realized at the time. These three connections, 305305/3, 356171/1 and 305305/5, were set up in the testing beam and the connecting bolts tightened down until the end-plates of the test connection and the testing beam were in full contact - this was necessary in order to ensure a 'rigid column'. It was realized during the tightening down that the welds would be pre-loaded to some degree, particularly the ends, but this pre-load was thought to be insignificant. During testing however, th pre-loading proved to be critical and the formation of a crack at the end o the tension weld was preceded by relatively large vertical deflections indicated by the dial gauge in position 6. It can be seen from the dial gauge readings, Tables 26 and 28, that the left-hand end of the tension flange was moving upwards, whereas the rest of the flange was moving downwa On further increase in the applied load the crack in the end of the tension weld propagated rapidly along the weld, thus causing weld failure at a load well below the expected value. Such a failure by propagation of an end crack in the tension weld has been designated as 'end mode failure'.

Specimen No.	V kN	M kNm
305127/1	19.20	57.22
" /2	77.97	59.39
" /3	203.4	57.00
" /4	276.0	23.43
" /5	299.5	2.58
356171/1	70.45	53.23
" /2	27.68	78.53
" /3	388.62	36.93
" /4	215.61	65.81
" /5	116.59	90.88
" /6	346.38	74.39
" /7	26.36	92.41
" /8	295.17	86.35
" /9	478.72	10.27
" /10	343.05	56.04
" /11	404.24	7.06
" /12	351.94	57.72
305305/1	40.56	111.42
" /2	483.63	10.40
" /3	26.91	77.29
" /4	395.94	68.08
" /5	189.90	48.71
" /6	322.67	124.95
" /7	447.17	34.8
" /8	772.26	22.81
" /9	368.05	102.16
" /10	171.0	133.6

Table 34. Calculated Results. Beam-Column Connections.

Fig. 82 Relationship Between V and M, Beam-column Connections

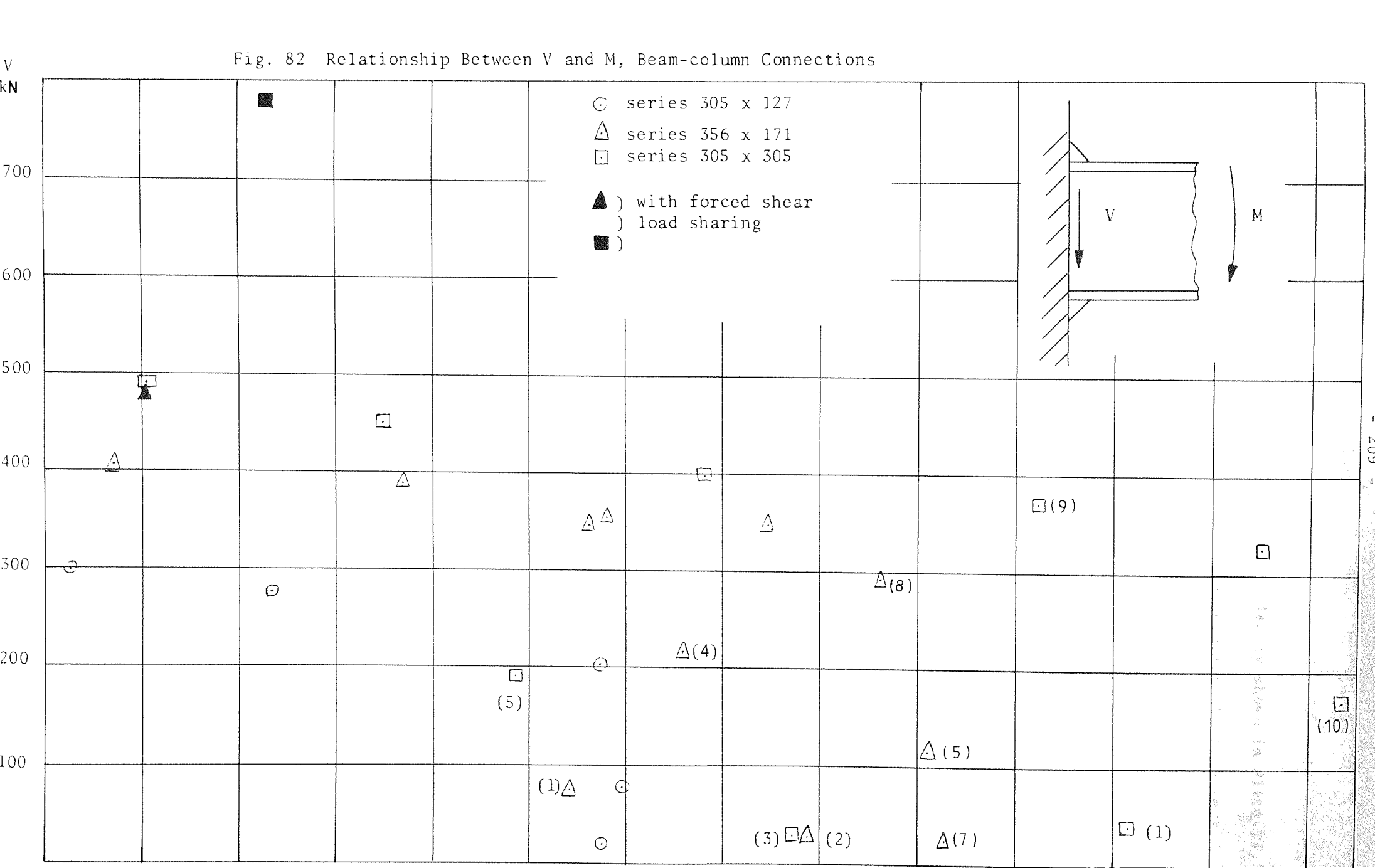

The propagating crack 'end mode failure' is clearly shown in Plate 11, 'Tension Weld No.3'. Complete failure of such a weld results in a very uneven and jagged fracture surface as can be seen in Plate 12, 'Tension Weld No.5', and plate 10, 'Tension Weld No.1'. The 'end mode failure' causes twisting of the connection and possible cracking of the compression weld at its right-hand end - see Plate 10, 'Compression Weld No.1'. In fig. 82 points (3)□, (5)⊡, and (1)△, represent 'end-mode failures', and the effect on connection ultimate capacity is made very clear.

The next three specimens, 356171/4, 356171/2 and 305305/1, were welded up using severe constraint and this resulted in only slight residual distortion in the end-plates which again was considered to be insignificant. However, even this slight distortion proved to be significant during the testing and, resulted in the definite 'end mode failure' of connection 305305/1, and the suspected 'end mode failure' of connections 356171/2 and 356171/4. Once again, the dial gauge readings confirmed the mode of failure, see Table 24 (gauge 6) and Tables 13 and 15 (gauge 5). The failure of these three specimens was not so dramatic as the previous three, but evidence of the mode of failure can be seen in Plate 8, 'Tension Weld Nos.2 and 4' which show the uneven and jagged fracture surfaces.

All subsequent test connections were welded with constraint, and then bolted to the testing beam with packing shims inbetween the plates - thus pre-loading of the welds was avoided. The placing of packing shims was rather a tedious operation, and in retrospect, machining of the end-plates would have been a better solution to the problem.

The aforementioned six tests were repeated and the results obtained fit well with the general trend as can be seen in fig.82; △(8), △(5), △(7), ⊡(9), and ⊡(10) different e/d.

The effect of weld pre-loading, resulting from poor fit-up of end-plates, on the connection ultimate capacity has been clearly demonstrated by these six tests.

Two connections were modified prior to testing, 356171/9 and 305305/8 by the addition of plates welded in position inbetween the flanges, directly underneath the welds, see Plates 11 and 12. This modification had the effect of more or less eliminating flange deformation and forcing an approximately equal shear load sharing between the two welds, resulting in an increased ultimate capacity as shown in fig. 82. It will be noted the approximate increase in shear load for the 305305 connection is 60%, and that for the 356171 connection is only 20%. The explanation of the difference lies in the effective flange width which is discussed later in this chapter.

If the 'end mode failures' and forced shear load results are ignored, the following general points can be drawn from fig.82.

(1) the relationship between V and M is approximately elliptic, centre origin,

(2) at V/M equals zero the ultimate bending moment is directly proportional to the flange width for all three beam sections (M_{ult} for section 356 x 171 was reduced by a factor 305/356 for this comparison). This implies that flange width is fully effective in resisting a pure bending moment,

(3) the ultimate shear load is well below the expected value especially for the wide flange section, 305 x 305. At this stage it is possible to conclude only that the flange width is not fully effective in resisting the shear load.

Plate 7 Fractured Beam-column Connections, Series 305 x 127

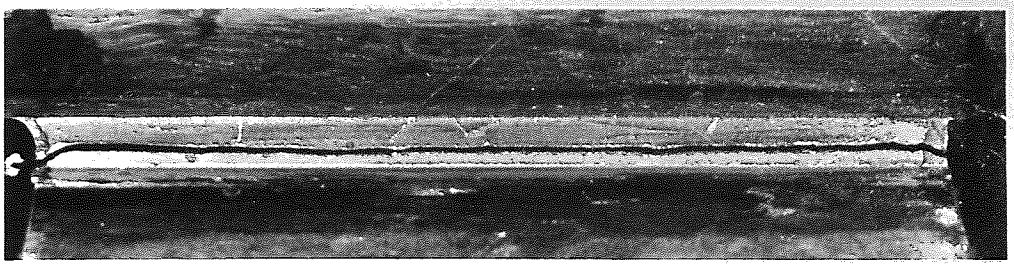

Tension Weld No.1

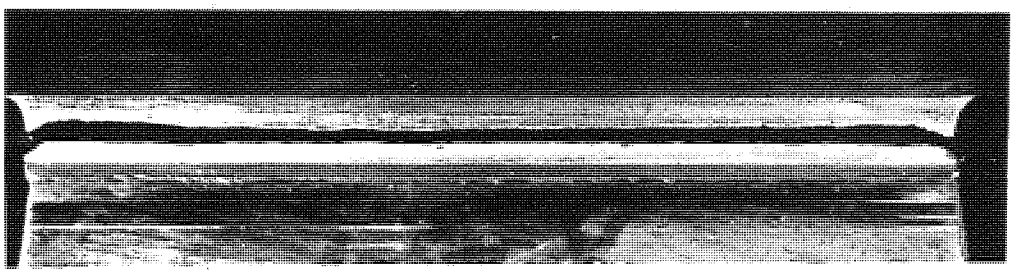

Tension Weld No.2

Tension Weld No.3

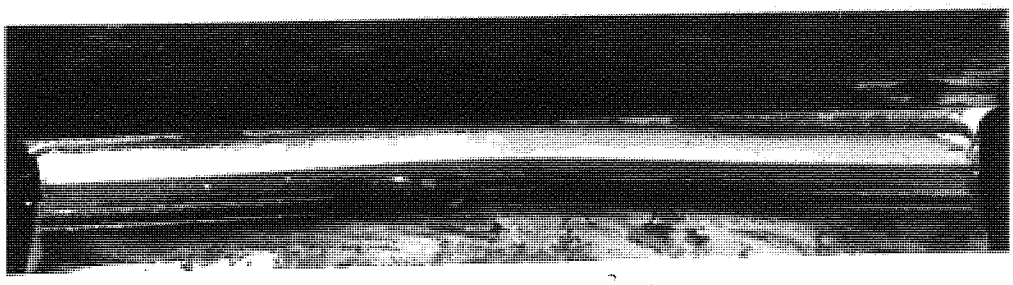

Compression Weld No.4

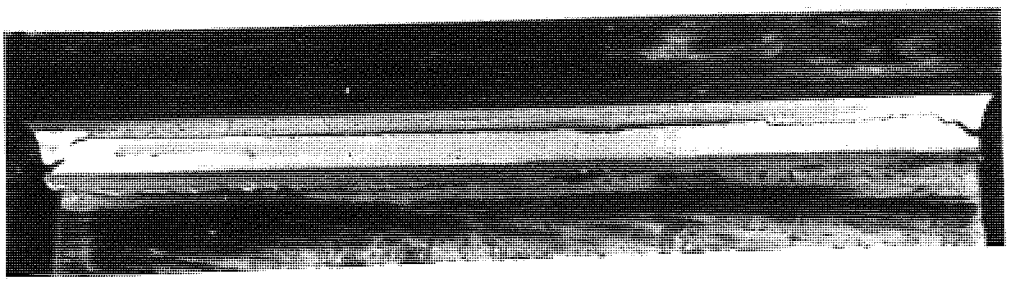

Tension Weld No.4

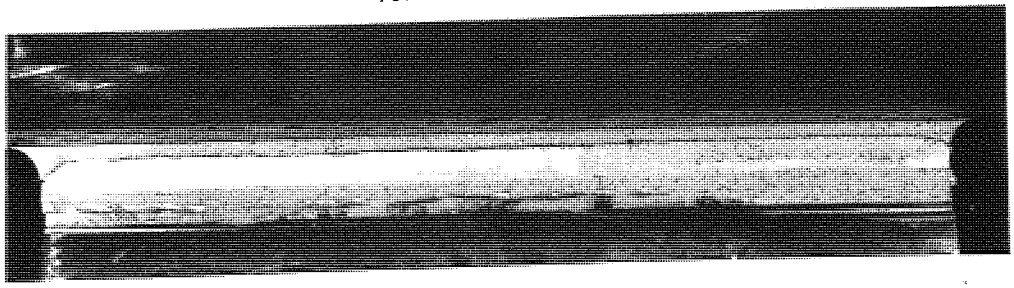

Tension Weld No.5

Plate 8 Fractured Beam-column Connections, Series 356 x 171

Tension Weld No.7

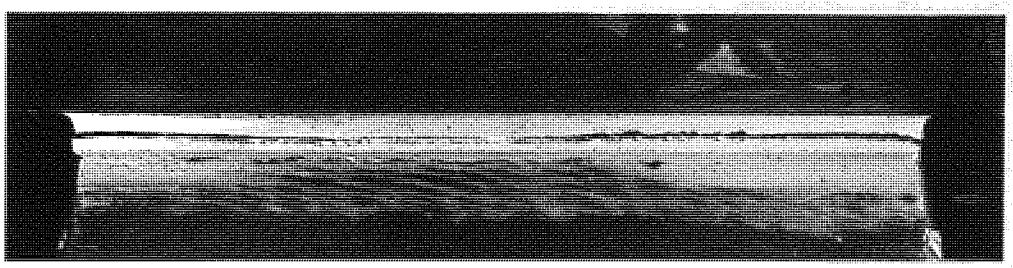

Tension Weld No.2

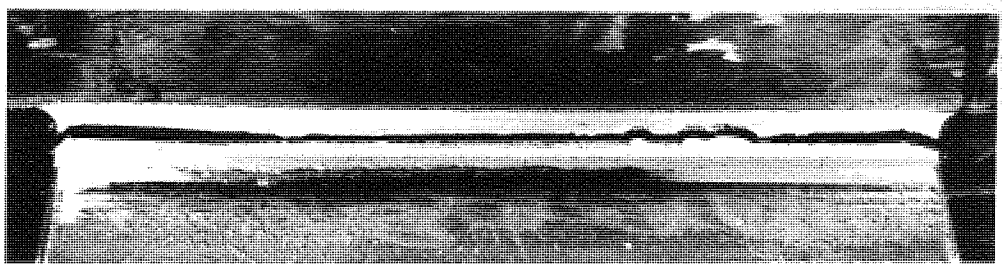

Tension Weld No.5

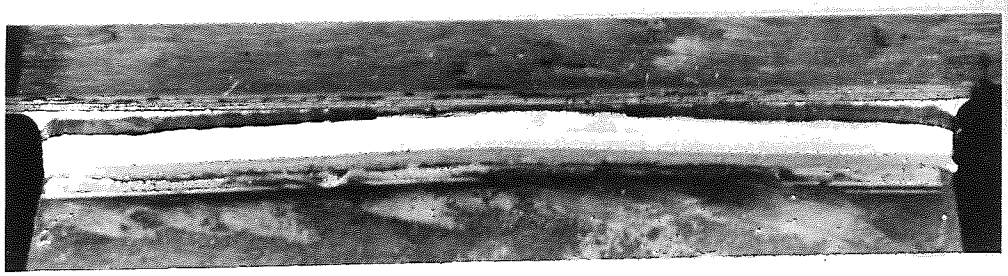

Compression Weld No.5

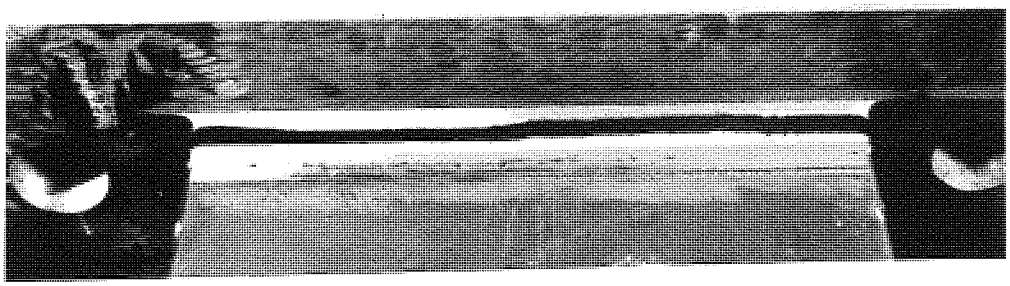

Tension Weld No.4

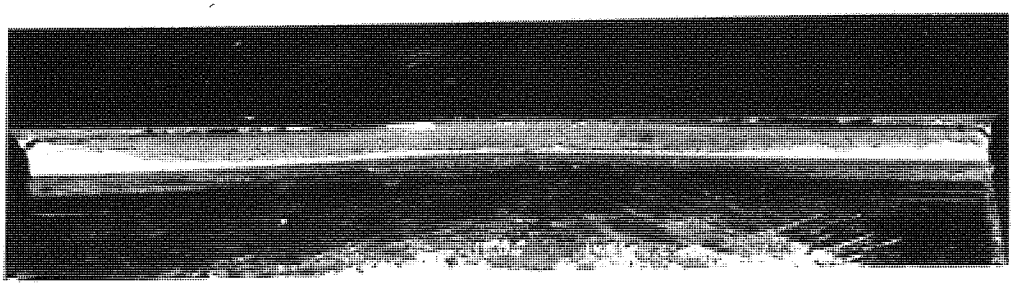

Compression Weld No.4

Plate 9 Fractured Beam-column Connections, Series 356 x 171

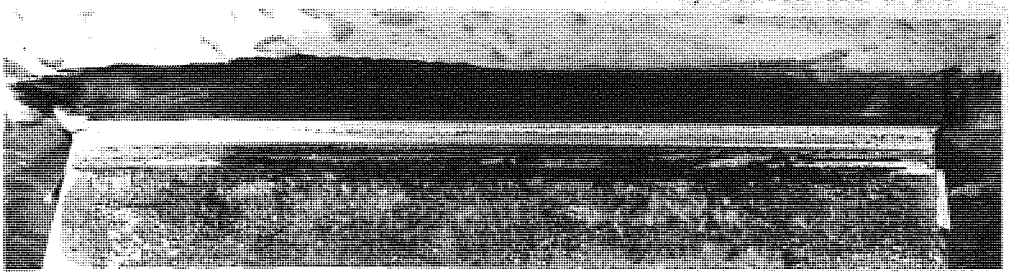

Tension Weld No.8 305 x 305

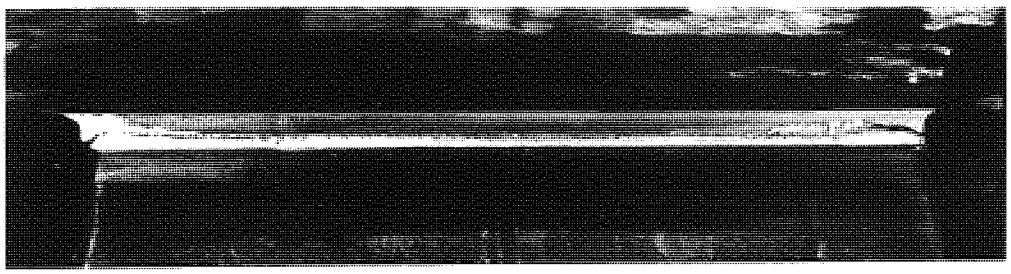

Tension Weld No.8

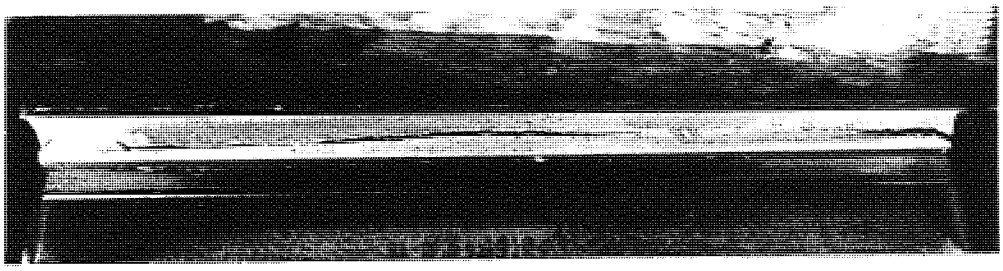

Tension Weld No.6

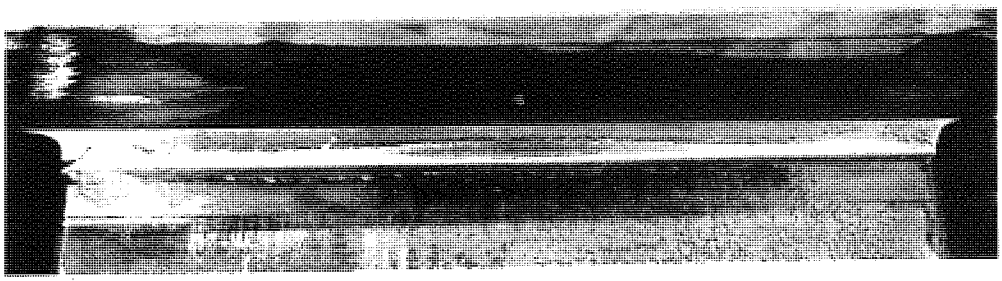

Tension Weld No.10

Tension Weld No.12

Tension Weld No.3

Plate 10 Fractured Beam-column Connections, Series 356 x 171

Tension Weld No.9

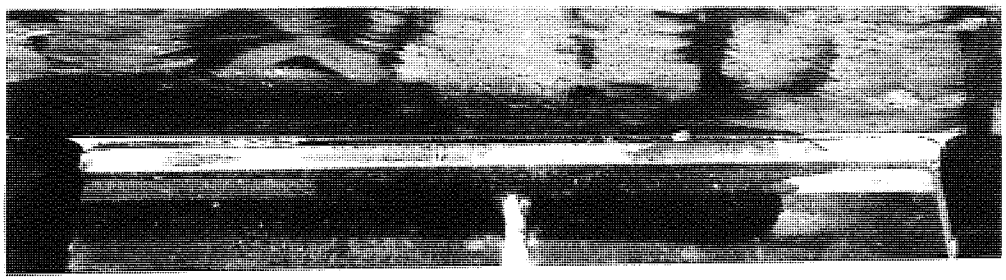

Compression Weld No.9

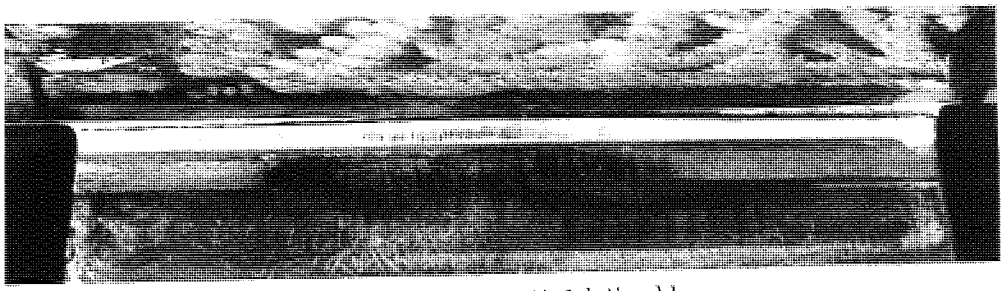

Compression Weld No.11

Tension Weld No.1

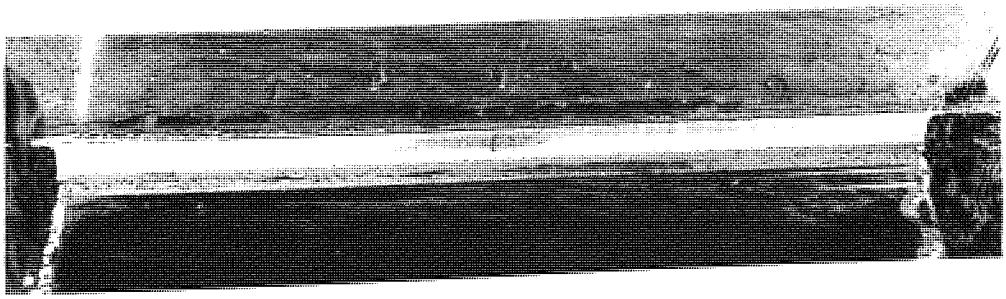

Compression Weld No.1

Plate 11 Fractured Beam-column Connections, Series 305 x 305

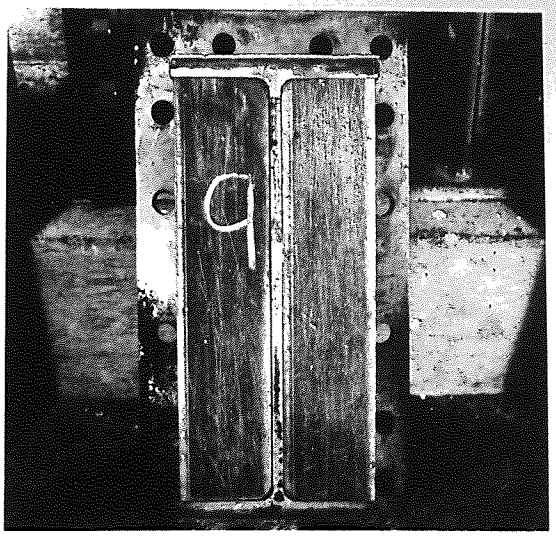

Stiffened Connection No.356171/9

Tension Weld No.3

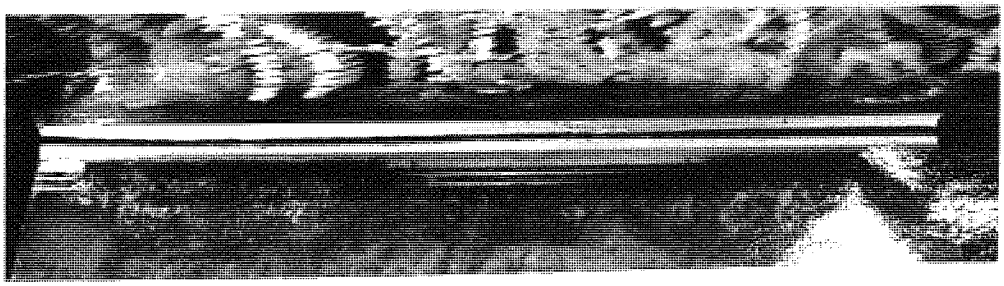

Tension Weld 1

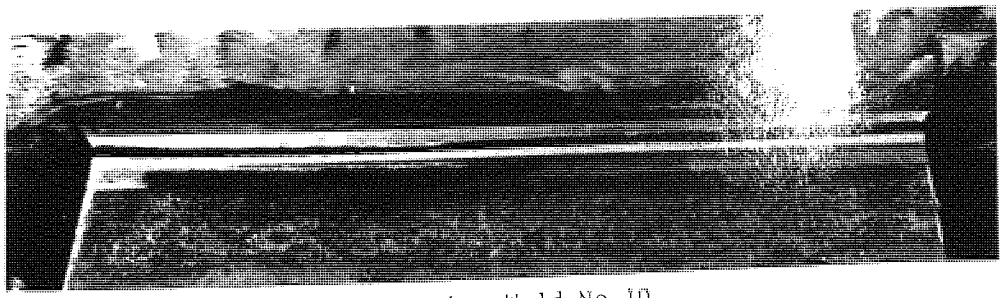

Tension Weld No.10

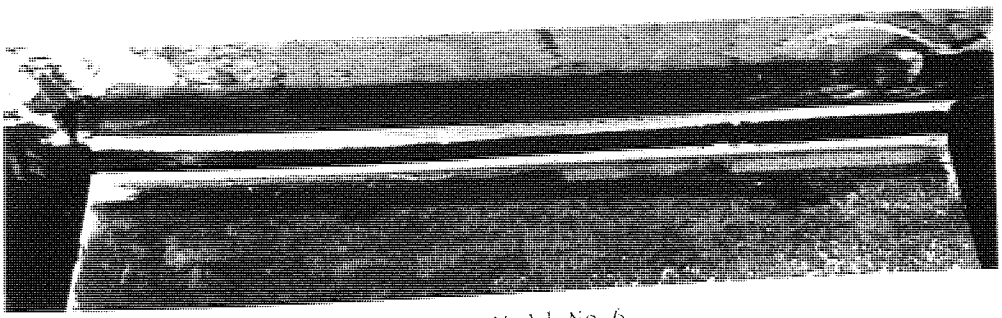

Tension Weld No.6

Plate 12 Fractured Beam.column Connections, Series 305 x 305

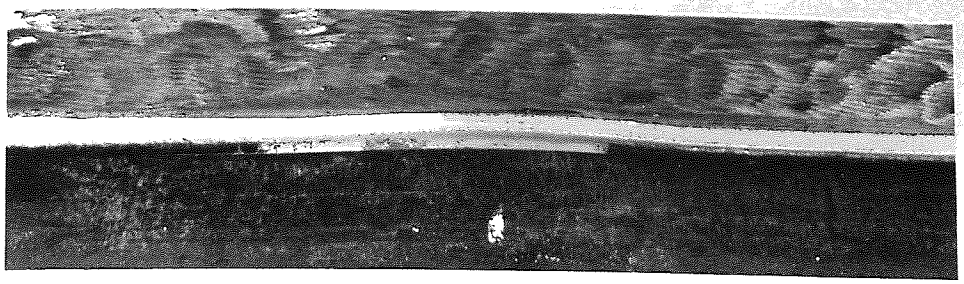

Compression Weld No.6

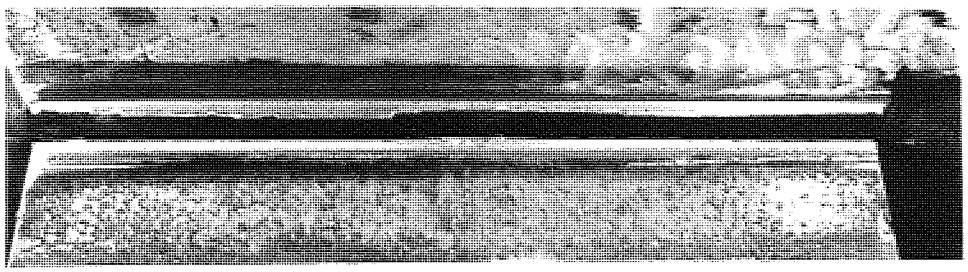

Tension Weld No.9

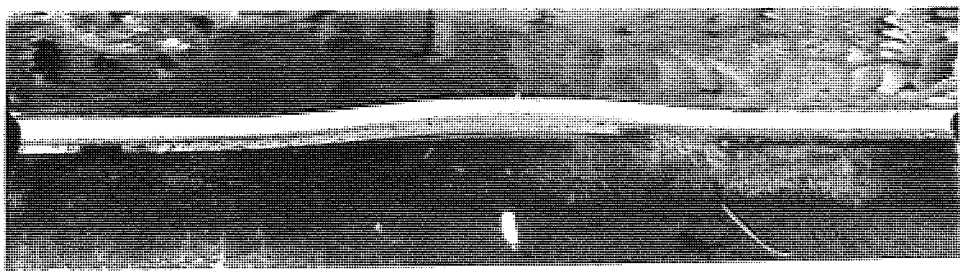

Compression Weld No.9

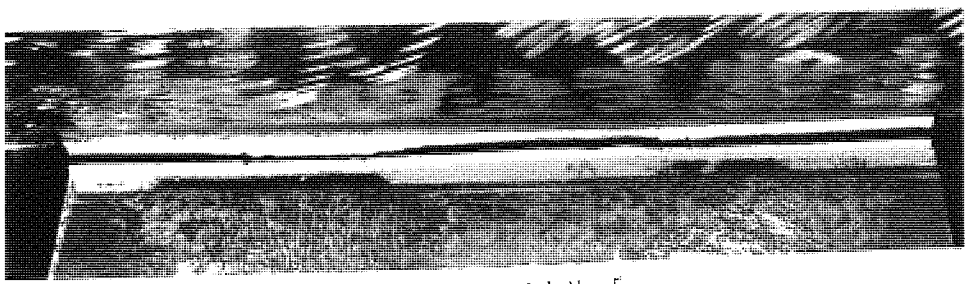

Tension Weld No.5

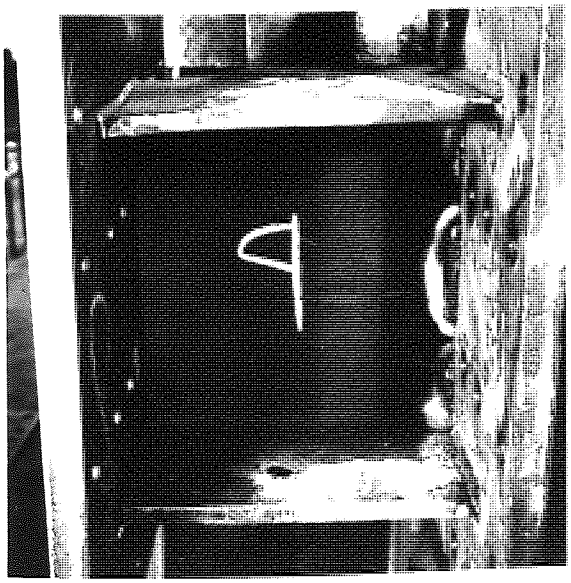

Compression Flange, No.9

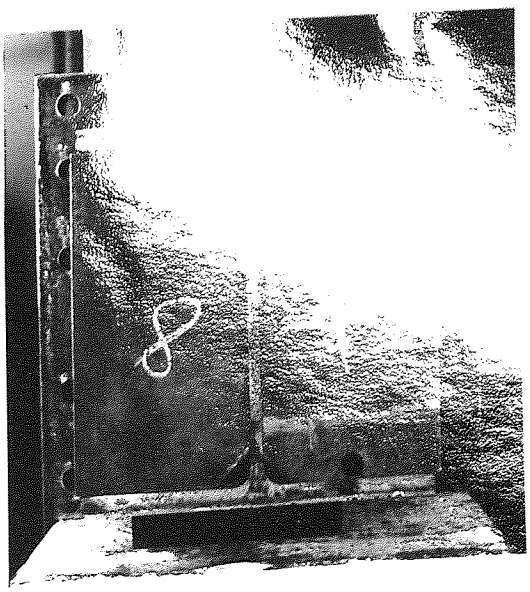

Stiffened Connection No.305305/8

Plate 15 Fractured Beam-column Connections, Series 305 x 305

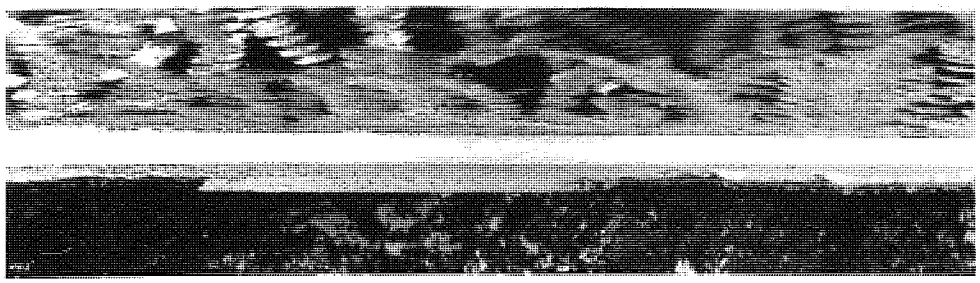

Tension Weld No.4

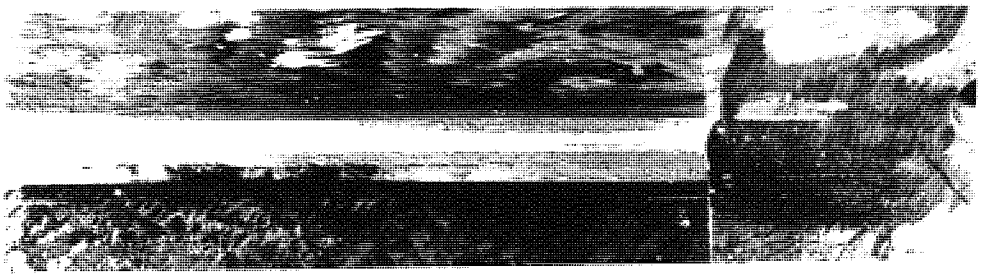

Compression Weld No.4

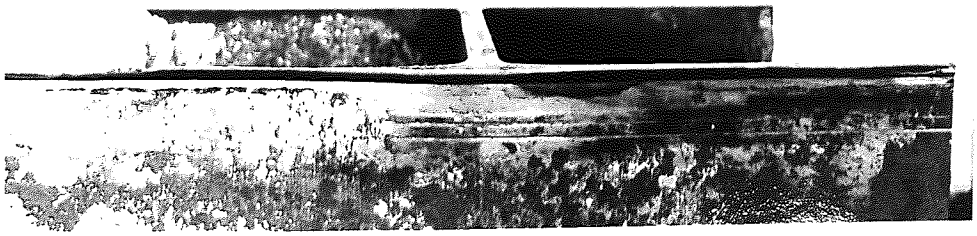

Compression Weld No.2

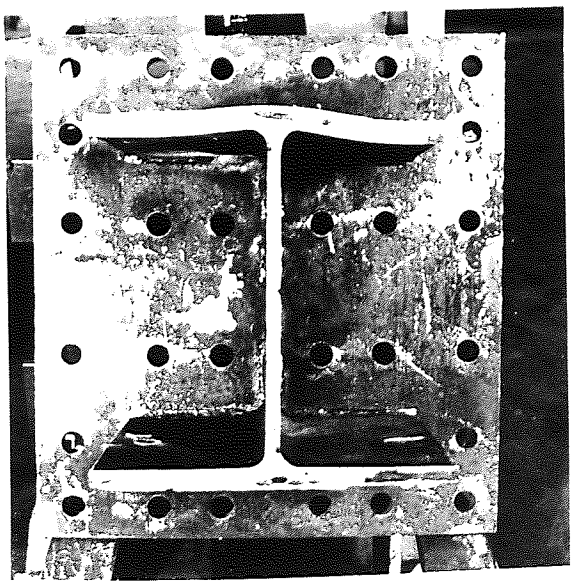

Compression Flange, No.7

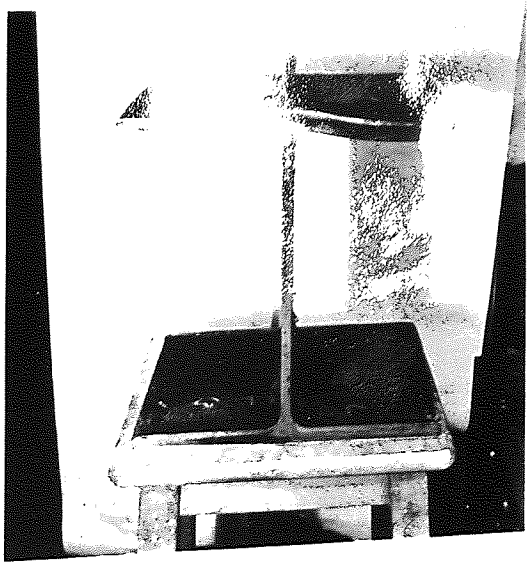

Compression Flange No.2

Further analysis of the results is required in order to investigate the outstanding issues of

1. shear load sharing between welds,
2. distribution of shear load along flange welds,
3. position of axis/centre of rotation,
4. effects of web flexibility

6.4 Analysis of Dial Gauge Readings

Dial gauge readings are given for all tests (except for connection 356171/1 which was exploratory) in Tables 8 to 33 inclusive, and dial gauge positions are shown in figs. 60, 61 and 62.

Because the flange/weld deflections were relatively small in many instances, it was considered necessary to correct the readings, taking account of the relative rotation between the end-plate and the test connection beam. The rotation of the connections was determined at the same time as the calculation of dial gauge reading corrections as shown in fig.83, in which average horizontal flange/weld deflections are represented by

$$\frac{(\Delta_i + \Delta_{ii})}{2} \quad \text{and} \quad \frac{(\Delta_{iii} + \Delta_{iv})}{2}$$

The connection rotation was determined as follows,

$$\text{Rotation, } \theta \text{ radians} = \frac{(\Delta_i + \Delta_{ii} + \Delta_{iii} + \Delta_{iv})}{2s_3}$$

and the corrections to horizontal flange/weld dial gauge readings are represented by $-\theta_{s_1}$ and $-\theta_{s_2}$. The corrections to the dial gauge readings at, or, very slightly less than the ultimate load have been made and are given in Tables 8 to 33 as 'Corrected Deflections'. The direction of

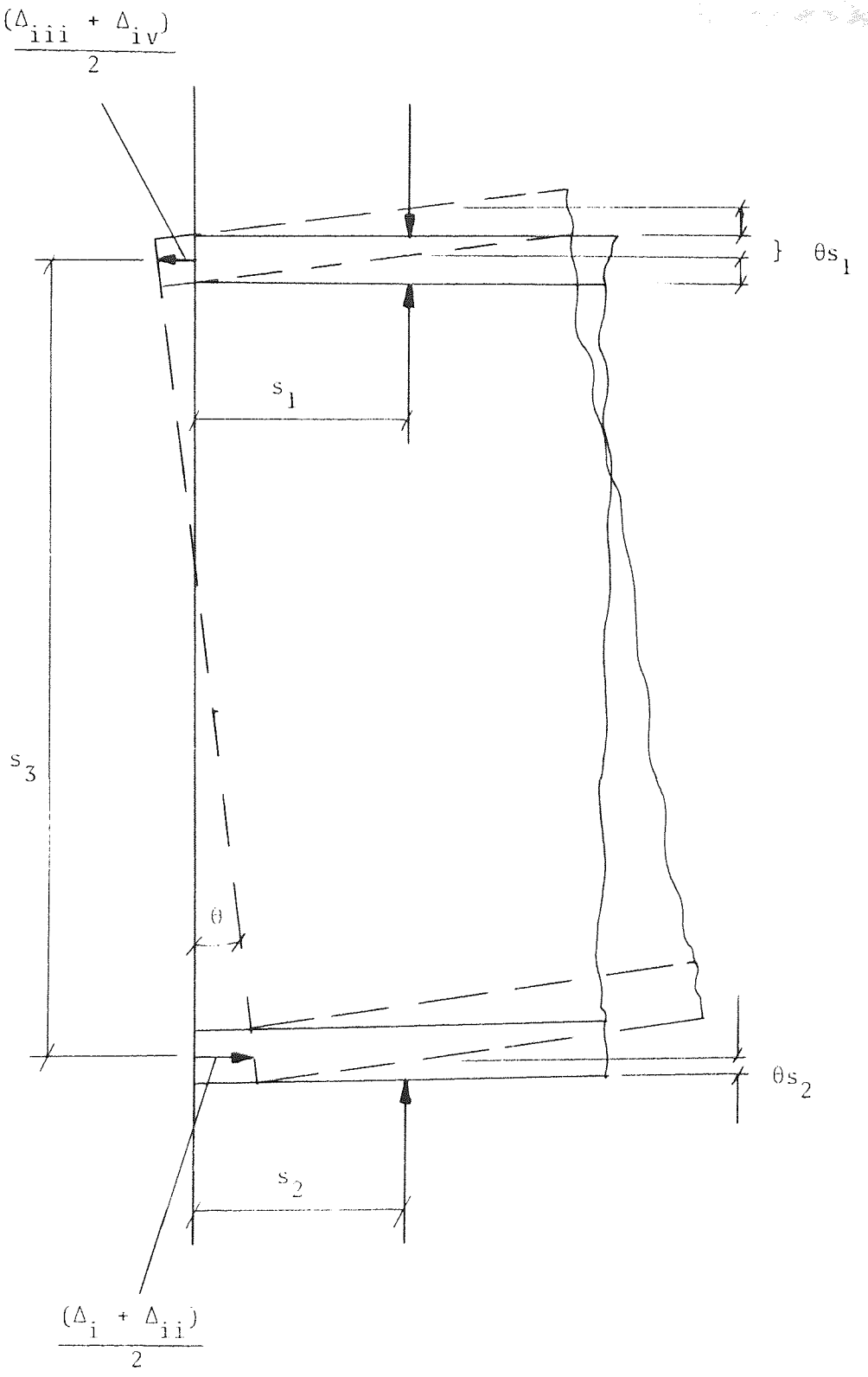

Fig.83 Dial Gauge Correction

the deflections relative to the unloaded position of the flanges are also to be found in these tables.

In the opinion of the author the dial gauges were placed close enough to the welds for the readings to be regarded as representing equally the deflections of the weld and flange.

Joint rotations will be found later in the chapter.

The corrected flange/weld deflections have been plotted, with reference to flange width, in figs. 84, 85 and 86. The implications of these flange/weld deflection patterns will be discussed later in the chapter.

6.5 Modes of Failure

The first thing to establish is whether or not one of the two welds fails before the other. Archer et al[22] stated that in all their tests the tension weld had failed first. No evidence of this claim was offered. Consider the two extremes of loading. When V/M equals zero it is reasonable to suppose that rotation of the connection takes place about or very near to, the compression weld. Under this condition, only the tension weld would offer resistance to the applied bending moment, and would of course fail first, rapidly followed by connection failure if the bending moment was maintained. The connections tested under low values of the ratio V/M failed as expected, the compression welds remaining intact after removal of the load.

For the other extreme when V/M equals infinity, one could only expect the two welds to fail simultaneously if (a), compression and tension welds behave in exactly the same manner, and (b) the connection beam-section is rigid.

Fig. 84 Flange/Weld Vertical Deflection, Series 305 x 127

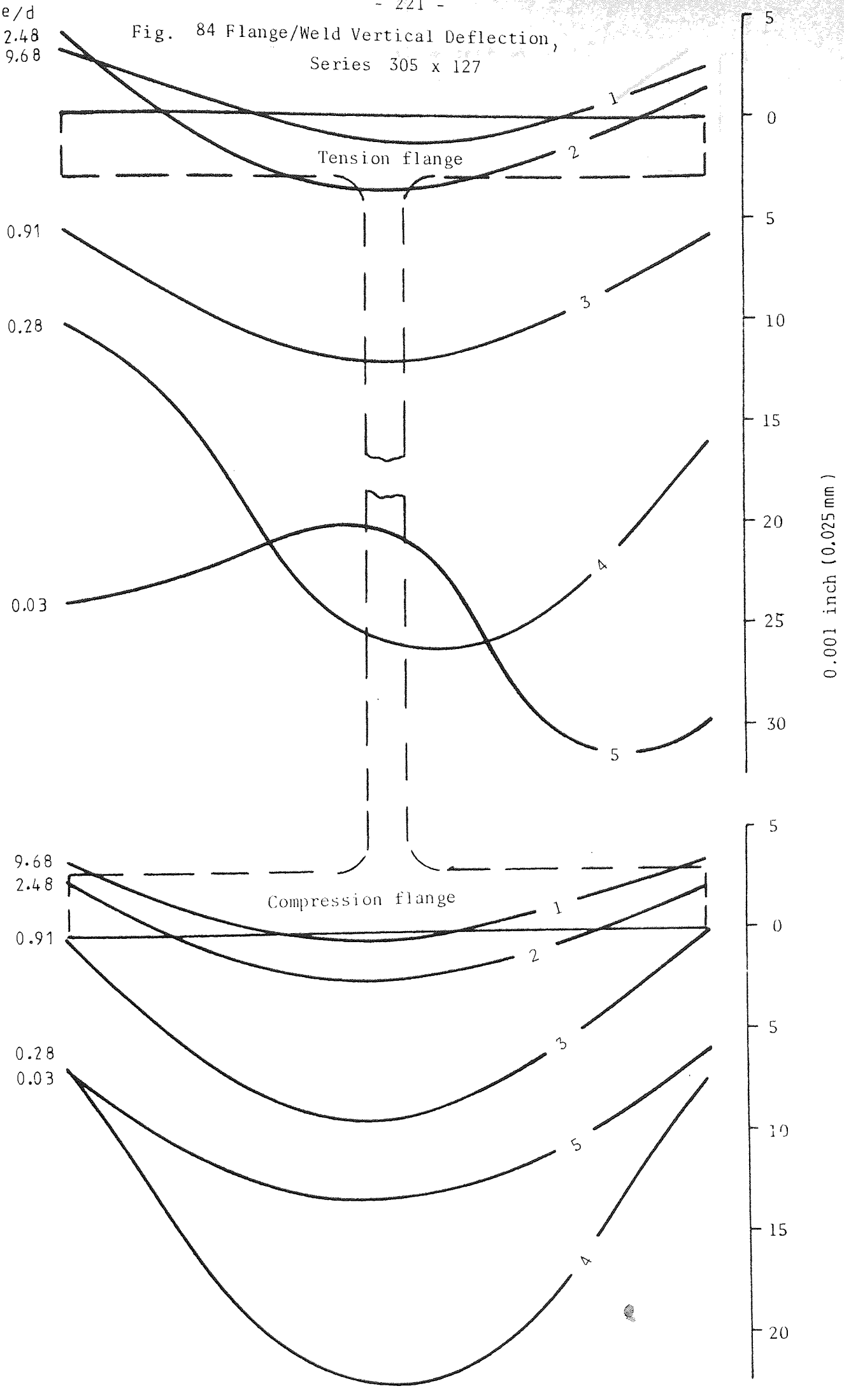

Fig. 85 Flange/Weld Vertical Deflection,

Series 356 x 171

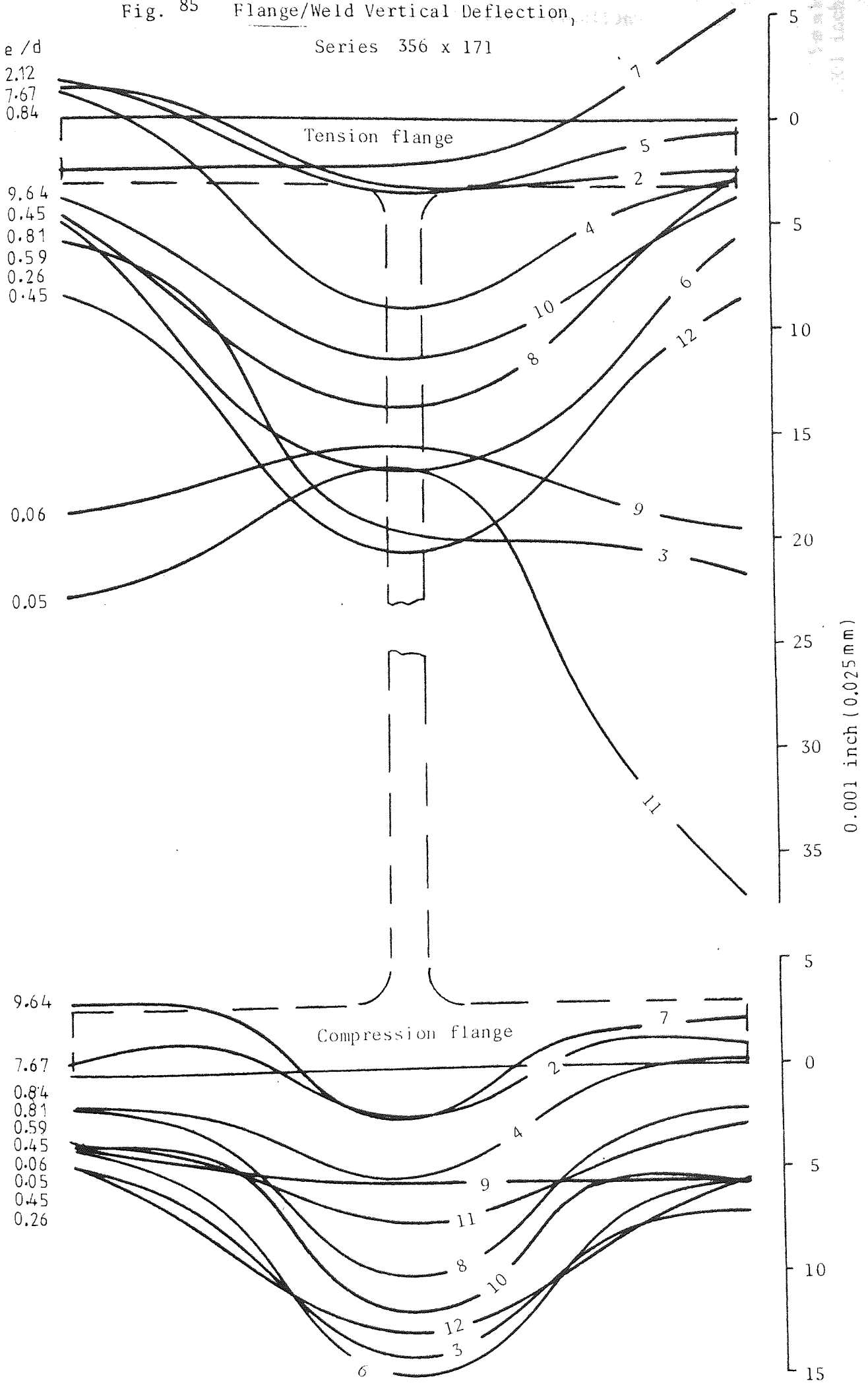

Fig. 86 Flange/Weld Vertical Deflection,
Series 305 x 305

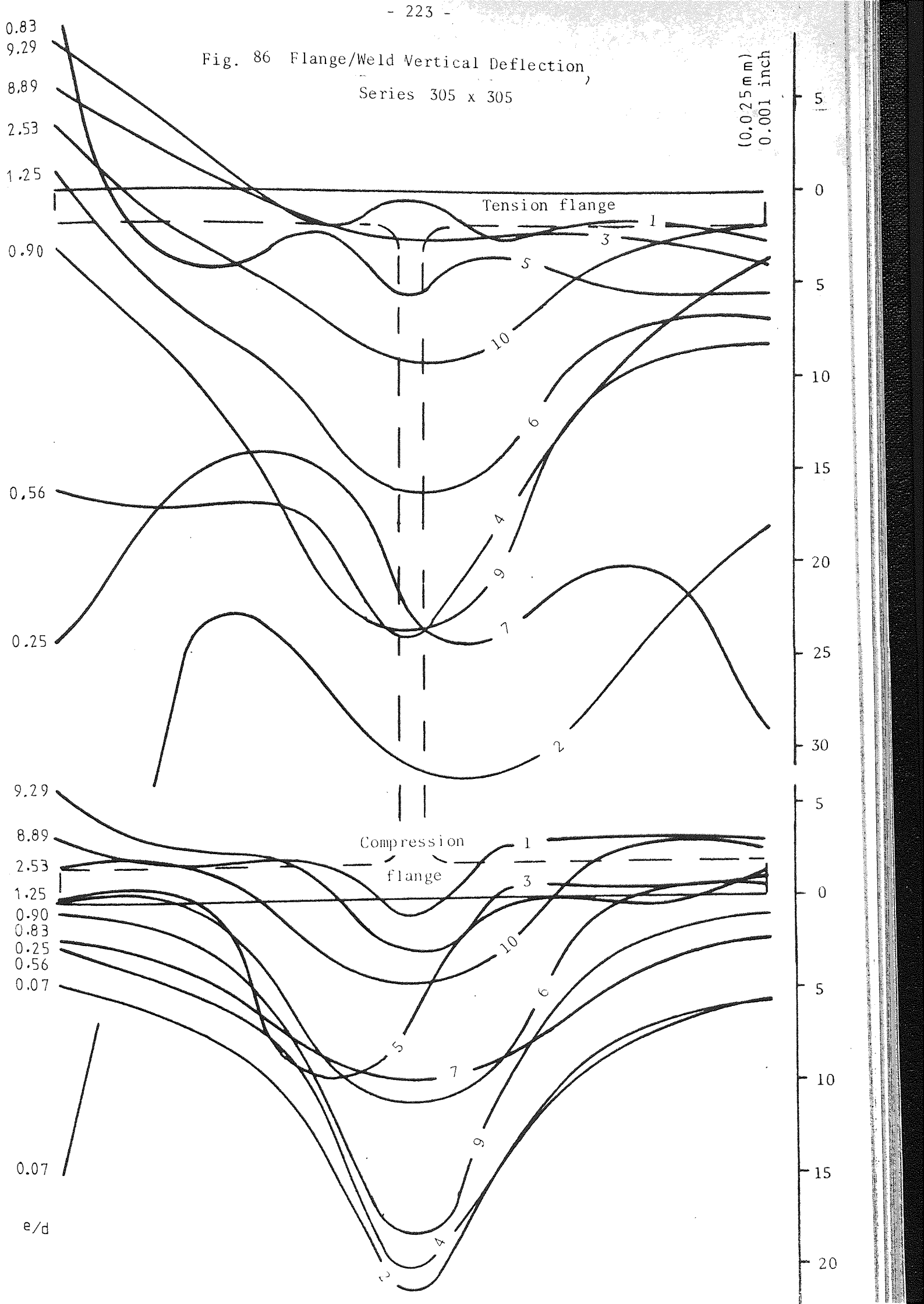

It has already been shown by the author, in Chapter Five, that the weld under a single compressive force is in fact weaker than when under a single tensile force. The connection beam-sections are certainly not rigid, and elastic compression of the web will ensure that the shear load is not equally shared between tension and compression welds. Logically the tension weld is bound to resist the greater proportion of the shear load, and therefore likely to fail first.

The failures of the test connections under high values of V/M tended to be very sudden, in both welds, and it was not possible to observe which weld failed first, or indeed, if they both failed together. However, there is evidence from four sources which proves beyond doubt that the tension weld is the critical one, and always fails first. The four sources of evidence are

1. the fracture plane angles of the failed compression welds,
2. the flange/weld deflection patterns,
3. the compression flange deformation which results from the failure,

and 4. comparison of tension and compression flanges after failure.

1. Fracture plane angles: in all cases where the compression weld failed, the fracture surface was planar at an angle of 90° to the flange face regardless of the ratio of V/M. This condition indicates that all the compression welds failed under the same loading condition. Corresponding tension welds did fracture at angles related to the applied loading ratio of V/M (these fracture angles will be presented later in the chapter).

2. Flange/weld deflection patterns (figs. 84, 85 and 86): in all but one or two cases the maximum deflection of the tension weld is relatively much greater than the maximum deflection of the compression flange. If it is assumed that the load/deflection characteristics of both welds are similar, then it must be concluded that the tension weld reaches a critical state before the compression weld (load/deflection characteristics will be examined later).

3. Compression flange deformation: compression flange profiles were traced after connection failure and are shown in figs. 87, 88 and 89. For series 305 x 127 and 356 x 171 the profiles after failure are compared with profiles before failure (see figs.76 to 80 for profiles before testing). Such a comparison was considered not necessary for series 305 x 305 because of such large deformations. It will be noted from figs. 84, 85 and 86 that flange deflections just prior to failure are negligible when compared with the difference of flange profile before and after testing as shown in figs. 87, 88 and 89. The only conclusion that can be drawn from these comparisons is that the tension weld failed first and transferred its share of the shear load to the compression weld which then deformed and failed under the weight of the total shear load.

4. Comparison of tension and compression flanges: the argument here is that it is not possible for the compression weld to deform more than the tension weld if it fails before, or simultaneously with the tension weld. Sufficient evidence is shown in Plate 12. 'Tension Weld No.9' and 'Compression Weld No.9'; Plate 13 'Compression Flange No.7', and 'Compression Flange No.2', and Plate 8, 'Tension Weld No.4' and 'Compression Weld No. 4'.

In view of the above evidence there can be no doubt that all connections tested (except 305305/4) failed in the tension weld first. This is a very important fact since a method of ultimate load prediction can now be based on the tension weld alone.

Test connection 305305/4 was 'frozen' at the failure load by a sudden release of the load as soon as it was realized that failure was beginning. The connection was examined thoroughly and the following points were noted:

Fig. 87 Deformation of Compression Flange/Weld Resulting from Connection Failure , Series 305 x 127

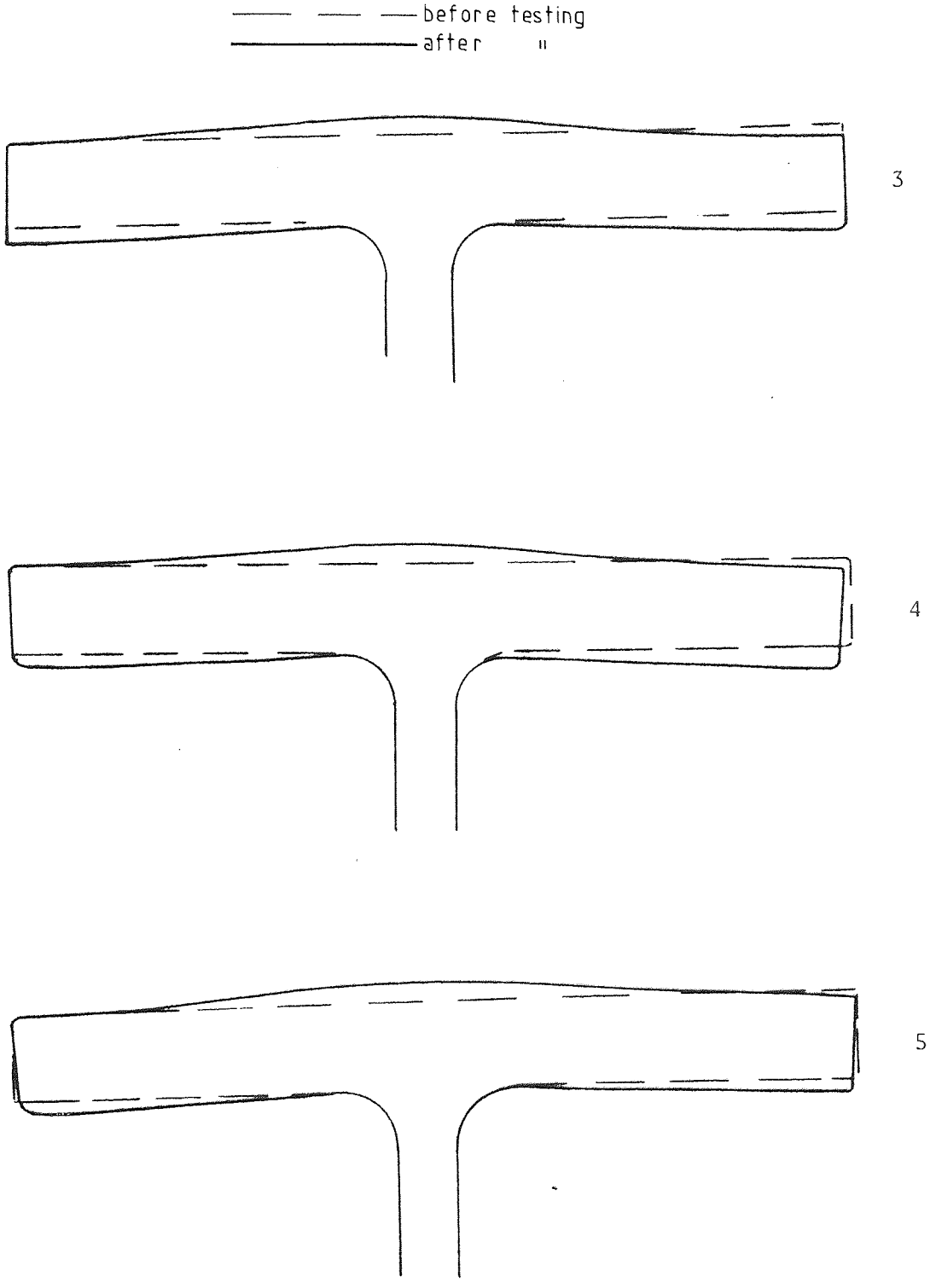

Fig. 88 Deformation of Compression Flange/Weld Resulting from Connection Failure , Series 356 x 171

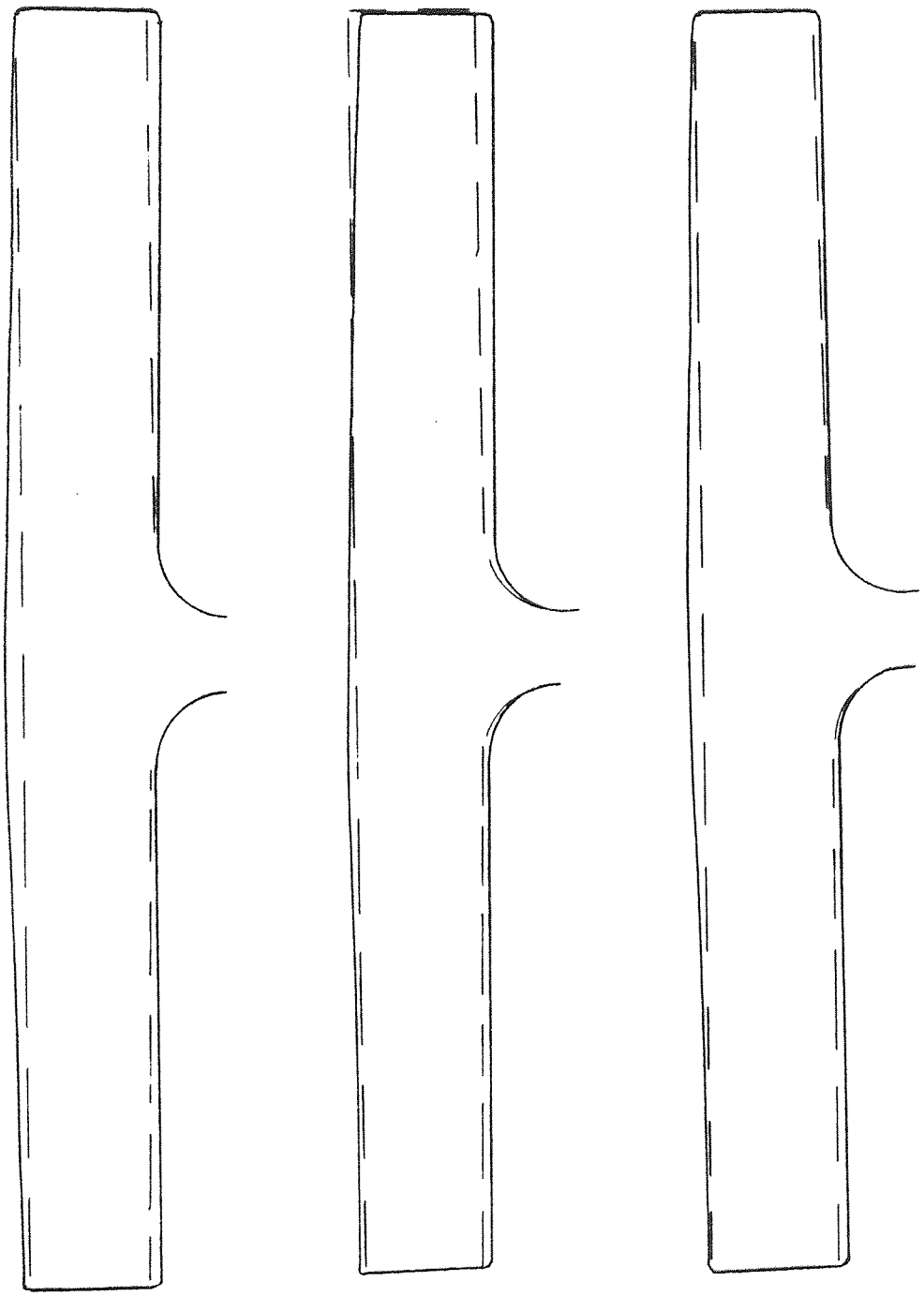

12 3 11

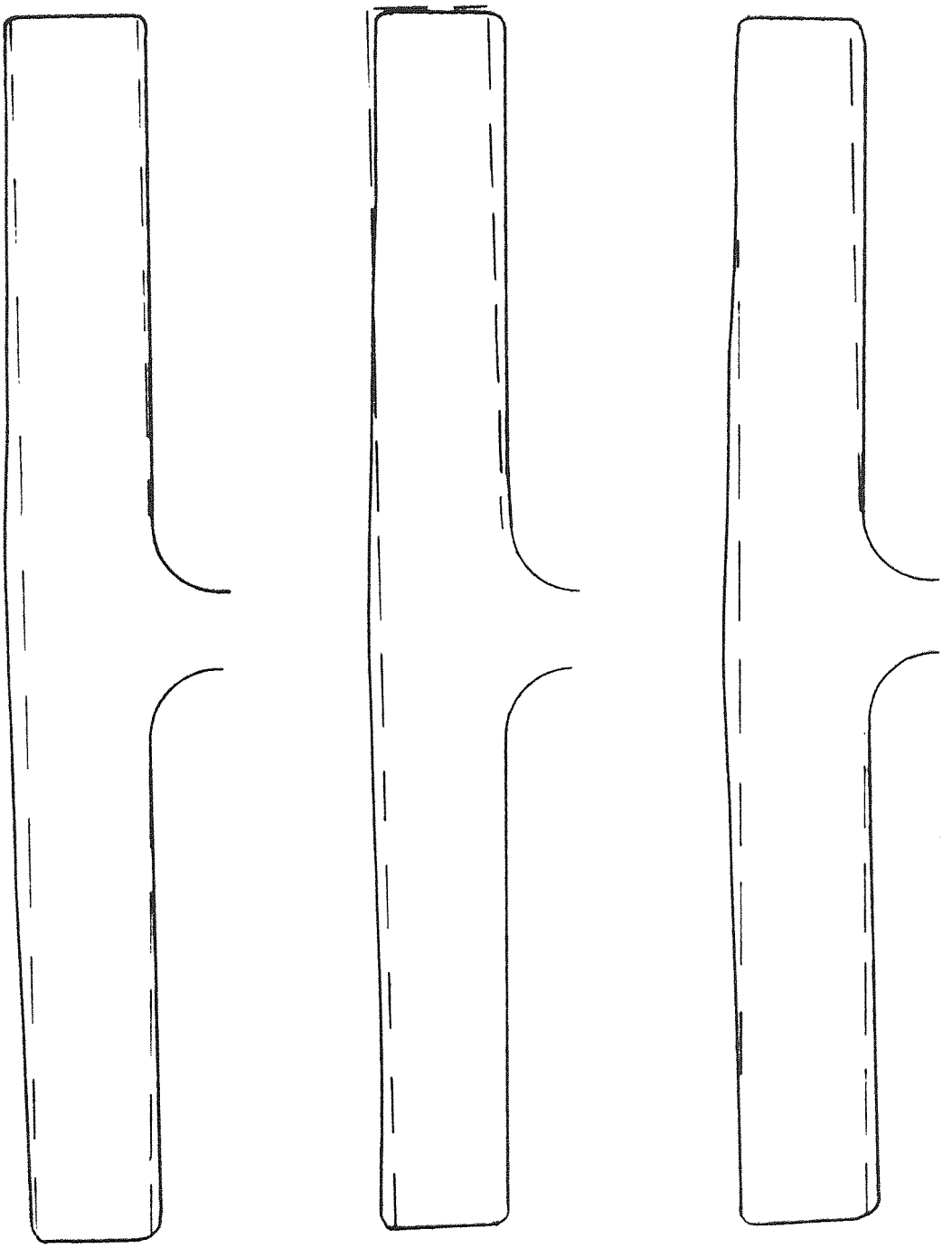

8 6 10

Fig. 89 Deformation of Compression Flange/Weld Resulting from Connection Failure, Series 305 x 305

(scale: 2/3 full size)

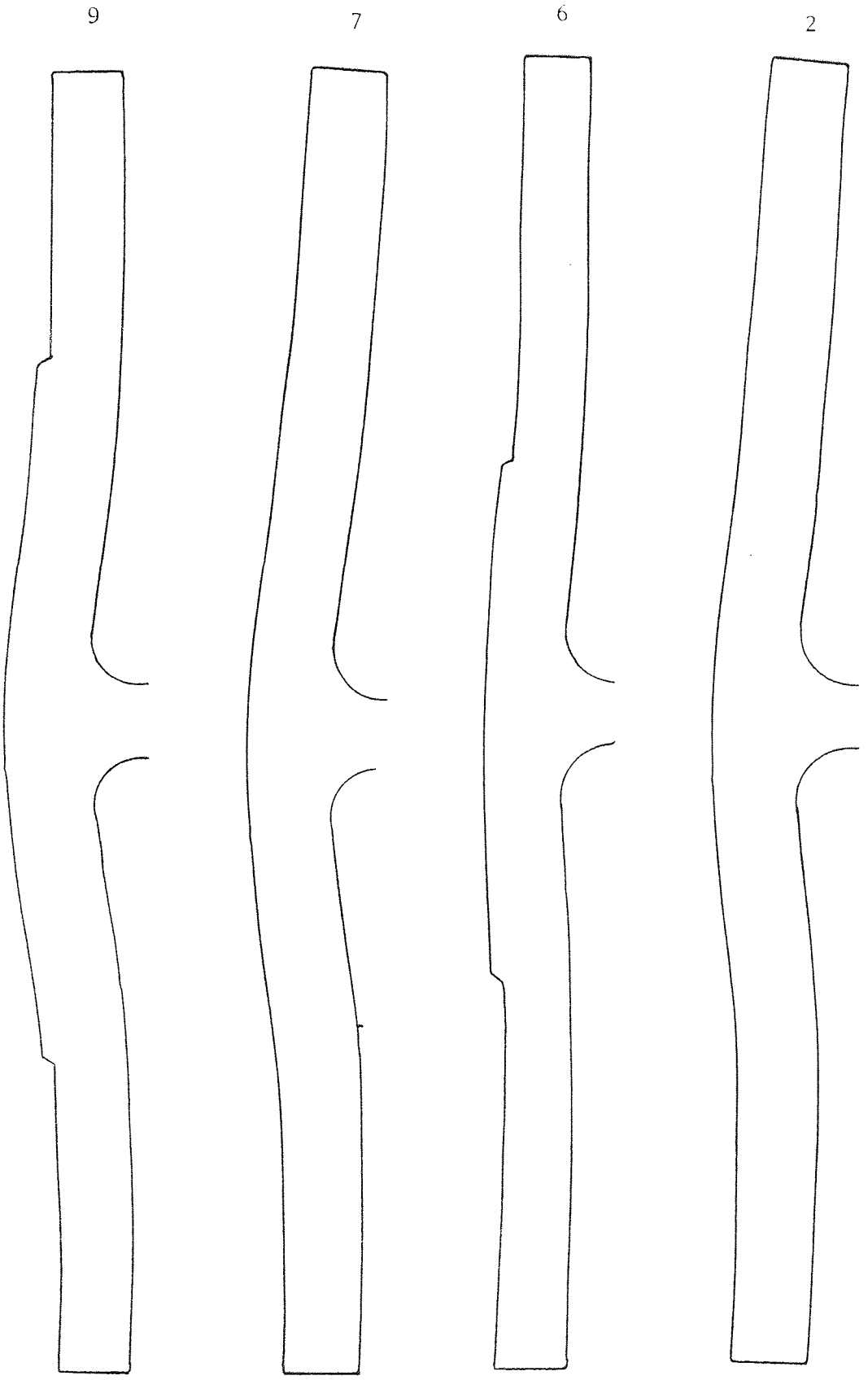

(1) there was a crack at the right-hand end of the compression weld approximately 30 mm in length,

(2) a yield line of approximately 80 mm in length extended from the above crack,

(3) the tension weld beneath the web had yielded over a length of approximately 100 mm,

(4) there was a small crack at the right-hand end of the tension weld which had not propagated.

This 'frozen' condition is illustrated in plate 13, 'Tension Weld No.4' and Compression Weld No.4. The dial gauges had indicated massive creep in the tension weld around the web and there is little doubt the tension weld would have failed first if the load had been sustained.

A study of the tension weld fracture plane angles, see Table 35, will reveal a sudden large increase at a value of e/d of approx.. unity (or a value of V/M of approx. 4) e.g. for series 305 x 127 - a change from 15° to 74°. Such a change of angle signifies a change from the loading situation F_x dominant, to the loading situation F_y dominant, see fig. 90.

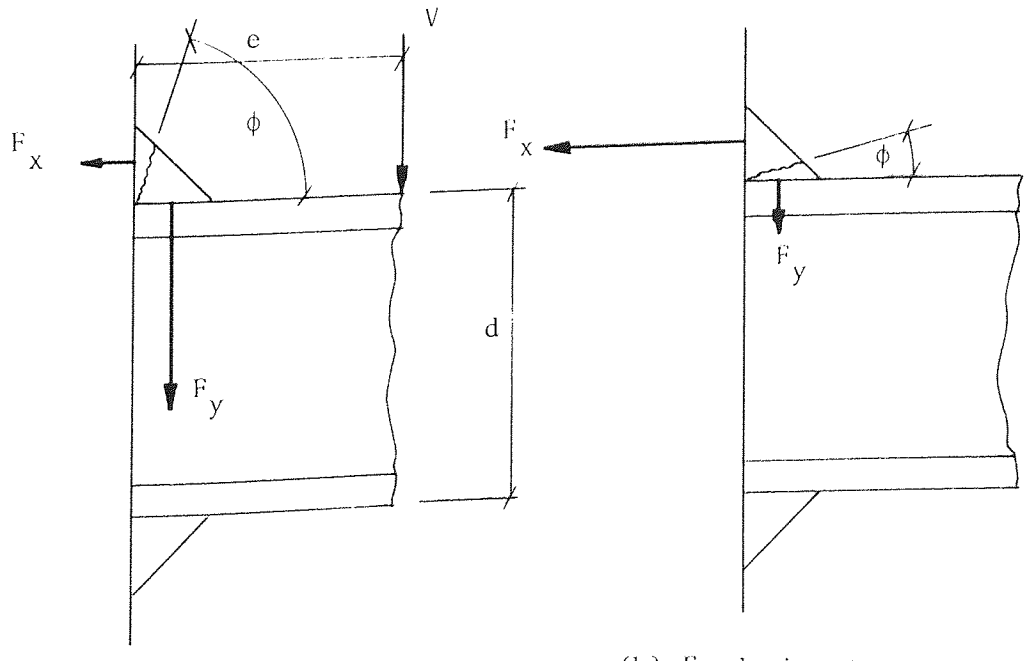

(a) F_y dominant (b) F_x dominant

Fig.90 Sudden Change of Fracture Plane Angle, ϕ

In the F_x dominant loading situation the shear load, V, will be relatively small compared to the bending moment, M, and hence, only small vertical weld deflections would be anticipated, and conversely, large horizontal deflections. Horizontal deflections were measured with dial gauges and are shown in figs. 91, 92 and 93. If a comparison is made with the vertical deflections of the tension weld, see figs. 84, 85 and 86, the above expectation regarding the relative size of the horizontal and vertical deflections will be corroborated. For an example of this comparison see 305127/1 and 2. Since the F_x dominant loading situation produces large deflections in the F_x direction, failure of the tension weld is bound to be in the same direction. This being the case, the flange width can be regarded as fully effective with respect to the length of weld. This is confirmed by the experimental results and well illustrated by uniform fractures of the tension weld, see Plate 7 'Tension Weld No.1' and 'Tension Weld No.2'. Apart from the extreme ends of the welds the fractures are reasonably planar and smooth.

Failure under the F_x dominant loading situation will be referred to as 'bending mode failure' since the ratio V/M will be small when F_x is dominant.

When the F_y dominant loading situation prevails the converse of the above argument will be true, i.e. shear load, V, will be relatively high, producing large vertical deflections with accompanying small horizontal deflections. Comparison of deflection patterns will show this to be true. Failure of the weld will obviously take place in the vertical direction, and will be referred to as 'shear mode failure' since the ratio V/M will be large when F_y is dominant.

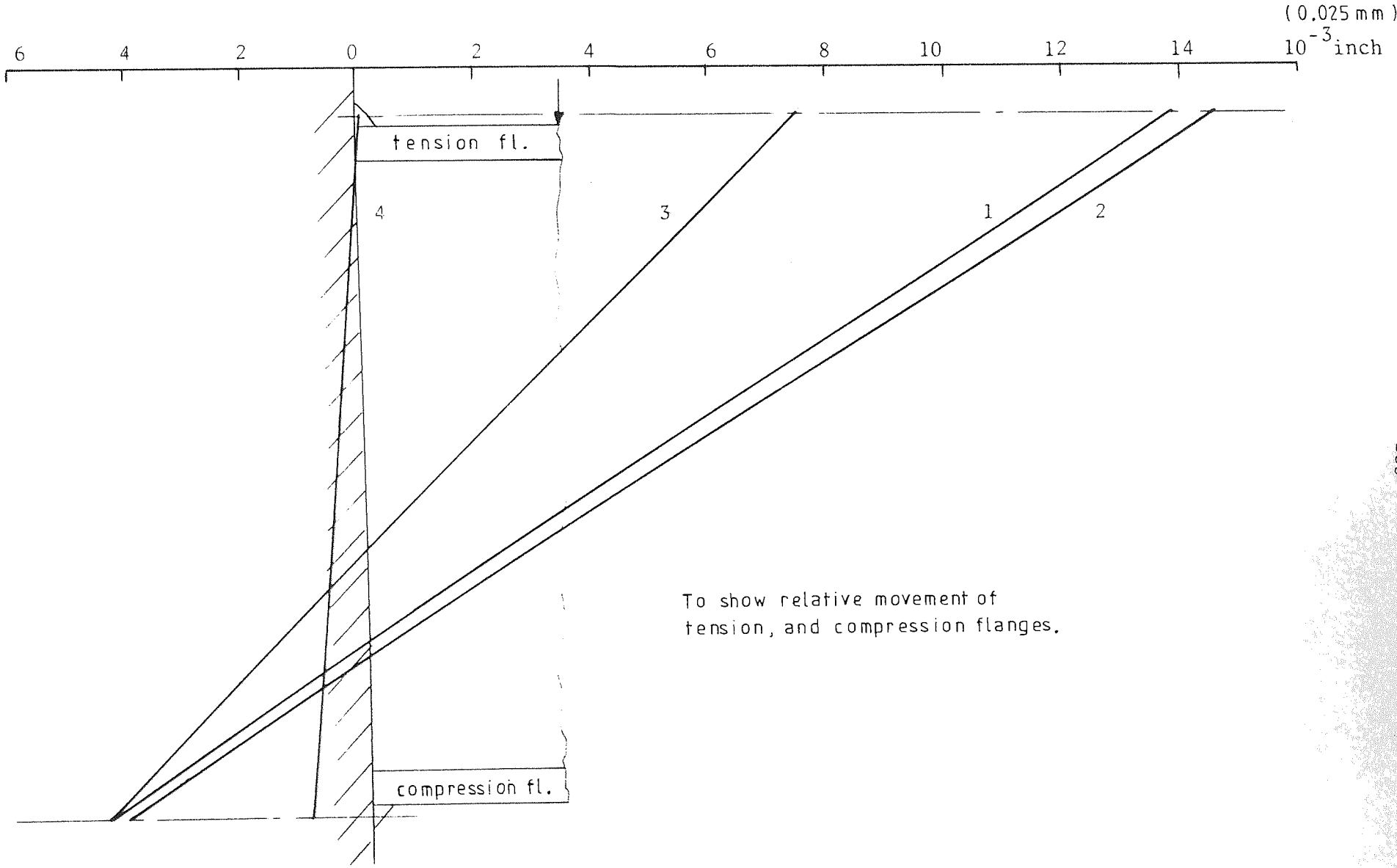

Fig.91 Horizontal Deflection, Series 305 x 127.

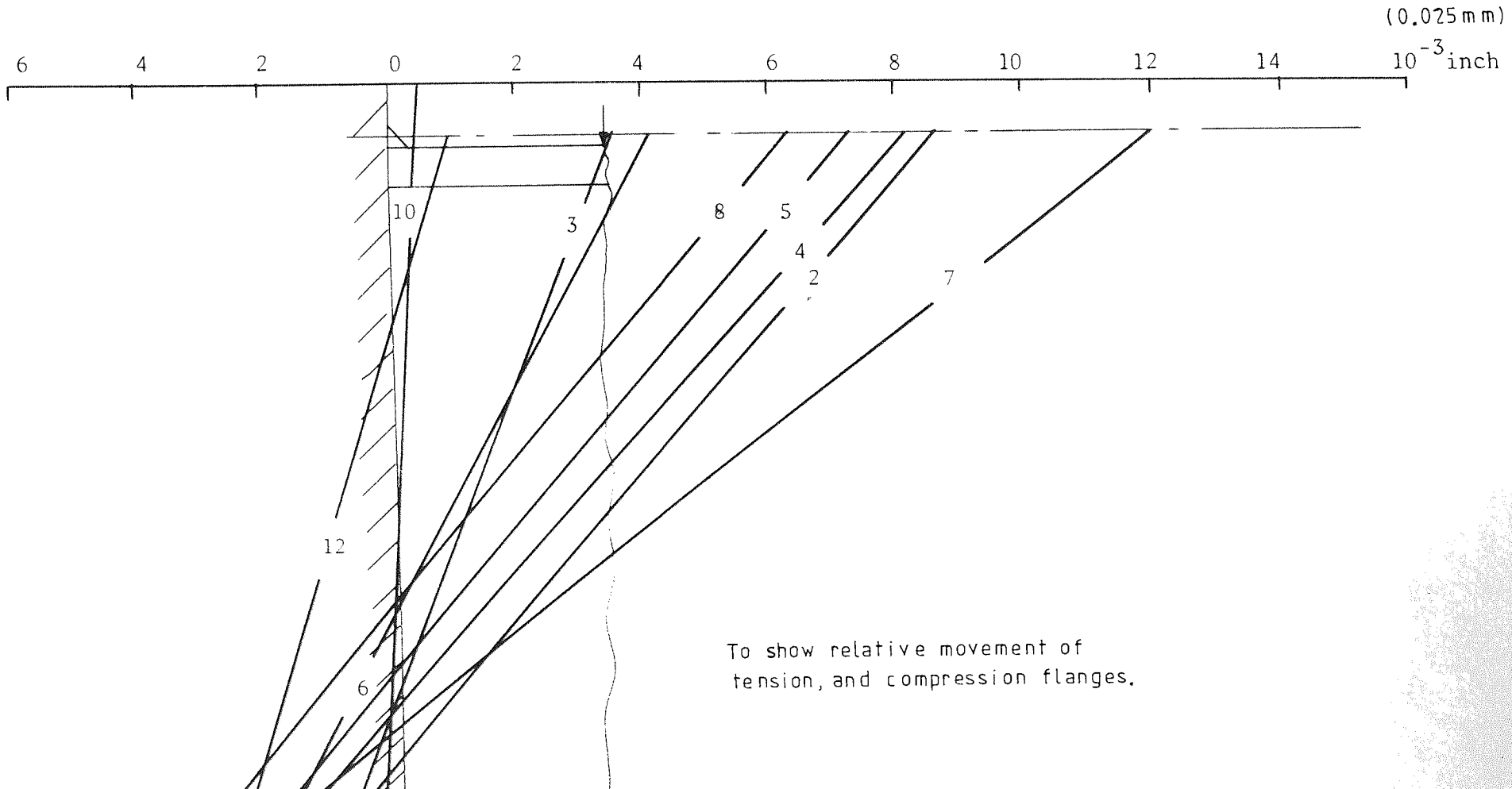

Fig. 92 Horizontal Deflection, Series 356 x 171

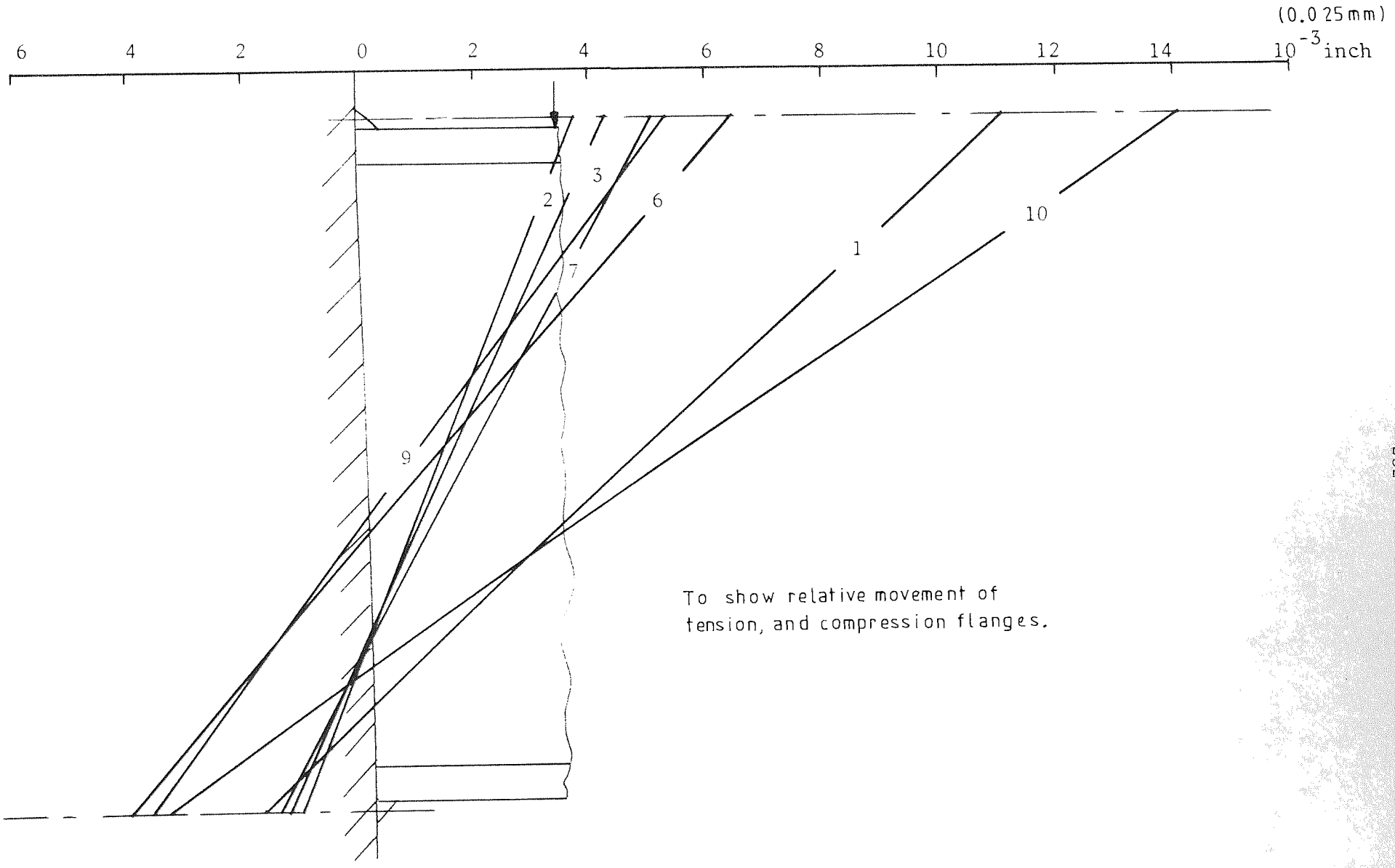

Fig. 93 Horizontal Deflection, Series 305 x 305.

Typical 'shear mode failures' are illustrated in Plate 7, 'Tension Weld No.4' and 'Tension Weld No.5' (for 'narrow' flanges) and Plate 9 'Tension Weld Nos 6, 10 and 12'(for 'wide' flanges).

The most important difference between the 'bending mode' and 'shear mode failures lies in the effective flange width - unless the flange is 'narrow', it will not be fully effective under the 'shear mode failure'. The vertical deflection patterns are probably indicative of the shear load distribution along the flange welds, this being so, it will be seen that the flange width becomes less effective as the ratio of V/M increases. There are a few anomolies in the patterns, these resulting from the right-hand testing-beam support being positioned directly under the tension flange of the test connection (this support is referred to as a '50 mm bearing'). The obvious effect of the 50 mm bearing is to induce a more uniform tension flange/weld deflection pattern and hence, a greater resistance to the shear load. Connections tested under this condition will obviously give higher ultimate capacities than would be expected otherwise.

There are obviously loading situations in which neither F_x, nor F_y can be considered dominant. One would expect the mode of failure under such a circumstance to be somewhere inbetween the 'bending' and 'shear' modes. It is reasonable to assume that the tension weld would fail in the mode giving the lowest ultimate capacity if joint restraint was low enough (this is with reference to the loading condition with F_x/F_y is approximately unity). Using this argument, it is the author's contention that when F_x/F_y is approximately unity, the tension weld would fail in the 'shear mode' because the flange width is not fully effective in this mode, whereas in the 'bending mode' it is - the weld would fail at the lower ultimate capacity.

This type of failure would account for the sudden change in fracture plane angle which is indicative of a sudden change from the 'bending mode' to the 'shear mode' failure. This unpredictable shear mode failure will be referred to as 'artificial shear mode'. This mode of failure is only possible with flexible flanges. The flanges used by Archer et al[22] were reasonably rigid, being only 50 mm wide, and produced fracture plane angles inbetween the two extremes achieved by the author - these results will be reviewed later in the chapter. Fracture plane angles have been plotted against the ratio e/d and are shown in fig.94. The sudden change of failure mode can be easily seen to take place at a value of e/d of approximately 0.8 at which the fracture plane angle is approximately 15° - at e/d equals 0.5 the average fracture plane angle is 72°. The results of Archer et al[22] show the expected gradual change from the 'bending mode' to the 'shear mode failure'.

The relationship between e/d and ϕ, shown in fig. 94,can be related to the relationship between F_x/F_y and $\tan\phi$ of the failure criteria specimens shown in fig. 72 - this will be done later.

Welds which failed in the 'bending mode' generally produced uni-planar fracture surfaces, the angles of which being fairly consistant. As a result of flange flexibility, welds which failed in the 'shear mode' generally produced bi-planar fracture surfaces. The fracture angles recorded are those of the 'prime' plane along which failure was initiated, i.e. the central part of the weld around the web which yielded first thus precipitating connection failure. The weld deflection patterns, figs. 84, 85 and 86, illustrate this mechanism, and Plate 9 'Tension Weld Nos.6, 10 and 12' clearly shows the 'prime' plane in the central part of the weld. The length of the 'prime' plane is indicative of the effective flange width.

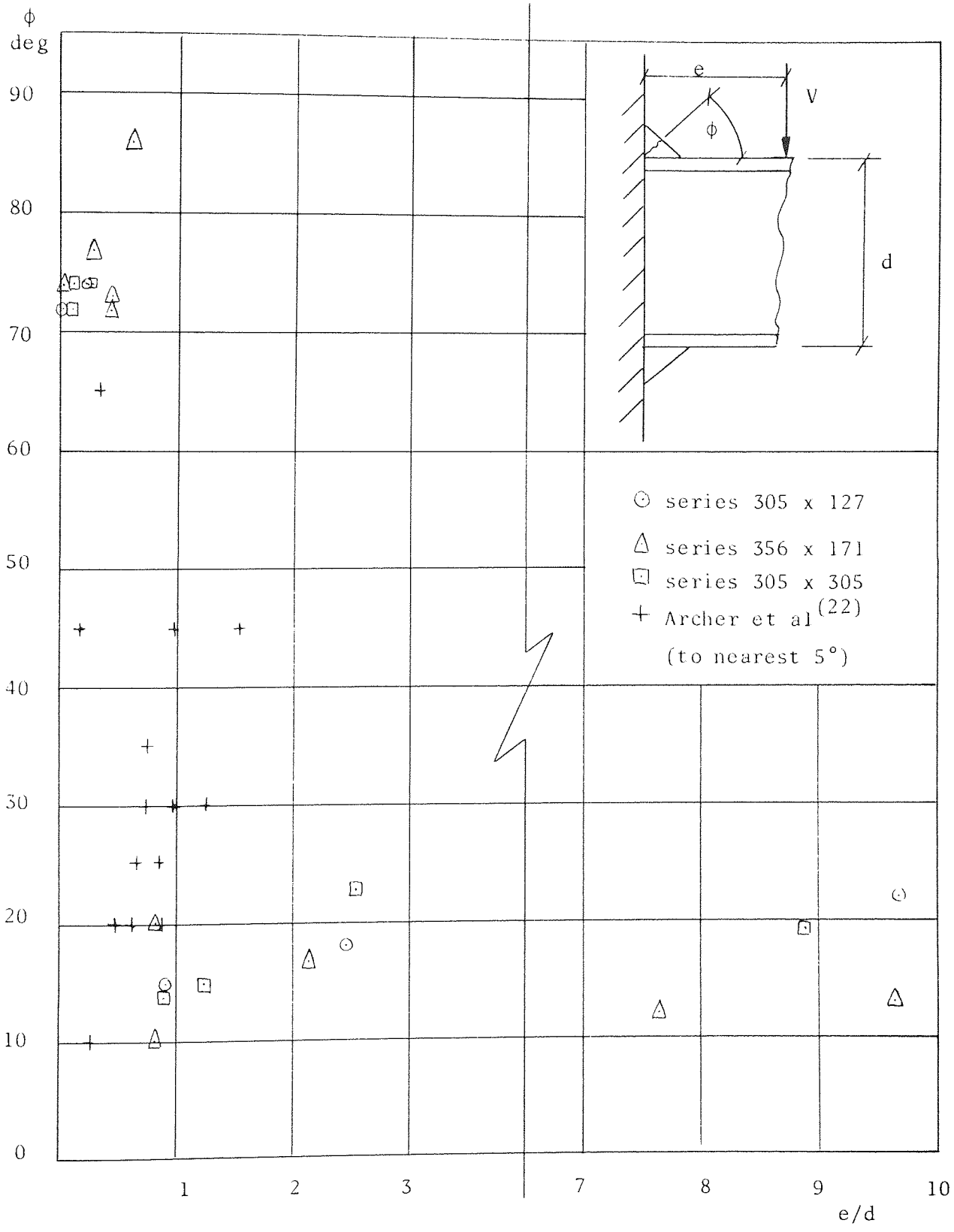

Fig. 94 Relationship Between e/d and ϕ

Specimen No.	e/d	Fracture angle ϕ		Connection rotation θ deg	Mode of failure
		Tension weld	Compression weld		
305127/1	9.68	22	n.f.	0.08745	bending
/2	2.48	18	"	0.08933	"
/3	0.91	15	90	0.05734	"
/4	0.28	74	90	0.00565	shear
/5	0.03	72	90	neg.	"
356171/7	9.64	13	n.f.	0.04885	bending
/2	7.67	12	n.f.	0.04135	"
/5	2.12	17	"	0.04052	"
/4	0.84	10	90	0.04217	"
/8	0.81	20	90	0.04119	"
/6	0.59	86	90	0.02739	shear
/10	0.45	72	90	0.00345	"
/12	0.45	73	90	0.01568	"
/3	0.26	77	90	0.01919	"
/9	0.06	c.m.a.	90	neg.	"
/11	0.05	74	90	"	"
/1	Exploratory test, invalid results				
305305/3	9.29	p.f.	n.f.	0.0271	bending
/1	8.89	19	n.f.	0.06087	"
/10	2.53	23	n.f.	0.08355	"
/6	1.25	15	90	0.05081	"
/9	0.9	14	90	0.043	"
/5	0.83	c.m.a.	n.f.	0.01485	"
/4	0.56	n.a.	n.a.	0.01856	shear Δ
/7	0.25	74	90	0.01706	shear
/8	0.1	74	90	neg.	"
/2	0.07	72	90	0.02375	"

n.f. - not failed
n.g. - negligible
n.a. - not applicable
c.m.a. cannot be meaningfully assessed
p.f. - partial failure
Δ - assessed from dial gauge readings

Table 35. Experimental Results, Beam-Column Connections

6.6 Web Flexibility

Prior to testing it was thought possible that web buckling would take place thus affecting the shear load sharing between tension and compression welds. For several of the tests under high values of V/M dial gauges were positioned to record movements of the web - virtually no movement was detected, i.e. there was no web buckling. This being so, the difference in deflectionsof the tension and compression welds immediately above the web must be due to elastic compressive strain of the web. Such elastic strain will directly affect the shear load sharing between the two welds.

6.7 Shear Load Sharing

Before the failure criterion, established in Chapter 5, can be applied to the tension weld in order to develop a method of ultimate load prediction for the beam-column connection, the proportion of the total shear load, V, that it carries must be determined. There is no doubt that it might be possible to arrive at a shear load sharing relationship from the theoretical consideration of elastic compression of the web, and elastic/plastic deformation of the flange/weld combination. Such an approach is not likely to lead to a simple solution applicable for use in the design office, and inevitably empirical load/deformation characteristics for both the welds would have to be incorporated. The author considers a more fruitful approach would be to combine the flange/weld deflection patterns with weld load/deformation characteristics.

Although load/deformation characteristics have been produced by Archer[19], Ligtenberg[20], Clark[26], Butler et al[30], Dawe[42], Biggs[55], and Tzogius[56], it was felt that these might not be applicable to large joints (they had all been established from relatively small joints) tested here.

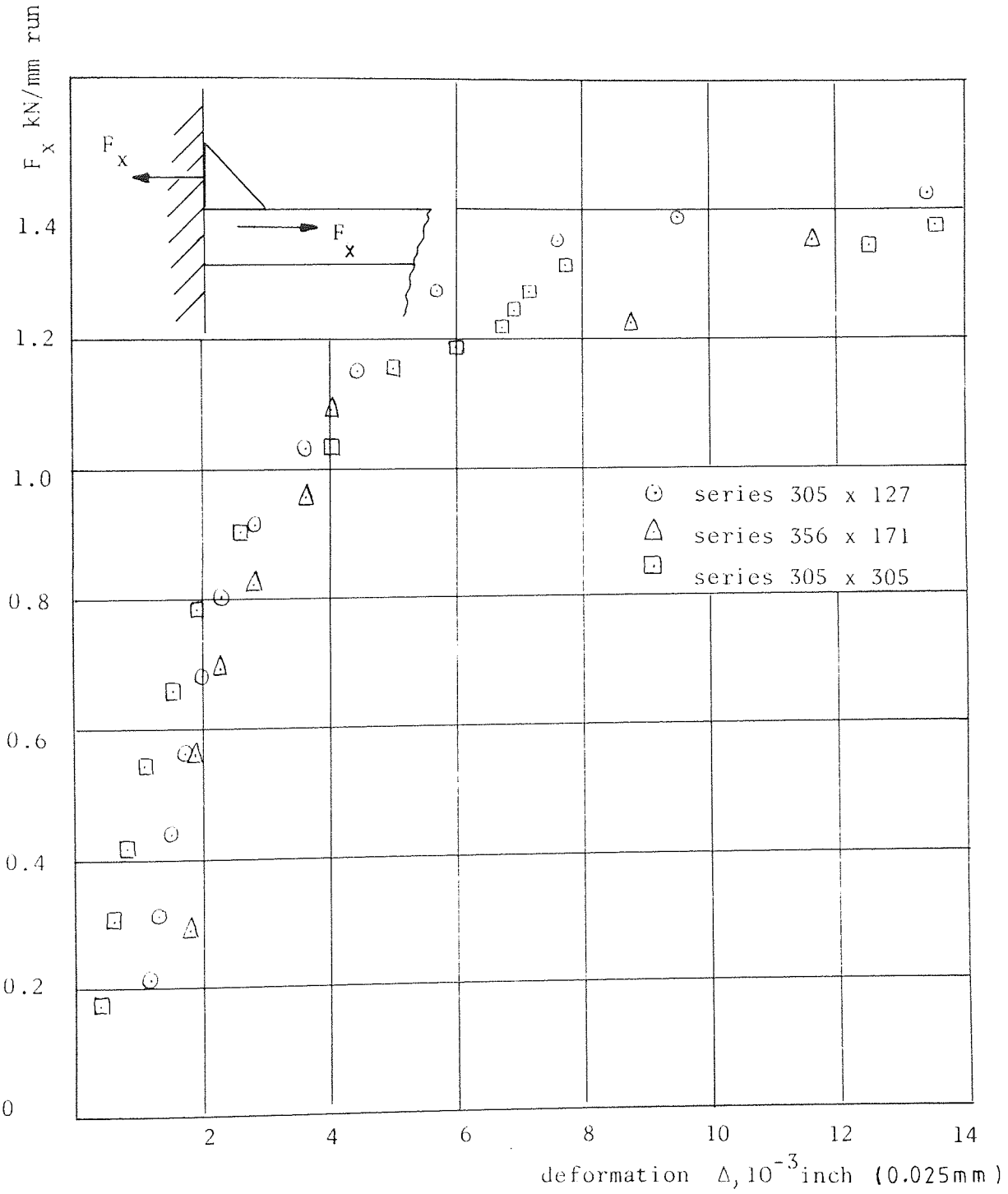

Fig.95 Load-Deformation Characteristics - Beam-Column Connection

A load/deformation characteristic can be obtained for the tension weld of the beam-column connections tested under very low ratios of V/M. For such low ratios of V/M the effect of the small shear load can be ignored and if the connection is considered to rotate about the compression weld, then

$$V.e = F_x.d$$

Three test connections, tested under low ratios of V/M, were chosen 305127/1, 356171/7 and 305305/10, and the calculated deformations are given in Table 36 and plotted in fig. 95. The ultimate values of the F_x force for the three connections are:

305127/1: 1.463 kN/mm run

356171/7: 1.485 kN/mm run

305305/10: 1.398 kN/mm run

The best-fit circle failure criterion, see figs. 67 and 70, predicts a value of 1.399 kN/mm run, and the average experimental value from the biaxially-loaded specimens is 1.495 kN/mm run. This comparison shows the applicability of the circle criterion to the beam-column connections, at least in the F_x dominant situation. Of course, for short or rigid welds, the F_x and F_y dominant situations are the same with regard the circle criterion.

It can be seen from fig.95 that the ultimate load is reached at a deformation of approximately 14 x 10^{-3} inch (or 0.36 mm). The characteristic produced by Clark[26], see fig. 37 (c) and (d), gives values of 0.7 mm and 1.55 mm and that by Butler et al[30], see fig. 40, a value of 28 x 10^{-3} inch, or 0.7 mm.

Table 36. Experimental Results, Load-Deformation Characteristics

Specimen No.	Load P tonne	Shear load V kN	F_x kN/mm run	Deformation Δ 10^{-3} inch (0.025mm)
305127/1	0.3	2.72	0.207	1.17
	0.6	4.26	0.324	1.28
	0.9	5.81	0.443	1.52
	1.2	7.35	0.560	1.75
	1.5	8.9	0.679	2.0
	1.8	10.44	0.796	2.3
	2.1	11.99	0.914	2.82
	2.4	13.53	1.031	3.57
	2.7	15.08	1.15	4.45
	3.0	16.62	1.267	5.72
	3.2	17.65	1.346	7.6
	3.3	18.17	1.385	9.5
	3.4	18.68	1.425	12.35
	3.4	18.68	1.425	13.4
	3.5	19.20	1.463	failure
356171/7	1.0	5.11	0.288	1.75
	2.0	9.83	0.554	1.8
	2.5	12.20	0.688	2.25
	3.0	14.56	0.821	2.8
	3.5	16.92	0.954	3.55
	4.0	19.28	1.087	4
	4.5	21.64	1.220	8.85
	5.0	24.0	1.353	11.65
	5.3	25.42	1.433	12.65
	*5.5	26.36	1.485	17
305305/10	2	20.18	0.169	0.4
	4	35.02	0.29	0.6
	6	49.86	0.413	0.8
	8	64.7	0.537	1.1
	10	79.54	0.66	1.45
	12	94.38	0.783	1.9
	14	109.2	0.906	2.6
	16	124.1	1.03	4.05
	18	138.9	1.152	5.0
	18.5	142.6	1.183	6.0
	19	146.3	1.213	6.7
	19.5	150.0	1.244	6.9
	20	153.7	1.275	7.15
	20.5	157.5	1.307	7.7
	21	161.2	1.337	12.45
	21.5	164.9	1.368	13.5
	22	168.6	1.398	failure

* Failure Load

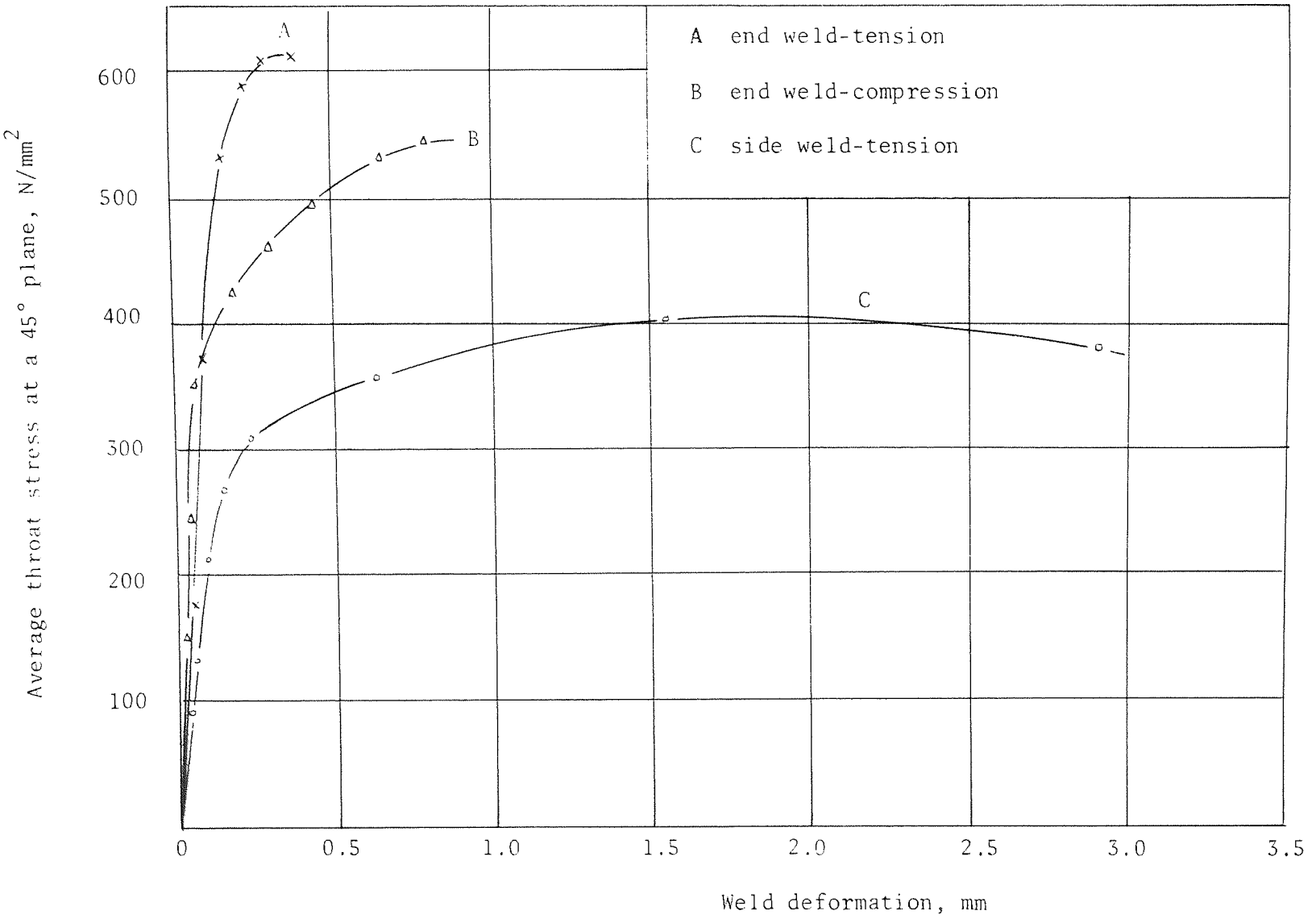

Fig.96 Load-deformation Characteristics by Tzogius

The characteristic presented by Ligtenberg[20] is of little use since it is only an estimation, and those produced by Archer et al[19] and Biggs[55] do not extend to the ultimate state. Specimens tested by Tzogius[56] were of similar design to the biaxially-loaded specimens and the same welding technique was used (his welds were also machined to an exact profile). Tzogius is the only investigator to have established a load/deformation characteristic for the end weld under compression, see fig. 96. The corresponding deformation for the weld under tension is approximately 0.35 mm. The characteristic produced by Tzogius[56] is the only one which bears comparison with that produced by the author.

Two important facts are implied by Tzogius' characteristics, firstly, the ultimate strength of the weld under compression is only 0.895 of that under tension (the author's average value was 0.916), and secondly, when the weld under tension has reached its ultimate capacity the weld under compression has only reached 0.89% of its ultimate capacity, or, 79.2% of the ultimate capacity of the weld under tension. This second fact is of prime importance in the beam-column connection where the applied shear load is shared between the tension, and compression welds. Unfortunately it is not possible to obtain a compression weld load/deformation characteristic from the results of the beam-column connections, but since the author's tension weld characteristic is in general agreement with that of Tzogius it was decided it would be possible to adopt the one proposed by Tzogius.

The amount of shear load carried by the two welds of the test connections could now be determined by relating the flange/weld deflection patterns, figs. 84, 85 and 86, to the load/deformation characteristics, figs.95 and 96. Such an exercise would prove to be rather complex unless the load/deformation characteristics could be expressed simply. Even if

this were possible, the resulting prediction of shear load sharing is unlikely to approximate the reality of the situation for the following reasons;

(1) the tension weld load/deformation characteristics presented are for the F_x dominant loading situation in which the test connection is constrained to fail in the F_x direction by virtue of its rotation about the compression weld. In the F_y dominant situation, movement in the F_x direction is virtually unrestricted and a different characteristic may apply,

(2) in between the two dominant situations the welds would be subjected to loading in two directions, the resultant deformation being at a variable angle to the weld leg - load/deformation characteristics for such a situation are unknown,

(3) some peak vertical deflections of the tension flange/weld well exceed the limit of the characteristic shown in fig. 95. There are two possible explanations for this, firstly the characteristic may not be complete, and secondly, the part of the weld having reached these large deflections may have already failed and transferred its load either to the remaining parts of the weld which still have deformation capacity or, to the compression weld,

(4) the flange/weld deflections were measured at the maximum load or slightly before, and hence are not representative of the ultimate deflection. This distinction is of great importance because the shear load carried by the compression weld is directly affected by the deflection which takes place after the tension weld has reached its ultimate load.

6.8 Effective Flange Width

The flange/weld vertical deflection patterns are indicative of the effective flange width which would appear to decrease as the ratio of V/M

increases. The exceptionsto this general trend are the specimens tested with a 50 mm bearing directly under the tension flange. The presence of the bearing obviously affected the deflection of the tension flange by making it more uniform, and hence a more uniform shear load distribution was obtained, thus making the flange width more effective, see fig.84, 4 and 5; fig.85, 3 and 11, and fig. 86, 2 and 7. The deflection of the compression flange was not affected.

It would be expected that the wider the flange the less effective it would be. This is demonstrated by a comparison of actual and expected ultimate shear loads (at $V/M = \infty$):

flange width, mm	expected shear load, kN	actual shear load, kN	ratio of actual and expected
127	368.3	300	0.814
171	495.9	410	0.827
305	884.5	490	0.554

The 127 and 171 mm flanges appear to be as equally effective at approximately 80%, but the 305 mm flange appears much less effective at 55%. It has to be remembered that these figures incorporate the shear load sharing, and the effects of the 50 mm bearing under the tension flange.

The expected ultimate shear loads are based upon the average values of F_x, @ $F_z/F_x = 0$, i.e. 1.495 kN/mm run for tension weld and 1.405 kN/mm run for compression weld of the criterion specimens, see fig. 67.

Two of the beam-column connections were tested with stiffening plates welded inbetween the flanges, see Plates 11 and 12. The stiffening plates had two affects on the behaviour of the connections:

(1) they virtually eliminated elastic compression of the web thus forcing a sharing of the shear load between the two welds, and

(2) made the flanges rigid thus ensuring a uniform shear load distribution along the two welds.

Under these conditions the expected ultimate shear loads would be achieved if it were not for difference in the load/deformation characteristics, see fig. 96, which implies that the compression weld would reach only approximately 90% of its ultimate capacity when the tension weld was at the point of failure. The ultimate shear capacities of these two connections were as follows:

356171/9, 478.7 kN @ V/M = 46.63

305305/8, 772.3 kN @ V/M = 33.85

Although the testing ratios of V/M were not infinity, they were high enough for comparison to be made with the expected ultimate shear loads already mentioned. It will be seen from the comparison that the actual capacities are less, this being probably due to differing load/deformation characteristics of the tension and compression welds.

The effective flange width in the 'bending mode failure' is evidently fully effective as the comparison between actual and expected ultimate bending moments shows (at V/M = 0):

section size	expected ultimate bending moment kNm	actual ultimate bending moment kNm
305 x 127	57.91	57.5
356 x 171	93.3	92.4
305 x 305	139.1	134.0

The expected ultimate bending moments are based on the assumptions that only the tension weld is effective, and that rotation takes place about the compression weld;

$$M_{ult} = 1.495 \frac{kN}{mm} \text{ x flange width x d.}$$

6.9 Existing Theories for Ultimate Load Prediction

In order that results and theories could be directly compared, the shear load and bending moment are represented by the dimensionless ratios V/V_o and $M/V_o.d$, respectively, where V_o equals the ultimate shear capacity of the tension weld when $V/M = \infty$.

The existing theories are those of Ligtenberg[20], Archer et al[22], Dawe[42], the I.I.W.[47] and BS 449[6]. The I.I.W. method is to allocate the shear load to the web welds, and hence is not applicable to the connection under consideration. The BS 449 method is known to be conservative, this was demonstrated by Archer et al[22]. The method proposed by Dawe[42] requires a very lengthy iterative procedure which shows little promise for use in the design office, and besides which, no account is taken of effective flange width which would inevitably lead to over-estimation of strength. The theory of Archer et al[22] also involves iteration, but this can be avoided since their theory was presented in the form of a design graph. Only the theories of Ligtenberg[20] and Archer et al[22] have been presented here.

(a) Ligtenberg's Method.

His method was based on the following assumptions:

(1) neutral axis at half-beam height,

(2) shear load is shared equally between the two welds,

(3) tension and compression welds behave in the same manner,

(4) the critical plane is at the throat,

(5) failure criterion is the I.S.O. comparative stress criterion

$$\sigma_c = \sqrt{\sigma_1^2 + 1.8(\tau_1^2 + \tau_{11}^2)},$$

(6) both welds are at critical state at joint failure.

All these assumptions have been shown to be partially, or totally in error.

By direct substitution into the comparative stress equation,

$$\sigma_c^2 = \{2.8(M/d)^2 - 0.8MV/d + 2.8V^2/4\}/ (t\ell)^2 \qquad (1)$$

For pure bending $M = 0.85\ t\ell d\sigma_c/\sqrt{2}$ then,

$$V_o = 0.85t\ell\sigma_c/\sqrt{2} \qquad (2)$$

substituting (2) into (1)

$$\frac{V}{V_o} = \frac{2}{1.195\sqrt{2.8(e/d)^2 - 0.8(e/d) + 0.7}} \qquad (3)$$

using the I.S.O. 1976 comparative stress equation

$$\frac{V}{V_o} = \frac{2}{\sqrt{4(e/d)^2 - 2(e/d) + 1}} \qquad (4)$$

Ligtenberg did suggest that for wide flanges only half the flange width was effective, then using the I.S.O. 1976 equation

$$\frac{V}{V_o} = \frac{2}{\sqrt{4(e/d)^2 - 2(e/d) + 4}} \qquad (5)$$

(b) The Method of Archer et al.

The method was based on the following assumptions:

(1) rotation takes place about the neutral axis at half-beam height,

(2) the horizontal forces acting on the two welds are equal,

(3) the shear load is shared between the two welds to the relationship (see fig. 27)

$$F_{y1} = \alpha V$$

where

$$\alpha = (3/4 - e/4d) \quad \text{for } e/d \leq 1$$

$$= 1/2 \quad \text{for } e/d > 1$$

(4) the tension weld fails first,

(5) the failure criterion is $\tau_{ult} = \sqrt{\sigma_\phi^2 + 4\tau_\phi^2}$

Archer et al presented their theory in the form of a design graph, see fig. 28. Their test results have been converted to the dimensionless forms already mentioned and are shown plotted in fig. 97, along with their ultimate load prediction curve. The most striking feature of the plot is the high degree of scatter which can only be due to poor quality of test welds (this matter has already been discussed in Chapter 2). The intercept of the V/V_o axis is at 1.333 which represents Archer's assumed shear load sharing factor. The section sizes of Archer's test specimens were 152 x 51 and 102 x 51, and with such narrow flanges, could be considered fairly rigid. Archer et al did not discuss effective flange width and one can only assume they regarded their flanges to be fully effective (the same applies to Dawe[42]). This being the case, it is difficult to understand why such a shear load sharing factor was chosen, other than to make the predicted curve fit the experimental results. The intercept of the $M/V_o d$ axis represents equal resistance by both welds to the bending moment. The curve of predicted capacity suggests that the F_x dominant, or 'bending mode failure' situation obtains up to a value of e/d of just more than 0.5 . There is no evidence in the results of a sudden jump to the 'shear mode failure', and it would not be expected with such narrow flanges which were probably equally as effective in both the F_x and F_y directions.

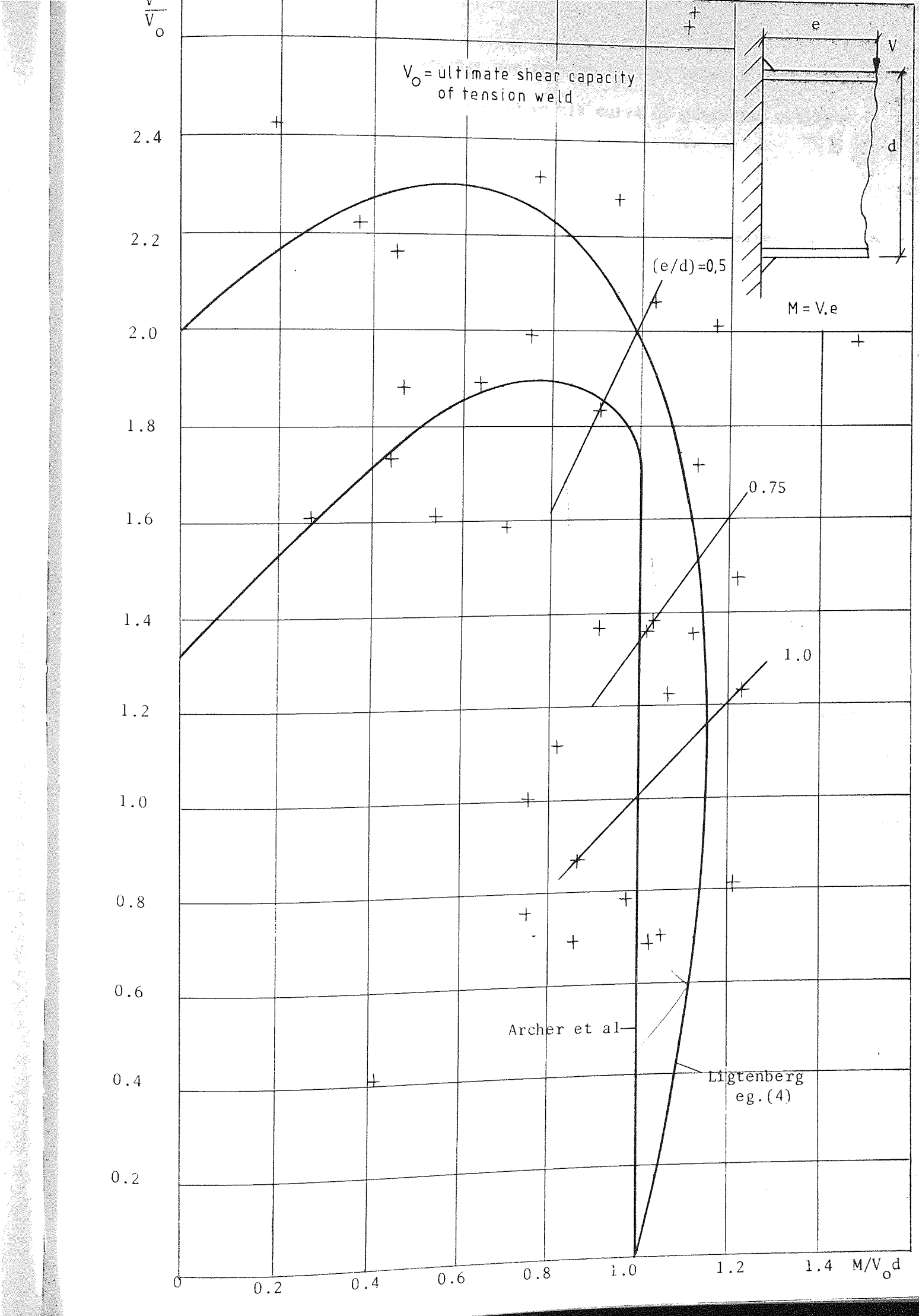
V/V_o
V_o = ultimate shear capacity of tension weld
e
V
d
M = V.e
(e/d)=0,5
0.75
1.0
Archer et al
Ligtenberg eq.(4)
2.4
2.2
2.0
1.8
1.6
1.4
1.2
1.0
0.8
0.6
0.4
0.2
0
0.2
0.4
0.6
0.8
1.0
1.2
1.4
M/V_o d

Ligtenberg did not present any results for the type of beam-column connection under consideration, and so his curve of predicted ultimate capacity is shown in fig. 97.

The only results that are available for this flange welded connection are those by Archer et al, the author, and just two results of little value by Uhler and Jensen[2].

The curve by Ligtenberg in fig. 97 is based on fully effective flanges and the 1976 I.S.O. criterion. It appears to fit the results of Archer et al as equally as well as their own prediction. The intercept of the V/V_o axis at 2 indicates 100% effective flange width and equal shear load sharing. The same applies to the $M/V_o d$ axis intercept as it did to the curve of Archer et al. It will be noticed that the Ligtenberg curve shows the ultimate value of F_x to be increasing as the force F_y is increased from zero, and then decreasing to its original value at V/V_o equals 2. This is a characteristic of the relationship between F_x and F_y as described by the I.S.O. comparative stress equation. The author's circle criterion also predicts this characteristic, see fig.70, and the characteristic is demonstrated by Jensen's[5] results of style (a) weld in fig. 12(a). The same figure also shows the relationship between F_x and F_y when the latter is compressive, style (b) weld and a large difference is readily apparent. The curve of Archer et al shows a constant value of F_x as F_y is increased up to V/V_o of approximately 1.7 . This constancy is in fact a simplification that was made by Archer et al to their predicted curve based upon their failure criterion which does show a similar rising characteristic to that of Ligtenberg.

The author's results of test connections have been converted to the dimensionless quantities, and are shown plotted in fig. 98 (the end mode

Fig.98 Test Results by the Author

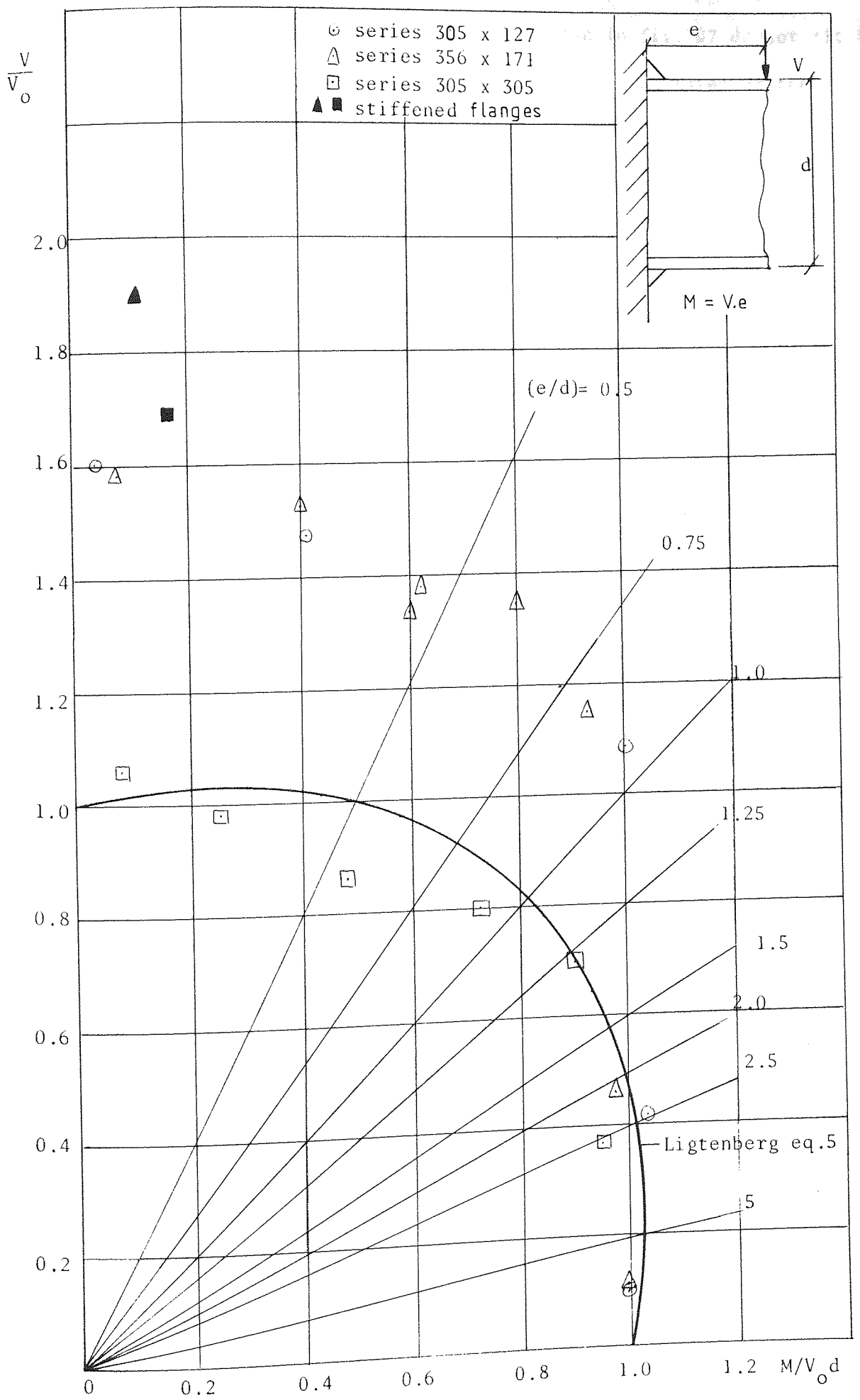

failure' results have been omitted). It can be immediately seen that the theories of Ligtenberg and Archer et al as shown in fig. 97 do not fit the results. This is not surprising since no account was taken of the effective flange width. However, Ligtenberg did suggest that 'wide' flanges were only 50% effective in resisting the shear load, see equation (5), and this prediction is shown plotted in fig. 98. It appears to fit quite well the results of the series 305 x 305, but this can only be regarded as coincidental in view of the assumptions that Ligtenberg made, see page 245. It is clear from the author's results that if a method of ultimate load prediction is to be applicable to all section sizes, then account must be taken of the effects of flange and web stiffnesses. No method so far presented has taken account of web stiffness, and only Ligtenberg made an attempt at assessing the importance of flange width.

The experimental results shown in fig.98 indicate that the two series 305 x 127 and 356 x 171, behave in a very similar manner although both the flange widths and section depths are different. Superficially, one would expect the series to give results inbetween the other two series because of the greater section depth and wider flange. A closer study of the section dimensions reveals that the flanges and webs of the series 305 x 127 and 356 x 171 are of comparable stiffness:

section	web thickness	flange thickness
305 x 127	8.5	12
356 x 171	9.5	16
305 x 305	10.5	15.5

The shear load distribution along the compression weld is determined solely by the flange/weld stiffness whilst that along the tension weld by the flange contour/stiffness and type of load application e.g. single point, line, or surface as with the 50 mm bearing support. The shear load sharing between the two welds is probably determined by a complex relationship

between flange stiffness (width and thickness) web stiffness (depth and thickness), ratio e/d, load/deformation characteristics, and possible frictional forces arising out of plate-bearing. A theoretical solution involving all the above variables in conjunction with the circle failure criterion would undoubtedly result in a method of load prediction requiring lengthy computer analysis, and of no use in the design office. Simplifications and approximations are obviously called for.

6.10 Effects of Plate-bearing

Dawe[43] assumed that bearing took place between both the flange and web ends (from the neutral axis) and the column face. He further assumed that the bearing stress over the flange end face reached the yield value of the material. In the field situation it is most unlikely that perfect fit-up would be achieved and as a result the compression flange might be in bearing for only a part of its length, or even not at all. With regards the test connections, care was taken by the author to ensure full bearing between the beam ends and the end-plate, but no doubt the surface preparation of the beam ends, especially the flange ends (by hand filing), resulted in the presence of local asperities which under the bearing forces would yield, and account for a major proportion of the horizontal deformations measured at the compression flange/end-plate interface. After the collapse of these local asperities bearing would be taken up along the entire length of the compression flange, but only along the outer edge of the flange owing to the rotation of the beam relative to the end-plate. Yielding of the flange along the edge would probably then follow thus allowing the flange end to settle down and take up full bearing.

A minor proportion of the measured horizontal deformations must be attributed to the elastic strain of the flanges (both tension, and compression

flanges) since the dial gauges were anchored to the flange sides at a distance of 30mm from the flange ends. This elastic strain is at a maximum when the ratio e/d is at a maximum, and the bearing force is necessarily at maximum value. Using a modulus of elasticity of 200 kN/mm^2 and the values of the maximum bearing force as shown in Table 36, the average elastic strain is estimated to be 0.61×10^{-3} inch (0.0153mm).

For connnections tested by the author the greatest value of the horizontal force F_x was 1.485 kN/mm run, see Table 36, and if this is considered to act over the full depth of the flange, after the initial collapse of local asperities and flange edge, the resultant average bearing stress is 92.8 N/mm^2. If the compression weld is considered to resist the horizontal force over its depth then the average bearing stress is reduced to 74.3 N/mm^2 which is well below the yield stress. If the contribution of the compression weld to the resistance of the bearing forces is assessed from the load/deformation characteristic in fig. 95 (fig. 96 is not accurate enough for this purpose), then a horizontal compression of say 3.5×10^{-3} inch (0.0875mm), which is typical for high values of e/d, see fig. 99(b) implies a resistive force of approximately 0.9 kN/mm run. This leaves a residual bearing force of 0.585 kN/mm to be resisted by the flange and web. If the flange is considered alone, then the average bearing stress is 36.5 N/mm^2.

The existence of a residual bearing force may lead to a frictional force resisting the applied shear load. Such a frictional force can only

exist if there is relative vertical movement between the flange end and column face. Average vertical deflections of the compression flange/weld are shown in fig. 99(a), and it is clear from this that vertical movements of approximately only 1×10^{-3} inch were recorded at high values of e/d. It is very doubtful whether such a small movement gave rise to a frictional force.

In the case of the 'shear mode failure' i.e. low values of e/d, it will be seen from fig.99 that average vertical deflections are relatively high, being sufficient for the creation of sliding friction, but on the other hand, the horizontal deflections of the compression flange/weld are relatively low,implying small bearing forces. An assessment of the frictional resistance to the shear load for the loading situation, $e/d \triangleq 0.5$ (an examination of the deflection characteristics in fig. 99 will show that at the ratio of $e/d \triangleq 0.5$, the frictional resistance is likely to be at its maximum) is given below .

Specimen 356171/12.

$e/d = 0.45, \quad V = 351.94$ kN

from fig. 98,

$M/V_o d = 0.62$

then assuming the horizontal resistive force of the compression weld and the bearing force act at the same point,

$F_x d = 0.62 V_o d$

$F_x = 0.62 \times 1.485 = 0.921$ kN/mm run

The horizontal deflection of the compression weld = 2.4×10^{-3} inch(0.06mm) which indicates a resistive force of 0.80 kN/mm from the load/deformation characteristic, fig. 95.

Residual bearing force = 171(0.921-0.80) = 20.7 kN

Frictional resistance = 0.28 x 20.7 = 5.8 kN

(assuming $\mu = 0.28$)

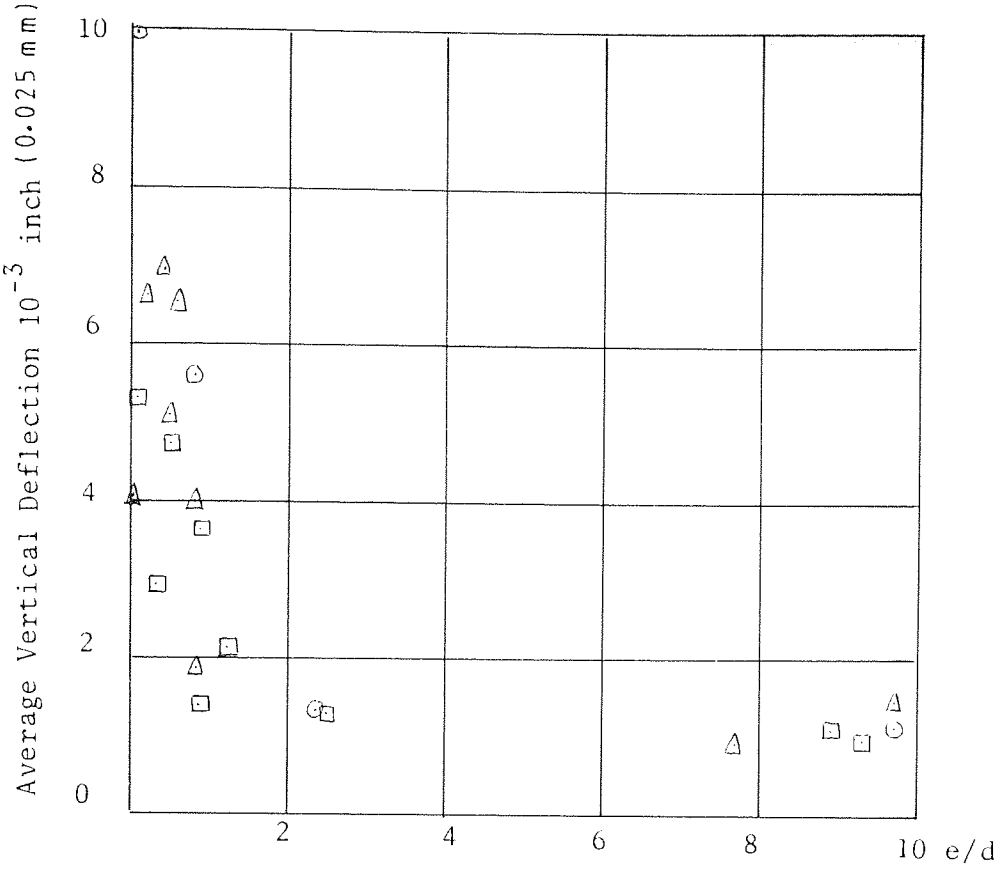

(a) Average Vertical Deflection

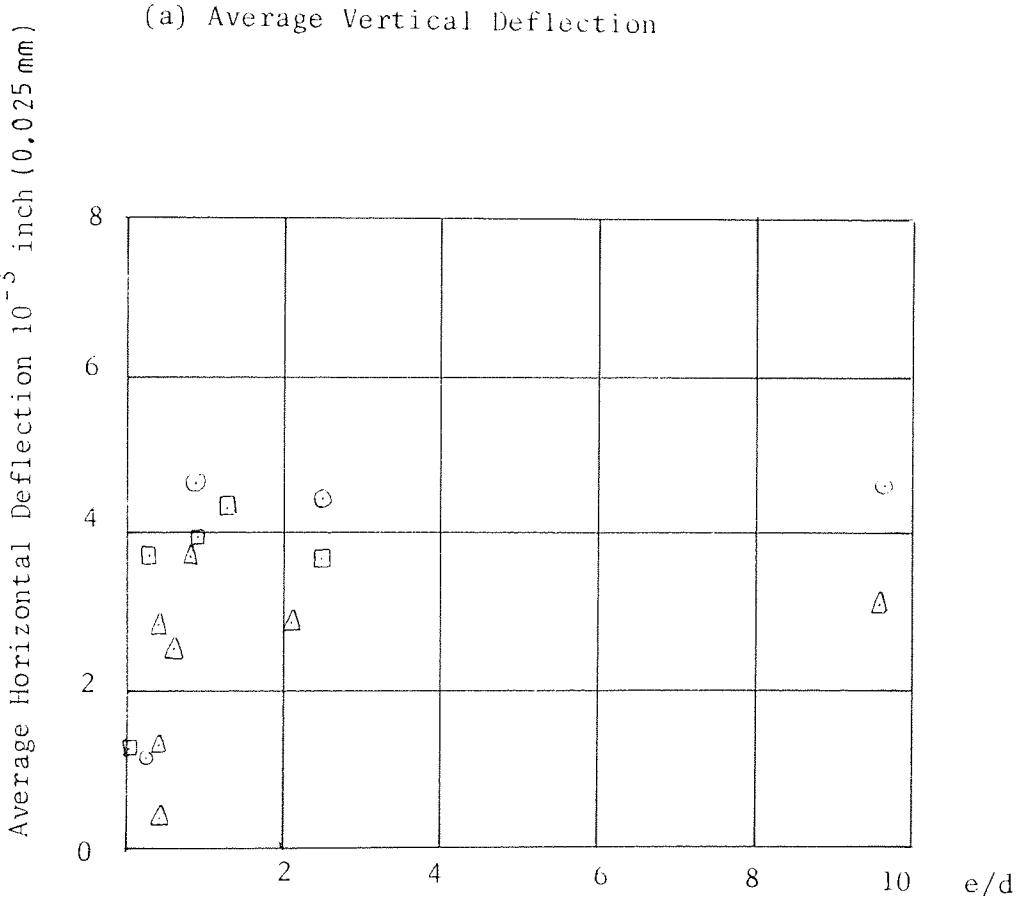

(b) Average Horizontal Deflection

Fig.99 Relationship Between Compression Flange Deflection and e/d

This frictional force is a very small percentage of the applied shear load of 351.94 kN. Even using the average horizontal deflection of 1.4×10^{-3} inch the resultant frictional force of 17.8 kN represents only 5 % of the applied shear load.

A visual examination was made of some of the compression flanges and no evidence was found of sliding friction.

On the basis of the arguments set out above the author considers the frictional resistance to the shear load to be of little significance.

The position of the axis of rotation, commonly referred to as the neutral axis, is obviously affected by the degree of plate-bearing. If the bearing zone is considered to be restricted to the flange only, and the bearing force to act at the same position as the compression weld horizontal resistive force, then the axis of rotation will be coincidental with the line of action of the bearing force, see fig. 100.

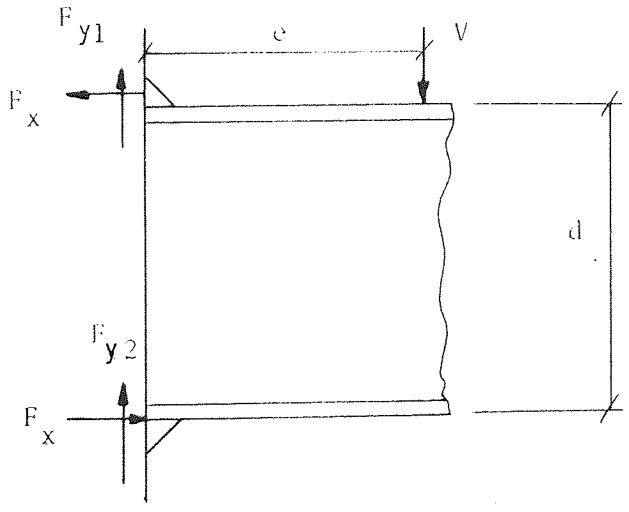

Fig. 100 Force Equilibrium Condition

In the real situation the compression weld horizontal resistive force would probably act at half leg height, and the bearing force at one third flange thickness (assuming a triangular bearing stress distribution), the distance between the lines of action being approximately 7 mm. This distance when compared to the depth of the beam section, d, can be regarded as insignificant in the calculation of bending moment resistance.

Since the compression weld horizontal resistive force and the bearing force are considered to act at the same point, then the position of the axis of rotation is of no importance in the determination of the moment resistance of the connection (with reference to test connections only).

The information regarding horizontal deflections, as presented in figs. 91, 92 and 93, cannot be used for the assessment of the position of the axis of rotation, since the deflections of the compression weld/flange represent local plastic deformation rather than gross movement.

6.11 Proposed Method of Load Prediction

It has been shown that for all ratios of e/d the tension weld will fail first. Sufficient evidence has been presented to show that the frictional resistance to the shear load can be regarded as insignificant. It has been argued that the horizontal compression weld resistance and bearing forces may be considered to act at the same point. The force equilibrium diagram, fig. 100, is based upon the above findings.

Two general loading situations have been discussed, i.e. F_x dominant and F_y dominant. and their corresponding failure modes of 'bending' and 'shear' respectively. It has been argued that the sudden change in fracture plane angles, see fig. 94, is indicative of a sudden change in

the failure mode from 'bending' to 'shear', at a ratio of F_x/F_y around unity, as e/d is decreased. This sudden change was attributed to the fact that the flange is rigid in the F_x direction but flexible in the F_y direction. The preceding general arguments will now be related to the experimental results, fig. 98, and the circle failure criterion predictions, figs.67, 70, 70(a) and 72.

Results from all three series indicate a value of unity for the intercept of the $M/V_o d$ axis - this confirms the belief that the flange width is fully effective in the pure bending situation, i.e. e/d equals ∞. The value of V_o was based upon the average ultimate value of the F_x force, 1.495 kN/mm run, from the biaxially-loaded specimens, fig. 67. The circle failure criterion predicts a value of 1.399 kN/mm run for both F_x and F_y, see figs. 67 and 70. The average fracture plane angle of the test connections tested at e/d = 9.68, 9.64 and 8.89 was 18° compared to a value of 17.25° for the basically-loaded specimens when $F_x/F_z = \infty$, fig. 70(a). The circle failure criterion is a little inaccurate at this extreme with a predicted angle of only 6.8°.

As the ratio of e/d is decreased from infinity and shear load, V, is applied, the moment resistance, M of the connection should increase as indicated by the failure criterion relationship between F_x and F_y in fig. 70 (this relationship is assumed to be symmetrical about $F_x/F_y = 1$). It is seen from this relationship that as F_y is increased from zero there is an initial increase in F_x which means an increase in the moment resistance M. Such an increase is not evidenced by the experimental results, the explanation of which now follows. The distribution of the shear load, the F_y force, has shown to be not uniform, by the flange/weld deflection patterns, figs. 84, 85 and 86,and since the distribution of the F_x force is

uniform, the ratio of F_y/F_x will vary along the length of the weld - being a maximum over the web and a minimum at the ends. In other words, the ultimate strength of the weld will vary along its length according to the relationship between F_x and F_y, fig. 70, being a maximum in the middle, and a minimum at the ends. This means that as the load is increased the ends of the welds will become critical and transfer their load to the remaining section of the weld which of course is progressively stronger towards the centre. In reality then, the weld does have an effective length when resisting the bending load (combined with a limited amount of shear) and this accounts for the absence of the expected increase in moment resistance.

As the shear load is increased further the criterion in fig. 70 predicts a peak in weld strength and then a decline to a value approximately equal to the starting value at a ratio of F_x/F_y of unity. So, at F_x/F_y equals unity the value of $M/V_o d$ should be approximately unity. The value of F_x/F_y of unity can now be related to a value of e/d by considering the fracture plane angles in fig. 94. With F_x/F_y equal unity the expected fracture plane angle would be 45°, but none of the connections tested produced this angle since at this ratio, the failure mode would have switched from 'bending' to the 'shear mode'. If the compression and tension welds were of equal strength, the flanges were fully effective, and the shear load was equally shared, then the corresponding ratio of e/d would be 0.5. This is obviously not the case in practice.

The absence of the expected rise in moment resistance as the shear load is increased from zero has been explained, but the probably behaviour of the test connections as the shear load is further increased has not. The effective weld length in the F_x direction will probably decrease as the shear load is increased because of initial weld failure at the critical ends -

this could well result in a decrease of the moment resistance below the value at the $M/V_o d$ axis intercept. Such behaviour might appear on the F_x/F_y criterion as shown by the dotted lines in fig. 101, but as has

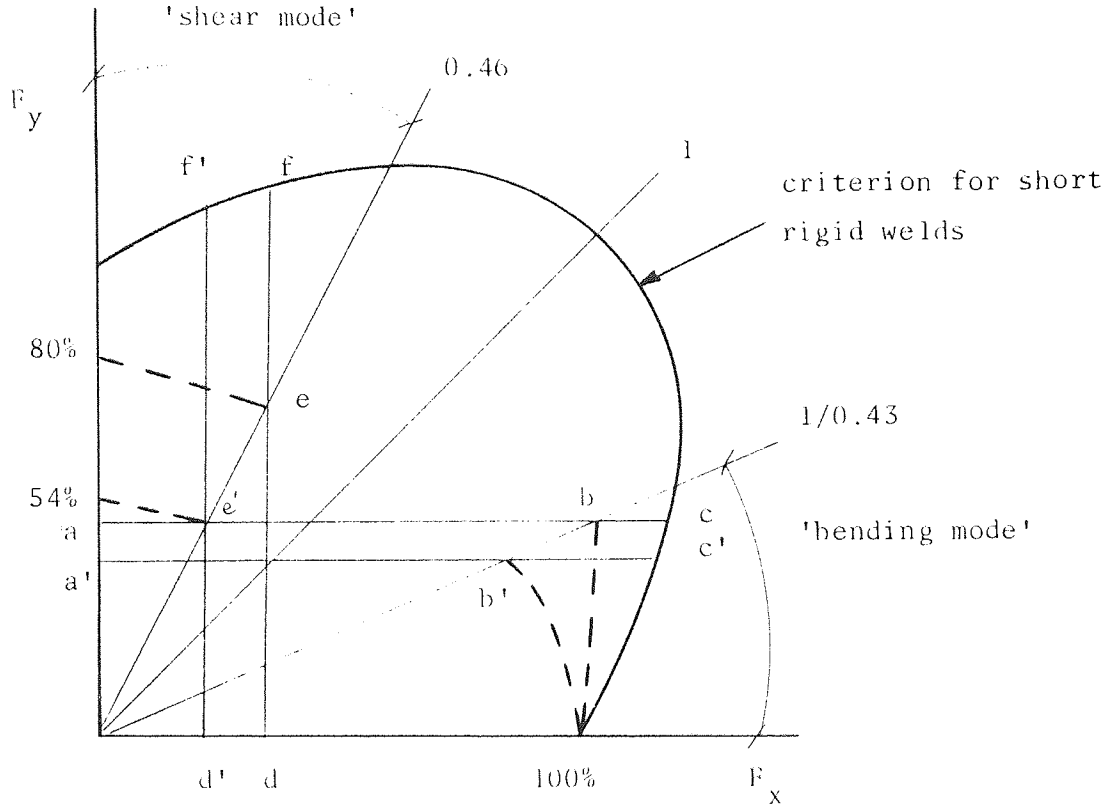

Fig. 101 Modification to F_x/F_y Criterion

already been shown, the failure mode will change abruptly before F_x/F_y reaches unity. It will be seen from Table 35 that these abrupt changes take place between ratios of e/d as follows:

series	change of fracture angle	change of e/d
305 x 127	15 → 74	0.91 → 0.28
356 x 171	20 → 86	0.81 → 0.59
305 x 305	14 → 74	0.9 → 0.25

which means the points plotted to the left of e/d = 0.75, fig. 98, represent 'shear mode failures'. It can now be seen from fig. 98 that the moment resistance does fall below that of the $M/V_o d$ axis intercept for all three series of connections and especially the 305 x 305 series, having by far the most flexible flanges. The average fracture angle reached after which abrupt change in failure mode occurred in 16.33° and this corresponds to a predicted value of F_x/F_y of 1/0.43 by the circle criterion, see fig. 72. It is most probable that the ratio of F_x/F_y at which the abrupt change takes place will be influenced by the beam section stiffness, and therefore, the concept of an average value presented above is an over-simplification of reality, but little more can be done with these limited results.

The effective flange width in the F_x direction just prior to the sudden change in failure mode is represented by ab/ac in fig.101. For the series 305 x 127 and 356 x 171 this is approximately 90% and for series 305 x 305, 66% (a'b'/a'c').

The first results in the 'shear mode failure' are at e/d equals 0.59 and 0.56 with an average fracture angle of 72.5° which corresponds to a ratio of F_x/F_y of 0.46 according to the circle criterion. In this mode the F_x force will be uniformly distributed whilst the distribution of the F_y force, will be non-uniform, as already discussed, and thus the ratio of F_x/F_y will vary along the length of weld as it did for the 'bending mode failure'. However, because of the much greater vertical deflections of the central region of the flange the central portion of the weld will reach a critical state long before the ends of the weld - failure will be initiated in the central region and load will be transferred towards the weld ends. This mechanism is opposite to that described for the 'bending mode failure'.

In the 'bending mode' only the strength of the tension weld was considered, but in the 'shear mode' both welds offer resistance to the shear load. The relative strengths of the two welds and the factors involved in the sharing of the shear load have already been discussed, and so for the sake of simplicity, the welds will be considered together. The effective flange width at the ratio of F_x/F_y equals 0.46 is represented in fig. 101 by the ratio de/df. For the series 305 x 127 and 356 x 171 this is approximately 60%, and for series 305 x 305 (d'e'/d'f'), approximately 39% (assuming both welds of equal strength and the same state with reference to the F_x/F_y criterion). These effective flange widths are much less than those before the sudden change in failure mode - credibility is thus given to the argument presented accounting for the sudden change.

As the ratio of e/d is further decreased, a reduction in connection shear resistance would be expected because flanges would become less effective, and the tension weld would carry an increasingly greater proportion of the total shear load as a result of further elastic compression of the web. The results however show an increasing shear resistance and this can only be due to the presence of the 50 mm bearing acting directly across the tension flange. This bearing produces a fairly uniform vertical deflection of the tension weld thus making the tension flange virtually fully effective.

If the two welds are considered together, the effective flange width at the V/V_o intercept is approximately 80% for series 305 x 127 and 356 x 171 and 54% for series 305 x 305. If the tension flange is considered to be fully effective, then the effectiveness of the compression flange becomes approximately 60% for series 305 x 127 and 356 x 171, and 10% for

series 305 x 305. If a point, or line bearing were to be used instead of 50 mm surface bearing, the shear load resistance would inevitably be greatly reduced, perhaps to half of that shown by the test connections.

The results of the two stiffened connections, 356171/9 and 305305/8, are plotted in fig. 98 and they demonstrate quite clearly the role of flange flexibility and web stiffness.

It is not feasible, as it was hoped, to develop a general method of ultimate load prediction for beam-column connections from the results of the limited testing programme presented here. The results have been analysed in conjunction with the circle failure criterion, and an accurate picture of connection behaviour and mechanisms of weld failure has been established.

Figure 98 can be used for design purposes, but its use must necessarily be restricted to those beam sections tested by the author. Its use only necessitates the value of V_o to be established under field conditions.

CHAPTER 7

CONCLUSIONS

With reference to short fillet welds subject to static loading in the F_x and F_z directions:

1. With regard to the relative strengths of welds;
   (i) welds under tension, and compression are of equal ultimate strength for the range of F_x/F_z from 0 to 2,
   (ii) welds under compression are weaker for the range of F_x/F_z from 2 to ∞, and
   (iii) when F_x/F_z equals infinity the average ratio of weld strengths is 0.916.

2. The level of residual stress does influence the ultimate strength of fillet welds. Failure of the fillet weld is initiated at the weld root, the important factor controlling the initiation being weld ductility. The level of residual stress determines to a large extent the weld (root) ductility. The greater the residual stress, the lower the weld (root) ductility and ultimate strength.

3. The influence of residual stress is greatest when the F_z force is dominant.

4. Stress relieving at 600°C resulted in a 30% increase in ultimate strength when F_x/F_z equalled infinity, and 12% increase when F_x/F_z equalled zero.

5. The critical, or fracture plane is only at the throat when F_x/F_z equals zero, or for the weld loaded in F_x and F_y directions, when F_x/F_y equals unity.

6. Critical plane angles vary from 15.25^o to 45^o (measured from the weld leg) for the welds under tension, and from 0 to 45^o for the welds under compression.

In connection with the development of the Crofts & Martin[45] failure criterion:

7. Insufficient results were obtained in the shear/compression zone of the failure criterion field - no advance has been made on the Crofts & Martin criterion in this respect.

8. Sufficient results were obtained in the shear/tension zone and various best-fit curves were applied. Extension of the linear criterion was found unsuitable and was abandoned in favour of the best-fit circle criterion. The circle criterion provides the most realistic fit to the experimental results and is the most suitable for further development.

9. Using the circle failure criterion, ultimate state relationships between F_x and F_y, F_x and F_z, and F_x, F_y and F_z have been established for short fillet welds subjected to tensile loading on the weld legs and longitudinal shear (see pages 163 and 163a). The solution of these relationships necessitates the evaluation of the critical plane angle, ϕ, but this may be avoided in the design office by using graphical representations of the relationships between F_x and F_z, and F_x and F_y as shown in figs 67 and 70. The intending user would first have to establish a value of F_x to suit his own field conditions - a double-lapped end weld test specimen similar to that in fig.55 is recommended for this purpose.

With regard to the beam-column connections tested the conclusions can be summarized as follows:

1. The flange weld under tension is critical and always fails first regardless of the ratio of e/d - this was evidenced by,

(i) shear load transfer to the compression weld subsequent to the failure of the tension weld,

(ii) fracture plane angles of compression welds, if failed, were always 90° to the flange face,

(iii) relative deflections of the two welds in relation to the load/deformation characteristics.

2. Web buckling does not occur, only elastic compression.

3. Under pure bending the moment resistance is directly proportional to the flange width.

4. Bearing stresses at the compression flange reach a probable maximum of 36.5 N/mm^2.

5. Frictional resistance to the applied shear load is insignificant when bearing forces were high, average vertical deflections were in the order of 0.001in (0.025mm) and little frictional resistance could have existed; when bearing forces were low, average vertical deflections were in the order of 0.008 in. (0.2mm) and frictional resistance was estimated to be a maximum of 5% of the applied shear load.

6. Bearing force acts at the same position as the horizontal resistance force of the compression weld and hence, position of the axis of rotation has no effect on the moment resistance of the connections (test connections only).

7. Shear load sharing between the tension and compression welds is a complex function of,

(i) elastic compression of the web,

(ii) elastic/plastic deformation of the flange/weld combination,

(iii) load/deformation characteristics of both the tension and compression welds,

(iv) type of load application to the tension flange.

8. Three distinct modes of connection failure are possible:

(1) 'End mode' - as a result of poor fit-up caused by distortion, tightening down can impose large enough pre-loads to cause the appearance of cracks at the weld ends, and from these failure can be initiated and propagate during loading which will result in failure loads well below normal. In the worst case the load attained was only 50% of the normal.

(2) 'Bending mode', or F_x dominant - occurs between ratios of e/d from ∞ to 0.8 and is characterised by complete failure of tension weld and non-failure of the compression weld. The failure mode was evidenced by

(i) fracture plane angles related to the circle failure criterion, and

(ii) relatively large horizontal deflections compared to vertical deflections.

The flange width was 100% effective for all sections at e/d = ∞, and a minimum of 60% at e/d = 0.8, for section 305 x 305.

(3) 'Shear mode', or F_y dominant - occurs between ratios of e/d from 0.59 to 0 and is characterised by initial failure of the tension weld in the central region, and subsequent transfer of shear load to the compression weld which then fails in the central region under large deformation of compression flange. The mode shows an increasing effective flange width as a result of the 50 mm surface bearing across the tension flange. The failure mode was evidenced by,

(i) elastic compression of the web,

(ii) fracture plane angles of the tension weld in relation to the circle failure criterion, and

(iii) relatively high vertical deflections compared to the horizontal deflections.

The effective flange width for sections 305 x 127 and 356 x 171 is 60% at e/d = 0.56, and 80% at e/d = 0. For section 305 x 305, 39% at e/d = 0.56 and 54% at e/d = 0.

The change from the 'bending mode' to the 'shear mode', as e/d is decreased occurs abruptly owing to the flange width being less effective in the vertical direction than in the horizontal direction.

9. The stiffened connections reached loads of approximately 95% of the maximum possible in a rigid connection.

10. No existing methods of ultimate load prediction, including that of Archer et al[22], are applicable to the connections tested. All overestimate the ultimate load to a greater or lesser degree.

11. There are insufficient results for the development of a general method of ultimate load prediction for beam-column connections. Results are presented in a dimensionless form in a design graph which can be used for ultimate load prediction, but only for those section sizes tested by the author. The design graph could be used as a guide for other section sizes. Before the graph can be used, the intending user should establish the ultimate weld strength, V_o, for his particular field conditions.

CHAPTER 8

RECOMMENDATIONS FOR FURTHER WORK

1. Insufficient results were obtained in the shear/compression zone from which to gain a complete picture of the failure criterion. A new style of specimen is required in which the fillet weld can be loaded in compression on both legs without the existence of plate-bearing.

2. The shear load sharing between the tension and compression welds is a complex function of beam-section stiffness parameters, style of loading and load/deformation characteristics. Before a general method of ultimate load prediction can be developed this complex function must be determined. This can only be done through the investigation of individual parameters in isolation from the others. The most important parameter is the flange width which may have an effectiveness ranging from 10 - 100%. The tension and compression flanges would have to be considered separately because they are loaded in different manners - the tension flange by a line or surface load, and the compression flange by virtually a point load via the web. Variables for a suitable test programme would be flange width, flange thickness, and distance of applied load from the weld.

Elastic compression of the web needs to be studied with reference to web thickness, web depth, and distance of load from the weld.

The load/deformation characteristic for the compression weld produced by Tzogius[56] needs to be confirmed for long welds.

3. After the shear load sharing functions have been established other types of connections should be investigated:

(i) flange welded (inner welds only)
(ii) flange welded (inner and outer welds)
(iii) web welded
(iv) all-round welded.

REFERENCES

1. Bibber,L.C. "The Theory of Stresses in Welds". The Welding Journal, 9, 4, 1930.
2. Uhler,E.H. and Jensen,C.D. "An Investigation of Welded Connections Between Beams and Columns", The Welding Journal, April 1930.
3. Schuster,L.W. "Welded Pressure Vessels". The Welding Journal No.5, May 1930.
4. Freeman,F.R. "The Strength of Welded Joints". The Welding Journal, June 1932.
5. Jensen,C.D. "Combined Stresses in Fillet Welds". The Welding Journal. No.2, February 1934.
6. BS 449. Specification for the Use of Structural Steel in Building,1970.
7. Schreiner,N.G. "The Behaviour of Fillet Welds when Subjected to Bending Stresses". Journal of the American Welding Society. Vol.14, No.9, September 1935.
8. Jennings,C.H. "Welding Design". The Welding Journal, October 1936.
9. Solakian,A.G. "Stress in Transverse Fillet Welds by Photoelastic Methods". The Welding Journal, Vol.13, 1934.
10. Blackwood,R.R. "The Strength of Electric Arc Welds in Structural Mild Steel". The Commonwealth Engineer. September 1930.
11. Vogel,A. "Design of Joints for Welded Structures". The Welding Journal. Vol.8, April 1929.
12. Jensen,C.D. & Crispen,R.E. "Stress Distribution in Welds Subject to Bending". The Welding Journal - Research Supplement, October 1938.
13. Professor Shedd. "Structural Design in Steel", John Wiley & Sons.Inc., (Publishers).
14. Johnston,B.J. & Deits,G.R. "Tests of Miscellaneous Welded Building Connections". The Welding Journal - Research Supplement. January 1942.
15. Koenigsberger,F. "Design Stresses in Fillet Weld Connexions". Proceedings of the Institute of Mechanical Engineers, 165, 1951.

16. Vreedenburgh,C.G.J. "New Principles for the Calculation of Welded Joints The Welding Journal, Vol.33, No.8, August 1954

17. Kist,N.C. "Berechnung der Schweissnahte unter Berucksichtigung konstanter Gestaltsanderrungs-energie" Vorbenricht 2, Kongress Int.Ver.fur Bruchenbau und Hochbau, 1936.

18. Kist,N.C. Theoretische beschouwing en proeven ter bepating van de draagkracht van gelaste constructies. Ontwerp Voorsch. V.H.Ontwerpen en v.h.vervaardigen met de electrische vlamboog g laste bruggen, Horld-commissie v.d. Normalisatie in Nederland, Sept.1940, V.1017 pp.14-29

19. Archer,F.E.,Fischer,H.K. & Kitchen,E.M. "Fillet Welds Subjected to Bendin and Shear". Civil Eng.& Public Works Review. Vol.54,No.634, April 1959.

20. Ligtenburg,F.K. "Recent Tests on the Welded Beam-Column Connection". Int.Inst. of Welding Document, Commission XV, 1959. Netherlands.

21. Commission XV.(IIW) "Calculation formulae for Welded Connections Subject to Static Loads". Welding in The World,Vol.2,4, 1964.

22. Archer,F.E.,Kitchen,E.M.& Fischer,H.K. "Strength of Fillet Welds", UNICIV Report R6, University of New South Wales, Australia. Nov.1964.

23. L.W.A.v.d.Elzen, "Welding Seams in Beam-to-Column Connections without the Use of Stiffening Plates". Report 6-66-2, I.I.W.Document,XV-213-66.

24. Higgins,T.R. & Preece,F.R., "Proposed Working Stresses for Fillet Welds in Building Construction". The Welding Journal Research Supplement. October 1968.

25. Ligtenburg,F.K. "International Test Series, Final Report". Document IIS/IIW-330-69-Z.

26. Clark,P.J. "Basis of Design for Fillet-Welded Joints Under Static Loading" Conference Proc.Vol.1.,1971. Welding Institute-Improving Welding Product Design. Paper 10.

27. Van Douwen,A.A. & Witteveen,J. "Proposed Modification of the I.S.O. Formulae for the Calculation of Welded Joints", Lastechniek,32,(6),1966.

28. I.I.W., "The Relationship Between Stress and Strain in Fillet Welds with Static Loading". I.I.W. Document XV-170-64.

29. Abolitz, "Plastic Design of Eccentrically Loaded Fasteners". Eng.Journal of AISC, 3, (3), July 1966.

30. Butler,L.J. & Kulak,G.L. "Strength of Fillet Welds as a Function of Direction of Load". The Welding Journal Research Supplement, May 1971.

31. Fisher, J.W. "Behaviour of Fasteners and Plates with Holes", Journal of the Structural Division ASCE. Vol.91, No.ST6, December 1965.

32. Kato,B. et al. "The Maximum Strength of Beam to Column Connections without Stiffening Plates". I.I.W. Document XV-311-71.

33. Naka,T. & Saito,H. "Investigation of the Strength of Welded Beam-Column Connections, Part 9 - Distribution of Beam Force into Column Web". Transaction of the Architectorial Institute of Japan, No.60, October 1958.

34. Miki,S. et al. "Some Problems on the Strength and Rigidity of Beam-to-Column Connections in Steel Frames". Kawasaki Dockyard Co.Ltd., Steel Structure Division, November 1964.

35. Igarashi,S. & Sakamoto,J. "Stress Analysis of the Welded Steel Connection - H-line Beam-to-Column Connection". Transaction of the Architectural Institute of Japan, No.68, June 1961.

36. Hoshino,M., Horikawa,K. & Okumiera,T. "Strength of Connection due to Structural Discontinuities". Document X-572-70. I.I.W.

37. de Geeter,P.J. "Effective Weld Length of Beam-to-Column Connections With and Without Stiffeners". I.I.W. Document XV-244-68.

38. Roloos,A. "The Effective Weld Length of Beam to Column Connections Without Stiffening Plates - Final Report". I.I.W. Document XV-276-69.

39. Strating, J. et al. "The Influence of a Longitudinal Stress on the Strength of Statically Loaded Fillet Welds". Welding in The World. Vol.10, No 5/6 1972.

40. Newmann,A. & Ziethe,H. "Bending Tests on Welded Beams with Prestressed Welds Connecting Flanges to Webs". I.S.O./T.C. 44/SC 2/1 (Germany 1-51).

41. Butler,L.J., Pal.S., & Kulak,G.L. "Eccentrically Loaded Welded Connections". Journal of the Structural Division. ASCE. No ST5 May 1972.

42. Dawe,J.L. "Behaviour of Welded Connections Under Combined Shear and Moment". M.Sc.Thesis, Department of Civil Engineering, University of Alberta, Edmonton, Alberta.

43. Dawe,J.L. & Kulak,G.L. "Welded Connections under Combined Shear and Moment". Journal of the Structural Division, ASCE. No.ST4, April 1974.

44. Crofts,M.R. "An Evaluation of Three Design Methods for Fillet Welds" M.Sc.Thesis, October 1974. University of Aston.

45. Crofts,M.R. & Martin,L.H. "A Failure Criterion for Fillet Welds". Welding Research International, Vol.6,2, May, pp.23-30. 1976.

46. Higgs,J.D. "Failure Criteria of Fillet Welds and Plate Bearing Effect of Structural Welded Connections Under Combined Bending and Shear". M.Sc.Thesis, October 1975, University of Aston.

47. "Design Rules for Arc-welded Connections in Steel Submitted to Static Loads". I.I.W. Document 504-76.

48. Greene,T.W. "Evaluation of Effect of Residual Stresses". Welding Journal, Research Supplement. 1949, Vol.28, pp.193s - 203s.

49. Kihara,H., & Masubuchi,K. "Effect of Residual Stress on Brittle Fracture". Welding Journal, Research Supplement, 1959, Vol.38. pp.159s - 168s.

50. Hall,W.J., Nordell,W.J. & Munse,W.H. "Studies of Welding Procedures". Welding Journal, Research Supplement. 1962, Vol.41, pp.505s - 518s.

51. Mcgeady,L.J. "The Effect of Preheat on Brittle Fracture of Carbon Steel for Pressure Vessels". Welding Journal, Research Supplement, 1962, Vol.41, pp.355s - 367s.

52. Parker,E.R. "Stress Relieving of Weldments". Welding Journal, Research Supplement, 1957, October, pp.433s - 441s.

53. Wheatley,J.M. & Baker,R.G."Mechanical Properties of a Mild Steel Weld Metal Deposited by the Metal-Arc Process".British Welding Journal,1962. Vol.9, pp.378 - 387.

54. Idem. "Microstructural Factors Governing the Yield Strength of a Mild Steel Weld Metal Deposited by the Metal-Arc Process". British Welding Journal, 1963. Vol.1. pp.23 - 28.

55. Biggs,M.S.A.B. "A Failure Criterion for Welded Joints Subject to Static Load". Thesis as partial fulfilment of an M.Sc. in Welding Technology and Management at the University of Aston in Birmingham, 1977.

56. Tzogius,A. "Weld Groups Subject to Torsion and Shear". Thesis as partial fulfilment of an M.Sc. in Welding Technology and Management at the University of Aston in Birmingham, 1980.

57. BS 4360, 1979. Specification for Weldable Structural Steels.

58. BS 3692, 1967. I.S.O. Metric Precision Hexagon Bolts, Screws and Nuts.

APPENDIX 1

Details of Biaxial Loading Jig

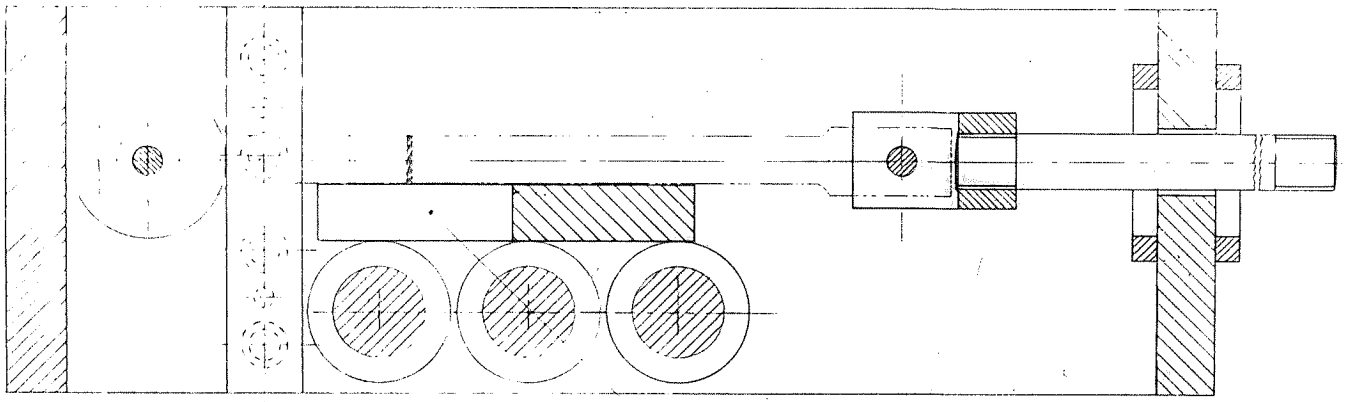

SECTION A-A

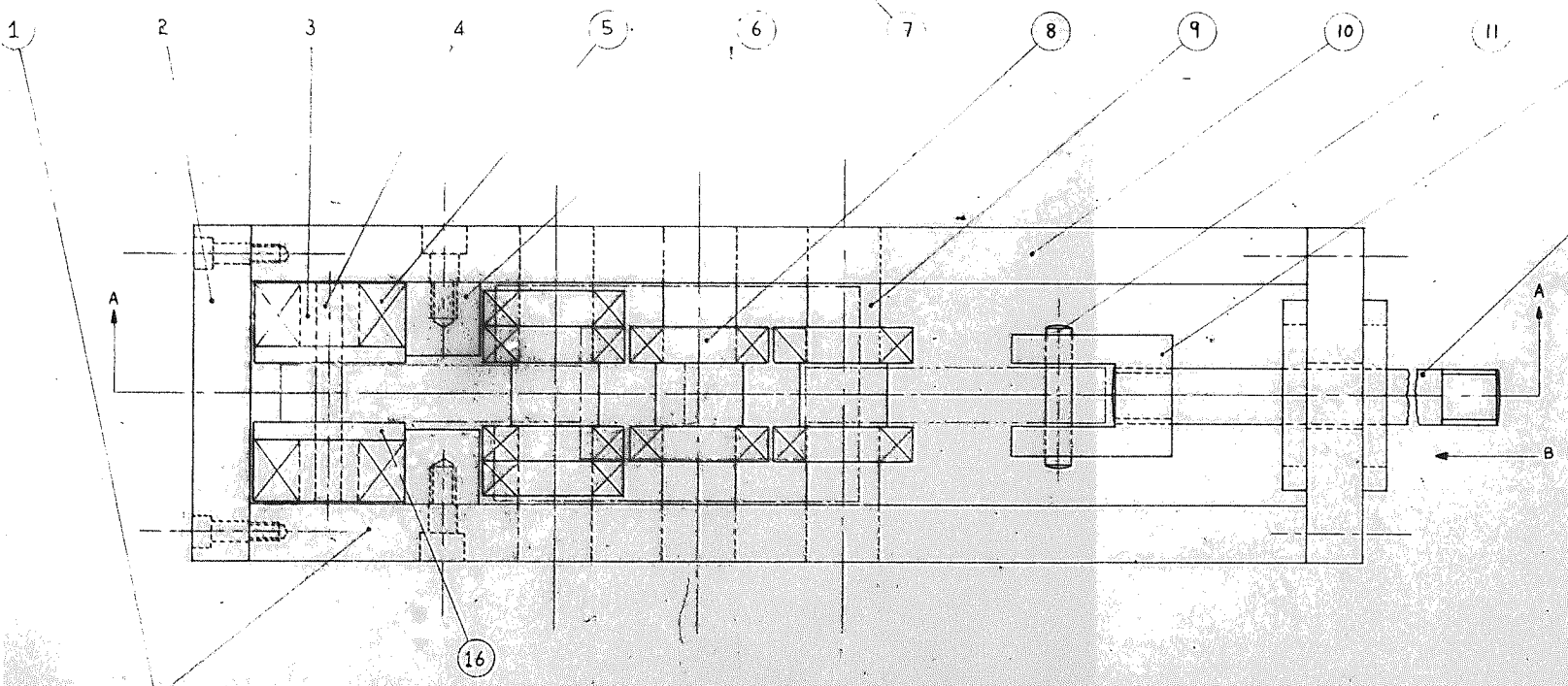

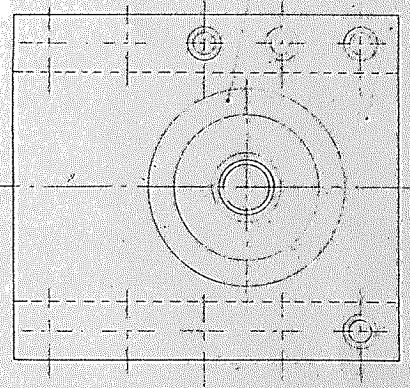

ELEVATION - B

GENERAL ARRANGEMENT OF BIAXIAL LOADING JIG FOR SHORT FILLET WELDS | DRAWN BY : J.D. HIGGS | DATE : 10. 6. 76 | SCALE : FULL SIZE

(1) SIDE PLATE (L.H.) M.S.

(10) SIDE PLATE (R.H) NOT ILLUS.

FIRST ANGLE PROJECTION

(1) ¼" B.S.W TAPPED HOLES 10mm DEEP

4 - COUNTERBORED HOLES TO SUIT ¼" B.S.W SOCKET HEAD CAP SCREWS

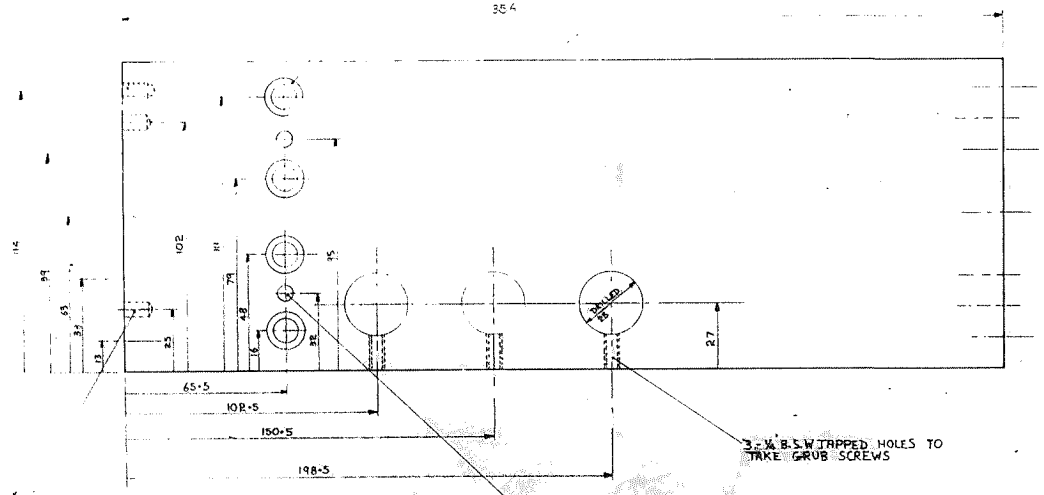

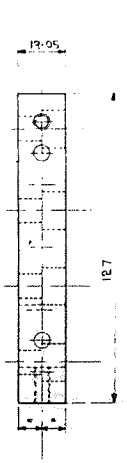

(3) BEARING PUSH, 2 OFF IN MILD STEEL INTERFERENCE FIT TO ITEM 5.

(11) CLEVIS PIN - ½" DOWEL, 2" LONG.

(4) BEARING PIN - ½" DOWEL, 3" LONG.

(5) ROLLER BEARING - SKF NU 2304 E. 2 OFF

(8) ROLLER BEARING - SKF 6005, 8 OFF.

(15) END PLATE MATL B.D.M.S. (2) END PLATE, AS ITEM 15 LESS 22mm DIA. HOLE.

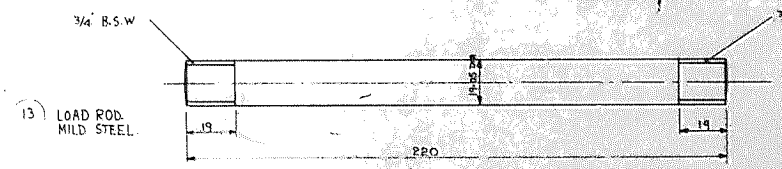

(13) LOAD ROD. MILD STEEL.

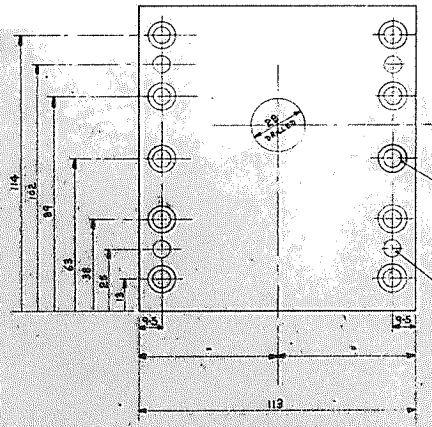

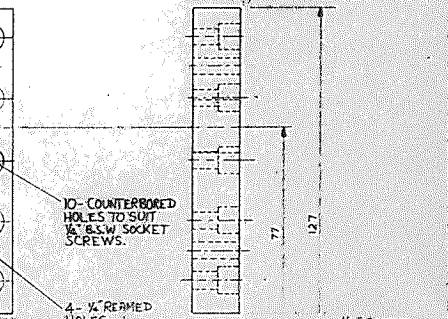

(16) DISTANCE PIECES. 2 OFF MATL. M.S.

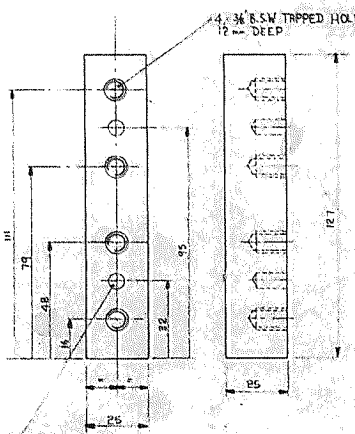

(6) REACTION POST. 2-OFF IN MILD STEEL.

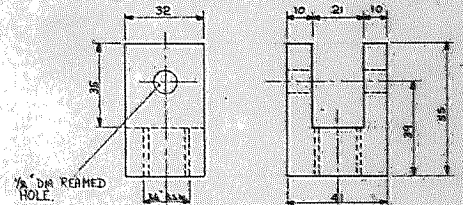

(12) CLEVIS. MILD STEEL.

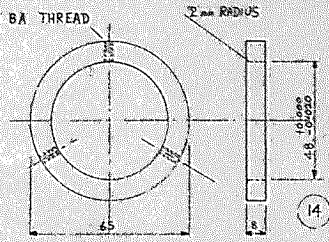

(14) RAM LOCATION RING. 2-OFF IN MILD STEEL. TO BE TACK WELDED IN POSITION.

(9) SHAFT. 3 OFF MATL. M.S.

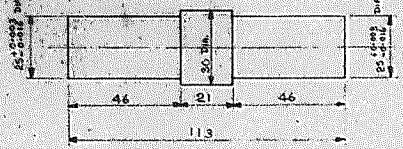

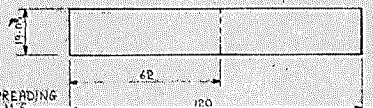

(7) SHEAR LOAD SPREADING PLATE

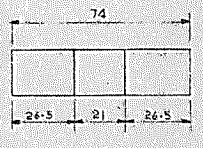

DETAILS OF BIAXIAL LOADING RIG FOR SHORT FILLET WELDS | TOLERANCES UNLESS

APPENDIX 2

Details of 1130 kNm, 1000 kN Testing Beam

ALL DIMENSIONS ARE IN MILLIMETRES.
DO NOT SCALE. IF IN DOUBT, ASK.

THIRD ANGLE PROJECTION

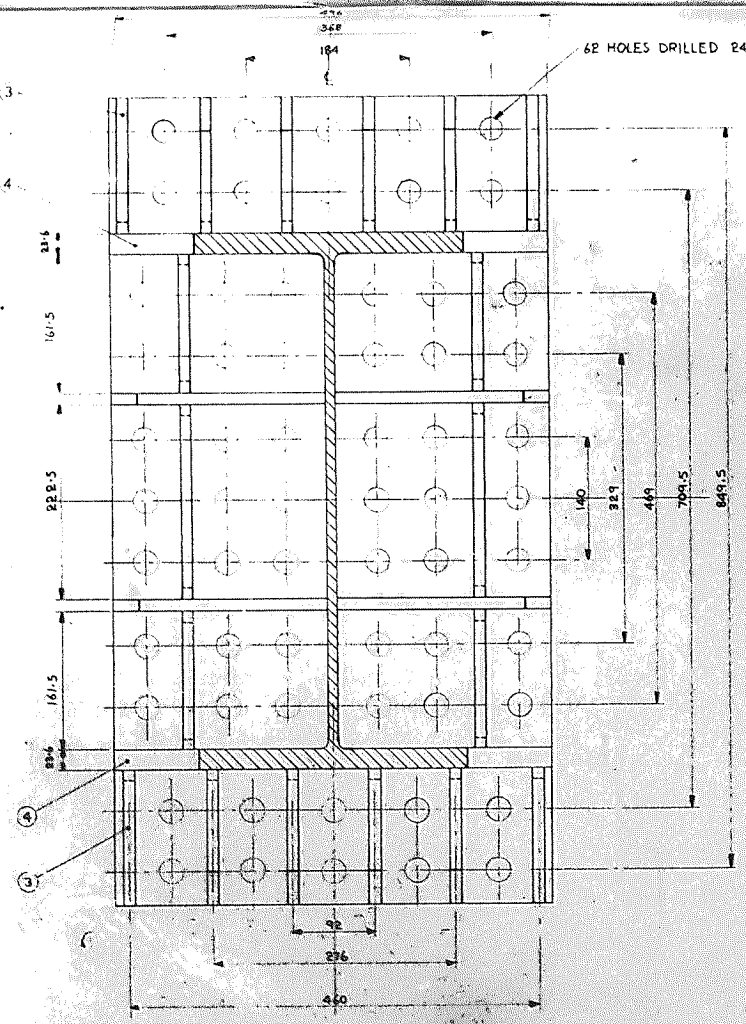

SECTION ON A-A

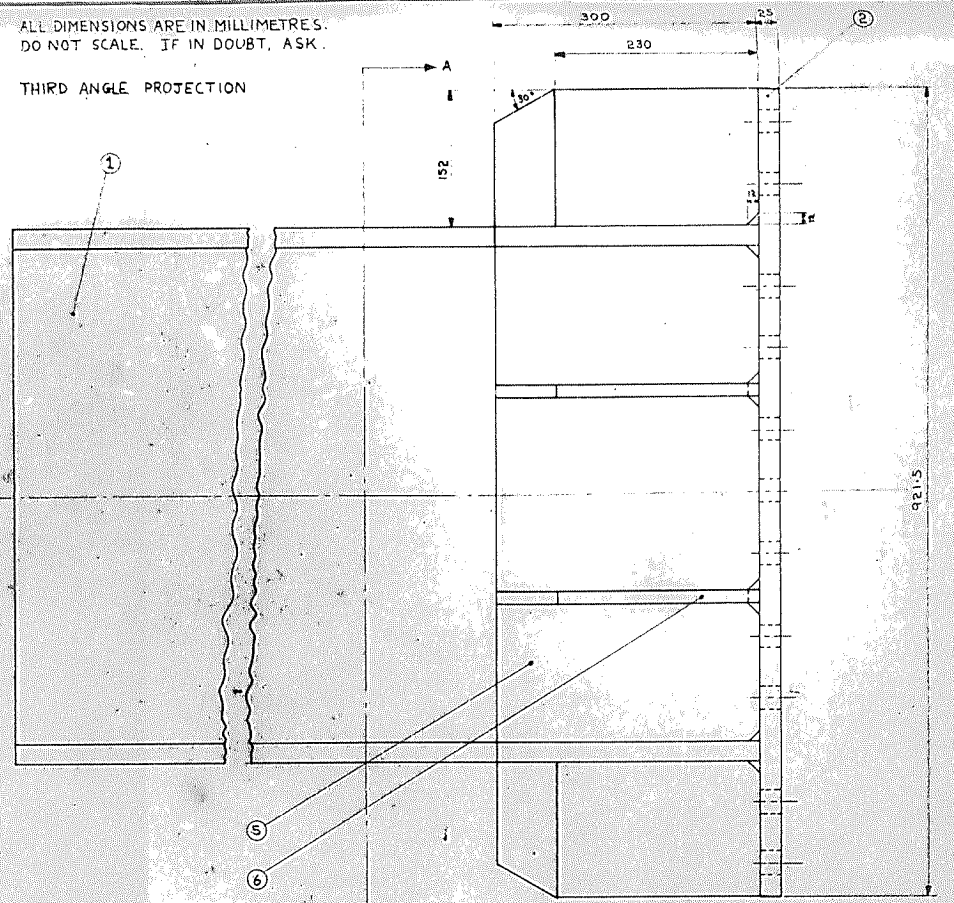

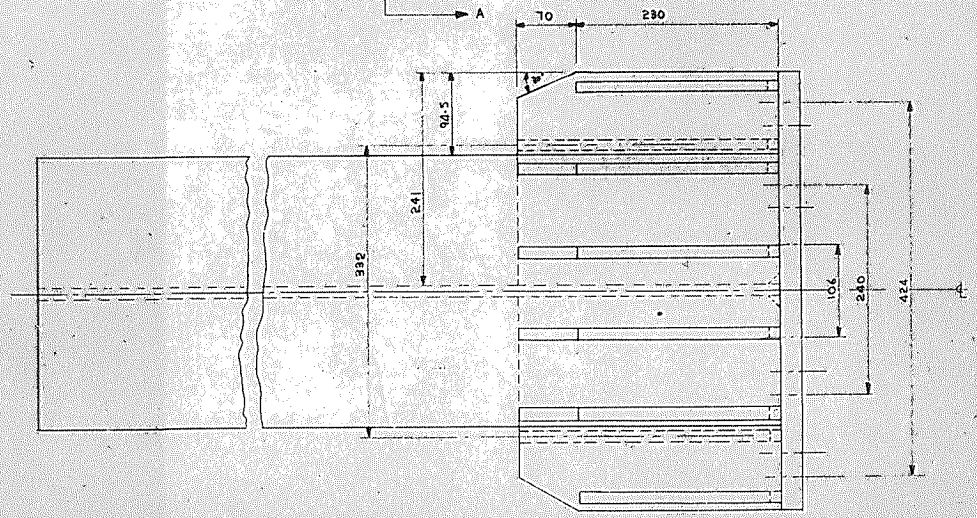

ITEM	MATERIAL	DESCRIPTION
1	HIGH YIELD STEEL	UNIVERSAL BEAM 610 X 305 @ 179 kg/m. 2 LENGTHS @
2	STRUCTURAL STEEL GRADE 50 TO BS 4360	END PLATE. 2 @ 921·5 X 496 X 25
3	"	FLANGE GUSSETS. 12 @ 300 X 152 X 12 . 8 @ 230 X 152 X 12
4	"	FLANGE GUSSETS. 8 @ 300 X 94·5 X 23·6
5	"	END PLATE STIFFENER. 8 @ 300 X 161·5 X 12 . 4 @ 300 X 228·5 X 12.
6	"	WEB GUSSETS. 8 @ 300 X 241 X 12.
7	STRENGTH GRADE 6·8 , BS 3692	130 STEEL BOLTS (COARSE THREAD SERIES) SIZE M24, LENGTH 100 mm. 130 STEEL NUTS TO SUIT.
8	MILD STEEL	260 FLAT WASHERS SIZE M24

TITLE :	DETAILS OF 1130kNm, 1000KN TESTING BEAM			
SCALE :	1/3 FULL SIZE	DATE :	14. 1. 76	TOLERANCES ON HOLE CENTRES : ± 0·05 mm. ON GUSSET CENTRES : ± 1·0 mm. ON GUSSET, STIFFENER AND END PLATE DIMENSIONS : +0·00 −0·50 mm.
DRAWN BY:	J. D. HIGGS	MACHINING:	ALL EDGES TO BE MACHINED.	

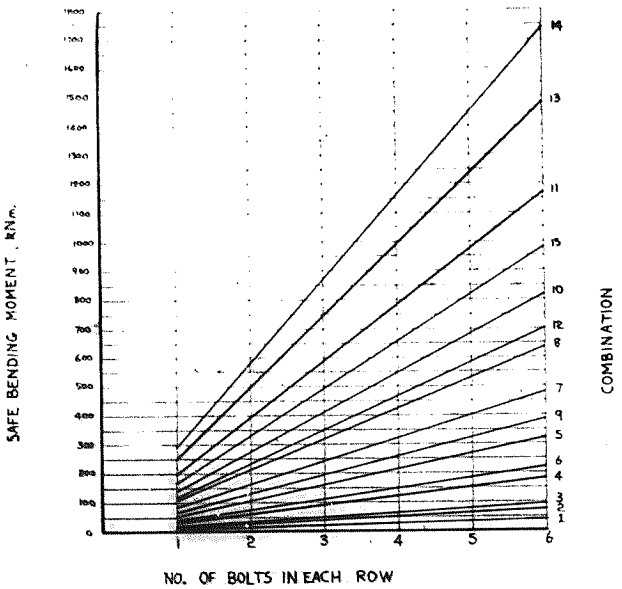

GRAPHICAL REPRESENTATION OF SAFE BENDING MOMENT

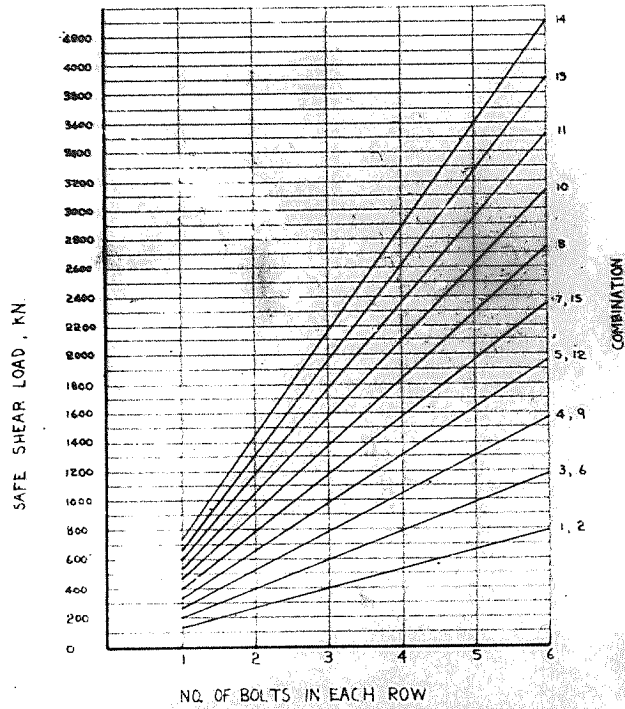

GRAPHICAL REPRESENTATION OF SAFE SHEAR LOAD

KEY TO ROW COMBINATIONS

COMBINATION	CONTAINS ROWS :
1	5~6 OR 6~7
2	5~7
3	5,6~7
4	4,5,6~7
5	4,5,6,7~8
6	4,6~8
7	3,4,5,6,7~8
8	3,4,5,6,7,8~9
9	3,5,7~9
10	2,3,4,5,6,7,8~9
11	2,3,4,5,6,7,8,9~10
12	2,4,6,8~10
13	1,2,3,4,5,6,7,8,9~10
14	1,3,4,5,6,7,8,9,10~11
15	1,3,5,7,9~11

KEY TO ROW NUMBERS

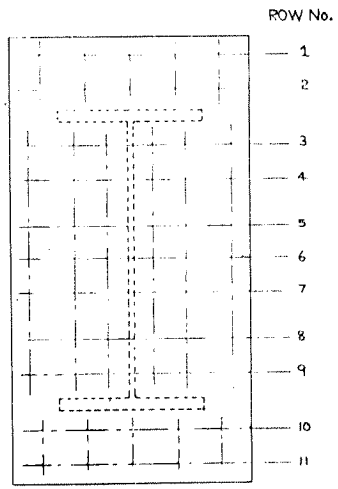

EXPLANATORY NOTES

The values obtained for the safe loads are based on the following assumptions :

1. close tolerance turned bolts are used.
2. their strength grade is 6.8, BS 3692.
3. the safe bending moment is calculated for pure bending situation.
4. the safe shear load is calculated for a pure shear situation.

COMBINATION	SAFE SHEAR LOAD, kN — NUMBER OF BOLTS IN EACH ROW						SAFE BENDING MOMENT, kNm — NUMBER OF BOLTS IN EACH ROW					
	1	2	3	4	5	6	1	2	3	4	5	6
1	130	260	390	520	650	780	6·2	12·4	18·6	24·8	31	37·2
2	130	260	390	520	650	780	12·4	24·8	37·2	49·6	62	74·4
3	195	390	585	780	975	1170	15·5	31	46·5	62	77·5	93
4	260	520	780	1040	1300	1560	30	60	90	120	150	180
5	325	650	975	1300	1625	1950	53·6	107	161	214	266	320
6	195	390	585	780	975	1170	36·3	72·4	109	145	181	218
7	390	780	1170	1560	1950	2340	79·4	159	238	318	397	476
8	455	910	1365	1820	2275	2730	105	210	316	420	525	630
9	260	520	780	1040	1300	1560	64·1	128	192	256	320	384
10	520	1040	1560	2080	2600	3120	136	272	408	544	681	817
11	585	1170	1755	2340	2925	3510	194	389	582	776	970	1164
12	325	650	975	1300	1625	1950	117	234	351	468	585	700
13	650	1300	1950	2600	3250	3900	246	492	738	984	1230	1476
14	715	1430	2145	2860	3575	4290	288	576	864	1152	1440	1730
15	390	780	1170	1560	1950	2340	163	326	489	652	815	977

TABLE OF SAFE LOADS

SAFE BOLT LOADS FOR 1130 kNm 1000 kN TESTING BEAM				
DRAWN BY :	J.D HIGGS	DATE :	19. 1. 76	

APPENDIX 3

Details of End-plates

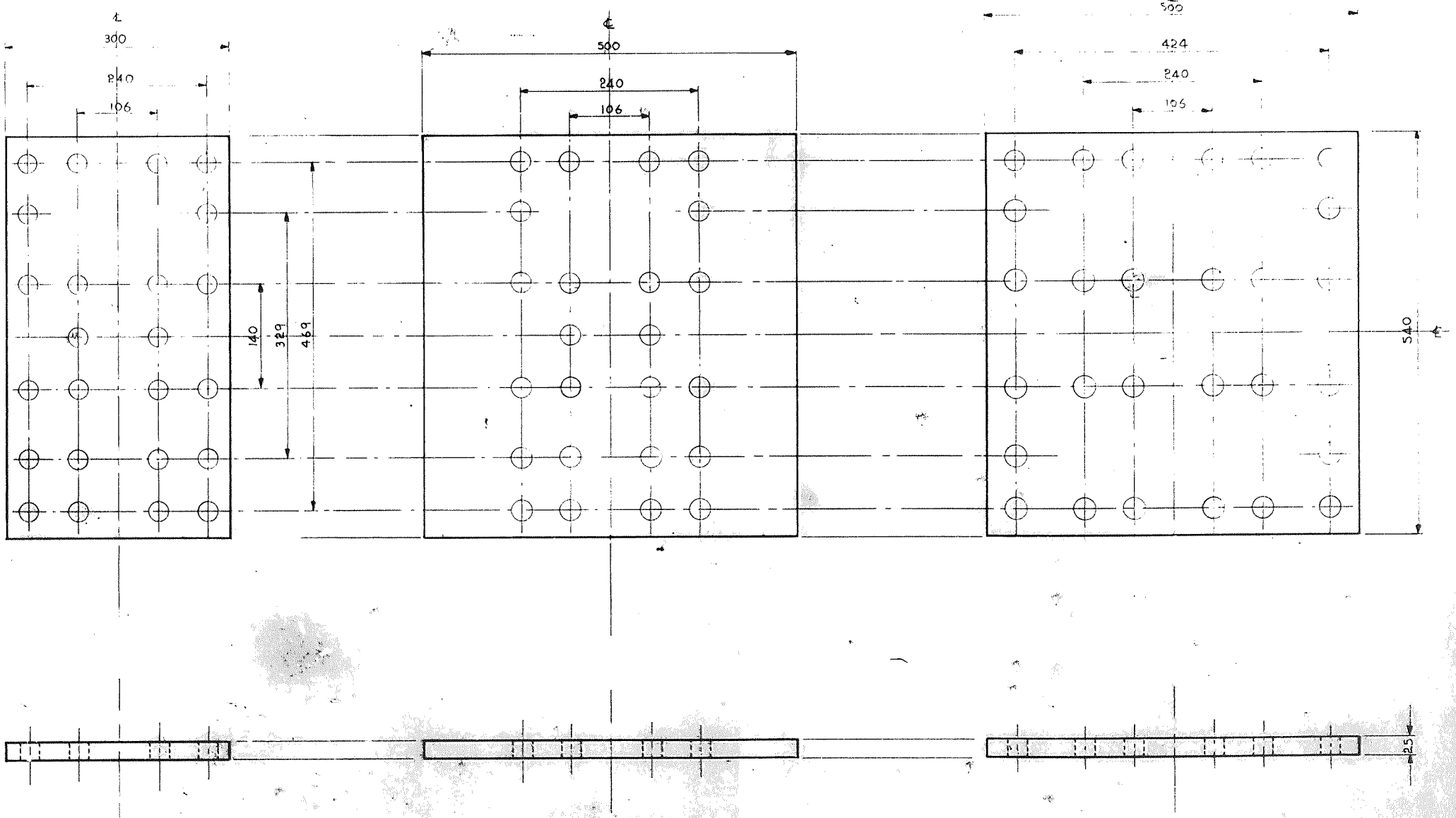

TYPE - A

TYPE - B

TYPE - C

HOLES TO BE DRILLED 24 mm

TITLE:	DETAILS OF END PLATES FOR WEB AND FLANGE TEST PIECES			
SCALE:	1/3 FULL SIZE	DATE:	23. 9. 76	TOLERANCES
DRAWN BY:	J.D HIGGS	M'CHG:	—	ON HOLE CENTRES: ±0.05mm

APPENDIX 4

Calibration Charts for Ram/Pressure Gauges

Calibration Chart for Ram/Pressure Gauge No.8531870

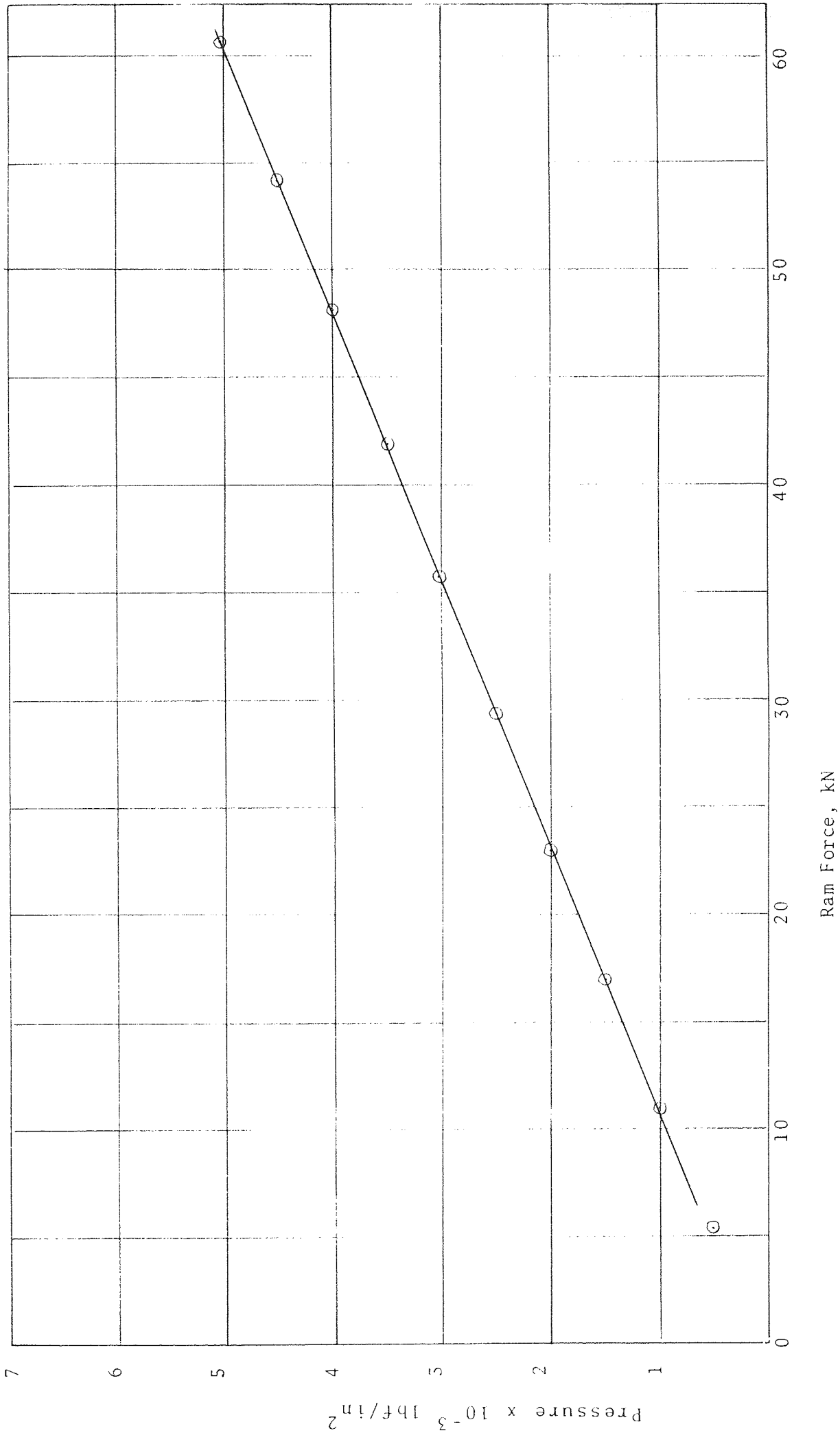

Calibration Chart for Ram/Pressure Gauge, No.9231569

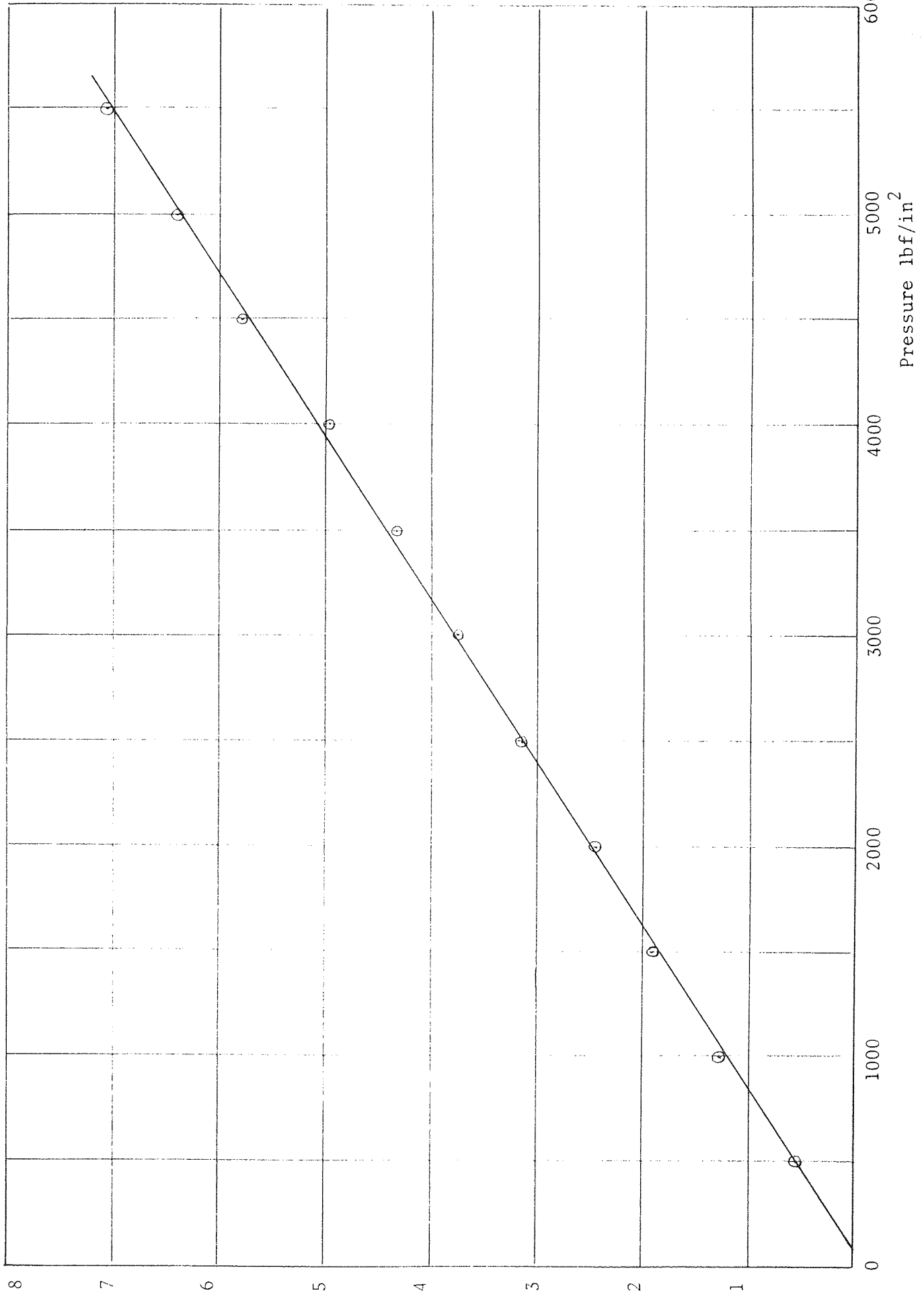

Calibration of Ram/Pressure Gauge No. 9581699